frontiers | Research Topics

Mineral solubilizing microorganisms (MSM) and their applications in nutrient bioavailability, bioweathering and bioremediation, volume II

Edited by
Muhammad Zahid Mumtaz, Maqshoof Ahmad, Hassan Etesami and Adnan Mustafa

Published in
Frontiers in Microbiology

ISSN 1664-8714
ISBN 978-2-8325-4810-3
DOI 10.3389/978-2-8325-4810-3

About Frontiers

Frontiers is more than just an open access publisher of scholarly articles: it is a pioneering approach to the world of academia, radically improving the way scholarly research is managed. The grand vision of Frontiers is a world where all people have an equal opportunity to seek, share and generate knowledge. Frontiers provides immediate and permanent online open access to all its publications, but this alone is not enough to realize our grand goals.

Frontiers journal series

The Frontiers journal series is a multi-tier and interdisciplinary set of open-access, online journals, promising a paradigm shift from the current review, selection and dissemination processes in academic publishing. All Frontiers journals are driven by researchers for researchers; therefore, they constitute a service to the scholarly community. At the same time, the *Frontiers journal series* operates on a revolutionary invention, the tiered publishing system, initially addressing specific communities of scholars, and gradually climbing up to broader public understanding, thus serving the interests of the lay society, too.

Dedication to quality

Each Frontiers article is a landmark of the highest quality, thanks to genuinely collaborative interactions between authors and review editors, who include some of the world's best academicians. Research must be certified by peers before entering a stream of knowledge that may eventually reach the public - and shape society; therefore, Frontiers only applies the most rigorous and unbiased reviews. Frontiers revolutionizes research publishing by freely delivering the most outstanding research, evaluated with no bias from both the academic and social point of view. By applying the most advanced information technologies, Frontiers is catapulting scholarly publishing into a new generation.

What are Frontiers Research Topics?

Frontiers Research Topics are very popular trademarks of the *Frontiers journals series*: they are collections of at least ten articles, all centered on a particular subject. With their unique mix of varied contributions from Original Research to Review Articles, Frontiers Research Topics unify the most influential researchers, the latest key findings and historical advances in a hot research area.

Find out more on how to host your own Frontiers Research Topic or contribute to one as an author by contacting the Frontiers editorial office: frontiersin.org/about/contact

Mineral solubilizing microorganisms (MSM) and their applications in nutrient bioavailability, bioweathering and bioremediation, volume II

Topic editors

Muhammad Zahid Mumtaz – The University of Lahore, Pakistan
Maqshoof Ahmad – The Islamia University of Bahawalpur, Pakistan
Hassan Etesami – University of Tehran, Iran
Adnan Mustafa – Brno University of Technology, Czechia

Citation

Mumtaz, M. Z., Ahmad, M., Etesami, H., Mustafa, A., eds. (2024). *Mineral solubilizing microorganisms (MSM) and their applications in nutrient bioavailability, bioweathering and bioremediation, volume II*. Lausanne: Frontiers Media SA.
doi: 10.3389/978-2-8325-4810-3

Table of contents

04 Editorial: Mineral solubilizing microorganisms (MSM) and their applications in nutrient bioavailability, bioweathering and bioremediation, volume II
Muhammad Zahid Mumtaz, Maqshoof Ahmad, Hassan Etesami and Adnan Mustafa

07 Bio-removal of rare earth elements from hazardous industrial waste of CFL bulbs by the extremophile red alga *Galdieria sulphuraria*
Anjali Singh, Mária Čížková, Vít Náhlík, Dana Mezricky, Dominik Schild, Marian Rucki and Milada Vítová

19 Insight into phytase-producing microorganisms for phytate solubilization and soil sustainability
Sheikh Rizwanuddin, Vijay Kumar, Pallavi Singh, Bindu Naik, Sadhna Mishra, Mansi Chauhan, Per Erik Joakim Saris, Ankit Verma and Vivek Kumar

32 Recovery of valuable metals from spent lithium-ion batteries using microbial agents for bioleaching: a review
Basanta Kumar Biswal and Rajasekhar Balasubramanian

57 Nutrient availability and acid erosion determine the early colonization of limestone by lithobiontic microorganisms
Jin Chen, Qing Zhao, Fangbing Li, Xiangwei Zhao, Yang Wang, Limin Zhang, Jinan Liu, Lingbin Yan and Lifei Yu

68 Soil nutrient management influences diversity, community association and functional structure of rhizosphere bacteriome under vegetable crop production
Adekunle R. Raimi, Obinna T. Ezeokoli and Rasheed A. Adeleke

84 Plant growth promotion under phosphate deficiency and improved phosphate acquisition by new fungal strain, *Penicillium olsonii* TLL1
Erinjery Jose Suraby, Valiya Nadakkakath Agisha, Savitha Dhandapani, Yee Hwui Sng, Shi Hui Lim, Naweed I. Naqvi, Rajani Sarojam, Zhongchao Yin and Bong Soo Park

frontiers | Frontiers in Microbiology

TYPE Editorial
PUBLISHED 04 January 2024
DOI 10.3389/fmicb.2023.1345161

OPEN ACCESS

EDITED AND REVIEWED BY
David Emerson,
Bigelow Laboratory for Ocean Sciences,
United States

*CORRESPONDENCE
Muhammad Zahid Mumtaz
✉ zahidses@gmail.com

RECEIVED 27 November 2023
ACCEPTED 12 December 2023
PUBLISHED 04 January 2024

CITATION
Mumtaz MZ, Ahmad M, Etesami H and Mustafa A (2024) Editorial: Mineral solubilizing microorganisms (MSM) and their applications in nutrient bioavailability, bioweathering and bioremediation, volume II.
Front. Microbiol. 14:1345161.
doi: 10.3389/fmicb.2023.1345161

Editorial: Mineral solubilizing microorganisms (MSM) and their applications in nutrient bioavailability, bioweathering and bioremediation, volume II

Muhammad Zahid Mumtaz[1,2]*, Maqshoof Ahmad[3], Hassan Etesami[4] and Adnan Mustafa[5]

[1]Institute of Molecular Biology and Biotechnology, The University of Lahore, Lahore, Pakistan, [2]College of Agronomy, Gansu Agricultural University, Lanzhou, China, [3]Department of Soil Science, The Islamia University of Bahawalpur, Bahawalpur, Pakistan, [4]College of Agriculture and Natural Resources, University of Tehran, Karaj, Iran, [5]Key Laboratory of Vegetation Restoration and Management, South China Botanical Garden, Chinese Academy of Sciences, Guangzhou, China

KEYWORDS

mineral solubilizing microorganisms, phosphate solubilizing microorganisms, nutrient bioavailability, bioweathering, bioremediation, mineral-microbe interactions, recovery of metals

Editorial on the Research Topic
Mineral solubilizing microorganisms (MSM) and their applications in nutrient bioavailability, bioweathering and bioremediation, volume II

Soil microorganisms are involved in mineral weathering, nutrient bioavailability, and bioremediation in the soil ecosystem. In this regard, microbes' mineral interactions can assist exogenic biogeochemical reactions. Various microorganisms cause weathering and rock decomposition through biocorrosion, bioerosion, and bioperforation by inhabiting rock surfaces or crevices (Bin et al., 2008). Microbes acquire nutrients from rock surfaces by building complex organic ligands and encouraging the release of mineral elements. Bioperforation in rock surface by microbial colonization promotes the exposed surface area of rock and intensifies its weathering by mechanical erosion, microbial destruction, and deterioration of rock particle cementation structure (Ehrlich, 1998). Microorganisms also boost mineral weathering through acidification by producing organic acids, microbial water retention, and release of CO_2 due to microbial respiration (Chen et al., 2000). Microorganisms enhance mineral availability from geological resources through mineral breakdown and rock deterioration. Furthermore, microbial technology exploits low-grade mineral resources available for plant uptake, accelerating soil formation (Kumar et al., 2018).

Microorganisms promote soil physicochemical characteristics and nutrient cycling in soil solution (Li et al., 2006). Roots exudates facilitate mineral solubilizing microorganisms (MSM) to perform their activity. In response to the plant's nutritional needs, exudation rates increase with root surface area (Aoki et al., 2012). In addition, plants emit sugars, amino acids, enzymes, fatty acids, sterols, growth factors, vitamins, and secondary metabolites. They transform the rhizosphere into a nutrient-rich environment that may support a diverse microbial population (Vives-Peris et al., 2020). The MSM in the rhizospheric area promotes a more intense mineral bioavailability than bulk soil. Microorganisms solubilize insoluble minerals through various mechanisms,

including direct dissolution, redox reactions, and enzymatic production of various acid phosphatases and phytases (Kumar et al., 2013). They solubilize minerals from the soil directly through microbial weathering and promote plant growth by improving root development, modulating phytohormones, producing siderophores and hydrogen cyanide, increasing plant enzymatic activities, controlling phytopathogen under normal as well as stress conditions (Mumtaz et al., 2017; Etesami and Adl, 2020; Saeed et al., 2021).

Industrialization in the current era negatively affects soil and crop productivity by accumulating vast amounts of minerals, including heavy metals. These heavy metals are cytotoxic even at low concentrations and cause human cancer. Their toxicity causes higher production of reactive oxygen species that reduce the antioxidant systems and affect an organism's normal functioning, ultimately leading to cell death (Tarfeen et al., 2022). The MSM can perform bioremediation of contaminated agricultural soil. These microorganisms perform bioremediation of metal minerals through biosorption to cell walls, precipitation, capturing in extracellular capsules, efflux outside the cell, transformation of metal minerals to a less toxic state, and ligation inside cell leading to adsorption of metal minerals ions (Riseh et al., 2022). Bioremediation of metal minerals depends on environmental factors (temperature, pH, electron acceptor, nutrients, etc.), contaminant properties, biodegradative genes in organisms, and bioavailability of contaminants to degrading microorganisms within the site (Maier, 2000). In the current Research Topic, metal bioavailability was considered to be the most crucial factor in bioremediation. The bioavailability of minerals also has a vital role in rocks and minerals weathering and nutrient availability for crop growth and productivity. The MSM have biologically activated metabolic systems that are eco-friendly and cost-effective and have various mechanisms for weathering, bioavailability, and bioremediation of minerals.

This Research Topic aims to uncover the role of MSM in mineral weathering, nutrient availability, and bioremediation. This topic presents two reviews and four original research papers by 39 authors from seven countries that span the research on mineral-solubilizing microorganisms. This topic publishes one article on weathering, three articles on nutrient bioavailability and plant growth promotion, and two articles on the bioremediation or recovery of metal minerals. These articles give insight into ongoing issues and provide a basis for further study on the application of MSM in nutrient availability and bioremediation. Here, we summarized some highlights from the six articles published on this Research Topic.

Mineral bioweathering through mineral solubilizing microorganisms

Microbial diversity is a crucial factor for soil formation from rock weathering. Chen et al. reported a higher abundance of fungi over bacteria during premature colonization on limestone. Fungal communities were remarkably unaffected by nutrient solutions, organic acid, inorganic acid, and microbial competition, while bacterial communities were robust and constant. They observed the dominant fungal phyla were Ascomycota, Basidiomycota, and Chytridiomycota, while the dominant bacterial phyla were Proteobacteria, Bacteroidota, and Actinobacteriota, which have their application in weathering of limestone.

Nutrient bioavailability through mineral solubilizing microorganisms

The MSM are associated with plants to promote essential mineral uptake. Suraby et al. reported the solubilization of insoluble phosphate compounds, including $AlPO_4$, $FePO_4{\cdot}4H_2O$, $Ca_3(PO_4)_2$, and hydroxyapatite by fungal strain *Penicillium olsonii* TLL1. This strain promoted Arabidopsis, Bok choy, and rice growth in vermiculite soil under phosphorus-limiting conditions. Rizwanuddin et al. emphasized the solubilization of soil organic phytate by phytase-producing microorganisms. MSM produces phytase enzymes that enhance the phytate mineralization through the cleavage of phytate ester bonds. Transgenic plants are generated by inserting microbial phytase-producing genes to promote phytate mineralization and phosphorus availability in plants. Raimi et al. reported that organic fertilizers support highly functional and more robust interactions within the rhizosphere bacterial community. Organic fertilizers demonstrated functionally versatile bacterial community structures characterized by plant growth-promoting genera such as Agromyces, Bacillus, and Nocardioides over traditional fertilizers. Rhizospheric bacterial communities had higher diversity richness and unique bacterial genera in organic farms than in conventional farms.

Bioremediation through mineral solubilizing microorganisms

Metal minerals at high doses are recalcitrant contaminants that can harm living organisms. Singh et al. reported the bioaccumulation/removal of rare earth elements from hazardous industrial waste of compact fluorescent lamp acid extract using synchronous culture of extremophilic red algae *Galdieria sulphuraria*. The algal efficiency to accumulate rare earth elements was augmented by adding 6-benzylaminopurine and 1-naphthaleneacetic acid, which could be the solution for the removal or recycling of wastes containing rare earth elements. Biswal and Balasubramanian reviewed the performance of various microbial agents to extract cobalt and lithium from the solid matrix of spent lithium-ion batteries. Bioleaching of dissolved metal from spent lithium-ion batteries is effective through bacterial strains, including *Acidithiobacillus ferrooxidans* and *Acidithiobacillus thiooxidans,* and the fungal strain *Aspergillus niger*. The production of sulfuric acid from bacterial strains and citric acid, gluconic acid, and oxalic acid from fungal strains are the dominant metabolites involved in cobalt and lithium bioleaching.

Author contributions

MM: Conceptualization, Data curation, Formal analysis, Investigation, Methodology, Project administration, Supervision, Validation, Writing—original draft, Writing—review & editing. MA: Formal analysis, Supervision, Validation, Writing—review & editing. HE: Formal analysis, Validation, Writing—review &

editing. AM: Data curation, Formal analysis, Writing—review & editing.

Funding

The author(s) declare that no financial support was received for the research, authorship, and/or publication of this article.

Conflict of interest

The authors declare that the research was conducted in the absence of any commercial or financial relationships that could be construed as a potential conflict of interest.

Publisher's note

All claims expressed in this article are solely those of the authors and do not necessarily represent those of their affiliated organizations, or those of the publisher, the editors and the reviewers. Any product that may be evaluated in this article, or claim that may be made by its manufacturer, is not guaranteed or endorsed by the publisher.

References

Aoki, M., Fujii, K., and Kitayama, K. (2012). Environmental control of root exudation of low-molecular weight organic acids in tropical rainforests. *Ecosystems* 15, 1194–1203. doi: 10.1007/s10021-012-9575-6

Bin, L., Ye, C., Lijun, Z., and Ruidong, Y. (2008). Effect of microbial weathering on carbonate rocks. *Earth Sci. Front.* 15, 90–99. doi: 10.1016/S1872-5791(09)60009-9

Chen, J., Blume, H. P., and Beyer, L. (2000). Weathering of rocks induced by lichen colonization-a review. *Catena* 39, 121–146. doi: 10.1016/S0341-8162(99)00085-5

Ehrlich, H. L. (1998). Geomicrobiology: its significance for geology. *Earth Sci. Rev.* 45, 45–60. doi: 10.1016/S0012-8252(98)00034-8

Etesami, H., and Adl, S. M. (2020). "Plant growth-promoting rhizobacteria (PGPR) and their action mechanisms in availability of nutrients to plants," in *Phyto-Microbiome in Stress Regulation. Environmental and Microbial Biotechnology*, eds M. Kumar, V. Kumar, and R. Prasad (Singapore: Springer), 147–203.

Kumar, P. S., Yaashikaa, P. R., and Baskar, G. (2018). "Biomining of natural resources," in *Waste Bioremediation*, S. J. Varjani, E. Gnansounou, B. Gurunathan, D. Pant, and Z. A. Zakaria (Singapore: Springer), 313–342.

Kumar, V., Singh, P., Jorquera, M. A., Sangwan, P., Kumar, P., Verma, A. K., et al. (2013). Isolation of phytase-producing bacteria from Himalayan soils and their effect on growth and phosphorus uptake of Indian mustard (*Brassica juncea*). *World J. Microbol. Biotechnol.* 29, 1361–1369. doi: 10.1007/s11274-013-1299-z

Li, Y., Zhang, Q., Wan, G., Huang, R., Piao, H., Bai, L., et al. (2006). Physical mechanisms of plant roots affecting weathering and leaching of loess soil. *Sci. China Ser. D Earth Sci.* 49, 1002–1008. doi: 10.1007/s11430-006-1002-4

Maier, R. M. (2000). "Bioavailability and its importance to bioremediation," in *Bioremediation*, ed J. J. Valdes (Dordrecht: Springer), 59–78.

Mumtaz, M. Z., Ahmad, M., Jamil, M., and Hussain, T. (2017). Zinc solubilizing *Bacillus* spp. potential candidates for biofortification in maize. *Microbiol. Res.* 202, 51–60. doi: 10.1016/j.micres.2017.06.001

Riseh, R. S., Vazvani, M. G., Hajabdollahi, N., and Thakur, V. K. (2022). Bioremediation of heavy metals by rhizobacteria. *Appl. Biochem. Biotechnol.* 195, 1–23. doi: 10.1007/s12010-022-04177-z

Saeed, Q., Xiukang, W., Haider, F. U., Kučerik, J., Mumtaz, M. Z., Holatko, J., et al. (2021). Rhizosphere bacteria in plant growth promotion, biocontrol, and bioremediation of contaminated sites: a comprehensive review of effects and mechanisms. *Int. J. Mol. Sci.* 22, 10529. doi: 10.3390/ijms221910529

Tarfeen, N., Nisa, K. U., Hamid, B., Bashir, Z., Yatoo, A. M., Dar, M. A., et al. (2022). Microbial remediation: a promising tool for reclamation of contaminated sites with special emphasis on heavy metal and pesticide pollution: a review. *Processes* 10, 1358. doi: 10.3390/pr10071358

Vives-Peris, V., de Ollas, C., Gómez-Cadenas, A., and Pérez-Clemente, R. M. (2020). Root exudates: from plant to rhizosphere and beyond. *Plant Cell Rep.* 39, 3–17. doi: 10.1007/s00299-019-02447-5

frontiers | Frontiers in Microbiology

TYPE Original Research
PUBLISHED 13 February 2023
DOI 10.3389/fmicb.2023.1130848

OPEN ACCESS

EDITED BY
Muhammad Zahid Mumtaz,
The University of Lahore,
Pakistan

REVIEWED BY
Chayakorn Pumas,
Chiang Mai University,
Thailand
Giovanna Salbitani,
University of Naples Federico II,
Italy

*CORRESPONDENCE
Milada Vítová
✉ milada.vitova@ibot.cas.cz

SPECIALTY SECTION
This article was submitted to Microbiological Chemistry and Geomicrobiology, a section of the journal Frontiers in Microbiology

RECEIVED 23 December 2022
ACCEPTED 24 January 2023
PUBLISHED 13 February 2023

CITATION
Singh A, Čížková M, Náhlík V, Mezricky D, Schild D, Rucki M and Vítová M (2023) Bio-removal of rare earth elements from hazardous industrial waste of CFL bulbs by the extremophile red alga *Galdieria sulphuraria*. *Front. Microbiol.* 14:1130848. doi: 10.3389/fmicb.2023.1130848

Bio-removal of rare earth elements from hazardous industrial waste of CFL bulbs by the extremophile red alga *Galdieria sulphuraria*

Anjali Singh[1], Mária Čížková[1], Vít Náhlík[1,2], Dana Mezricky[3], Dominik Schild[3], Marian Rucki[4] and Milada Vítová[1,5]*

[1]Laboratory of Cell Cycles of Algae, Centre Algatech, Institute of Microbiology, Czech Academy of Sciences, Třeboň, Czechia, [2]Faculty of Fisheries and Protection of Waters, South Bohemian Research Center of Aquaculture and Biodiversity of Hydrocenoses, Institute of Aquaculture and Protection of Waters, University of South Bohemia, České Budějovice, Czechia, [3]Institute of Medical and Pharmaceutical Biotechnology, IMC FH Krems, Krems, Austria, [4]Laboratory of Predictive Toxicology, National Institute of Public Health, Prague, Czechia, [5]Centre for Phycology, Institute of Botany, Czech Academy of Sciences, Třeboň, Czechia

In recent decades, a shift has been seen in the use of light-emitting diodes over incandescent lights and compact fluorescent lamps (CFL), which eventually led to an increase in wastes of electrical equipment (WEE), especially fluorescent lamps (FLs) and CFL light bulbs. These widely used CFL lights, and their wastes are good sources of rare earth elements (REEs), which are desirable in almost every modern technology. Increased demand for REEs and their irregular supply have exerted pressure on us to seek alternative sources that may fulfill this demand in an eco-friendly manner. Bio-removal of wastes containing REEs, and their recycling may be a solution to this problem and could balance environmental and economic benefits. To address this problem, the current study focuses on the use of the extremophilic red alga, *Galdieria sulphuraria*, for bioaccumulation/removal of REEs from hazardous industrial wastes of CFL bulbs and the physiological response of a synchronized culture of *G. sulphuraria*. A CFL acid extract significantly affected growth, photosynthetic pigments, quantum yield, and cell cycle progression of this alga. A synchronous culture was able to efficiently accumulate REEs from a CFL acid extract and efficiency was increased by including two phytohormones, i.e., 6-Benzylaminopurine (BAP - Cytokinin family) and 1-Naphthaleneacetic acid (NAA - Auxin family).

KEYWORDS

compact fluorescent lamp, industrial wastes, extremophile, Rhodophyta, *Galdieria sulphuraria*, bio-removal, plant hormones

Introduction

Rare earth elements (REEs) are a group of 17 chemical elements that comprise yttrium (Y), scandium (Sc), and a series of 15 lanthanides. REEs have practically identical physical and chemical properties although they have rather unique magnetic and catalytic properties (Cheisson and Schelter, 2019; Čížková et al., 2021). These properties make them desirable in a wide range of industries such as electrical, electronics, laser, glass, magnetic materials, energy technology, aquaculture, and agriculture (Hu et al., 2004; Chakhmouradian and Wall, 2012; Balaram, 2019). In recent decades, the use of fluorescent lamps (FLs), involving both tubes and compact fluorescent lamps (CFLs), has increased globally to improve energy efficiency. However, due to the presence of mercury and REEs as essential components, their use can be environmentally harmful (Balaram, 2019; Pagano et al., 2019). The shift from incandescent lights and CFLs to light-emitting diodes has generated a considerable amount of waste electrical equipment (WEE) (Baldé et al., 2017; Gwenzi

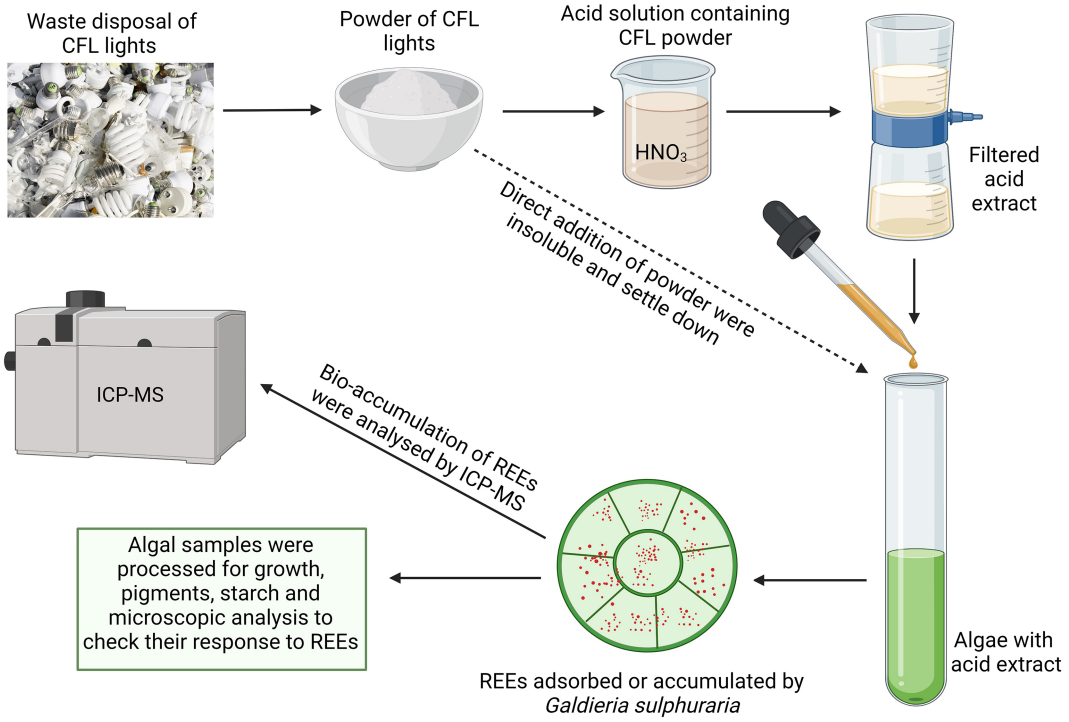

et al., 2018; Pagano et al., 2019). Among the most common elements present in WEE are the REEs yttrium (Y), europium (Eu), and terbium (Tb). These economically important REEs are usually discarded into our environment as wastes, having a consequential effect on the linear flow of goods throughout the economy (Balaram, 2019). Increased demands for REEs, has exerted pressure on industrialized countries to look for alternatives to fulfill their demand in an eco-friendly manner. Bio-removal of WEE containing REEs, and their recycling can have a positive impact, balancing both environmental and economic benefits.

The role of plants, microbes (i.e., bacteria, cyanobacteria, and fungi), and algae as REE accumulators, bio-removers, and potential bio-miners have been studied extensively (Dubey and Dubey, 2011; Qu and Lian, 2013; Pinto et al., 2020; Jalali and Lebeau, 2021). Among these, algae-based bioaccumulation/bio-removal is considered to be one of the most promising methods due to its high efficiency, wide applicability and the low-cost recovery. However, mostly contaminated water, soil or red mud were used as secondary sources of REEs (Pinto et al., 2020; Lima and Ottosen, 2021). Regarding WEE (e.g., CFL lights) as secondary source of REEs, only a few studies have demonstrated the use of microalgae as potential REE accumulators/sorbents or removers (Čížková et al., 2021). However, several studies have been conducted that demonstrate the growth of green and red algae in the presence of a single REE, or waste containing a mixture of REEs (Čížková et al., 2021; Pinto et al., 2021). The growth of green algae *Chlamydomonas reinhardtii*, *Chlorella* sp. or *Arthrospira* sp. improved in the presence of REEs (Liu and Shizong, 1999) whereas, another study showed that due to the presence of multiple REEs in CFL powder, *Galdieria* growth and dry matter accumulation slowed compared to the control (Čížková et al., 2021).

In addition, extensive research has been conducted to investigate heavy metal (HM) bioaccumulation/bioremediation by algae employing different chemical agents and phytohormones. However, the underlying mechanisms controlling the effect of phytohormones on bioremediation are elusive (Piotrowska-Niczyporuk et al., 2012, 2018). Unlike HM bioremediation, fewer studies have been conducted to understand REE bio-removal/bioaccumulation (Pinto et al., 2020; Čížková et al., 2021; Pinto et al., 2021). Literature describing the use of chemical agents commonly employed in bioremediation, or phytohormones that affect the biosorption/bio-removal of REEs are also scarce. This study is the first showing the use of two phytohormones, 6-Benzylaminopurine (BAP - Cytokinin family, known to affect cell division) and 1-Naphthaleneacetic acid (NAA - Auxin family, generally known as growth stimulators) on REE accumulation by the red algae *G. sulphuraria*.

Recently, algae from the extremophile group of cyanidiophyceae, especially the unicellular red alga *Galdieria*, has been proposed as suitable models that have the potential to accumulate or adsorb different REEs (Minoda et al., 2015; Čížková et al., 2019, 2021). *G. sulphuraria* grows under thermo-acidophilic conditions, and inhabits hot sulfur springs, toxic metal-containing and geothermal habitats (Gross et al., 1998; Yoshimura et al., 1999; Reeb and Bhattacharya, 2010; Minoda et al., 2015). The organism is known to thrive over in moderate/high temperatures ranging from 35°C to 56°C (Reeb and Bhattacharya, 2010; Carfagna et al., 2015; Bottone et al., 2019), and pH ranging from 0.2 to 6 (Yoon et al., 2006; Náhlík et al., 2021; Abiusi et al., 2022). Its resistance to toxic metals and REEs is exceptional among other eukaryotic algae, thus it is a suitable organism to achieve bioaccumulation/bio-removal of metals from waste material (Yoshimura et al., 1999; Minoda et al., 2015; Čížková et al., 2021). Unlike other microalgae, *G. sulphuraria* produces highly branched and low molecular weight glycogen as an energy and carbon reserve instead of starch supplying energy for processes related to cell multiplication such as DNA replication, nuclear division, cytokinesis, daughter cell formation and release of autospores (Vítová et al., 2015; Martinez-Garcia et al., 2017). The accumulation of starch during the cell cycle, and its consumption during the cell division in dark phase has been described in several synchronized cultures of

green algae (Brányiková et al., 2011; Vítová et al., 2015). Recently, Náhlík et al. studied the accumulation of glycogen in *G. sulphuraria* throughout the cell cycle following light and dark phases. Results showed that some accumulated glycogen was consumed during cell division (Náhlík et al., 2021). Like other microalgae, *G. sulphuraria* divides by multiple fission and releases 2^n autospores from a single mother cell within one cell cycle (Jong et al., 2021).

One of the important fluorescence parameters followed in photosynthetic microalgae is the F_v/F_m ratio, a valuable bio-indicator for overall photosynthetic performance, indicating maximal photochemical quantum efficiency of photosystem II (PSII). The F_v/F_m index also indicates stress conditions such as temperature, light, pH, nutrient concentration, or toxic metals (Schreiber et al., 1986; Iovinella et al., 2020). The ratio of F_v/F_m differs in photosynthetic organisms from plant to cyanobacteria, in land plants F_v/F_m varies between ~0.75–0.8, and slightly lower values ~0.7 were reported in green algae. However, red algae and cyanobacteria have significantly lower values of F_v/F_m ratio between ~0.5–0.6 and ~0.2–0.4, respectively (Oesterhelt et al., 2007; Iovinella et al., 2020). Like photosynthetic efficiency, photosynthetic pigments are also vulnerable to stress conditions. Until now, the effect of REEs on photosynthetic pigments have not been investigated thoroughly, although research has shown that exposure to Lu^{3+} (lutetium) and Sc^{3+} (scandium) significantly reduced levels of photosynthetic pigments in *Parachlorella kessleri* (Goecke et al., 2017).

In the present study, we describe the effect of a CFL acid extract on a synchronous culture of *G. sulphuraria* throughout the cell cycle. Furthermore, accumulated glycogen and the photosynthetic pigment profile of a synchronously growing and dividing culture were analyzed. This study provides insight into the impact of REEs on the cell cycle of *G. sulphuraria*. The study also determined how efficiently this red alga could accumulate REEs from a CFL extract and the effect of two synthetic plant hormones (BAP and NAA).

Materials and methods

Algal culture and growth conditions

The experimental organism, unicellular red alga *G. sulphuraria* (Galdieri) Merola, 002 was acquired from the Algal Collection of the University "Federico II" of Naples, Italy.[1] In general, algal cells were cultivated photoautotrophically in a Galdieria-nutrient medium (modified Allen medium) prepared to the following final composition of macroelements ($g\,L^{-1}$): 1.31 $(NH_4)_2SO_4$, 0.27 KH_2PO_4, 0.25 $MgSO_4{\cdot}7H_2O$, 0.02 $C_{10}H_{12}O_8N_2NaFe$, 0.14 $CaCl_2{\cdot}2H_2O$, and microelements diluted 500x from the stock solution ($mg\,L^{-1}$): 31 H_3BO_3, 1.25 $CuSO_4{\cdot}5H_2O$, 22.3 $MnSO_4{\cdot}4H_2O$, 0.88 $(NH_4)_6Mo_7O_{24}{\cdot}4H_2O$, 2.87 $ZnSO_4{\cdot}7H_2O$, 1.46 $Co(NO_3)_2{\cdot}6H_2O$, 0.014 $V_2O_4(SO_4)_3{\cdot}16H_2O$, 0.3 $Na_2NO_4{\cdot}7H_2O$, 1.19 KBr, 0.83 KI, 0.91 $CdCl_2$, 0.78 $NiSO_4$, 0.12 CrO_3, 4.74 $Al_2(SO_4)_3K_2SO_4{\cdot}24H_2O$ (all chemicals from Penta, Chrudim, Czech Republic) in distilled water, autoclaved for 20 min. The synchronization of the cultures was carried out by changing the light and dark periods (16 l/8D) according to Náhlík et al. (2021). The culture was cultivated under optimal conditions of pH 3, temperature of 40°C, and light intensity of 350 µmol photons $m^{-2}\,s^{-1}$. The photobioreactors, in the shape of glass cylinders (300 ml) or flat cuvettes (2.5 l), were placed in a thermostatic water bath and illuminated by a panel of dimmable fluorescent lamps (OSRAM DULUX L55 W/950 Daylight, Milano, Italy). Algal culture suspensions were supplied with a gas mixture of air and CO_2 (2% v/v), at a flow rate of 15 L h^{-1}. The experiments were carried out in a batch culture regime under controlled light and temperature conditions.

Preparation of CFL acid extract

Luminophore powder from e-waste of CFL light bulbs was provided by RECYKLACE EKOVUK a.s. (Příbram, Czech Republic). The particle size of CFL powder was 25 µm[3] and it was insoluble in water or Galdieria-nutrient medium. Based on the preliminary study with different acids, acid mixtures, and their concentrations, the best solubility of CFL particles was observed in 10% HNO_3 acid. To prepare the CFL acid extract with a final concentration of 40 µg mL^{-1}, 4 g of CFL powder was extracted into 100 ml of 10% HNO_3. The solution was shaken on a horizontal shaker (at 150 rpm) for 1 h and then extracted at room temperature for 12 h, followed by 3 h of shaking. The suspension was centrifuged at 4000 rpm for 3 min and the supernatant was filtered through a 0.45 µm filter to avoid the remaining solid particles. The resulting clear CFL acid extract solution has an approximate pH of 0.5. The stock solution was used in all experiments.

CFL acid extract treatment

To study the effect of CFL extract on various parameters of the cell cycle and the accumulation of REEs, 4% CFL acidic extract (v/v) was used to treat the algal culture. After adding the CFL extract to nutrient medium, the pH dropped to 2, and was adjusted with approximately 0.5 ml of NH_4OH to pH 3. For CFL treatment, the synchronous cultures of *G. sulphuraria*, at an initial concentration of $1{\times}10^6$ cells L^{-1}, were cultivated in 4% of CFL extract for 24 h. Samples of the algal culture were collected at desired time intervals for further analyses. Along with CFL–treated culture, a control (untreated culture) was also inoculated with the same initial culture concentration and incubated for 24 h.

Plant hormone treatment

To study the effect of hormones on REEs accumulation, one set of asynchronous cultures of *G. sulphuraria* was cultivated with CFL and hormones for 24 h. For this study two synthetic plant hormones, 6-Benzylaminopurine (BAP-Cytokinin family) and 1-Naphthaleneacetic acid (NAA-Auxin family) (Sigma-Aldrich) were used at a final concentration of 5 mg L^{-1} for this study. At the end of the experiment, cultures with and without plant hormones were harvested by centrifugation (3,000 rpm, 5 min), freeze dried and analyzed by ICP-MS.

Dry matter and doubling time determination

Dry matter was determined from 5 ml of algal suspension centrifuged at 4000 rpm for 5 min in dried and pre-weighed 5 ml test tubes. The pellet was dried at 105°C for 24 h and weighed on a Sartorius TE214S-0 CE analytical balance.

1 http://www.acuf.net/index.php?lang=en

Doubling time (DT) was calculated for both the control and treated cultures of *G. sulphuraria* based on dry matter (DM) according to the equation $DT(h) = \frac{(T_t - T_0) * \log(2)}{(\log(DM_t) - \log(DM_0))}$, where T_t is the time of the end of the light phase, T_0 is the starting time, and DM_t is the value of dry matter at T_t and DM_0 is the value of dry matter at T_0.

Pigment analysis

To determine the content of chlorophyll *a* (Chl *a*) and carotenoids (car), 10 ml of homogenized suspension of both the control and CFL–treated cultures were centrifuged at 4000 rpm for 5 min. Harvested pellets were suspended in 1 ml of phosphate buffer (containing 0.1 M KH_2PO_4: 0.1 M $Na_2HPO_4{\cdot}12H_2O$, 1:9; pH 7.7) and 10 µg of $MgCO_3$. The pellets were then each mixed with 500 µl of 0.75–1.00 mm glass beads (P-LAB, Prague, Czech Republic) and vortexed for 5 min to break the cell walls. For pigment extraction, 4 ml of 100% acetone was added, mixed well, and centrifuged at 4000 rpm for 5 min. After the first round of extraction, the supernatant was transferred to a calibrated tube with a stopper and placed in a dark block. The extraction process was repeated with 80% acetone and the supernatant was transferred to the same calibrated tube. The final volume of extract was made up to 10 ml using 80% acetone. The absorbance of the solution was recorded at 750, 664, 647, 470, and 450 nm by UV-1800 spectrophotometer, Shimadzu Corporation (Kyoto, Japan). The content of chlorophyll *a* and carotenoids were calculated according to Wellburn (1994).

Phycobiliproteins were extracted in 10 ml of homogenized control and CFL–treated culture samples. Each culture was centrifuged at 4000 rpm for 10 min at room temperature and the pellet was washed twice with distilled water. Finally, the culture was re-suspended in 20 mM acetate buffer (pH 5.1) containing 40 mM NaCl and 0.02 M sodium azide, followed by bead beating and repeated freeze-thawing until the phycobiliproteins were released into the supernatant. The collected supernatant was measured in a UV–VIS spectrophotometer (Shimadzu 1800-UV, Shimadzu Corp., Japan). The estimation of phycobiliproteins, expressed in mg mL^{-1}, was carried out by following the equations of Bennett and Bogorad (1973) and Johnson et al. (2014). All chemicals were supplied by Penta (Chrudim, Czech Republic).

Photosynthesis evaluation

Photosynthetic activity was evaluated by fluorimeter as the quantum yield (F_v/F_m). Two milliliters aliquots were withdrawn from the culture and placed into 10 × 10-mm plastic cuvettes for 30 min in the dark. Quantum yield was measured using an AquaPen-C 100 PAM fluorimeter (Photon Systems Instruments, Drasov, Czech Republic).

Determination of glycogen content

Glycogen content was determined by the anthrone method (McCready et al., 1950) according to the modified protocol of Brányiková et al. (2011). Briefly, 10 ml algal samples were harvested by centrifugation at 3000 rpm for 3 min and the cell pellet was stored at −20°C. 250 µl zirconium beads (0.7 mm diameter) and 500 µl dH_2O were added to thawed samples and vortexed (Vortex Genie 2, Scientific Industries, Inc., Bohemia, NY, United States) for 5 min at 3,200 rpm for cell breakage. For depigmentation of algae, 1 ml of 80% ethanol was added to the sample then vortexed and incubated at 68°C for 15 min in a water bath. This process was repeated 3–4 times until the pellet was clear (green color free). The glycogen-containing cell pellets were hydrolyzed with 1.5 ml of 30% perchloric acid for 15 min at room temperature, then centrifuged and supernatants were collected into pre-prepared calibration test tubes. This process was repeated twice more, and the extracts were combined and made up to 5 ml using 30% $HClO_4$. The colorimetric reaction was then carried out by mixing 500 µl of ice-cold extract with 2.5 ml of anthrone reagent (2 g of anthrone in 1 l of 72% (v/v) ice-cold sulphuric acid). The mixture was boiled at 100°C for 8 min followed by cooling and quantification at 625 nm (A_{625}) using a Shimadzu UV-spectrophotometer UV-1800 (UV-1800, Shimadzu, Kyoto, Japan). The same procedure was followed for the blank (500 µl of 30% $HClO_4$) and standard tubes (500 µl of glucose (100 mg L^{-1}) in 30% $HClO_4$). Glycogen calibration was carried out simultaneously using glucose as the standard. To obtain the calibration curve for glycogen determination, the values measured for glucose were multiplied by 0.9. The data were expressed as picograms (pg) of glycogen per cell.

Confocal microscopy

Confocal images of treated and control cells were captured with an inverted Zeiss LSM 880 laser scanning confocal microscope (Carl Zeiss Microscopy GmbH, Oberkochen, Germany) equipped with a Plan-Apochromat 63x/1.4 NA Oil DIC M27 immersion objective. SYBR-Green was excited by Argon laser 488 nm (laser power 0.03%), its emission was captured by GaAs-detector at wavelengths 499–571 nm, Gain 750. Likewise, chlorophyll auto-fluorescence was excited by Argon laser 488 nm (laser power 0.15%) and detected at 695–759 nm (PMT detector, using photon counting mode). This track was on top of that used to create T-PMT signal (transmission) using Gain 370. The pinhole for this excitation wavelength was kept at 69 µm diameter. MBS was chosen 488 and pixel dwell time was given 16.38 µs. The images were then processed using ImageJ software.

Statistical analysis

All experiments were performed in three biological replicates ($n = 3$). The presented results are the averages and standard deviations from all three replicates. The data statistics analysis was generated using the Real Statistics Resource Pack software (Release 8.4) for MS Excel 2013. Copyright (2013–2021) Charles Zaiontz[2] (accessed on 3 January 2023). To quantify the relationship between predictor variables (time, treatment) and a response variable (concentration of pigments, or concentration of glycogen, or F_v/F_m ratio) multiple linear regression model was used. The fitted regression model was: ß1 + (ß2*time) + (ß3*treatment) + (ß4*time^2) + (ß5*(time*treatment)), where the coefficient values correspond to predictors: ß1 - Intercept, ß2 - Time, ß3 - Treatment, ß4-Time^2, ß5 – Time*Treatment. The comparison of individual REE concentration levels at different time

2 https://www.real-statistics.com/free-download/real-statistics-resource-pack/

points or between experimental treatments (CFL, CFL + hormones) was performed using the one-way ANOVA test and Tukey's HSD test. A value of $p < 0.05$ was considered significant.

Quantitative REE analysis by ICP-MS

Samples of CFL alone and CFL-treated algal biomass were digested with 30% H_2O_2 and 67% HNO_3 (Merck, Suprapure) in a PTFE microwave oven (MLS1200 MEGA, Gemini bv, Apeldoorn, The Netherlands) at 250–600 W for 20 min. Quantitative analysis of REEs was performed using an Elan DRC-e (Perkin Elmer, Concord, ON, Canada) which is equipped with a concentric PTFE nebulizer and cyclonic spray chamber. Algal samples were passed through a 0.45 µm nylon syringe filter (Millipore, Molsheim, France) and diluted 1:10 with distilled water. Values were expressed as micrograms per gram dry weight (µg g^{-1} DM).

Results

Before conducting the experiments and because CFL was extracted into 10% HNO_3, the effect of 10% HNO_3 on a synchronous culture of *G. sulphuraria* was studied. Results of this preliminary study showed that there was no negative effect of 10% HNO_3 on the cell shape, size, or growth of this organism (Supplementary Figures S1, S2).

Effect of CFL on growth of *Galdieria sulphuraria*

Growth of the control culture of *G. sulphuraria* and the culture treated with CFL extract was expressed as dry matter in mg mL^{-1} (Figure 1). Our results showed a progressive increase in dry matter of both control and treated cultures up to 16 h (light regime), after which, a decline was observed due to a light limitation. The control culture of *G. sulphuraria* reached a dry matter content of 0.42 mg mL^{-1} during the light phase whereas the culture treated with CFL extract achieved only 0.30 mg mL^{-1} dry matter. The loss of dry matter from 0.42 mg mL^{-1} to 0.28 mg mL^{-1} in the control culture and from 0.30 mg mL^{-1} to 0.17 mg mL^{-1} in CFL–treated culture during the dark phase (Figure 1, dark phase) could be due to losses by respiration (night biomass loss). The calculated mass doubling time (see Methods for the equation) was 10.09 h ± 0.30 for the control culture and 12.10 h ± 0.48 for the culture treated with CFL extract.

The effect of CFL on photosynthetic pigments

The effect of CFL extract on chlorophyll *a*, carotenoids, and phycocyanin contents was observed at 4 hourly intervals over the period from 0 to 24 h synchronous culture. Figure 2 shows the comparative effect of CFL–treated and control cultures on pigment content. Results showed that all three photosynthetic pigments progressively increased with increasing duration of the experiment, although CFL–treated cells showed lower pigment levels than the control culture. Figure 2A shows the synthesis of chlorophyll *a*, which was affected by CFL treatment throughout the experiment. At the end of the light phase (16 h), the Chl *a* content was recorded as 3.0 mg L^{-1} in the control culture whereas, in

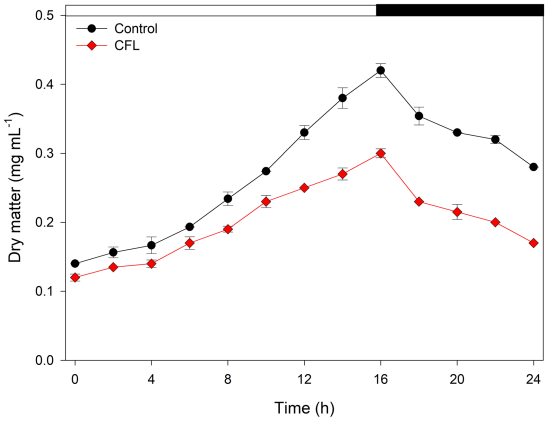

FIGURE 1
Growth of synchronous culture of *Galdieria sulphuraria* in control (black circles) and CFL–treated (red diamonds) medium, at pH 3, a light intensity of 350 µmol photons m^{-2} s^{-1} and a temperature of 40°C, expressed as dry matter (DM) in µg mL^{-1}. The dark phase is indicated by the black bar above the graph. The data are plotted as means of biological triplicates. The error bars represent standard deviations (±SD) and are shown when larger than the symbol size.

the CFL–treated culture, Chl *a* content was only 2.2 mg L^{-1}. This loss in chlorophyll content could be due to CFL extract stress on the algae. In contrast, carotenoids, which are known to play a role in defense of algae against stress, increased till 4 h to 110 mg L^{-1} under CFL treatment compared with 78 mg L^{-1} in the control culture (Figure 2B). Later, the trend of values reversed, and at 16 h (end of the light phase), the CFL–treated culture yielded 209 mg L^{-1} carotenoids as compared to 270 mg L^{-1} in the control culture (Figure 2B). Like chlorophyll *a*, phycocyanin content also increased progressively throughout the experiment. The control culture showed a slightly higher level of phycocyanin at 16 h, i.e., 191 mg L^{-1} as compared to 176 mg L^{-1} in the CFL–treated culture (Figure 2C). Interestingly as compared to chlorophyll and carotenoids, phycocyanin was the pigment least affected by CFL acid extract stress.

Multiple linear regression was used to test if time (hours of cultivation) and treatment (control vs. CFL) significantly predicted the concentration of pigments (chlorophyll *a*, carotenoids, and phycocyanin) in the algal biomass (Figure 2). For fitted regression model see Methods. The overall regression was statistically significant for Chl *a* ($R^2 = 0.97$, $F(4, 9) = 132.56$, $p = 5.43E\text{-}08$), carotenoids ($R^2 = 0.94$, $F(4, 9) = 61.55$, $p = 1.55E\text{-}06$), and also for phycocyanin ($R^2 = 0.97$, $F(4, 9) = 125.25$, $p = 6.98E\text{-}08$). Both time and time^2 significantly predicted the concentration of all three pigments. Treatment alone did not significantly predict their concentration, however, the interaction term time*treatment did significantly predict the concentration of chlorophyll *a*, and carotenoids. The treatment influence was therefore significantly time-dependent. There was no time-dependency for phycocyanin, and its concentration in both cultures was not significantly different. For β coefficients and corresponding *p*-values see Supplementary Table S1.

The effect of CFL on photosynthesis efficiency (F_v/F_m)

In the present study photosynthetic performance was determined as quantum yield (ratio F_v/F_m) which is the parameter commonly reflecting reduced function or impairment of the PSII

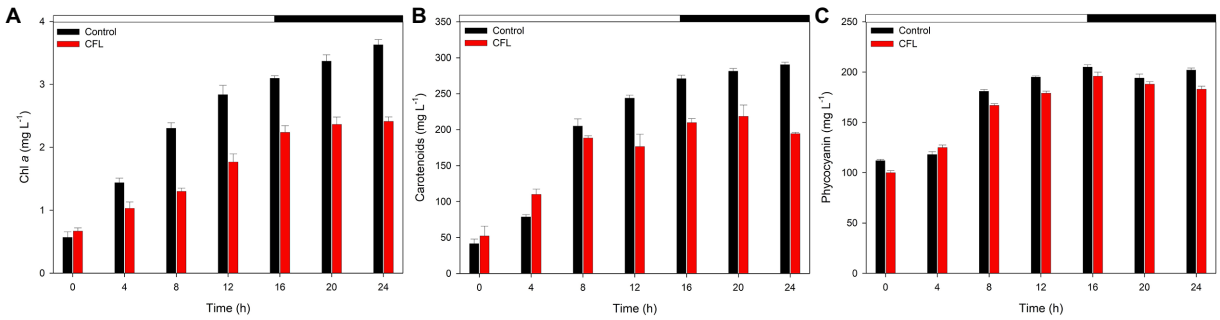

FIGURE 2
Photosynthetic pigments in synchronous control (black bar) and CFL–treated (red bar) *Galdieria sulphuraria* cultures, expressed as mg L^{-1} **(A)** chlorophyll *a*, **(B)** carotenoids, **(C)** phycocyanin. The dark phase is indicated by the black bar above the graph. The data are plotted as means of biological triplicates. The error bars represent standard deviations (±SD). For details of statistical analysis (multiple linear regression) see Supplementary Table S1.

reaction centers. At the beginning of the experiment, the F_v/F_m ratio was recorded as 0.58 in the control culture and 0.55 in the CFL–treated culture (Figure 3). With progression of the cell cycle, at 6 h, the F_v/F_m ratio fell to its minimum, i.e., 0.36 and 0.17 in the control and CFL–treated cultures, respectively, (light phase of Figure 3). This decrease in F_v/F_m in the control culture recovered to almost its initial value, i.e., 0.53–0.56 at 18–24 h during the dark phase. The F_v/F_m ratio in the CFL–treated culture recovered to a value of approximately 0.45, which is slightly lower than its original value (Figure 3, dark phase).

Multiple linear regression was used to test if time (hours of cultivation) and treatment (control vs. CFL) significantly predicted the F_v/F_m ratio in the algal biomass (Figure 3). For fitted regression model see Methods. The overall regression was statistically significant ($R^2 = 0.65$, $F(4, 21) = 12.92$, $p = 1.84E\text{-}05$). Both time and time^2 significantly predicted the F_v/F_m ratio. Treatment alone significantly predicted the F_v/F_m ratio, however, the interaction term time*treatment did not. For β coefficients and corresponding *p*-values see Supplementary Table S1.

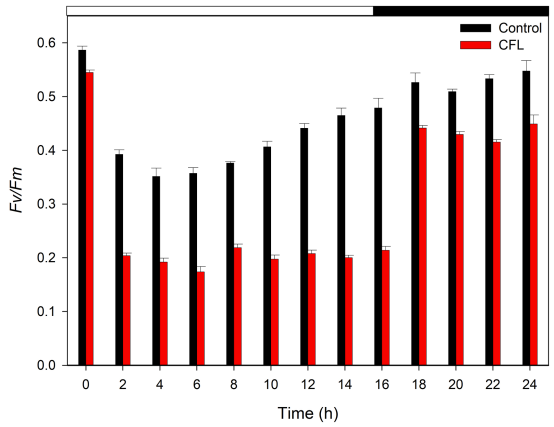

FIGURE 3
F_v/F_m ratio of synchronous control (black bar) and CFL–treated (red bar) *Galdieria sulphuraria* cultures, showing the photochemical maximum quantum efficiency of PSII. The dark phase is indicated by the black bar above the graph. The data are plotted as means of biological triplicates. The error bars represent standard deviations (±SD). For details of statistical analysis (multiple linear regression) see Supplementary Table S1.

The effect of CFL on glycogen content

The accumulation of glycogen in *G. sulphuraria* was followed throughout the cell cycle and samples were withdrawn every 2 h from both control and CFL–treated cultures (Figure 4). The net content of glycogen in both cultures progressively increased from the beginning of the cell cycle, showing the highest content, i.e., 8.0 pg. $cell^{-1}$ in the control and 5.11 pg. $cell^{-1}$ in the CFL–treated culture, at 16 h (at the end of the light phase). This represents and approximately 8-fold increase in glycogen in the control culture and 5.5-fold increase in the CFL-treated cells during the light phase; around 1/3 of the glycogen content was consumed during the dark phase in both cases (Figure 4).

Multiple linear regression was used to test if time (hours of cultivation) and treatment (control vs. CFL) significantly predicted the concentration of glycogen in the algal biomass (Figure 4). For fitted regression model see Methods. The overall regression was statistically significant [$R^2 = 0.92$, $F(4, 21) = 75.24$, $p = 3.84E\text{-}12$]. Regarding the β coefficients and corresponding p-values in the Supplementary Table S1, it can be concluded that all predictor variables significantly predicted the concentration of glycogen. The treatment influence was significantly time-dependent, and the difference in glycogen concentration between control and CFL-treated culture was statistically significant.

Course of the cell cycle

In this study, cell cycle development of *G. sulphuraria* was assessed by confocal microscopy using SYBR Green dye for nuclear staining (Figure 5). At the beginning of the cell cycle, during the light phase of the experiment, the single-nuclei daughter cells of both control (Figure 5A) and CFL–treated cultures (Figure 5B) were released from their mother cell walls (Figure 5A – 0 h). The cells started to grow in both cultures (Figure 5A – 8 h). In the control culture, chloroplasts and nuclei started to divide into two at 12 h (Figure 5A – 12 h). Protoplast division into two occurred at 14 h (Figure 5A – 14 h). At 16 h of the cell cycle, cells started to divide into four (Figure 5A – 16 h) which included the second chloroplast, nuclei, and protoplast fissions. At 24 h of the cell cycle, all the cells finished the division into four daughter cells, which remained by the mother cell wall (Figure 5A – 24 h). CFL-treated cells (Figure 5B) followed the same time course of the cell cycle as control cells, with the exception that the first cell division was delayed by 1–2 h (Figure 5B 12 h, 16 h).

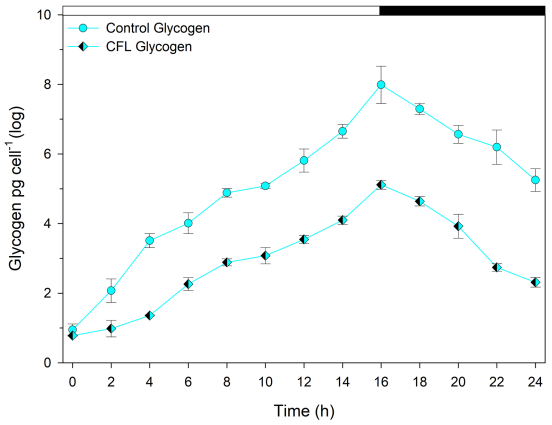

FIGURE 4
Concentration of total glycogen in synchronous *Galdieria sulphuraria* cultures. Control culture (cyan diamonds), CFL–treated culture (cyan-black diamonds). The dark phase is indicated by the black bar above the graph. The data are plotted as means of biological triplicates. The error bars represent standard deviations (±SD) and are shown when larger than the symbol size. For details of statistical analysis (multiple linear regression) see Supplementary Table S1.

The effect of CFL on accumulation of REEs in algal biomass

ICP-MS analysis was conducted to observe the accumulation of REEs by a synchronous culture of *G. sulphuraria*. REE levels in the CFL acid extract were also analyzed using ICP-MS. The most abundant elements in the extract were La, Y, and Ce followed by Tb, Eu and Gd, respectively (Table 1). The results showed that specific REEs accumulated differently at different phases of the cell cycle. For example, at 2 h of the cell cycle (growth phase), Y and Eu levels were recorded as 42 and 2.7 $\mu g\,g^{-1}$ DM respectively, which increased to 803 $\mu g\,g^{-1}$ and 145 $\mu g\,g^{-1}$ DM, respectively, at 10 h of the cell cycle (commitment point before the first division) (Figure 6). In contrast, at 2 h of the cell cycle, cerium (Ce) and La levels were 101 and 35 $\mu g\,g^{-1}$ DM respectively, which drastically decreased to 2 and 10 $\mu g\,g^{-1}$, respectively, at 24 h of the cell cycle (end of the cell cycle; cell division finished) (Figure 6). The most abundant lanthanides accumulated by *G. sulphuraria* were Y followed by Eu, La, and Ce (Figure 6). However, the uptake of REEs was not related to their abundance in the CFL acid extract (compare Figure 6; Table 1). There is an apparent increase in the content of Y and Eu in the biomass during the cell cycle, while a decrease of La and Ce was detected. Although Tb and gadolinium (Gd) were quite abundant in the CFL acid extract, their accumulation was less than 5 $\mu g\,g^{-1}$ DM throughout the cell cycle (Table 1; Figure 6). This suggests a concentration-independent accumulation of REEs by *G. sulphuraria*.

A one-way ANOVA was performed to compare the effect of time (different phases of the cell cycle-2 h, 10 h, 24 h) on the concentration of individual REEs in the biomass of *G. sulphuraria*. The analysis revealed a statistically significant difference in the concentration of individual REEs between at least two groups, for statistical values see Supplementary Table S2A. Tukey's HSD test for multiple comparisons found that the mean value of the concentration of individual REEs was significantly different between the groups marked by asterisks in the Supplementary Table S2B. Overall, the concentration of all elements differed significantly between 2 h and 10 h and also between 2 h and 24 h, with the exception of two elements La and Ce, where the difference in their concentration was significant between all groups (2 h, 10 h, 24 h).

The effect of plant hormones on REEs accumulation

Two synthetic plant hormones, i.e., BAP and NAA, were tested to determine their effect on the accumulation of REEs from the CFL acid extract. Before conducting this experiment, we studied the effect of these

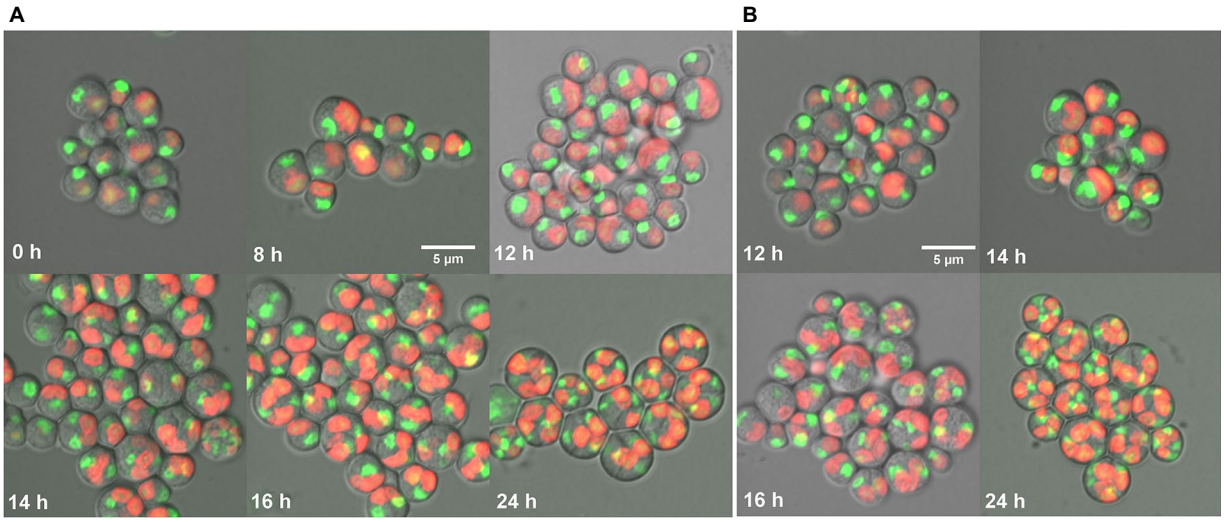

FIGURE 5
Fluorescent photomicrographs of cells of *Galdieria sulphuraria* under control conditions **(A)**, and in a CFL–treated culture **(B)**. Control culture: daughter cells - 0h, growing single cells - 8h, 1st division of chloroplast and nuclei - 12h, division into 2 cells - 14h, division into 4 cells, protoplast division apparent - 16h, four daughter cells growing inside the original mother cell wall before their release - 24h. CFL–treated culture: chloroplast and nuclei started to divide - 12h, apparent division into 2 cells - 14h, started division into 4 cells and protoplast fission apparent - 16h, four daughter cells growing inside the original mother cell wall before their release - 24h. Nuclei in green were stained by SYBR Green I, chloroplasts in red - autofluorescence of chlorophyll. The bar represents 5 µm.

TABLE 1 Concentration of individual REEs in a CFL acid extract.

REE	μg g^{-1}±SD
Y	7,019 ± 280.76
La	10,387 ± 259.68
Ce	6,176 ± 222.34
Pr	0.3 ± 0.009
Nd	0.5 ± 0.0195
Sm	0.1 ± 0.004
Eu	594 ± 17.82
Gd	234 ± 5.85
Tb	2,929 ± 244.11
Dy	1.6 ± 0.08
Tm	0.2 ± 0.007
Yb	2.6 ± 0.065
Lu	39 ± 3.86

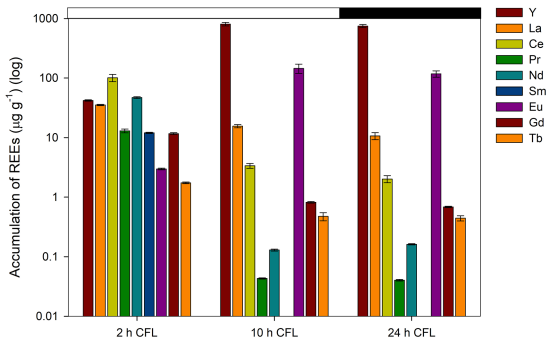

FIGURE 6
Accumulation of individual REEs in synchronous cultures of *Galdieria sulphuraria* under CFL–treatment expressed as concentration in μg g^{-1}. The Y axis has a logarithmic scale. The X axis represents three different phases of the cell cycle (growth phase, commitment point, end of the cell cycle). The dark phase is indicated by the black bar above the graph. The error bars represent standard deviations (±SD). For details of statistical analysis (one-way ANOVA, Tukey's HSD) see Supplementary Table S2.

two hormones on cell shape, size, and growth of *G. sulphuraria*. Results showed that these hormones did not affect these parameters (Supplementary Figures S3, S4). The results showed that both hormones dramatically affected REE accumulation, but NAA had the more significant effect. The asynchronous culture of *G. sulphuraria*, after 24 h of growth, accumulated 3,596 and 319 μg g^{-1} DM of Y and Eu respectively, which increased to 6,556 (1.82-fold) and 451 (1.4-fold) μg g^{-1} DM, respectively, in the presence of NAA (Figure 7A). BAP also increased the accumulation of Y and Eu to 3,870 and 298 μg g^{-1} DM, respectively, (Figure 7A). Figure 7B shows the accumulation of La, Ce, Gd and Tb from the same experiment. NAA increased the accumulation of La from 19 to 27 μg g^{-1} DM, Ce from 7 to 10.5 μg g^{-1} DM, Gd from 20 to 29 μg g^{-1} DM and Tb from 16 to 21.5 μg g^{-1} DM (Figure 7B). However, BAP did not increase the accumulation of La, Ce, Gd, and Tb like Y and Eu (compare BAP in the Figures 7A,B). Compared to BAP, NAA had a more pronounced effect on the accumulation of REEs.

A one-way ANOVA was performed to compare the effect of treatment (CFL extract alone, CFL + BAP hormone, CFL + NAA hormone) on the concentration of individual REEs in the biomass of *G. sulphuraria*. The analysis revealed that there was a statistically significant difference in the concentration of individual REEs between at least two groups, for statistical values see Supplementary Table S3A. Tukey's HSD test for multiple comparisons found that the mean value of the concentration of individual REEs was significantly different between the groups marked by asterisks in the Supplementary Table S3B. Altogether, valid for all elements, there was no significant difference in concentration of individual REEs in the biomass treated by CFL alone and CFL+ BAP. On the other hand, the concentration of REEs in the biomass treated by CFL + NAA was significantly different in comparison with the other two groups (CFL alone and CFL + BAP).

Discussion

The extremophilic red alga *G. sulphuraria* was selected for the present study due to its ability to grow in a range of diverse habitats including those having thermophilic, acidophilic, halophilic and toxic metal conditions (Oesterhelt et al., 2007; Weber et al., 2007). The growth of cyanobacteria and algae in the presence of REEs has been demonstrated previously. Dubey and Dubey reported on the growth of three cyanobacteria, *Phormidium*, *Oscillatoria* and *Lyngbya*, in presence of red mud (Dubey and Dubey, 2011). Similarly, the growth of 6 living macroalgae species, i.e., *Ulva lactuca, Ulva intestinalis, Fucus spiralis, Fucus vesiculosus, Osmundea pinnatifida* and *Gracilaria* sp. in laboratory-prepared seawater solution containing REEs (Y, La, Ce, praseodymium (Pr), neodymium (Nd), Eu, Gd, Tb, dysprosium (Dy)) has been studied (Pinto et al., 2021). However, until now, only a few studies have been conducted to evaluate the growth and accumulation of REEs present in waste luminophores. Interestingly, this is the first study that examines the effect of a CFL acid extract on growth and the bioaccumulation of REEs present in electronic waste of CFL lights. Prior to this study, Čížková et al., used the unicellular red alga *Galdieria phlegrea* to examine the growth and bioaccumulation of REEs from luminophore powder (of two different sources such as energy saving light bulbs - CFL, and fluorescent lamps - FL) (Čížková et al., 2021). The findings of the present study confirmed that the growth of *G. sulphuraria* was optimal under the acidic conditions (Supplementary Figures S1, S2). Thus low growth (dry matter) observed in the presence of the CFL acid extract compared to the control culture (Figure 1) could have been due to a negative effect of REEs.

The biomass loss recorded in the dark phase of both control and treated cultures (Figure 1, dark phase) was due to the phenomenon of night biomass loss or respiration loss. This phenomenon is an essential property of photosynthetic algae, and acts as a tax on day biomass gains; approximately 30% of the algal biomass produced during the day can be lost at night (Guterman et al., 1989; Hu et al., 1998; Edmundson and Huesemann, 2015). Edmundson and Huesemann, studied night biomass loss in three potential commercial biomass-producing algal strains, *Chlorella sorokiniana*, *Nannochloropsis salina* and *Picochlorum* sp. They reported that specific night biomass loss rates were highly variable, and varied between −0.006 and −0.59 μ_{dark} day^{-1} (Edmundson and Huesemann, 2015). The result also showed that night biomass loss was species-specific and influenced by environmental conditions such as culture temperature and light intensity prior to and during the dark phase. The night biomass loss was positively corelated with increasing cultivation temperature (Torzillo et al., 1991; Edmundson and

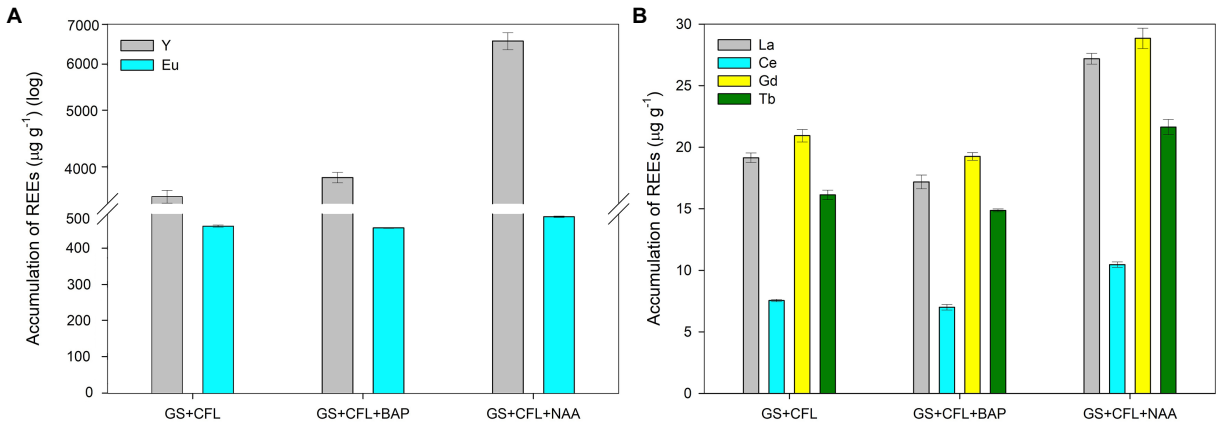

FIGURE 7
Effect of plant hormones NAA and BAP on the accumulation of individual REEs in *Galdieria sulphuraria* under CFL treatment. **(A)** Y and Eu accumulation following NAA and BAP treatments, and **(B)** La, Ce, Gd and Tb accumulation under NAA and BAP treatments. Expressed as concentrations in µg g^{-1}. The error bars represent standard deviations (±SD). For details of statistical analysis (one-way ANOVA, Tukey's HSD) see Supplementary Table S3.

Huesemann, 2015). Given the high optimal cultivation temperature (40°C) of *G. sulphuraria*, loss of biomass during the dark phase was not surprising.

All three photosynthetic pigments increased with progression of the cell cycle in both control and CFL–treated cultures (Figure 2). However, the CFL–treated culture showed reduced levels of Chl *a* as compared to the control, probably due to adverse effects of REEs present in the CFL acid extract (Figure 2A). A negative effect of abiotic stresses on photosynthetic pigments of algae and cyanobacteria has also been reported (Sun et al., 2014; Fu et al., 2020). In the present experiment, the phycocyanin was least affected pigment by CFL acid stress (Figure 2C). The reason could be a high stability of phycocyanin of extremophilic *G. sulphuraria* which was significantly more stable compared to phycocyanin of common cyanobacteria *Spirulina platensis* (Wan et al., 2021). All the members of cyanidiophyceae were considered as best organisms for the production of stable phycobiliproteins (Carfagna et al., 2018; Ferraro et al., 2020). Regarding carotenoids, their function also comprises a defense mechanism to mitigate the damaging effects of stress in photosynthetic organisms (Shi et al., 2020; Potijun et al., 2021). Microalgae respond to an increased exposure to dissolved metals by accumulating carotenoids as antioxidant compounds (Gauthier et al., 2020). In the present study, carotenoid content increased during the initial 4 h of the cell cycle (Figure 2B), probably to mitigate the stress caused by prime accumulation of REEs (Figure 6; 2 h) in the CFL–treated culture. Nonetheless, due to increased accumulation of certain REEs (e.g., Y, Eu) with the progression of the cell cycle (Figure 6; 10 h, 24 h) and due to their toxicity, carotenoids were not able to cope with this stress and levels began to decrease (Figure 2B). It is known that under acute metal stress the antioxidant capacity of microalgae can be depleted (Pinto et al., 2003). Similarly to this study, a selenium (Se) concentration of up to 75 mg L^{-1} increased both the chlorophyll and carotenoid contents in *Chlorella vulgaris*; a higher concentration (>75 mg L^{-1}) of Se caused a significant decline in the overall content of carotene and chlorophyll *a* (Sun et al., 2014). This result showed that if the level of stress was higher, then no defense mechanism of the cell could protect it. Similarly, Cheng et al., showed that an increasing concentration and exposure time to cadmium (Cd) can cause a decline in Chl *a*, Chl *b* and carotenoids in *C. vulgaris* (Cheng et al., 2016). Like other metal stresses, photosynthetic pigments of *Trachydiscus minutus* and *Parachlorella kessleri* were evaluated after exposure to several single REEs and monazite (Goecke et al., 2017). Results showed that pigment content was variable according to the element and algal species used.

The F_v/F_m ratio signifies the maximum potential quantum yield of photosystem II, once all the reaction centers are exposed. It is used as an indicator of stress on PSII. Under stress conditions, the photosynthetic efficiency of PSII is reduced as the cell activates all photo-protective mechanisms. The determined starting values of F_v/F_m ratio (0.58; 0.55) are typical for red algae (Oesterhelt et al., 2007; Iovinella et al., 2020), and are not comparable with green algae or plants due to a fluorescence interference of phycocyanin present in red algae. Our results showed that both the control and CFL–treated cultures expressed a fall in the F_v/F_m ratio at the initial hour of the experiment, which could be due to sudden light exposure after a long (8 h) dark phase (Figure 3). Comparable F_v/F_m values and pattern were determined during the cell cycle of *G. sulphuraria* treated with red mud extract (Náhlík et al., 2022). Fu et al. also observed a similar pattern in *Galdieria partita*, where the F_v/F_m value started to decrease rapidly within 1 h of high light exposure (Fu et al., 2020). In our study, after the 1st h of incubation, the control culture began to adapt to the new condition and eventually recovered significantly during the dark phase of the cell cycle. Nevertheless, CFL–treated cells were unable to recover significantly during the light phase of the experiment due to simultaneous light and CFL stress (Figure 3). Likewise, the maximum photochemical quantum yield (F_v/F_m) of the PSII reaction center decreased under La exposure in *D. quadricauda* (Ashraf et al., 2021). However, in *G. sulphuraria,* high light conditions stimulated cell growth and dry matter in both control and CFL–treated cultures. Recently, Kselíková et al., studied the effect of two different concentrations of deuterated water and three different light intensities on the F_v/F_m ratio in *C. reinhardtii* and *D. quadricauda*. They observed reduced F_v/F_m ratios with increasing light intensity and the concentration of deuterated water (Kselíková et al., 2022). The studies by Kselíková et al., and Ashraf et al., support results observed in the present study showing that increasing stress can reduce the photosynthetic efficiency of PSII (Ashraf et al., 2021; Kselíková et al., 2022).

Glycogen synthesis exactly followed the pattern of dry matter accumulation throughout the cell cycle in both control and CFL–treated cultures. Around 20–30% of the glycogen content produced in the light phase was consumed during the dark phase (Figure 4). Náhlík et al.

observed a similar pattern of glycogen synthesis in synchronized cultures of *G. sulphuraria* (Náhlík et al., 2021). So far, the accumulation of glycogen during the cell cycle in *Galdieria* has not been studied. However, the consumption of glycogen during cell division was comparable to consumption of starch during the cell cycle in green algae (Vítová et al., 2015).

The algal cell cycle is associated with the nature of algal species and growth conditions. In the present study, the control culture of *G. sulphuraria* attained its 1st division at 12 h and 2nd at 16 h of the cell cycle (Figure 5A). Under the same growth conditions, *G. sulphuraria* attained the first cell division into two cells at 12 h and the second division into four cells at the 16th h of the cell cycle (Náhlík et al., 2021). Although, CFL–treated cells showed a 1–2 h delay in cell division which could be a toxicity adaptation time, eventually they completed their second division within the time course of the cell cycle (Figure 5B). At the end of the cell cycle (24 h of experiment) all cells had divided into four daughter cells in both control and CFL–treated cultures, but not released from the mother cell wall (Figures 5A,B). The 2 h shift was also confirmed by the calculation of the mass doubling time being about 10 h in the control culture and 12 h in the CFL treated culture. Although the cells finished the division to four in the CFL treated culture, the biomass gain was lower implying the daughter cell size had to be smaller (compare Figures 1, 5, 24 h). In contrast to *Cyanidioschyzon*, in *Galdieria* and *Cyanidium*, the divided cells (autospores) were surrounded by the mother cell wall before hatching (Jong et al., 2021). There was also a correlation between the number of following cell divisions and commitment cell size in cyanidialean red algae, including *G. sulphuraria*. The delayed cell division of the CFL–treated culture could be due to slower growth for cells to reach commitment size, as compared to the control culture (Jong et al., 2021). However, CFL–treated cells also finished the 2nd division during the dark phase of the 24 h cell cycle. Similarly, *Pseudokirchneriella subcapitata*, a freshwater alga was exposed to different metals, i.e., cadmium (Cd), chromium (Cr) and copper (Cu), and their growth, cell volumes, and cell divisions were investigated over a period of 72 h (Machado and Soares, 2014). Results showed that the highest metal concentrations of Cr(VI) and Cu(II) arrested cell growth before the first nuclear division whereas Cd(II) arrested the cell after the second nuclear division but before the release of autospores from the mother cell wall (Machado and Soares, 2014). This variable impact of metals on the cell cycle of algae suggests that different metals trigger different toxicity mechanisms.

In the present study, REE accumulation was concentration-independent and highly selective with the progression of the cell cycle (Figure 6; Table 1). In *G. sulphuraria*, the accumulation of single REEs was not concentration dependent, e.g., the concentration of La and Ce was very high in the CFL acid extract, however the accumulation of Y and Eu was greater than the accumulation of La and Ce (Figures 6, 7). The increased or decreased metal concentration in cells at different phases of the cell cycle could be due to the selective behavior of *G. sulphuraria* towards individual REEs. If the cells were not able to tolerate toxicity of several REEs such as Ce and La, they excluded these metals from cells in a later phase of the cell cycle. This phenomenon could be a base for a future selective "extraction" of lanthanides from medium by continuous sampling during the cultivation. Similar findings were observed in *Galdieria phlegrea*, where the ratio of accumulated REEs differed significantly from their ratio in the growth medium (Čížková et al., 2021). Several studies show that the accumulation of light lanthanides, i.e., La, Ce, Pr, Nd, promethium (Pm), samarium (Sm) were preferred by organisms over heavy lanthanides (González et al., 2015; Yang and Wilkinson, 2018). Our results clearly showed that *G. sulphuraria* has tremendous capacity for lanthanide bio-mining/bio-removal, but further investigation is required to understand the detailed mechanisms behind the bioaccumulation/biosorption of REEs from e-waste (CFL lights) containing environments.

Interestingly, almost no research to date has been conducted on the effect of hormones on the bioaccumulation of REEs by microalgae. This is the first study that shows the accumulation of Y and Eu can be doubled in the presence of the plant hormones NAA and BAP (Figures 7A,B). However, the mechanism behind increased REE accumulation following NAA exposure remains elusive. A possible explanation could be that the application of exogenous cytokinins and auxins mitigated the toxicity of REEs and promoted cell growth, development, and regulated their adsorption similar to HM adsorption in green algae *C. vulgaris* and *Acutodesmus obliquus* (Piotrowska-Niczyporuk et al., 2012, 2018).

Conclusion

Being acidophilic in nature, the red alga *G. sulphuraria* can grow in the presence of a CFL acid extract containing 10% HNO_3, although growth was slightly slower than the control culture. Photosynthetic pigments such as chlorophyll *a*, carotenoids and phycocyanin were also decreased under CFL treatment, although carotenoid synthesis minimized the deleterious effects of CFL up to the initial 4th h of the cell cycle. During the light phase of the cell cycle, photosynthetic performance, expressed as the ratio F_v/F_m, was negatively affected by CFL treatment, but later in the dark phase, recovered significantly. In the initial hours of the cell cycle, cell division was delayed by about 2 h with CFL treatment, although later cells were able to complete their 2nd division within 24 h of the cell cycle. The produced daughter cells were of smaller size. Accumulation of REEs by *G. sulphuraria* was concentration-independent and selective. The REEs most accumulated by *G. sulphuraria* were Y and Eu, followed by La, Ce, Gd, and Tb, respectively. The plant hormone NAA stimulated the accumulation of REEs and almost doubled Y accumulation. BAP also had a pronounced effect on Y and Eu accumulation, although it did not increase the accumulation of other REEs. Waste luminophores like CFL bulbs could be a great secondary source of REEs, and using the red alga *G. sulphuraria* may be promising in REE bio-removal/accumulation technology. Recovery of REEs from algal biomass could lead to an economic and eco-friendly solution for the removal of hazardous waste from CFL lights and for the generation of REEs for future use.

Data availability statement

The original contributions presented in the study are included in the article/Supplementary material, further inquiries can be directed to the corresponding author.

Author contributions

MV, DS, and DM: conceptualization and funding acquisition. AS, MČ, and VN: methodology, investigation, and writing—original draft preparation. DS and DM: validation. MR: formal analysis. AS and MČ:

resources. MV and DM: data curation, writing—review and editing, and project administration. MV and MR: visualization. MV: supervision. All authors contributed to the article and approved the submitted version.

Funding

This research was funded by the European fund for regional development, the program Interreg V-A Austria – Czech Republic, the Project ATCZ172 REEgain, the COST Action 19116 – PLANTMETALS and by the institutional support RVO 61388971 and RVO 67985939 of the Czech Academy of Sciences.

Acknowledgments

We acknowledge J. D. Brooker for critical reading and language editing of the text and Barbora Šedivá for confocal imaging. We are very thankful to the technical staff of the Laboratory of Cell Cycles of Algae for excellent technical support.

Conflict of interest

The authors declare that the research was conducted in the absence of any commercial or financial relationships that could be construed as a potential conflict of interest.

Publisher's note

Supplementary material

The Supplementary material for this article can be found online at: https://www.frontiersin.org/articles/10.3389/fmicb.2023.1130848/full#supplementary-material

References

Abiusi, F., Fernández, P. M., Cansiani, S., Janssen, M., Wijffels, R. H., and Barbosa, M. (2022). Mixotrophic cultivation of *Galdieria sulphuraria* for C-phycocyanin and protein production. *Algal Res.* 61:102603. doi: 10.1016/j.algal.2021.102603

Ashraf, N., Vítová, M., Cloetens, P., Mijovilovich, A., Bokhari, S. N. H., and Küpper, H. (2021). Effect of nanomolar concentrations of lanthanum on *Desmodesmus quadricauda* cultivated under environmentally relevant conditions. *Aquat. Toxicol.* 235:105818. doi: 10.1016/j.aquatox.2021.105818

Balaram, V. (2019). Rare earth elements: a review of applications, occurrence, exploration, analysis, recycling, and environmental impact. *Geosci. Front.* 10, 1285–1303. doi: 10.1016/j.gsf.2018.12.005

Baldé, C. P., Forti, V., Gray, V., Kuehr, R., and Stegmann, P. (2017). *The Global e-Waste Monitor 2017: Quantities, Flows and Resources*. Bonn/Geneva/Vienna: United Nations University, International Telecommunication Union, and International Solid Waste Association.

Bennett, A., and Bogorad, L. (1973). Complementary chromatic adaptation in a filamentous blue-green alga. *J. Cell Biol.* 58, 419–435. doi: 10.1083/jcb.58.2.419

Bottone, C., Camerlingo, R., Miceli, R., Salbitani, G., Sessa, G., Pirozzi, G., et al. (2019). Antioxidant and anti-proliferative properties of extracts from heterotrophic cultures of *Galdieria sulphuraria*. *Nat. Prod. Res.* 33, 1659–1663. doi: 10.1080/14786419.2018.1425853

Brányiková, I., Maršálková, B., Doucha, J., Brányik, T., Bišová, K., Zachleder, V., et al. (2011). Microalgae—novel highly efficient starch producers. *Biotechnol. Bioeng.* 108, 766–776. doi: 10.1002/bit.23016

Carfagna, S., Landi, V., Coraggio, F., Salbitani, G., Vona, V., Pinto, G., et al. (2018). Different characteristics of C-phycocyanin (C-PC) in two strains of the extremophilic *Galdieria phlegrea*. *Algal Res.* 31, 406–412. doi: 10.1016/j.algal.2018.02.030

Carfagna, S., Napolitano, G., Barone, D., Pinto, G., Pollio, A., and Venditti, P. (2015). Dietary supplementation with the microalga *Galdieria sulphuraria* (*Rhodophyta*) reduces prolonged exercise-induced oxidative stress in rat tissues. *Oxidative Med. Cell. Longev.* 2015, 1–11. doi: 10.1155/2015/732090

Chakhmouradian, A. R., and Wall, F. (2012). Rare earth elements: minerals, mines, magnets (and more). *Elements* 8, 333–340. doi: 10.2113/gselements.8.5.333

Cheisson, T., and Schelter, E. J. (2019). Rare earth elements: Mendeleev's bane, modern marvels. *Science* 363, 489–493. doi: 10.1126/science.aau7628

Cheng, J., Qiu, H., Chang, Z., Jiang, Z., and Yin, W. (2016). The effect of cadmium on the growth and antioxidant response for freshwater algae *Chlorella vulgaris*. *Springer Plus* 5:1290. doi: 10.1186/s40064-016-2963-1

Čížková, M., Mezricky, P., Mezricky, D., Rucki, M., Zachleder, V., and Vítová, M. (2021). Bioaccumulation of rare earth elements from waste luminophores in the red algae, *Galdieria phlegrea*. *Waste and Biomass Valorization* 12, 3137–3146. doi: 10.1007/s12649-020-01182-3

Čížková, M., Vítová, M., and Zachleder, V. (2019). The red microalga *Galdieria* as a promising organism for applications in biotechnology. *Microalgae Physiol. Appl.* 1:17. doi: 10.5772/intechopen.89810

Dubey, K., and Dubey, K. P. (2011). A study of the effect of red mud amendments on the growth of cyanobacterial species. *Biorem. J.* 15, 133–139. doi: 10.1080/10889868.2011.598483

Edmundson, S. J., and Huesemann, M. H. (2015). The dark side of algae cultivation: characterizing night biomass loss in three photosynthetic algae, *Chlorella sorokiniana*, *Nannochloropsis Salina* and *Picochlorum* sp. *Algal Res.* 12, 470–476. doi: 10.1016/j.algal.2015.10.012

Ferraro, G., Imbimbo, P., Marseglia, A., Lucignano, R., Monti, D. M., and Merlino, A. (2020). X-ray structure of C-phycocyanin from *Galdieria phlegrea*: determinants of thermostability and comparison with a C-phycocyanin in the entire phycobilisome. *Biochim. Biophys. Acta Bioenerg.* 1861:148236. doi: 10.1016/j.bbabio.2020.148236

Fu, H.-Y., Liu, S.-L., and Chiang, Y.-R. (2020). Biosynthesis of ascorbic acid as a glucose-induced photoprotective process in the extremophilic red alga *Galdieria partita*. *Front. Microbiol.* 10:3005. doi: 10.3389/fmicb.2019.03005

Gauthier, M. R., Senhorinho, G. N. A., and Scott, J. A. (2020). Microalgae under environmental stress as a source of antioxidants. *Algal Res.* 52:102104. doi: 10.1016/j.algal.2020.102104

Goecke, F., Vítová, M., Lukavský, J., Nedbalová, L., Řezanka, T., and Zachleder, V. (2017). Effects of rare earth elements on growth rate, lipids, fatty acids and pigments in microalgae. *Phycol. Res.* 65, 226–234. doi: 10.1111/pre.12180

González, V., Vignati, D. A., Pons, M.-N., Montarges-Pelletier, E., Bojic, C., and Giamberini, L. (2015). Lanthanide ecotoxicity: first attempt to measure environmental risk for aquatic organisms. *Environ. Pollut.* 199, 139–147. doi: 10.1016/j.envpol.2015.01.020

Gross, W., Kuever, J., Tischendorf, G., Bouchaala, N., and Büsch, W. (1998). Cryptoendolithic growth of the red alga *Galdieria sulphuraria* in volcanic areas. *Eur. J. Phycol.* 33, 25–31. doi: 10.1080/09670269810001736503

Guterman, H., Ben-Yaakov, S., and Vonshak, A. (1989). Automatic on-line growth estimation method for outdoor algal biomass production. *Biotechnol. Bioeng.* 34, 143–152. doi: 10.1002/bit.260340202

Gwenzi, W., Mangori, L., Danha, C., Chaukura, N., Dunjana, N., and Sanganyado, E. (2018). Sources, behaviour, and environmental and human health risks of high-technology rare earth elements as emerging contaminants. *Sci. Total Environ.* 636, 299–313. doi: 10.1016/j.scitotenv.2018.04.235

Hu, Q., Kurano, N., Kawachi, M., Iwasaki, I., and Miyachi, S. (1998). Ultrahigh-cell-density culture of a marine green alga *Chlorococcum littorale* in a flat-plate photobioreactor. *Appl. Microbiol. Biotechnol.* 49, 655–662. doi: 10.1007/s002530051228

Hu, Z., Richter, H., Sparovek, G., and Schnug, E. (2004). Physiological and biochemical effects of rare earth elements on plants and their agricultural significance: a review. *J. Plant Nutr.* 27, 183–220. doi: 10.1081/PLN-120027555

Iovinella, M., Carbone, D. A., Cioppa, D., Davis, S. J., Innangi, M., Esposito, S., et al. (2020). Prevalent pH controls the capacity of *Galdieria maxima* to use ammonia and nitrate as a nitrogen source. *Plan. Theory* 9:232. doi: 10.3390/plants9020232

Jalali, J., and Lebeau, T. (2021). The role of microorganisms in mobilization and phytoextraction of rare earth elements: a review. *Front. Environ. Sci.* 9:688430. doi: 10.3389/fenvs.2021.688430

Johnson, E. M., Kumar, K., and Das, D. (2014). Physicochemical parameters optimization, and purification of phycobiliproteins from the isolated *Nostoc* sp. *Bioresour. Technol.* 166, 541–547. doi: 10.1016/j.biortech.2014.05.097

Jong, L. W., Fujiwara, T., Hirooka, S., and Miyagishima, S.-Y. (2021). Cell size for commitment to cell division and number of successive cell divisions in cyanidialean red algae. *Protoplasma* 258, 1103–1118. doi: 10.1007/s00709-021-01628-y

Kselíková, V., Husarčíková, K., Zachleder, V., and Bišová, K. (2022). Cultivation of the microalgae *Chlamydomonas reinhardtii* and *Desmodesmus quadricauda* in highly deuterated media: balancing the light intensity. *Front. Bioeng. Biotechnol.* 10:960862. doi: 10.3389/fbioe.2022.960862

Lima, A. T., and Ottosen, L. (2021). Recovering rare earth elements from contaminated soils: critical overview of current remediation technologies. *Chemosphere* 265:129163. doi: 10.1016/j.chemosphere.2020.129163

Liu, A., and Shizong, L. (1999). Effects of La on growth and the chlorophyll contents of *Chlorella* in heterotrophic culture. *Chin. Rare Earths* 20, 38–40.

Machado, M. D., and Soares, E. V. (2014). Modification of cell volume and proliferative capacity of *Pseudokirchneriella subcapitata* cells exposed to metal stress. *Aquat. Toxicol.* 147, 1–6. doi: 10.1016/j.aquatox.2013.11.017

Martinez-Garcia, M., Kormpa, A., and Van Der Maarel, M. J. (2017). The glycogen of *Galdieria sulphuraria* as alternative to starch for the production of slowly digestible and resistant glucose polymers. *Carbohydr. Polym.* 169, 75–82. doi: 10.1016/j.carbpol.2017.04.004

McCready, R., Guggolz, J., Silviera, V., and Owens, H. (1950). Determination of starch and amylose in vegetables. *Anal. Chem.* 22, 1156–1158. doi: 10.1021/ac60045a016

Minoda, A., Sawada, H., Suzuki, S., Miyashita, S.-I., Inagaki, K., Yamamoto, T., et al. (2015). Recovery of rare earth elements from the sulfothermophilic red alga *Galdieria sulphuraria* using aqueous acid. *Appl. Microbiol. Biotechnol.* 99, 1513–1519. doi: 10.1007/s00253-014-6070-3

Náhlík, V., Čížková, M., Singh, A., Mezricky, D., Rucki, M., Andresen, E., et al. (2022). Growth of the red alga *Galdieria sulphuraria* in red mud-containing medium and accumulation of rare earth elements. *Waste Biomass Valorization*. doi: 10.1007/s12649-022-02021-3

Náhlík, V., Zachleder, V., Čížková, M., Bišová, K., Singh, A., Mezricky, D., et al. (2021). Growth under different trophic regimes and synchronization of the red microalga *Galdieria sulphuraria*. *Biomol. Ther.* 11:939. doi: 10.3390/biom11070939

Oesterhelt, C., Schmälzlin, E., Schmitt, J. M., and Lokstein, H. (2007). Regulation of photosynthesis in the unicellular acidophilic red alga *Galdieria sulphuraria*. *Plant J.* 51, 500–511. doi: 10.1111/j.1365-313X.2007.03159.x

Pagano, G., Thomas, P. J., Di Nunzio, A., and Trifuoggi, M. (2019). Human exposures to rare earth elements: present knowledge and research prospects. *Environ. Res.* 171, 493–500. doi: 10.1016/j.envres.2019.02.004

Pinto, J., Costa, M., Henriques, B., Soares, J., Dias, M., Viana, T., et al. (2021). Competition among rare earth elements on sorption onto six seaweeds. *J. Rare Earths* 39, 734–741. doi: 10.1016/j.jre.2020.09.025

Pinto, J., Henriques, B., Soares, J., Costa, M., Dias, M., Fabre, E., et al. (2020). A green method based on living macroalgae for the removal of rare-earth elements from contaminated waters. *J. Environ. Manag.* 263:110376. doi: 10.1016/j.jenvman.2020.110376

Pinto, E., Sigaud-Kutner, T. C. S., Leitao, M. A. S., Okamoto, O. K., Morse, D., and Colepicolo, P. (2003). Heavy metal-induced oxidative stress in algae. *J. Phycol.* 39, 1008–1018. doi: 10.1111/j.0022-3646.2003.02-193.x

Piotrowska-Niczyporuk, A., Bajguz, A., Zambrzycka, E., and Godlewska-Żyłkiewicz, B. (2012). Phytohormones as regulators of heavy metal biosorption and toxicity in green alga *Chlorella vulgaris* (Chlorophyceae). *Plant Physiol. Biochem.* 52, 52–65. doi: 10.1016/j.plaphy.2011.11.009

Piotrowska-Niczyporuk, A., Bajguz, A., Zambrzycka-Szelewa, E., and Bralska, M. (2018). Exogenously applied auxins and cytokinins ameliorate lead toxicity by inducing antioxidant defence system in green alga *Acutodesmus obliquus*. *Plant Physiol. Biochem.* 132, 535–546. doi: 10.1016/j.plaphy.2018.09.038

Potijun, S., Yaisamlee, C., and Sirikhachornkit, A. (2021). Pigment production under cold stress in the green microalga *Chlamydomonas reinhardtii*. *Agriculture* 11:564. doi: 10.3390/agriculture11060564

Qu, Y., and Lian, B. (2013). Bioleaching of rare earth and radioactive elements from red mud using *Penicillium tricolor* RM-10. *Bioresour. Technol.* 136, 16–23. doi: 10.1016/j.biortech.2013.03.070

Reeb, V., and Bhattacharya, D. (2010). "The thermo-acidophilic cyanidiophyceae (Cyanidiales)" in *Red Algae in the Genomic Age* (Dordrecht: Springer), 409–426.

Schreiber, U., Schliwa, U., and Bilger, W. (1986). Continuous recording of photochemical and non-photochemical chlorophyll fluorescence quenching with a new type of modulation fluorometer. *Photosynth. Res.* 10, 51–62. doi: 10.1007/BF00024185

Shi, T.-Q., Wang, L.-R., Zhang, Z.-X., Sun, X.-M., and Huang, H. (2020). Stresses as first-line tools for enhancing lipid and carotenoid production in microalgae. *Front. Bioeng. Biotechnol.* 8:610. doi: 10.3389/fbioe.2020.00610

Sun, X., Zhong, Y., Huang, Z., and Yang, Y. (2014). Selenium accumulation in unicellular green alga *Chlorella vulgaris* and its effects on antioxidant enzymes and content of photosynthetic pigments. *PLoS One* 9:e112270. doi: 10.1371/journal.pone.0112270

Torzillo, G., Sacchi, A., Materassi, R., and Richmond, A. (1991). Effect of temperature on yield and night biomass loss in *Spirulina platensis* grown outdoors in tubular photobioreactors. *J. Appl. Phycol.* 3, 103–109. doi: 10.1007/BF00003691

Vítová, M., Bišová, K., Kawano, S., and Zachleder, V. (2015). Accumulation of energy reserves in algae: from cell cycles to biotechnological applications. *Biotechnol. Adv.* 33, 1204–1218. doi: 10.1016/j.biotechadv.2015.04.012

Wan, M., Zhao, H., Guo, J., Yan, L., Zhang, D., Bai, W., et al. (2021). Comparison of C-phycocyanin from extremophilic *Galdieria sulphuraria* and *Spirulina platensis* on stability and antioxidant capacity. *Algal Res.* 58:102391. doi: 10.1016/j.algal.2021.102391

Weber, A. P., Horst, R. J., Barbier, G. G., and Oesterhelt, C. (2007). Metabolism and metabolomics of eukaryotes living under extreme conditions. *Int. Rev. Cytol.* 256, 1–34. doi: 10.1016/S0074-7696(07)56001-8

Wellburn, A. R. (1994). The spectral determination of chlorophylls a and b, as well as total carotenoids, using various solvents with spectrophotometers of different resolution. *J. Plant Physiol.* 144, 307–313. doi: 10.1016/S0176-1617(11)81192-2

Yang, G., and Wilkinson, K. J. (2018). Biouptake of a rare earth metal (Nd) by *Chlamydomonas reinhardtii* – bioavailability of small organic complexes and role of hardness ions. *Environ. Pollut.* 243, 263–269. doi: 10.1016/j.envpol.2018.08.066

Yoon, H. S., Ciniglia, C., Wu, M., Comeron, J. M., Pinto, G., Pollio, A., et al. (2006). Establishment of endolithic populations of extremophilic Cyanidiales (*Rhodophyta*). *BMC Evol. Biol.* 6:78. doi: 10.1186/1471-2148-6-78

Yoshimura, E., Nagasaka, S., Sato, Y., Satake, K., and Mori, S. (1999). Extraordinary high aluminium tolerance of the acidophilic thermophilic alga, *Cyanidium caldarium*. *Soil Sci. Plant Nutr.* 45, 721–724. doi: 10.1080/00380768.1999.10415835

frontiers | Frontiers in Microbiology

TYPE Review
PUBLISHED 11 April 2023
DOI 10.3389/fmicb.2023.1127249

OPEN ACCESS

EDITED BY
Muhammad Z. Mumtaz,
The University of Lahore, Pakistan

REVIEWED BY
Sandhya Mishra,
National Botanical Research Institute (CSIR), India
Iqra Naseer,
Islamia University of Bahawalpur, Pakistan

*CORRESPONDENCE
Bindu Naik
✉ binnaik@gmail.com
Per Erik Joakim Saris
✉ per.saris@helsinki.fi

SPECIALTY SECTION
This article was submitted to Terrestrial Microbiology, a section of the journal Frontiers in Microbiology

RECEIVED 19 December 2022
ACCEPTED 10 March 2023
PUBLISHED 11 April 2023

CITATION
Rizwanuddin S, Kumar V, Singh P, Naik B, Mishra S, Chauhan M, Saris PEJ, Verma A and Kumar V (2023) Insight into phytase-producing microorganisms for phytate solubilization and soil sustainability.
Front. Microbiol. 14:1127249.
doi: 10.3389/fmicb.2023.1127249

Insight into phytase-producing microorganisms for phytate solubilization and soil sustainability

Sheikh Rizwanuddin[1], Vijay Kumar[2], Pallavi Singh[3], Bindu Naik[1]*, Sadhna Mishra[4], Mansi Chauhan[5], Per Erik Joakim Saris[6]*, Ankit Verma[2] and Vivek Kumar[2]

[1]Department Food Science and Technology, Graphic Era (Deemed to be University), Dehradun, India, [2]Himalayan School of Biosciences, Swami Rama Himalayan University, Dehradun, India, [3]Department of Biotechnology, Graphic Era (Deemed to be University), Dehradun, India, [4]Faculty of Agricultural Sciences, GLA University, Mathura, India, [5]Department of Microbiology, Graphic Era (Deemed to be University), Dehradun, India, [6]Department of Microbiology, Faculty of Agriculture and Forestry, University of Helsinki, Helsinki, Finland

The increasing demand for food has increased dependence on chemical fertilizers that promote rapid growth and yield as well as produce toxicity and negatively affect nutritional value. Therefore, researchers are focusing on alternatives that are safe for consumption, non-toxic, cost-effective production process, and high yielding, and that require readily available substrates for mass production. The potential industrial applications of microbial enzymes have grown significantly and are still rising in the 21st century to fulfill the needs of a population that is expanding quickly and to deal with the depletion of natural resources. Due to the high demand for such enzymes, phytases have undergone extensive research to lower the amount of phytate in human food and animal feed. They constitute efficient enzymatic groups that can solubilize phytate and thus provide plants with an enriched environment. Phytases can be extracted from a variety of sources such as plants, animals, and microorganisms. Compared to plant and animal-based phytases, microbial phytases have been identified as competent, stable, and promising bioinoculants. Many reports suggest that microbial phytase can undergo mass production procedures with the use of readily available substrates. Phytases neither involve the use of any toxic chemicals during the extraction nor release any such chemicals; thus, they qualify as bioinoculants and support soil sustainability. In addition, phytase genes are now inserted into new plants/crops to enhance transgenic plants reducing the need for supplemental inorganic phosphates and phosphate accumulation in the environment. The current review covers the significance of phytase in the agriculture system, emphasizing its source, action mechanism, and vast applications.

KEYWORDS

phosphorus, microbial phytase, bioinoculants, transgenic, growth inducer, soil sustainability, agriculture, nutrient cycle

Introduction

Phosphorus (P) is one of the Earth's (lithosphere) less-abundant macronutrients (0.1% of total), and soil phosphorus concentration depends on the phosphorus content of the parent material. Organic phosphorus (P_o) constitutes approximately 30%–65% of the total phosphorus; however, inorganic phosphorus (P_i) accounts for 30%–75% of the total soil phosphorus (Fujita et al., 2017; Wu et al., 2022). Its availability throughout the initial stages of plant development is vital for the establishment of plant reproductive component primordia. It is essential for boosting root strength and ramification, giving plant vigor and pathogen resistance. Moreover, it aids in the production of seeds and the early maturity of crops such as grains and legumes (Sharma et al., 2013). Figure 1 demonstrates the various routes of phosphorus utilization by the plants in the soil. Plants require phosphorus for their various fundamental processes such as photosynthesis, flowering, fruiting, and maturation. Significantly high phosphorus levels are required for cell division and in the development of meristematic tissues. It also promotes the growth of roots and helps in nitrogen fixation (Weil and Brady, 2017). While in the case of phosphorus deficiency, the plant is typically spindly, thin-stemmed, and stunted and has dark and almost bluish-green foliage, instead of light foliage. Therefore, phosphorus-deficient plants frequently appear relatively normal unless much larger and healthy plants are present to provide a comparison. In addition, delayed maturation, irregular flowering, and poor seed quality are traits of phosphorus-deficient plants. A significant phosphorus deficit can result in senescence and withering of leaves. Lack of phosphorus causes many plants to exhibit purple colors in their leaves and stems. Phosphorus is found aggregated in the form of myo-inositol hexabisphosphate in soil, which is chemically known as phytate/phytic acid. Soil phytate can be produced through microbial soil P_i transformation, plant tissues, and monogastric animal manures (Liu et al., 2022). Phytate mineralization is observed by many microorganisms and can be implemented in plant systems for induced agricultural sustainability. The previous study demonstrated that the exogenous addition of phytate-rich substrates and soil immobilization and transformation by P fertilizers are associated with phytate accumulation (Menezes-Blackburn et al., 2013).

Phytate is a chemical derivative of inositol (myo-inositol hexabisphosphate) and is the most widely distributed form of phosphorus in the soil (Duong et al., 2018). It is present mainly in the bound form with other minerals and significantly contributes to the organic soil phosphate pool (P_o) (Gerke, 2015). Structurally, it is a six-hydroxyl alcohol with phosphoric acid (six molecules) residues bound to its hydroxyl groups.

As the metallic cations of Ca, Fe, K, Mg, Mn, and Zn are tightly bound by the negatively charged phosphate in PA, they become insoluble and are hence not available for plants (Azeem et al., 2014; Sun et al., 2021). Small quantities of inorganic phosphorus added to the rhizosphere might act as a stimulator to phytic acid mineralization, thus improving plant phosphorus feeding (Elhaissoufi et al., 2022).

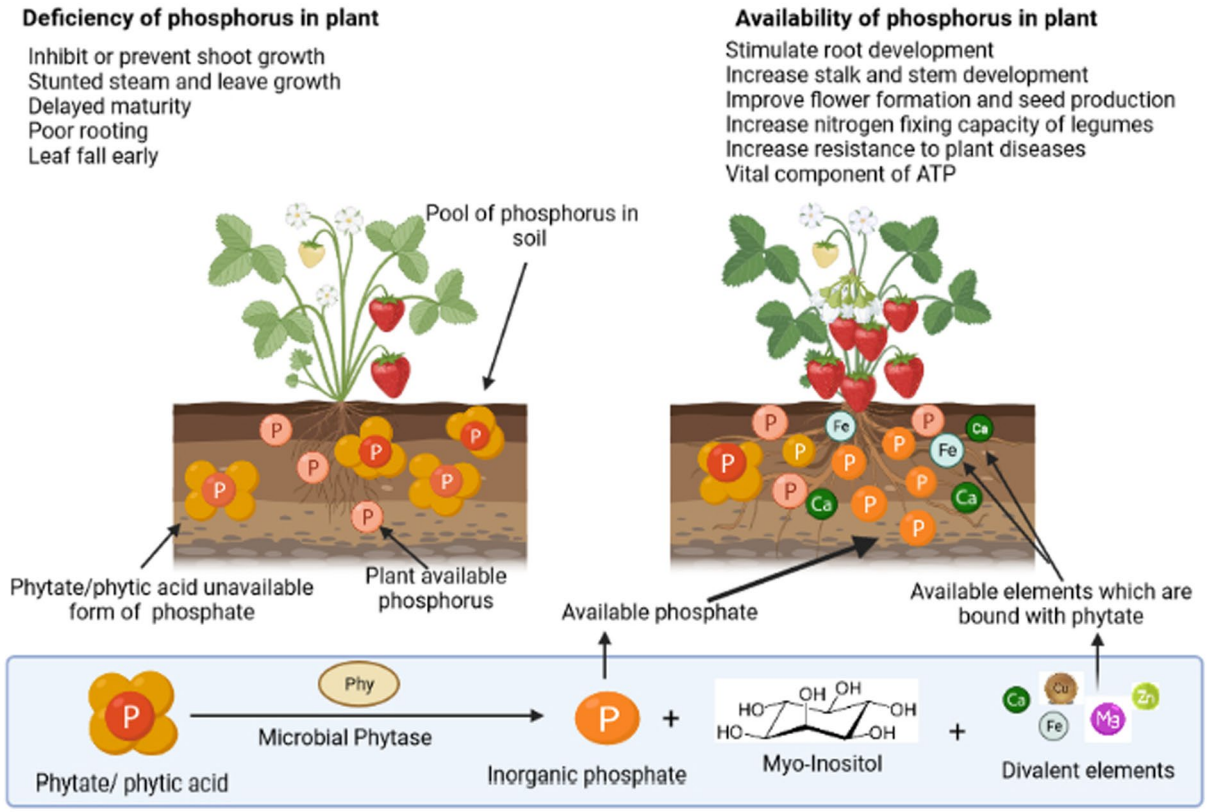

FIGURE 1
Depiction of the importance of phosphorus to a plant and the role of phosphate solubilizing microorganisms in the utilization of different forms of phosphorus *via* diverse processes.

However, the phytate present in the soil cannot be directly utilized by the plants. For soil phytate to contribute to plant P nutrition, phosphate ester (C-O-P), phosphoanhydride (P-O-P), or phosphonate (C-P) must first be dephosphorylated through phytase-mediated hydrolysis.

Phytases are abundantly found in nature. The primary sources include plants, microbes (bacteria and fungi), and some animal tissues (Cookson, 2002; Konietzny and Greiner, 2002). Due to their catalytic properties and simplicity of enzyme production, phytases of microbial origin are the most suitable for use in the commercial biotechnological production of enzymes. A few plant roots have been detected with phytases having low hydrolytic activity and not secreting phytase into the rhizosphere. Therefore, plants are unable to utilize soil phytates by their mechanism. Phytases are actively excreted by microscopic soil fungi and, to a lesser extent, by bacteria. Plant roots were shown to have weak phytase activity, but since the enzyme is not released into the rhizosphere, plants are unable to absorb the fixed phosphorus from soil phytates on their own (Kashirskaya et al., 2020).

Phytases are enzymes that catalyze the hydrolysis of phytic acid in different positions of the inositol ring and release phosphorus, zinc, and other minerals in inorganic form, thereby increasing the absorption of minerals by plants (Vats and Banerjee, 2004). The physicochemical properties of phytases affect their stability, mobility, and ability to hydrolyze soil phytate. Moreover, their enormous anion-holding capacity and surface area suggest that inositol phosphates have a strong affinity for soil colloids. Their activity is dependent on the soil type. Azeem et al. (2014) reported that clays and organic materials restrict enzyme activity more than diverse soil surfaces, with great specificity to soil characteristics and mineralogy. Moreover, after 28 days of phytase adsorption in sandy soil, 40% of the extra phytase remained active, but only 5% remained active in soil with higher clay percentages. A well-aerated soil will allow for faster phosphorus solubilization than saturated, wet soil. Interlaminar gaps in clay minerals reduced phytase activities more than 1:1 phyllosilicate.

Because of their global commercial importance, sources of phytases in microbes are rated more essential than other sources (Singh et al., 2020). Although plants cannot obtain phosphorus from phytate directly, the existence of phosphate-solubilizing microorganisms in the rhizosphere can compensate for this loss (Kaur, 2020). Microbial phytases were more effective than those extracted from plants (Azeem et al., 2014). Currently, microbial phytase is a highly researched area known to counter food toxicity and security concerns. A report in support of this fact has been published currently by Ladics et al. (2020). They studied the toxicity effects of PhyG (bacterial phytase variant) developed *via* fermentation using *Trichoderma reesei* and observed non-toxic when consumed on remarkably higher doses of consumption in broilers. Another study by Thorsen et al. (2021) evaluated the safety of Phytase HM derived from *Aspergillus oryzae*. They studied the effects *in vivo* and observed no mutagenic or inflammatory effects. Significantly, these produced positive responses to the growth and bone health of poultry animals.

Phytate: Organic phosphorus

Phosphorus deposition as phytate within soils is approximately 50 million metric tonnes annually, accounting for 65% of phosphorus fertilizer. Inositol hexakisphosphate (IP6), a chemical derived from phytate, was found in 1903 and is the primary P storage form in many soil and plant tissues (Azeem et al., 2014). Soil phytate may derive from plant tissues, monogastric animal manures, and microbial conversion from soil Pi. Plants and bacteria both produce phytate, although plants are the primary producer. Phytate exists in six inositol esters, i.e., Mono-, bis-, tris-, tetrakis-, pentakis-, and hexakis-phosphates (IP1–6), out of which, IP6 is the major form, making up to 83%–100% of IP (Hill et al., 2007). Moreover, IP6 exits in four stereoisomers with their abundance in the order: myo (56–90%) > scyllo (20%–50%) > Dchiro (6%–10%,) > neo (1%–5%) (Turner et al., 2012). IP6 stereoisomer is mostly contributed by plants while the rest of the stereoisomers are synthesized by microbes present in the soil. Phytate has a high degree of charge density and hence has strong interaction with soil and is responsible for binding Fe/Al-oxides in acidic soil and Ca/Mg minerals in alkaline soil. Due to pH dependency, and numerous hydroxyl- and oxo- groups on the surface, phytate develops a chelating affinity with mineral cations and forms phytate-mineral complexes. However, multiple hydroxyl groups allow phytic acid and its deprotonated phytate forms to form strong inter- and intra-molecular hydrogen bonds and aid in solubility and acidity in aqueous solutions (Liu et al., 2022). Despite the possibility of phytate being present in soil solution, there is not any proven record that plants directly absorb phytate from the soil. The soil phytate must first be dephosphorylated from phosphate ester (COP), phosphoanhydride (POP), or phosphonate (CP) *via* phytase-mediated hydrolysis to contribute to plant P nutrition.

Mechanisms of phytate solubilization

Phytate has a high affinity for soil; therefore, it gets accumulated in the soil as compared to other esters of phosphorus. Hence, its availability is low, thereby interfering with the interaction with phytase which reduces the cleavage of esters bonds of phytate and mineralization of the inositol ring (Tang et al., 2006). There are two approaches to improving phytate access by phytase: desorption and solubilization. Protons, organic acids, and phenolic acids can all desorbate or solubilize P in soil, with organic acids being the main solubilizer of the rarely available phosphorus (Richardson et al., 2011). There are three methods through which the carboxylate groups in organic acids can mobilize phytate. First, by substituting P with a carboxylate anion, carboxylates can desorb phosphate anions from the soil by ligand exchange. Due to its higher number of carboxyl groups and closer pK2 value (4.76 vs. 4.28) to soil pH (4.5–9.5), tribasic citrate releases more P than dibasic oxalate and causes oxalate to degrade more quickly (Menezes-Blackburn et al., 2016). Second, carboxylates can remove P sorption sites by solubilizing Fe and Al *via* H+. Finally, they can dissolve organic matter (OM) that binds to P *via* Fe/Al-bridges, releasing phosphate as the OM-Fe/Al-P complex (Gerke, 2010). Phytate solubilization in the soil is improved by chelating metals bound in metal-phytate complexes to release P and chelating metals to form complexes that bind to soils and prevent microbial degradation of organic acids (Gerke, 2015). Microbes can efficiently decompose organic acids in the soil solution, but their decomposition is slowed significantly by sorption onto the soil. For phytate to dissolve in soil, organic acids must be present in the soil solution and Gerke provided a summary of the impact of organic acids on plants' uptake of phytate-P (Gerke et al., 2000; Gerke, 2015).

Both the plant and microbial phytases play a significant role in the solubilization of phytate (Figure 2) present in the soil. Phytases catalyze the mineralization, or the conversion of organic phosphorus from phytate to inorganic phosphorus, which can be easily absorbed by plants (Ariza et al., 2013). The extracellular phytase secreted from the roots is crucial for soil phytate hydrolysis when there is a lack of P, these either stay attached to the cell walls of the roots or are discharged straight into the rhizosphere to catalyze phytate hydrolysis (Sun et al., 2022). By using genetic engineering tools, transgenic plants have been developed to express phytase genes of microbial origin to break down soil phytate. This improves plant phosphorus accumulation and increases biomass (Xiao et al., 2005; Balaban et al., 2017).

Factors regulating phytate solubilization

The plant can only absorb the inorganic phosphate produced by the hydrolysis of phytic acid. In various physicochemical circumstances, the phosphate ester bond in phytate is relatively stable. The negative charge of phytate is responsible for interaction with metals present in soil and the formed metal complexes affect its solubility (Celi et al., 2001). Metal phytate complexes are soluble as follows: in terms of metal species, Na, Ca, and Mg are preferred over Cu, Zn, Mn, Cd, and Al over Fe. In terms of pH, pH 5.0 is preferred over pH 7.5. Except for Al-phytate, most phytate-metal complexes resist acid hydrolysis, and dry complexes are typically stable at high pressure and temperature (except Ca phytate) (De Boland et al., 1975). At all pH ranges, phytate combines with calcium to form soluble complexes (Ca_1- or Ca_2- phytate) or insoluble precipitates such as Ca_3-phytate. Strong chelating chemicals like EDTA are insufficient to dissolve complexes of metals without first reducing the metals (like Fe) (Sun et al., 2021). Phytate may undergo severe immobilization, which prevents it from being hydrolyzed by phytase, resulting in its limited availability and significant accumulation in soils. This is supported by the fact that phytate has a higher reactivity than P_i and other P_o compounds (Celi and Barberis, 2005). The organic acids produced by plant exudates and microbes also affect the solubility of phytate in soil (Richardson et al., 2011). The phytate solubility in the soil is also dependent on the phytase enzyme. The activity of phytase is affected by soil pH and is optimum in the range of 2.5–8.0 and then decreases with an increase in pH. In addition, because of its sorption onto soil minerals like montmorillonite, phytase action is suppressed (Leprince and Quiquampoix, 1996). *Aspergillus niger* phytase varied in its ability to prevent metal complexes from being hydrolyzed by enzymes; however, it has been discovered that the Fe phytate complex showed the most outstanding inhibition. Strong chelating chemicals like EDTA are insufficient to dissolve complexes of metals without first reducing the metals (like Fe) (Sun et al., 2021). Moreover, the interactions among phytate-mineralizing bacteria, bacteria-eating nematodes, and mycorrhizal fungi also boost plant P uptake from phytate in soils with significant P adsorption (Ranoarisoa et al., 2020).

Types of phytases and their sources

Phytases were discovered in 1907 and are considered among the 10 most significant discoveries in agricultural processes during the last

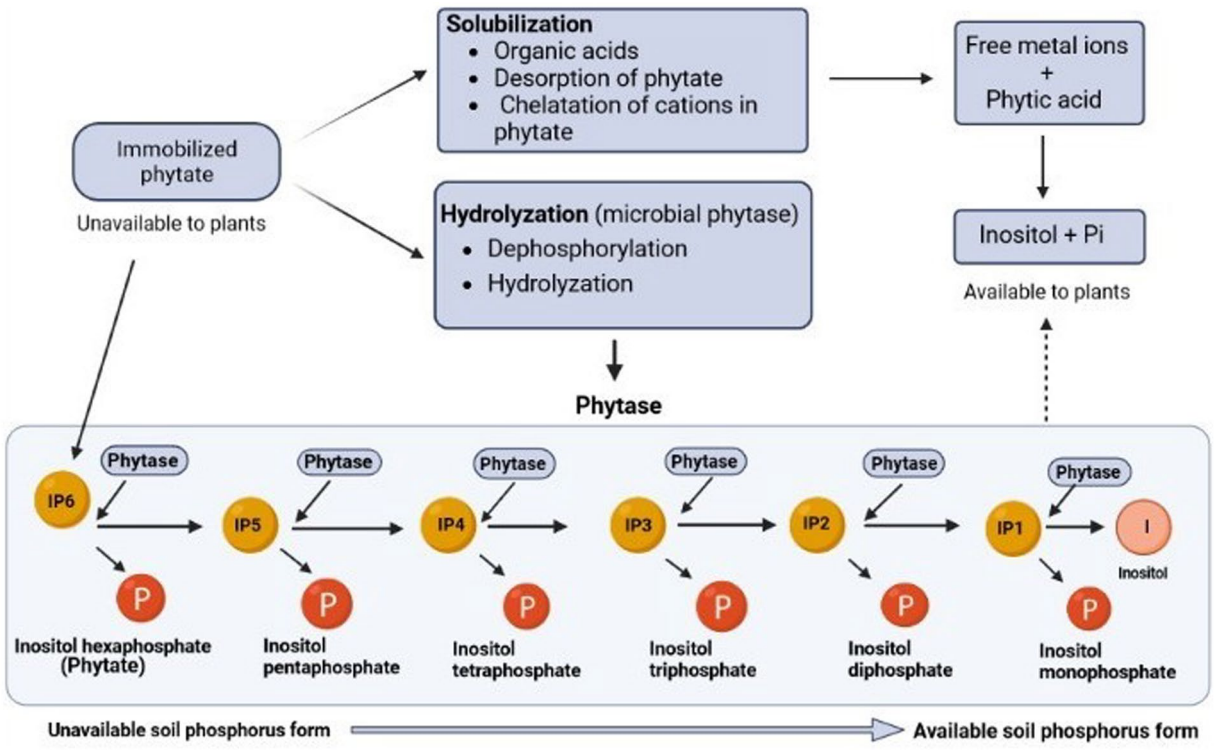

FIGURE 2
The various processes of phytate solubilization highlighting the breakdown of phytate (unavailable form) into simpler compounds (available form).

century. Phytase enzymes are phosphatases that may initiate the progressive dephosphorylation of phytate (Figure 3). They are classified according to their source, pH optimal (alkaline or acid phytases), and current catalytic processes. Although not all phytases have the exact catalytic mechanism, there are four separate categories of these enzymes with diverse structures and processes (Lei et al., 2013; Menezes-Blackburn et al., 2013) *viz.*, β-propeller phytase (BPPs), protein tyrosine phosphatase-like phytase (PTP-like phytase), purple acid phosphatase (PAPs), and last histidine acid phosphatases (HAPhy). Whereas HAPhy is further subdivided into multiple inositol polyphosphate phosphatases (MINPs) due to the observed difference in sequence homology. Cysteine phosphatase-like phytase (CP-phytase) and BPP are exclusively found in microbes, but HAP and PAPhy phytases have been found in plants. Because of the economic relevance of these enzymes, the structure and characteristics of microbial HAPs have been intensively researched (Madsen and Brinch-Pedersen, 2020). Furthermore, the catalytic process is related to molecular structure, which fluctuates substantially across and within different categories. On the other hand, the structural differences among phytases *via* the phytate dephosphorylation on the inositol ring at varying locations (3, 5, and 6) categorize it into 3-phytase, 5-phytase, and 6-phytase (Singh B. et al., 2018; Rix et al., 2022).

Because certain phytases are intracellular but may not participate in external phosphorus-phytate dephosphorylation, soil and manure phytase activity cannot be linked entirely to P nutrition. Rhizosphere phytase activity may enhance plant development in soils with inadequate P supplies (Liu et al., 2022). Although, this phytase activity is commonly regarded as a direct indication of the metabolic needs of the microbial population in several situations and circumstances. Xenobiotic phosphonates (flame retardants, detergent additives, pesticides, and antibiotics) are today's major effluents (Behera et al., 2014). Most organic molecules have high molecular weights and are often resistant to enzymatic hydrolysis; in such cases, phosphatases are one of the best-researched enzymes capable of biodegradation. Depending on the application, a phytase with commercial potential must meet several quality requirements. When added to feed, enzymes should be efficient in releasing phytate phosphate, stable to withstand heat inactivation from feed processing and storage, and inexpensive to produce. Since feed pelleting is frequently done at temperatures between 65°C and 95°C, thermostability is a crucial concern (Konietzny and Greiner, 2004).

Source of phytase

Phytases are extensively distributed among various life forms. Plants, microorganisms, and animals are the sources used to obtain

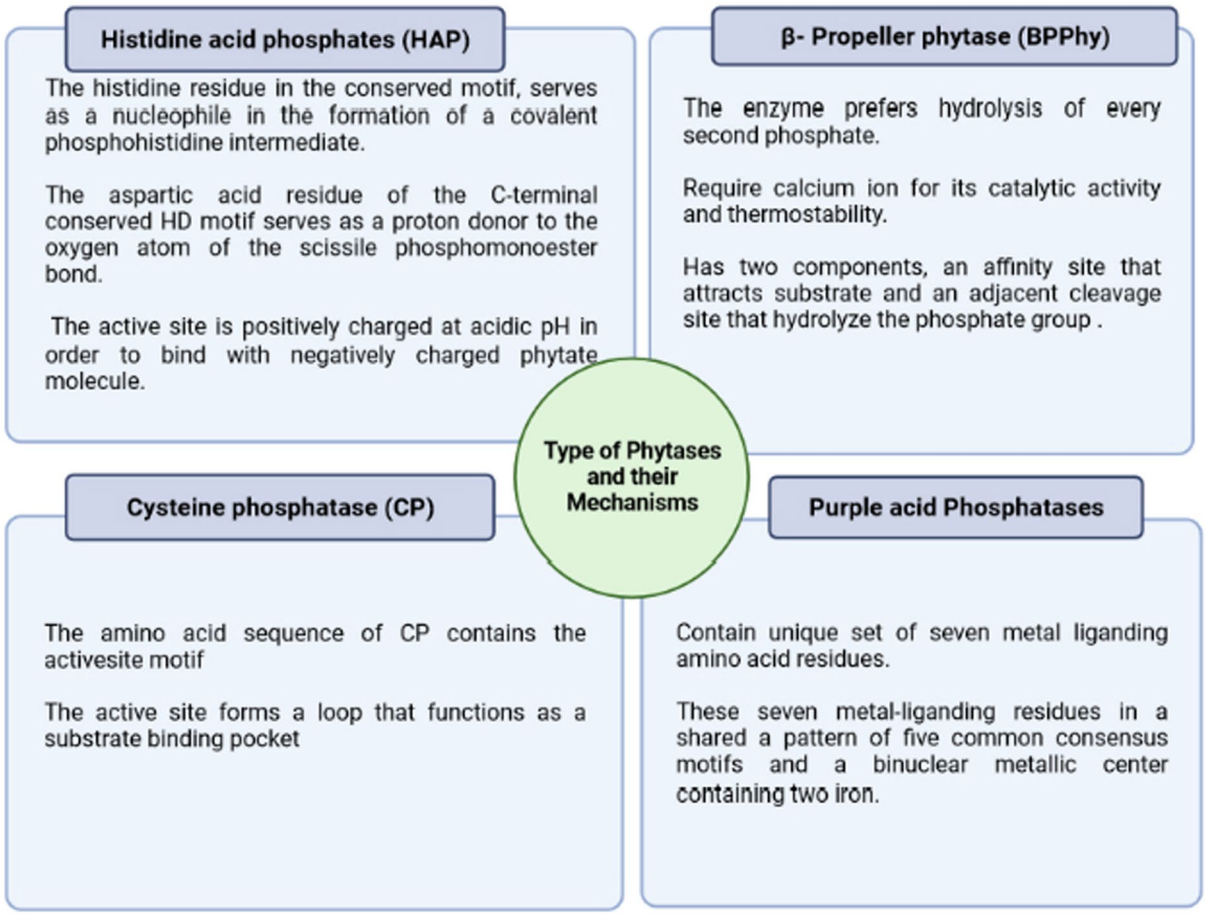

FIGURE 3
Major types of phytases and their different mechanism of action stating a basic criterion for their classification.

phytase (Figure 4). Among them, microbial phytase is the major source of phytases, produced by yeasts, bacteria, and fungi, followed by plants.

In plants, phytase may be found in higher concentrations in wheat, barley, and peas, while lower content in soybeans, maize, spinach, and so on. Phytase in the plant was first discovered in rice bran, which formed several phosphatidyl inositols as an intermediate or final product (Secco et al., 2017; Kumar and Sinha, 2018; Singh N. et al., 2018). Plant phytases can be MINPPs, PAPhys, or, in rare situations, HAPs, which are more similar to fungus HAPs than MINPPs. Plant phytases are typically produced during seed germination and can be expressed during grain filling. Phytases are usually linked with roots and are often extruded from them. Phytases exhibit wider mechanisms of action as discussed in the earlier sections, indicating their potential to work on other substrates. In plants, there is no obvious functional distinction between the phytase groups (Madsen and Brinch-Pedersen, 2020).

The majority of HAP family plant phytases begin phytate hydrolysis at position C6 of the myo-inositol hexaphosphate ring and are thus classified as type 6 phytases. Some plant phytases have been identified as alkaline or purple acid phosphatases. Plant phytase is inactive in dry seeds, but its activity increases during germination because phytase releases phosphorus to meet the plant's needs (Hussain et al., 2022); also reported to inhibit the translocation of heavy metals in plants, for instance, *Pteris vittata* PvPHY1, a new root-specific phytase expressed in tobacco was reported to promote growth and P accumulation by 10%–50% (Sun et al., 2022). Plant-derived phytase enzymes are unstable at pH levels below 4.0 and above 7.0, but phytase enzymes derived from bacteria are stable at pH levels above 8.0 and below 3.0. The optimum temperature range for plant phytase is 40–60°C, while higher temperatures of 70–90°C result in plant phytase deactivation. When the temperature surpasses 80°C, pellet formation results in the inactivation of plant phytase (Hussain et al., 2022). The main issue with generating plant phytases is that a cost-effective and efficient method of synthesizing the enzymes has yet to be established. Plant phytases have lower pH and heat stability than microbial phytases. However, manufacturing phytase from plants is time-consuming, complicated, and costly. This is also not economically advantageous. Due to the tough plant cell walls and phyto-depositions, the extraction of phytases generated by plants necessitates the use of chemicals and takes more time than that of microbes. Moreover, the price of chemicals may change depending on the type of plant source. On the other hand, by using an optimized substrate, growth conditions, and manufacturing techniques, microorganisms may be employed for mass production. As a result, the production of phytase from microbial origin has more significant potential (Dailin et al., 2019; Alemzadeh et al., 2022).

Microbial phytase

Microbial phytase activity was first discovered in *A. niger* mycelium more than a century ago (Gessler et al., 2018). Microbial phytases, preferably those derived from filamentous fungi such as *Mucor piriformis*, *Penicillium*, *Rhizopus*, *Aspergillus*, *Thermomyces*, and *Trichoderma*, constitute a large number of scientific reports published in response to this topic (Jatuwong et al., 2020). Fungi have more efficiency in phytate degradation due to certain factors, such as their hyphae can traverse longer distances in soil and extract P more efficiently and their ease of culture and excellent production yields (Shahryari et al., 2018). Fungi are also known to exhale a high concentration of organic acids, which act as a chelator and are considered the major process of inorganic phosphate solubilization. Microbial phytases do not require or release any toxic chemicals, thus they are safe biofertilizers and can also benefit farmers who practice organic farming (Gaind and Nain, 2015). Singh and Satyanarayana

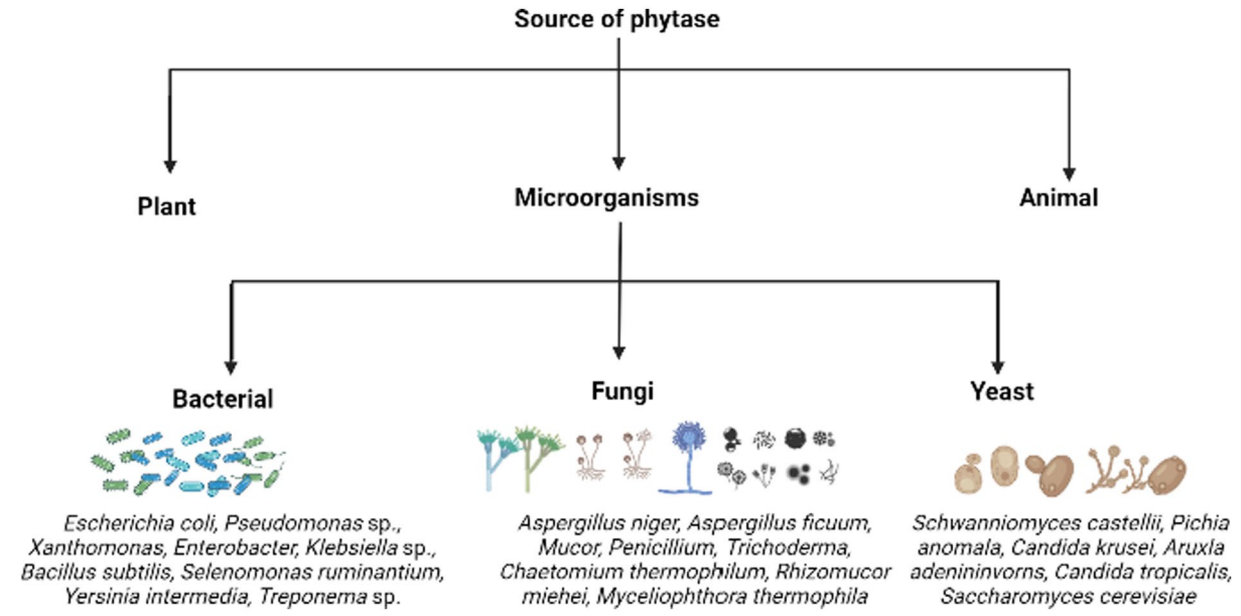

FIGURE 4
The various sources of phytases highlighting certain examples of phytate/phosphate solubilizing microorganisms.

(2015) reported *Schwanniomyces castellii* as the most phytase-yielding strain. Several reports revealed the diversity of phytase-producing yeasts such as *Candida otropicalis, Candida krusei*, *Arxula adeninivorans*, *Debaryomyces castelii*, *Kluyveromyces fragilis*, *Kluyveromyces lactis*, *Schwanniomyces castellii*, *Zygosaccharomyces bisporus*, *Zygosaccharomyces priorionus*, and *P. spartinae* (Kaur et al., 2007; Menezes et al., 2020; Soman et al., 2020; Molina et al., 2021). Phytases have been reported in bacteria such as *Aerobacter aerogenes*, *Bacillus* sp. (*Bacillus licheniformis*, *Bacillus subtilis* P6, and *B. subtilis*) (Zhao et al., 2021; Trivedi et al., 2022), *Enterobacterium*, anaerobic rumen bacteria (*Megasphaera elsdenii* and *Selenomonas ruminantium*), *Escherichia coli*, *Lactobacillus amylovorus, and Pseudomonas* sp. *Lactobacillus sanfranciscensis*, which were discovered as the highest phytase producers among the lactic acid bacterial strains recovered from sour doughs (Konietzny and Greiner, 2004). Bacterial phytases have high thermostability. Other characteristics of bacterial phytases include comparatively smaller structures (Hussain et al., 2022), high substrate specificity, proteolysis resistance, and catalytic efficiency.

Contribution of phytases in agriculture

Organic phosphorus, in the form of inositol phosphates, contributes 30%–80% of total phosphorus in soils. Phosphorus is inaccessible to plants due to interactions with reactive metals, such as Zn^{2+}, Al^{3+}, Cu^{2+}, Ca^{2+}, and Fe^{2+}, and calcareous and normal soils (Azeem et al., 2014). Phosphorus buildup as phytate in soils can reach up to 51 million metric tons annually, accounting for 65% of phosphorus fertilizer. Phytase/phosphatase enzymes serve as essential mediators of organic phosphorus mineralization to use the soil's organic phosphorus pool (Gaind and Nain, 2015). Protein and microbial-mediated degradation, partial or total incapacitation by adsorption onto soil particles and interaction with metal ions, microbial metabolites, and polyvalent anions are all important factors influencing phytase activity (Tang et al., 2006; Nannipieri et al., 2011).

Manures of monogastric animal and plant tissues and microbial conversion of soil inorganic phosphorus can all produce phytate (Liu et al., 2022). Phytase hydrolyzed the soluble forms of calcium and magnesium inositol phosphates; moreover, extracellular phytase activity has been identified in various plant species under phosphate stress situations. According to Wang et al. (2022), Mg-Al layered double hydroxides (LDHs) were found to be environmentally friendly materials to reduce phytate loss and promote the sustainable consumption of phytate when applied to the soil. Phytate or low phosphates are utilized by plants, which are present in soil and the utilization is enhanced when the soil contains phytase-producing microorganisms (Rao et al., 2009). Phytases provide a diverse role in various disciplines, but their major effects were studied in soil sustainability and feed additives.

Role of microbial phytases in soil sustainability

Soils are formed through the dissolution of rocks and the minerals contained within them, and except for carbon, hydrogen, oxygen, and some nitrogen, soil serves as the environment for the growth of roots, and plants rely on soil for all other nutrients and water. Earlier, only the soil's physical and chemical characteristics were thought to be significant. Yet, it is now well acknowledged that soil biodiversity plays a crucial role in preserving fertility and that soil biological activities are influenced by its physical and chemical properties. By the biotic operations of the microorganisms, the phytate can be found in soils in a variety of ways, including adsorbed to clays, as insoluble iron, calcium, and aluminum salt precipitates in acidic soils can be broken to the available form of phosphorus. Phytic acid also binds to the positively charged moiety of amino acids limiting their absorption; therefore, the proteins of leguminous plants consisting of more basic proteins are more readily bound to that of wheat proteins (Dersjant-Li et al., 2019). Phytases, from diverse sources in soil, are abundantly generated by numerous fungi, yeast, plants, animals, and bacteria, are necessary to hydrolyze phytic acid in the soil and are in charge of releasing phosphorus in rhizospheric regions of soil. The consumption of phosphorus from phytate is significantly influenced by the exogenous phytase activity of the roots of transgenic plants (Singh and Satyanarayana, 2011). There exist several phenomena of phytate utilization as discussed in the previous section "Mechanism of phytate solubilization." The degradation of phytates produces many by-products and final products that enhance soil health (Figure 5). Phytase activity of a microbial source can be induced using optimized substrate and inoculum levels, pH, temperature, nitrogen and carbon additives, and resistance and sensitivity to the various metal inhibitors implied (Sadaf et al., 2022).

Application of phytase-producing biofertilizers

High agricultural efficiency is based on lower synthetic chemical fertilizer doses and crop production costs. Phosphorus is supplied to crops in agricultural farming systems using produced phosphatic compounds. Because of their inherent value and possible agronomic capacity for plant development during prolonged phosphorus deprivation, bioinoculants may be a solution; phytases of microbial origin have emerged as an attractive target for commercial application (Kaur, 2020). Although several phosphate-solubilizing biofertilizer agents have been identified, they are primarily aimed at mobilizing rock phosphates in soil (Mohite et al., 2022).

Microbial phytases are thought to be a precise method for improving plant growth and productivity on a global level. Biofertilizers are regarded as very successful alternatives to synthetic fertilizers due to their simplicity, non-toxicity, environmental friendliness, and cost-effectiveness (Mazid and Khan, 2015). Biofertilizers have been demonstrated to increase the growth and development of plants by increasing the availability of macro and micronutrients to the plant system. *Azotobacter*, *Azosporillum*, *Phosphobacteria*, and *Rhizobium*-based biofertilizers are well-known and successful (Jorquera et al., 2008; Singh et al., 2014; Balogun et al., 2021; Chakraborty and Akhtar, 2021; Taj and Mohan, 2022). *Pseudomonas*, *Aspergillus* (*A. niger*, *A. flavus*, and *A. fumigatus*) (Balogun et al., 2021), *Burkholderia*, *Advenella* species, *Cellulosi microbium* sp. PB-09 (Singh et al., 2014), *Enterobacter,* and *Pantoea* isolates may release inorganic phosphate from phytate, thereby supporting agricultural sustenance. Microbial phytases are an appealing target for biofertilizers because they play an essential part in the soil phosphorus nutrient cycle. Many phosphate-solubilizing

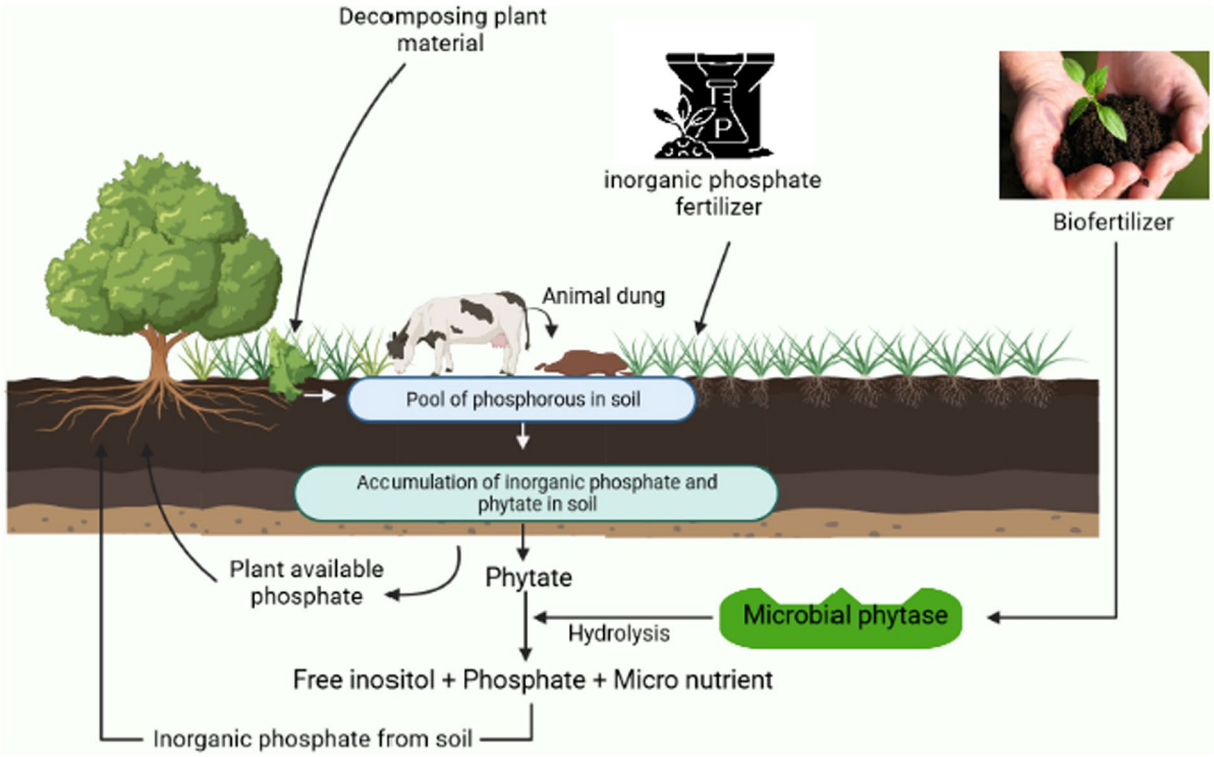

FIGURE 5
An overview to demonstrate the cyclic working process of a biofertilizer and the role of microorganisms in phytate solubilization.

biofertilizers have been discovered, although their main function is to mobilize rock phosphates in soil. Biofertilizers are required to solubilize immobilized phosphate forms, like phytate, into mobilized form (Mohite et al., 2022). Phytases are essential for maintaining the balance of phosphorus in the environment, especially in its organic form, phytic acid, which reduces the need for chemical fertilizers to make up for phosphorus shortfall. Natural soil bio-resources, such as soil microorganisms, can be a viable alternative to traditional inorganic fertilizers. Some of the potential phytase-producing microbial strains with plant growth-promoting attributes are summarized in Table 1.

Phytase-producing transgenic plants

By maximizing the use of soil-based phosphate pools, including residual phosphorus, biotechnologies must be applied to agriculture to increase the efficiency of phosphate usage in crop production. For instance, intercropping cereals and legumes has been recommended to boost crop yields (Yang and Yang, 2021). Moreover, rhizosphere modification for phytate absorption may be ineffective because of low environmental fitness, inadequate metabolite production, or inoculum variability (Shenoy and Kalagudi, 2005). With the aid of modern technology, phytase can now be genetically inserted into crops (transgenic plants), used as biofertilizers, or added to the soil as pure enzymes. This also applies to all applications of phytate as a source of high phosphorus for animals, especially farm animals. The expression of regulating microbial phytase gene resulting in nutritious transgenic plant varieties might bring a significant outcome to resolve soil phytate consumption issues, as well as a lower dependency on external rock phosphate supply or biofertilizer treatment (Singh and Satyanarayana, 2011). The general mechanism for the transgenic development procedure has been stated in Figure 6.

In the last decade, the genes involved in the synthesis of microbial phytases having a high affinity toward phytate have been utilized to produce transgenic plants. Phytase genes from bacteria, fungi, and yeasts such as *B. subtilis, Selenomonas ruminantium, E. coli, Aspergillus ficuum*, *A. niger*, and *Thermomyces lanuginosus* have been used to develop transgenic plants. The most studied *A. niger* enzyme has been successfully expressed in *Arabidopsis*, tobacco, wheat, maize, soybeans, alfalfa, and canola (Valeeva et al., 2018). Several studies back up the advantages brought forth by transgenic types, such as the high expression of a PHY US417-related gene in *Arabidopsis* that led to increased growth and inorganic phosphorus content without inducing inorganic phosphorus starvation-triggered (PSI) genes. Enhanced biomass and Pi were seen in plants co-cultured with ePHY overexpression when the PSI gene was suppressed (Belgaroui et al., 2016).

Bacillus phytase production in tobacco cell cytoplasm alters the balance of inositol phosphate biosynthesis, providing more accessible phosphate (Singh and Satyanarayana, 2012). *Arabidopsis thaliana*, a transgenic plant grown solely on phytate, demonstrated better growth, which was related to root overexpression of the *A. niger* histidine acidic phosphatase gene phyA. Using *Bacillus* phytases, researchers have acquired further positive results in a transgenic plant (Balaban et al., 2017).

Transgenic soybean plants grew faster and absorbed more P (Singh et al., 2020). Transgenic soy roots produced *A. ficuum* histidine

TABLE 1 Microorganisms producing phytase and having PGPR effects.

Microbial source	Microorganisms	Functions	Reference
Bacteria	*Klebsiella variicola*	Antioxidants Metabolites	Kusale et al. (2021)
	Cedecea davisae	Production of IAA, Ammonia, and phytase and solubilization of inorganic zinc and phosphate	Mazumdar et al. (2020)
	Rahnella aquatilis JZ-GX1	Promotes Seed Germination and Growth	Li et al. (2021)
	Bacillus amyloliquefaciens SQR9	IAA production	Shao et al. (2015)
	Proteus mirabilis BUFF14	Enhanced seed germination	Dhiman et al. (2019)
	Bacillus clausii	Produce lytic enzymes, Siderophores and solubilize inorganic phosphate.	Oulebsir-Mohandkaci et al. (2021)
	Streptomyces sp. (NCIM 5533)	Production of IAA, Ammonia, and phytase and solubilization of inorganic phosphate	Puppala et al. (2019)
	Bacillus subtilis	Enhancement of the growth performance of *Arabidopsis* and tobacco	Belgaroui et al. (2016)
	Bacillus aryabhattai RS1	IAA, ammonia, HCN, and siderophore production	Pal Roy et al. (2017)
	Burkholderia sp. AU4i	Promotes root and shoot elongation in pea	Usha et al. (2015)
	Pseudomonas sp. strain PSB-2	Solubilizing tricalcium phosphate	He and Wan (2022)
	Arthrobacter sp. strain PSB-5	Solubilizing tricalcium phosphate	He and Wan (2022)
Fungi	*Discosia* sp. FIHB 571	Production of siderophores, and biosynthesis of IAA- like auxins	Rahi et al. (2009)
	Penicillium spp. GP15-1	Stimulates growth and disease resistance	Hossain et al. (2014); Banerjee and Dutta (2019)
	Aspergillus awamori	Growth and seed production	Kour et al. (2019)
	Aspergillus niger	Solubilize the rock phosphate and make it available to plants	Din et al. (2019)
	Trichoderma sp.	Shoot and root growth	Kour et al. (2019); Cangussu et al. (2018)
	Rhizopus arrhizus KB-2	Stimulate plant growth	Evstatieva et al. (2020)
Yeast	*Candida tropicalis* HY	Stimulate rice seedling growth by production of IAA and ACC deaminase activity, deproteinization potential	Puppala (2018)
	Saccharomyces cerevisiae NCIM 3662	Hydrolyze phytate, probiotic and fortification properties	Puppala (2018)

acid phytase (afphyA), which had 3.5–6 times the catalytic activity as compared to wild-type control plants for inorganic phosphate (Li et al., 2009). Sapara et al. (2022) studied the effectiveness of phytase gene promoters in transgenic varieties of tomato and cucumber, which were known to enhance minerals and micronutrient concentration, thus supporting nutrigenomics. Some of the transgenic varieties obtained are tabulated in Table 2.

Despite these promising laboratory results, the situation in real-world soils would be less favorable. There is minimal evidence that such transgenic plants boost phosphate absorption and plant development in conventional soils; this has been supported by Blackburn (2012) in his experiments using *Trifolium subterraneum*, which resulted from better P absorption and more remarkable plant development found in agar was hampered when the same plants were exposed to the actual soil. One possible explanation is that phytases that have been released lose their action in soil due to adsorption. This rapid immobilization of the enzyme may limit the phytase's capacity to interact with phytic acid in the soil, negating the previously predicted benefits of such a transgenic method to improve plant metabolism (George et al., 2004).

Bacterial phytases are frequently less expensive to produce and more accessible to express in plants than their eukaryotic counterparts. When using a bacterial phytase to make transgenic plants, it is critical to use an effective expression system inside the plants. Transgenic phytases are frequently introduced into the rhizosphere to aid in the decomposition of soil phytate and the improvement of soil phosphorus bioavailability, further increasing soil fertility and nutrient absorption. Plants engineered to express microbial phytase genes can release extracellular enzymes into the rhizosphere, enhancing phosphorus accumulation in plants. Phytases might reduce the risk of malnutrition while also lowering the phosphorus level of animal excrement. Phytases have enormous commercial and environmental potential. According to the existing literature, either the variation in phytase activity across plants has minimal impact on the phosphate nutrition of soil-grown plants or the baseline levels of phytase activity among plants have equal hydrolytic capacities. However, it is more likely that a significantly more considerable proportion of phytase obtained from microorganisms will disguise the variations in plant-exuded phytase (Liu et al., 2022). A remarkable study by Song et al. (2022) evaluated the effectiveness of the CRISPR/Cas9 mechanism to induce mutation within the phytate utilizing gene expression. They successfully reported the reduced phytic acid content with the deletion of specific gene segments.

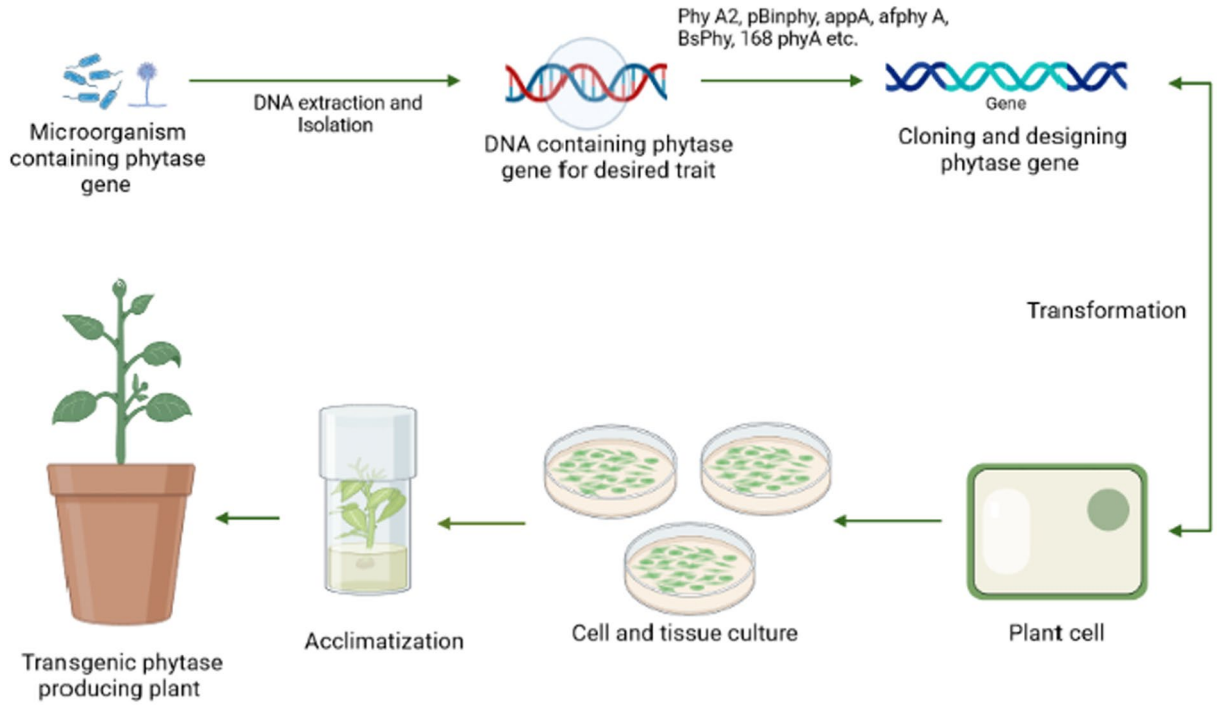

FIGURE 6
A pictorial representation of the steps involved in the generation of a transgenic plant beginning with the screening of an efficient microorganism possessing phytase gene followed by DNA extraction, cloning of phy gene, and transformation to the plant cell, which is further tested *in vivo* by plant tissue culture and then finally implemented to the field.

TABLE 2 Transgenic plants developed in response to positive outcomes.

Source of microorganism	Gene	Plant	Reference
A. niger	*PhyA2*	Maize	Hu et al. (2022); Geetha et al. (2019); Tan et al. (2017)
Aspergillus ficuum	*PhyA2*	Maize	Jiao et al. (2021)
LBA4404 *Agrobacterium*	*PBINphy*	*Brassica napus*	Xu et al. (2020)
Escherichia coli	*appA (mappA)*	Soybean	Zhao et al. (2019)
Aspergillus japonicas	*PhyA*	Wheat	Akhtar et al. (2020); Cangussu et al. (2018)
A. ficuum	*AfphyA*	Soybean	Li et al. (2009); Balaban et al. (2017)
B. subtilis phytase	*BsPhy*	Cucumber	Sapara et al. (2022)
E. coli	*AppA*	Potato	Chen et al. (2020)
A. niger	*PhyA*	*A. thaliana*	Valeeva et al. (2018); Balaban et al. (2017)
B. subtilis	*168phyA*	*A. thaliana*	Valeeva et al. (2018); Lung et al. (2005)
B. subtilis	*168phyA*	Tobacco	Lung et al. (2005)
Aspergillus niger	*PhyA*	*Trifolium subterraneum*	Giles et al. (2017)

Conclusion and future prospective

Microbial phytases have been a need for the current scenario, as such naturally produced enzymes have various advantages, i.e., they are non-toxic, readily available, environmentally safe, and low production cost. Microbial phytases are among the most researched concerning their significance, action mechanism, and mass production. It has been hypothesized that certain phytases have positive health benefits, including heart disease, kidney disorders, and in some types of cancer. The food sector may potentially be interested in employing phytases to generate functional meals as well as to increase mineral bioavailability by lowering the phytate level in a particular product.

Consumers of agricultural goods are worried about their quality, nutritional value, and health. Phosphate solubilizing microorganisms

(PSM) as inoculants is a measure for increased plant production. Although, their efficacy in replenishing the required plant nutrient is dependent on their establishment in the soil after competing for nutrients with natural flora. They are sensitive to plant pathogens due to the production of hydrogen cyanate, antibiotics, and antifungal metabolites. Their use is both environmentally and economically sound. Thus, using PSM as biofertilizers is a viable approach for increasing food production while posing no health risks and conserving the environment, and emerging the development of sustainable soil management. Genetic and protein engineering can be used to modify and improve the characteristics of enzymes. Transgenic plants and animals producing phytase and low-phytate crops are gaining popularity nowadays. Further advances in the creation of application-oriented phytases will usher in a new age in bioprocessing, broadening the scope of its efficiency and applicability. Furthermore, it emphasizes the use of advanced molecular techniques and genetic engineering to produce phytase genes of microbial origin for phytase synthesis. This strategy merits greater consideration since it can provide fresh research opportunities in future.

Author contributions

BN: conceptualization, analyzed the data, written the original draft, and reviewed the manuscript. SR: analyzed the data and wrote the original draft. VijK: conceptualization, analyzed the data, wrote the original draft, and reviewed the manuscript. PEJS: analyzed the data and wrote the original draft. PS: analyzed the data and wrote the original draft. MC: analyzed the data and wrote the original draft. VivK, AV, and SM: writing—review and editing revision. All authors contributed to the article and approved the submitted version.

Acknowledgments

The authors thank the Helsinki University, Helsinki, Finland for open access support.

Conflict of interest

The authors declare that the research was conducted in the absence of any commercial or financial relationships that could be construed as a potential conflict of interest.

Publisher's note

References

Akhtar, A., Rizvi, Z., Irfan, M., Maqbool, A., Bashir, A., and Abdulla Malik, K. (2020). Biochemical and morphological risk assessment of transgenic wheat with enhanced iron and zinc bioaccessibility. *J. Cereal Sci.* 91:102881. doi: 10.1016/j.jcs.2019.102881

Alemzadeh, I., Vaziri, A. S., Khosravi-Darani, K., and Monsan, P. (2022). Enzymes in functional food development. *Novel Food Grade Enzyme* 2022, 217–252. doi: 10.1007/978-981-19-1288-7_9

Ariza, A., Moroz, O. V., Blagova, E. V., Turkenburg, J. P., Waterman, J., Roberts, S. M., et al. (2013). Degradation of phytate by the 6-phytase from hafnia alvei: a combined structural and solution study. *PLoS One* 8:e65062. doi: 10.1371/journal.pone.0065062

Azeem, M., Riaz, A., Chaudhary, A. N., Hayat, R., Hussain, Q., Tahir, M. I., et al. (2014). Microbial phytase activity and their role in organic P mineralization. *Arch. Agron. Soil Sci.* 61, 751–766. doi: 10.1080/03650340.2014.963796

Balaban, N. P., Suleimanova, A. D., Valeeva, L. R., Chastukhina, I. B., Rudakova, N. L., Sharipova, M. R., et al. (2017). Microbial Phytases and Phytate: exploring opportunities for sustainable phosphorus Management in Agriculture. *Am J Mol Biol* 7, 11–29. doi: 10.4236/ajmb.2017.71002

Balogun, D. A., Oke, M. A., Rocha-Meneses, L., Fawole, O. B., and Omojasola, P. F. (2021). Phosphate solubilization potential of indigenous rhizosphere fungi and their biofertilizer formulations. *Agron. Res.* 20, 40–55. doi: 10.15159/ar.21.163

Banerjee, S., and Dutta, S. (2019). Plant growth promoting activities of a fungal strain *Penicillium commune* MCC 1720 and its effect on growth of black gram. *Pharm. Innov.* 8, 121–127.

Behera, B. C., Singdevsachan, S. K., Mishra, R. R., Dutta, S. K., and Thatoi, H. N. (2014). Diversity, mechanism and biotechnology of phosphate solubilising microorganism in mangrove—a review. *Biocatal. Agric. Biotechnol.* 3, 97–110. doi: 10.1016/j.bcab.2013.09.008

Belgaroui, N., Berthomieu, P., Rouached, H., and Hanin, M. (2016). The secretion of the bacterial phytase PHY-US 417 by Arabidopsis roots reveals its potential for increasing phosphate acquisition and biomass production during co-growth. *Plant Biotechol. J.* 14, 1914–1924. doi: 10.1111/pbi.12552

Blackburn, D. M. (2012). Biotechnological agronomic strategies for improving organic p cycling in andisols using cattle manure treated with phytases stabilized in nanoclays. Doctoral dissertation. Araucanía, Chile: Universidad De La Frontera).

Cangussu, A. S. R., Aires Almeida, D., Aguiar, R. W. D. S., Bordignon-Junior, S. E., Viana, K. F., Barbosa, L. C. B., et al. (2018). Characterization of the catalytic structure of plant phytase, protein tyrosine phosphatase-like phytase, and histidine acid phytases and their biotechnological applications. *Enzyme Res.* 2018:824069, 1–12. doi: 10.1155/2018/8240698

Celi, L., and Barberis, E. (2005). "Abiotic stabilization of organic phosphorus in the environment" in *Organic phosphorus in the environment*. eds. B. L. Turner, E. Frossard and D. Baldwin (Cambridge, MA: CABI), 113–132.

Celi, L., Presta, M., Ajmore-Marsan, F., and Barberis, E. (2001). Effects of pH and electrolytes on inositol hexaphosphate interaction with goethite. *Soil Sci. Soc. Am. J.* 65, 753–760. doi: 10.2136/sssaj2001.653753x

Chakraborty, T., and Akhtar, N. (2021). "Biofertilizers: prospects and challenges for future," In *Biofertilizers: Study and Impact*. eds. M. Inamuddin, I. Ahamed, R. Boddula and M. Rezakazem, 575–590.

Chen, B. C., Lin, H. Y., Chen, J. T., Chao, M. L., Lin, H. T., and Chu, W. S. (2020). Compositional analysis of the transgenic potato with high-level Phytase expression. *J. Food Nutr. Res.* 8, 231–237. doi: 10.12691/jfnr-8-5-3

Cookson, P. (2002). Variation in phosphatase activity in soil: a case study. *Agric. Sci.* 7, 65–72.

Dailin, D. J., Hanapi, S. Z., Elsayed, E. A., Sukmawati, D., Azelee, N. I. W., Eyahmalay, J., et al. (2019). "Fungal phytases: biotechnological applications in food and feed industries" in *Recent advancement in white biotechnology through fungi* (Cham: Springer), 65–99.

De Boland, A. R., Garner, G. B., and O'Dell, B. L. (1975). Identification and properties of phytate in cereal grains and oilseed products. *J. Agric. Food Chem.* 23, 1186–1189. doi: 10.1021/jf60202a038

Dersjant-Li, Y., Hruby, M., Evans, C., and Greiner, R. (2019). A critical review of methods used to determine phosphorus and digestible amino acid matrices when using phytase in poultry and pig diets. *J. Appl. Anim. Nutr.* 7:E2. doi: 10.1017/JAN.2019.1

Dhiman, S., Dubey, R. C., Maheshwari, D. K., and Kumar, S. (2019). Sulfur-oxidizing buffalo dung bacteria enhance growth and yield of Foeniculum vulgare mill. *Can. J. Microbiol.* 65, 377–386. doi: 10.1139/cjm-2018-0476

Din, M., Nelofer, R., Salman, M., Khan, F. H., Khan, A., Ahmad, M., et al. (2019). Production of nitrogen fixing Azotobacter (SR-4) and phosphorus solubilizing *Aspergillus niger* and their evaluation on Lagenaria siceraria and Abelmoschus esculentus. *Biotechnol Rep.* 22:e00323. doi: 10.1016/j.btre.2019.e00323

Duong, Q. H., Lapsley, K. G., and Pegg, R. B. (2018). Inositol phosphates: health implications, methods of analysis, and occurrence in plant foods. *J. Food Bioact.* 1, 41–55. doi: 10.31665/jfb.2018.1126

Elhaissoufi, W., Ghoulam, C., Barakat, A., Zeroual, Y., and Bargaz, A. (2022). Phosphate bacterial solubilization: a key rhizosphere driving force enabling higher P use efficiency and crop productivity. *J. Adv. Res.* 38, 13–28. doi: 10.1016/j.jare.2021.08.014

Evstatieva, Y., Ilieva, A., Valcheva, V., and Nikolova, D. (2020). Production of plant growth regulatory metabolites of *Rhizopus arrhizus* KB-2. *Bulg. J. Agric. Sci.* 26, 551–557.

Fujita, K., Kunito, T., Moro, H., Toda, H., Otsuka, S., and Nagaoka, K. (2017). Microbial resource allocation for phosphatase synthesis reflects the availability of inorganic 21 phosphorus across various soils. *Biogeochemistry* 136, 325–339. doi: 10.1007/s10533-017-0398-6

Gaind, S., and Nain, L. (2015). Soil–phosphorus mobilization potential of phytate mineralizing fungi. *J. Plant Nutr.* 38, 2159–2175. doi: 10.1080/01904167.2015.1014561

Geetha, S., Joshi, J. B., Kumar, K. K., Arul, L., Kokiladevi, E., Balasubramanian, P., et al. (2019). Genetic transformation of tropical maize (*Zea mays* L.) inbred line with a phytase gene from *Aspergillus niger*. *3 Biotech* 9, 208–210. doi: 10.1007/s13205-019-1731-7

George, T. S., Richardson, A. E., Hadobas, P. A., and Simpson, R. J. (2004). Characterization of transgenic *Trifolium subterraneum* L. which expresses phyA and releases extracellular phytase: growth and P nutrition in laboratory media and soil. *Plant Cell Environ.* 27, 1351–1361. doi: 10.1111/j.1365-3040.2004.01225.x

Gerke, J. (2010). Humic (organic matter)-Al (Fe)-phosphate complexes: an underestimated phosphate form in soils and source of plant-available phosphate. *Soil Sci.* 175, 417–425. doi: 10.1097/SS.0b013e3181f1b4dd

Gerke, J. (2015). Phytate (inositol hexakisphosphate) in soil and phosphate acquisition from inositol phosphates by higher plants- A review. *Plan. Theory* 4, 253–266. doi: 10.3390/plants4020253

Gerke, J., Beißner, L., and Römer, W. (2000). The quantitative effect of chemical phosphate mobilization by carboxylate anions on P uptake by a single root. I. the basic concept and determination of soil parameters. *J. Plant Nutr. Soil Sci.* 163, 207–212. doi: 10.1002/(sici)1522-2624(200004)163:2%3C207::aid-jpln207%3E3.0.co;2-p

Gessler, N. N., Serdyuk, E. G., Isakova, E. P., and Deryabina, Y. I. (2018). Phytases and the prospects for their application. *Appl. Biochem. Microbiol.* 54, 352–360. doi: 10.1134/s0003683818040087

Giles, C. D., George, T. S., Brown, L. K., Mezeli, M., Shand, C. A., Richardson, A. E., et al. (2017). Linking the depletion of rhizosphere phosphorus to the heterologous expression of a fungal phytase in *Nicotiana tabacum* as revealed by enzyme-labile P and solution 31P NMR spectroscopy. *Rhizosphere* 3, 82–91. doi: 10.1016/j.rhisph.2016.11.004

He, D., and Wan, W. (2022). Distribution of Culturable phosphate-solubilizing bacteria in soil aggregates and their potential for phosphorus acquisition. *Microbiol. Spectr.* 10:e0029022. doi: 10.1128/spectrum.00290-22

Hill, J. E., Richardson, A. E., and Turner, B. L. (2007). "Isolation and assessment of microorganisms that utilize phytate" in *Inositol phosphates: linking agriculture and the environment*. eds. B. L. Turner, A. E. Richardson and E. J. Mullaney (Wallingford, UK: CABI), 61–77.

Hossain, M. M., Sultana, F., Miyazawa, M., and Hyakumachi, M. (2014). The plant growth-promoting fungus *Penicillium* spp. GP15-1 enhances growth and confers protection against damping-off and anthracnose in the cucumber. *J. Oleo Sci.* 63, 391–400. doi: 10.5650/jos.ess13143

Hu, Y., Linghu, L., Li, M., Mao, D., Zhang, Y., Yang, X., et al. (2022). Nutritional components and protein quality analysis of genetically modified phytase maize. *GM Crops Food* 13, 15–25. doi: 10.1080/21645698.2021.2009418

Hussain, S. M., Hanif, S., Sharif, A., Bashir, F., and Iqbal, H. (2022). Unrevealing the sources and catalytic functions of Phytase with multipurpose characteristics. *Catal. Lett.* 152, 1358–1371. doi: 10.1007/s10562-021-03752-z

Jatuwong, K., Suwannarach, N., Kumla, J., Penkhrue, W., Kakumyan, P., and Lumyong, S. (2020). Bioprocess for production, characteristics, and biotechnological applications of fungal phytases. *Front. Microbiol.* 11:188. doi: 10.3389/fmicb.2020.00188

Jiao, P., Yuan, W. Y., Zhao, H. D., Qu, J., Wang, P. W., Guan, S. Y., et al. (2021). Construction of a new plant expression vector and the development of maize germplasm expressing the *Aspergillus ficuum* phytase gene PhyA2. *Genet. Resour. Crop. Evol.* 68, 1103–1115. doi: 10.1007/s10722-020-01052-w

Jorquera, M., Martínez, O., Maruyama, F., Marschner, P., and de la Luz Mora, M. (2008). Current and future bio-technological applications of bacterial phytases and phytase-producing bacteria. *Microbes Environ.* 23, 182–191. doi: 10.1264/jsme2.23.182

Kashirskaya, N. N., Plekhanova, L. N., Chernisheva, E. V., Eltsov, M. V., Udaltsov, S. N., and Borisov, A. V. (2020). Temporal and spatial features of phosphatase activity in natural and human-transformed soils. *Eurasian Soil Sci.* 53, 97–109. doi: 10.1134/s1064229320010093

Kaur, G. (2020). *Microbial phytases in plant minerals acquisition, in: molecular aspects of plant beneficial microbes in agriculture*, Cambridge, MA: Academic Press, pp. 185–194.

Kaur, P., Kunze, G., and Satyanarayana, T. (2007). Yeast phytases: present scenario and future perspectives. *Crit. Rev. Biotechnol.* 27, 93–109. doi: 10.1080/07388550701334519

Konietzny, U., and Greiner, R. (2002). Molecular and catalytic properties of phytate-degrading enzymes (phytases). *Int. J. Food Sci.* 37, 791–812. doi: 10.1046/j.1365-2621.2002.00617.x

Konietzny, U., and Greiner, R. (2004). Bacterial phytase: potential application, in vivo function and regulation of its synthesis. *Braz. J. Microbiol.* 35, 12–18. doi: 10.1590/s1517-83822004000100002

Kour, D., Rana, K. L., Yadav, N., Yadav, A. N., Singh, J., Rastegari, A. A., et al. (2019). "Agriculturally and industrially important fungi: current developments and potential biotechnological applications" in *Recent advancement in white biotechnology through fungi* (Cham: Springer), 1–64.

Kumar, V., and Sinha, A. K. (2018). *General aspects of phytases.In enzymes in human and animal nutrition* (pp. 53–72). Cambridge, MA: Academic Press.

Kusale, S. P., Attar, Y. C., Sayyed, R. Z., Malek, R. A., Ilyas, N., Suriani, N. L., et al. (2021). Production of plant beneficial and antioxidants metabolites by *Klebsiella variicola* under salinity stress. *Molecules* 26:1894. doi: 10.3390/molecules26071894

Ladics, G. S., Han, K. H., Jang, M. S., Park, H., Marshall, V., Dersjant-Li, Y., et al. (2020). Safety evaluation of a novel variant of consensus bacterial phytase. *Toxicol. Rep.* 7, 844–851. doi: 10.1016/j.toxrep.2020.07.004

Lei, X. G., Weaver, J. D., Mullaney, E., Ullah, A. H., and Azain, M. J. (2013). Phytase, A new life for an" old" Enzyme. *Annu. Rev. Anim. Biosci.* 1, 283–309. doi: 10.1146/annurev-animal-031412-103717

Leprince, F., and Quiquampoix, H. (1996). Extracellular enzyme activity in soil: effect of pH and ionic strength on the interaction with montmorillonite of two acid phosphatases secreted by the ectomycorrhizal fungus *Hebeloma cylindrosporum*. *Eur. J. Soil Sci.* 47, 511–522. doi: 10.1111/j.1365-2389.1996.tb01851.x

Li, G. E., Kong, W. L., Wu, X. Q., and Ma, S. B. (2021). Phytase-producing *Rahnella aquatilis* JZ-GX1 promotes seed germination and growth in corn (Zea mays L.). *Microorganisms.* 9:1647. doi: 10.3390/microorganisms9081647

Li, G., Yang, S., Li, M., Qiao, Y., and Wang, J. (2009). Functional analysis of an *Aspergillus ficuum* phytase gene in *Saccharomyces cerevisiae* and its root-specific, secretory expression in transgenic soybean plants. *Biotechnol. Lett.* 31, 1297–1303. doi: 10.1007/s10529-009-9992-6

Liu, X., Han, R., Cao, Y., Turner, B. L., and Ma, L. Q. (2022). Enhancing phytate availability in soils and phytate-P acquisition by plants: a review. *Environ. Sci. Technol.* 56, 9196–9219. doi: 10.1021/acs.est.2c00099

Lung, S. C., Chan, W. L., Yip, W., Wang, L., Yeung, E. C., and Lim, B. L. (2005). Secretion of beta-propeller phytase from tobacco and *Arabidopsis* roots enhances phosphorus utilization. *Plant Sci.* 169, 341–349. doi: 10.1016/j.plantsci.2005.03.006

Madsen, C. K., and Brinch-Pedersen, H. (2020). Globoids and phytase: the mineral storage and release system in seeds. *Int. J. Mol. Sci.* 21:7519. doi: 10.3390/ijms21207519

Mazid, M., and Khan, T. A. (2015). Future of bio-fertilizers in Indian agriculture: an overview. *Int. J. Agric. Res.* 3, 10–23. doi: 10.24102/ijafr.v3i3.132

Mazumdar, D., Saha, S. P., and Ghosh, S. (2020). Isolation, screening and application of a potent PGPR for enhancing growth of chickpea as affected by nitrogen level. *Int. J. Veg. Sci.* 26, 333–350. doi: 10.1080/19315260.2019.1632401

Menezes, A. G. T., Ramos, C. L., Cenzi, G., Melo, D. S., Dias, D. R., and Schwan, R. F. (2020). Probiotic potential, antioxidant activity, and phytase production of indigenous yeasts isolated from indigenous fermented foods. *Probiotics Antimicrob Proteins* 12, 280–288. doi: 10.1007/s12602-019-9518-z

Menezes-Blackburn, D., Inostroza, N. G., Gianfreda, L., Greiner, R., Mora, M. L., and Jorquera, M. A. (2016). Phytase-producing bacillus sp. inoculation increases phosphorus availability in cattle manure. *J. Soil Sci. Plant Nutr.* 16, 200–210. doi: 10.4067/S0718-95162016005000016

Menezes-Blackburn, D., Jorquera, M. A., Greiner, R., Gianfreda, L., and de la Luz Mora, M. (2013). Phytases and phytase-labile organic phosphorus in manures and soils. *Crit. Rev. Environ. Sci. Technol.* 43, 916–954. doi: 10.1080/10643389.2011.627019

Mohite, B. V., Marathe, K., Salunkhe, N., and Patil, S. V. (2022). "Isolation and screening of phytase producing microorganisms: an essential bioinput for soil fertility" in *Practical handbook on agricultural microbiology* (New York, NY: Humana), 337–341.

Molina, D. C., Poisson, G. N., Kronberg, F., and Galvagno, M. A. (2021). Valorization of an Andean crop (yacon) through the production of a yeast cell-bound pytase. *Biocatal. gric. Biotechnol.* 36:102116. doi: 10.1016/j.bcab.2021.102116

Nannipieri, P., Giagnoni, L., Landi, L., and Renella, G. (2011). "Role of phosphatase enzymes in soil" in *Phosphorus in action* (Berlin, Heidelberg: Springer), 215–243.

Oulebsir-Mohandkaci, H., BenzinaTihar, F., and Hadjouti, R. (2021). Exploring biofertilizer potential of plant growth-promoting rhizobacteria *Bacillus clausii* strain B8 (MT305787) on *Brassica napus* and *Medicago sativa*. *Not. Bot. Horti. Agrobot. Cluj. Napoca.* 49:12484. doi: 10.15835/nbha49412484

Pal Roy, M., Datta, S., and Ghosh, S. (2017). A novel extracellular low-temperature active phytase from *bacillus aryabhattai* RS1 with potential application in plant growth. *Biotechnol. Prog.* 33, 633–641. doi: 10.1002/btpr.2452

Puppala, K.R. (2018). Studies on Phytase producing yeasts and its application in food and agriculture. PhD Thesis. Pune, India: CSIR-National Chemical Laboratory.

Puppala, K. R., Bhavsar, K., Sonalkar, V., Khire, J. M., and Dharne, M. S. (2019). Characterization of novel acidic and thermostable phytase secreting Streptomyces sp. (NCIM 5533) for plant growth promoting characteristics. *Biocatal. Agric. Biotechnol.* 18:101020. doi: 10.1016/j.bcab.2019.101020

Ranoarisoa, M. P., Trap, J., Pablo, A. L., Dezette, D., and Plassard, C. (2020). Micro-food web interactions involving bacteria, nematodes, and mycorrhiza enhance tree P

nutrition in a high P-sorbing soil amended with phytate. *Soil Biol. Biochem.* 143:107728. doi: 10.1016/j.soilbio.2020.107728

Rahi, P., Vyas, P., Sharma, S., Gulati, A., and Gulati, A. (2009). Plant growth promoting potential of the fungus Discosia sp. FIHB 571 from tea rhizosphere tested on chickpea, maize and pea. *Indian J Microbiol.* 49, 128–133.

Rao, D.E.C.S., Rao, K.V, Reddy, T.P., and Reddy, V.D. (2009). Molecular characterization, physicochemical properties, known and potential applications of phytases: an overview. *Crit. Rev. Biotechnol.* 29, 182–198. doi: 10.1080/07388550902919571

Richardson, A. E., Lynch, J. P., Ryan, P. R., Delhaize, E., Smith, F. A., Smith, S. E., et al. (2011). Plant and microbial strategies to improve the phosphorus efficiency of agriculture. *Plant Soil* 349, 121–156. doi: 10.1007/s11104-011-0950-4

Rix, G. D., Sprigg, C., Whitfield, H., Hemmings, A. M., Todd, J. D., and Brearley, C. A. (2022). Characterization of a soil MINPP phytase with remarkable long-term stability and activity from *Acinetobacter* sp. *PLoS One* 17:e0272015. doi: 10.1371/journal.pone.0272015

Sadaf, N., Haider, M. Z., Iqbal, N., Abualreesh, M. H., and Alatawi, A. (2022). Harnessing the Phytase production potential of soil-borne fungi from wastewater irrigated fields based on eco-cultural optimization under shake flask method. *Agriculture* 12:103. doi: 10.3390/agriculture12010103

Sapara, K. K., Agarwal, P., Gupta, K., and Agarwal, P. K. (2022). Expression of *B. subtilis* phytase gene driven by fruit specific E8 promoter for enhanced minerals, metabolites and phytonutrient in cucumber fruit. *Int. Food Res. J.* 156:111138. doi: 10.1016/j.foodres.2022.111138

Secco, D., Bouain, N., Rouached, A., Prom-u-Thai, C., Hanin, M., Pandey, A. K., et al. (2017). Phosphate, phytate and phytases in plants: from fundamental knowledge gained in Arabidopsis to potential biotechnological applications in wheat. *Crit. Rev. Biotechnol.* 37, 898–910. doi: 10.1080/07388551.2016.1268089

Shahryari, Z., Fazaelipoor, M. H., Setoodeh, P., Nair, R. B., Taherzadeh, M. J., and Ghasemi, Y. (2018). Utilization of wheat straw for fungal phytase production. *Int. J. Recycl. Org. Waste Agric.* 7, 345–355. doi: 10.1007/s40093-018-0220-z

Shao, J., Xu, Z., Zhang, N., Shen, Q., and Zhang, R. (2015). Contribution of indole-3-acetic acid in the plant growth promotion by the rhizospheric strain *bacillus amyloliquefaciens* SQR9. *Biol. Fertil. Soils* 51, 321–330. doi: 10.1007/s00374-014-0978-8

Sharma, S. B., Sayyed, R. Z., Trivedi, M. H., and Gobi, T. A. (2013). Phosphate solubilizing microbes: sustainable approach for managing phosphorus deficiency in agricultural soils. *Springer Plus.* 2, 1–14. doi: 10.1186/2193-1801-2-587

Shenoy, V. V., and Kalagudi, G. M. (2005). Enhancing plant phosphorus use efficiency for sustainable cropping. *Biotechnol. Adv.* 23, 501–513. doi: 10.1016/j.biotechadv.2005.01.004

Singh, B., Boukhris, I., Kumar, V., Yadav, A. N., Farhat-khemakhem, A., Kumar, A., et al. (2020). Contribution of microbial phytases to the improvement of plant growth and nutrition: a review. *Pedosphere* 30, 295–313. doi: 10.1016/s1002-0160(20)60010-8

Singh, N., Kuhar, S., Priya, K., Jaryal, R., and Yadav, R. (2018). "Phytase: the feed enzyme, an overview" in *Advances in animal biotechnology and its applications*. eds. S. K. Gahlawat, J. S. Duhan, R. J. Salar, P. Siwach, S. Kumar and P. Kaur, 269–327.

Singh, P., Kumar, V., and Agrawal, S. (2014). Evaluation of phytase producing bacteria for their plant growth promoting activities. *Int. J. Microbiol.* 2014:426483. doi: 10.1155/2014/426483

Singh, B., and Satyanarayana, T. (2011). Microbial phytases in phosphorus acquisition and plant growth promotion. *Physiol. Mol. Biol. Plants* 17, 93–103. doi: 10.1007/s12298-011-0062-x

Singh, B., and Satyanarayana, T. (2012). "Plant growth promotion by phytases and phytase-producing microbes due to amelioration in phosphorus availability" in *Microorganisms in Sustainable Agriculture and Biotechnology*. eds. T. Satyanarayana, B. N. Johri and A. Prakash, 3–15.

Singh, B., and Satyanarayana, T. (2015). Fungal phytases: characteristics and amelioration of nutritional quality and growth of non-ruminants. *J. Anim. Physiol. Anim. Nutr.* 99, 646–660. doi: 10.1111/jpn.12236

Singh, B., Sharma, K. K., Kumari, A., Kumar, A., and Gakhar, S. K. (2018). Molecular modeling and docking of recombinant HAP-phytase of a thermophilic mould *Sporotrichum thermophile* reveals insights into molecular catalysis and biochemical properties. *Int. J. Biol. Macromol.* 115, 501–508. doi: 10.1016/j.ijbiomac.2018.04.086

Soman, S., Kumarasamy, S., Narayanan, M., and Ranganathan, M. (2020). Biocatalyst: phytase production in solid state fermentation by OVAT strategy. *Bioin. Res App Chem* 10, 6119–6127. doi: 10.33263/briac105.61196127

Song, J. H., Shin, G., Kim, H. J., Lee, S. B., Moon, J. Y., Jeong, J. C., et al. (2022). Mutation of GmIPK1 gene using CRISPR/Cas9 reduced phytic acid content in soybean seeds. *Int. J. Mol. Sci.* 23:10583. doi: 10.3390/ijms231810583

Sun, M., He, Z., and Jaisi, D. P. (2021). Role of metal complexation on the solubility and enzymatic hydrolysis of phytate. *PLoS One* 16:e0255787. doi: 10.1371/journal.pone.0255787

Sun, D., Zhang, W., Feng, H., Li, X., Han, R., Turner, B. L., et al. (2022). Novel phytase PvPHY1 from the as-hyper accumulator *Pteris vittata* enhances P uptake and phytate hydrolysis and inhibits as translocation in plant. *J. Hazard. Mater.* 423:127106. doi: 10.1016/j.jhazmat.2021.127106

Taj, M. Y., and Mohan, E. (2022). Growth performance of *coriandrum sativum* L. inoculated with biofertilizers - an initial study. *J. Adv. Agric.* 13, 396–399. doi: 10.55218/jasr.202213149

Tan, Y., Tong, Z., Yluang, Q., Sun, Y., Jin, X., Peng, C., et al. (2017). Proteomic analysis of phytase transgenic and non-transgenic maize seeds. *Sci. Rep.* 7, 9246–9211. doi: 10.1038/s41598-017-09557-8

Tang, J., Leung, A., Leung, C., and Lim, B. L. (2006). Hydrolysis of precipitated phytate by three distinct families of phytases. *Soil Biol. Biochem.* 38, 1316–1324. doi: 10.1016/j.soilbio.2005.08.021

Thorsen, M., Nielsen, L. A., Zhai, H. X., Zhang, Q., Wulf-Andersen, L., and Skov, L. K. (2021). Safety and efficacy profile of a phytase produced by fermentation and used as a feed additive. *Heliyon* 7:e07237. doi: 10.1016/j.heliyon.2021.e07237

Trivedi, S., Husain, I., and Sharma, A. (2022). Purification and characterization of phytase from *Bacillus subtilis* P6: evaluation for probiotic potential for possible application in animal feed. *Food Front.* 3, 194–205. doi: 10.1002/fft2.118

Turner, B. L., Cheesman, A. W., Godage, H. Y., Riley, A. M., and Potter, B. V. (2012). Determination of neo- and D-chiro-inositol hexakisphosphate in soils by solution 31P NMR spectroscopy. *Environ. Sci. Technol.* 46, 4994–5002. doi: 10.1021/es204446z

Usha, D., Indu, K., Reena, V. S., Lalit, K., Devender, S., and Gupta, A. (2015). Genomic and functional characterization of a novel *Burkholderia* sp. strain AU4i from pea rhizosphere conferring plant growth promoting activities. *Adv. Genet. Eng.* 4:129. doi: 10.4172/2169-0111.1000129

Valeeva, L. R., Nyamsuren, C., Sharipova, M. R., and Shakirov, E. V. (2018). Heterologous expression of secreted bacterial BPP and HAP phytases in plants stimulates *Arabidopsis thaliana* growth on phytate. *Front. Plant Sci.* 9:186. doi: 10.3389/fpls.2018.00186

Vats, P., and Banerjee, U. C. (2004). Production studies and catalytic properties of phytases (myoinositolhexakisphosphate phosphohydrolases): an overview. *Enzym. Microb. Technol.* 35, 3–14. doi: 10.1016/j.enzmictec.2004.03.010

Wang, W., Tan, J., Li, S., Guan, Y., Zhang, X., Wang, N., et al. (2022). Transport, retention and release of phytate in soil with addition of mg–Al layered double hydroxides. *J. Clean. Prod.* 379:134774. doi: 10.1016/j.jclepro.2022.134774

Weil, R. R., and Brady, N. C. (2017). *Soil organic matter. Nature and properties of soils*. (*15th ed.*). Pearson Education Limited, London, UK, 545–601.

Wu, Q., Zhou, W., Lu, Y., Li, S., Shen, D., Ling, Q., et al. (2022). Combined chemical fertilizers with molasses increase soil stable organic phosphorus mineralization in sugarcane seedling stage. *Sugar Tech.*, 1–10. doi: 10.1007/s12355-022-01196-2

Xiao, K., Harrison, M. J., and Wang, Z. Y. (2005). Transgenic expression of a novel *M. truncatula* phytase gene results in improved acquisition of organic phosphorus by arabidopsis. *Planta* 222, 27–36. doi: 10.1007/s00425-005-1511-y

Xu, L., Zeng, L., Ren, L., Chen, W., Liu, F., Yang, H., et al. (2020). Marker-free lines of phytase-transgenic *Brassica napus* show enhanced ability to utilize phytate. *Plant Cell Tissue Organ Cult.* 140, 11–22. doi: 10.1007/s11240-019-01706-3

Yang, M., and Yang, H. (2021). Utilization of soil residual phosphorus and internal reuse of phosphorus by crops. *Peer J* 9:e11704. doi: 10.7717/peerj.11704

Zhao, T., Yong, X., Zhao, Z., Dolce, V., Li, Y., and Curcio, R. (2021). Research status of bacillus phytase. *3 Biotech* 11, 415–414. doi: 10.1007/s13205-021-02964-9

Zhao, Y., Zhu, L., Lin, C., Shen, Z., and Xu, C. (2019). Transgenic soybean expressing a thermo stable phytase as substitution for feed additive phytase. *Sci. Rep.* 9, 1–7. doi: 10.1038/s41598-019-51033-y

frontiers | Frontiers in Microbiology

TYPE Review
PUBLISHED 31 May 2023
DOI 10.3389/fmicb.2023.1197081

OPEN ACCESS

EDITED BY
Muhammad Zahid Mumtaz,
The University of Lahore, Pakistan

REVIEWED BY
Amilton Barbosa Botelho Junior,
University of São Paulo, Brazil
Rajesh Ramdas Waghunde,
Navsari Agricultural University, India
Yayun Ma,
Central South University, China

*CORRESPONDENCE
Basanta Kumar Biswal
✉ pupun.biswal@gmail.com
Rajasekhar Balasubramanian
✉ ceerbala@nus.edu.sg

RECEIVED 30 March 2023
ACCEPTED 09 May 2023
PUBLISHED 31 May 2023

CITATION
Biswal BK and Balasubramanian R (2023) Recovery of valuable metals from spent lithium-ion batteries using microbial agents for bioleaching: a review.
Front. Microbiol. 14:1197081.
doi: 10.3389/fmicb.2023.1197081

Recovery of valuable metals from spent lithium-ion batteries using microbial agents for bioleaching: a review

Basanta Kumar Biswal* and Rajasekhar Balasubramanian*

Department of Civil and Environmental Engineering, National University of Singapore, Singapore, Singapore

Spent lithium-ion batteries (LIBs) are increasingly generated due to their widespread use for various energy-related applications. Spent LIBs contain several valuable metals including cobalt (Co) and lithium (Li) whose supply cannot be sustained in the long-term in view of their increased demand. To avoid environmental pollution and recover valuable metals, recycling of spent LIBs is widely explored using different methods. Bioleaching (biohydrometallurgy), an environmentally benign process, is receiving increased attention in recent years since it utilizes suitable microorganisms for selective leaching of Co and Li from spent LIBs and is cost-effective. A comprehensive and critical analysis of recent studies on the performance of various microbial agents for the extraction of Co and Li from the solid matrix of spent LIBs would help for development of novel and practical strategies for effective extraction of precious metals from spent LIBs. Specifically, this review focuses on the current advancements in the application of microbial agents namely bacteria (e.g., *Acidithiobacillus ferrooxidans* and *Acidithiobacillus thiooxidans*) and fungi (e.g., *Aspergillus niger*) for the recovery of Co and Li from spent LIBs. Both bacterial and fungal leaching are effective for metal dissolution from spent LIBs. Among the two valuable metals, the dissolution rate of Li is higher than Co. The key metabolites which drive the bacterial leaching include sulfuric acid, while citric acid, gluconic acid and oxalic acid are the dominant metabolites in fungal leaching. The bioleaching performance depends on both biotic (microbial agents) and abiotic factors (pH, pulp density, dissolved oxygen level and temperature). The major biochemical mechanisms which contribute to metal dissolution include acidolysis, redoxolysis and complexolysis. In most cases, the shrinking core model is suitable to describe the bioleaching kinetics. Biological-based methods (e.g., bioprecipitation) can be applied for metal recovery from the bioleaching solution. There are several potential operational challenges and knowledge gaps which should be addressed in future studies to scale-up the bioleaching process. Overall, this review is of importance from the perspective of development of highly efficient and sustainable bioleaching processes for optimum resource recovery of Co and Li from spent LIBs, and conservation of natural resources to achieve circular economy.

KEYWORDS

spent Li-ion batteries, cathode material, bioleaching, biohydrometallurgy, metal recovery, lithium and cobalt, sustainability, circular economy

1. Introduction

Lithium-ion batteries (LIBs) are widely used in electric vehicles, energy storage systems, mobile phones, and other portable electronic devices for energy storage applications (Martins et al., 2021; Miao et al., 2022). The use of LIBs as energy storage devices is mainly due to their high energy density, high reliability, higher output voltage, fast charging ability, higher resistance to self-discharge, light weight and longer lifetime (Miao et al., 2022; Alipanah et al., 2023). There is a huge demand for LIBs (USD$36.7 billion in 2019), and it is projected to increase by nearly fourfold (i.e., USD$129.3 billion) by 2027 (Dyatkin and Meng, 2020). The global LIB production capacity is estimated to increase from 455 GWh in 2020 to 1,447 GWh in 2025, i.e., with a compound annual growth rate (CAGR) of 26% (Alipanah et al., 2021). Notably, China was the major producer of LIBs, e.g., in 2020, contributing to 77% of the total LIBs production globally (Alipanah et al., 2021). Due to explosive production and usage of LIB-based portable and non-portable devices, a huge amount of spent LIBs is generated (Golmohammadzadeh et al., 2022). The amount of spent LIBs generated has been estimated to reach 640,000 metric tons in China by 2025 (Yang et al., 2022), while in Australia, it is expected to reach 137,000 metric tons by the end of 2036 (Golmohammadzadeh et al., 2022). With the assumption that the average lifespan of LIBs used in automotive applications (e.g., electric vehicles) is 10 years, it is projected that 700,000 metric tons of LIBs will reach their end of life by 2025 globally (Alipanah et al., 2021).

The different components of spent LIBs and their corresponding percentage in the total weight are: cathode (35%), battery case (25–30%), anode (15–18%), electrolyte (11–12%), plastic materials (5–6%) and others (mass loss during treatment, e.g., drying, 3–4%) (Horeh et al., 2016; Heydarian et al., 2018). $LiCoO_2$ (lithium cobalt oxide) is one of the most preferred cathodes than other lithium oxides-based cathodes and extensively used in portable electronic devices at the current time. The use of $LiCoO_2$ is likely to continue in the future primarily due to its high energy density and longevity (Zeng et al., 2014; Zhang et al., 2022). The two major metals in spent LIBs (with $LiCoO_2$ as cathode material) are cobalt (Co) which is detected up to 30.4% and lithium (Li) which is found up to 10.3% of the total weight of spent LIBs (Heydarian et al., 2018). Other elements detected in spent LIBs at varying concentrations include nickel (Ni), manganese (Mn), copper (Cu), aluminum (Al) and iron (Fe) (**Table 1**). The concentration of Cu, Ni and Mn in spent LIBs varies between 6–12%, 5–10% and 5–11%, respectively (Roy et al., 2021a; Ratnam et al., 2022). The concentration of these elements varies in natural ores depending on the types of minerals (e.g., primary vs. secondary minerals, or based on the chemical groups, e.g., sulfide, arsenide, carbonate, oxide-containing ores) (Dehaine et al., 2021). For example, carrollite which is a sulfide-containing mineral contains 28.56% Co, 20.53% Cu and 9.48% Ni, while skutterudite (arsenide containing mineral) contains only 17.95% Co and 5.96% Ni (Dehaine et al., 2021). There are variations of metal contents in spent LIBs which is possibly due to variations of manufactory (battery chemistry) (Xin et al., 2016; Sethurajan and Gaydardzhiev, 2021). As a result of a significant increase of LIBs production worldwide, the price of some of the metals used in LIBs considerably increased, e.g., the Co price increased nearly 4 times in the last 2 years, from US$ 22 /kg to US$ 81 /kg (Du et al., 2022). According to a recent study, the price of Li also increased by three-times (Ratnam et al., 2022). Fan et al. (2020) reported that the average price of Co was US$ 75,991.27/ton in 2018, which was 10 and 5 times higher than that of Mn and Ni, respectively. With the current trend of increasing production of LIBs, nearly 70% of the global Co reserves is expected to be spent for battery production by 2040, and the demand for LIBs is projected to go beyond its supply by 2030 (Alipanah et al., 2023). At present, 35% of the globally produced Li and 25% of globally produced Co are utilized for LIBs production and it is estimated that the Li consumption could be doubled (66%) by 2025 (Swain, 2017; Golmohammadzadeh et al., 2022). It should be noted that the global reserves for Co and Li are limited to nearly 145 million tons and 62 million tons, respectively (Fan et al., 2020).

Disposal of LIBs used in electronic applications as part of various solid waste streams due to their limited life span (e.g., the typical life span of $LiCoO_2$-based LIB is 1–2 years, 500–1,000 cycles) is an issue of concern (Aboelazm et al., 2021; Lin et al., 2021; Yu et al., 2022). The reason for this concern is that improper management and disposal of untreated spent LIBs could pose negative effects on human health, environment and ecosystems (Huang et al., 2019). Metals namely Co and Ni present in LIBs are categorized as carcinogenic and mutagenic materials. Furthermore, the toxic organic electrolytes/solvents used in LIBs could have adverse impacts on the human health and environment (Fan et al., 2020). The polymers like polyethylene and polypropylene used in separators could also pose negative environmental effects (e.g., cause microplastic pollution) (Golmohammadzadeh et al., 2022; Ratnam et al., 2022). The spent LIBs are considered as secondary source of metals, and sometimes, the metal quantity (e.g., concentration) is higher than what is available in the concentrated ores or natural ores (Xi et al., 2015). In view of the limited supply of Li and Co, it is important to reduce the high demand on the natural metal resources, save the valuable metals present in the spent LIBs and mitigate environmental pollution caused by the hazardous components of spent LIBs, spent LIBs should be appropriately handled and recycled.

Recycling could play a major role in the overall sustainability of future LIBs by recycling the secondary metallic resources and also contribute to the circular economy (Golmohammadzadeh et al., 2022). It is reported that recycling and reuse of valuable metals namely Co and Ni from spent LIBs could save 51.3% of natural resources and reduce the mining of metals from the virgin mineral sources (Dewulf et al., 2010). The recovered valuable metals from spent LIBs can be reused in LIBs or other products including supercapacitors (Ratnam et al., 2022). The commonly used recycling methods for spent LIBs include direct recycling, pyrometallurgy, hydrometallurgy and biohydrometallurgy (bioleaching) (Golmohammadzadeh et al., 2022; Roy et al., 2022). The major advantages and disadvantages of various types of recycling methods are given in **Table 2**. Among the various types of recycling methods, bleaching is cost-effective, environmentally friendly, simple in operation and less energy intensive (Golmohammadzadeh et al., 2022; Mokarian et al., 2022). As of 2018, the recycling rate of LIBs was only 8.86% (Mao et al., 2022), and the global rate of Li recycling is even lower (i.e., $< 1\%$) (Swain, 2017).

Although LIBs dominate in the various energy markets (e.g., from portable electronic devices to electric vehicles) (Wu Y. et al., 2019), from the sustainability perspectives (e.g., to reduce carbon footprint), recently increasing interest is given on the development of renewable/green energy (e.g., solar, wind and biomass-based energy) (Qazi et al., 2019; Ray et al., 2022). Specifically, in the biomass-based energy, diverse microalgae species are explored for their potential as a feedstock for biofuel production (Nayak et al., 2018, 2020). For the sustainable energy systems, biomass-based electrode materials (e.g., anode: bio-graphite) and bio-based solid electrolytes are explored in LIBs (Sagues et al., 2020; Raj et al., 2022). According to Sagues et al. (2020) the softwood-derived bio-graphite in a LIB cell shows 89% capacity retention over 100 cycles and more than 99% coulombic efficiency. Another study reported that the use of carbonated soybean oil-based electrolyte in LFP batteries exhibited the gravimetric capacity of 112 and 157 mAh/g at room temperature and 60 °C, respectively (Raj et al., 2022).

To understand the current state of knowledge on the recycling of spent LIBs, this review comprehensively analyzed the publication trend in the last 10 years (2013–2022) using the scientific database (e.g., Scopus) (**Supplementary Figure 1**). The two keywords used in the Scopus search engine are "spent Lithium-ion batteries" and "recycling" which resulted in 1,268 publications with only 15 publications in 2013, but 360 publications in 2022 (i.e., increased by 24 times). The continuous increase of publications pertaining to spent LIBs in the past 10 years indicates that there is an increasing interest among scientific communities to develop novel and sustainable technologies for the recycling of spent LIBs to recover valuable metals present in spent LIBs and contribute to environmental protection. A major fraction of these publications is related to the recycling of spent LIBs using the pyrometallurgy, hydrometallurgy or direct recycling. Previous studies have also reported that the above three methods are widely used for the recycling of spent LIBs (Zeng et al., 2014; Mao et al., 2022). In terms of the distribution of publications in various countries, around 60% of articles were published by researchers in China, followed by the United States (9%) and India (6%). Further analysis in the Scopus database employing the keywords namely "spent Lithium-ion batteries," "bioleaching" and/or "biohydrometallurgy" revealed a total of 53 publications (37 journal articles, 8 review articles, 6 book chapters and 2 conference papers), indicating that bioleaching is getting much attention as an emerging environmentally friendly method. The flowchart for the review methodology is presented in **Supplementary Figure 2**. However, it should be noted that bioleaching is largely explored in the lab-scale mode for the recovery of valuable metals from spent LIBs. The most articles included in each subsection are mostly peer-reviewed articles published in 2013–2022 which are collected from the various online scientific database namely Scopus, Web of Science, and Google Scholar by using the keywords relevant to the particular section. Additionally, the relevance and data quality were further checked by reading the abstract and/or specific sections of the article.

Our literature review shows that a few review papers dealing with bioleaching of valuable metals in spent LIBs have been published (Moazzam et al., 2021; Roy et al., 2021a, 2022; Sethurajan and Gaydardzhiev, 2021) among which one review mainly focused on the Li bioleaching (Moazzam et al., 2021). However, limited information is available on the comparative evaluation on the

TABLE 1 Metal contents in spent Li-ion batteries (LIBs) reported in various studies.

	Quantity of key metals in spent LIBs (%, w/w)							
Method	Co	Li	Cu	Mn	Fe	Al	Ni	References
Chemical digestion	22.05	3.03	2.55	0.44	0.38	4.27	0.05	Roy et al., 2021b
Chemical digestion	16.0	2.1	0.62	0.07	–	–	0.04	Biswal et al., 2018
Chemical digestion	7.44	5.16	2.82	9.1	0.97	0.62	15.96	Jegan-Roy et al., 2021
Chemical digestion	16.54	2.22	5.93	21.31	0.04	9.12	2.56	Horeh et al., 2016
Chemical digestion	30.4	10.3	0.6	5.2	2.2	0.3	8.2	Heydarian et al., 2018
Chemical digestion	15.6	4.2	8.1	20.5	0.5	4.8	15	Xin et al., 2016
Chemical digestion	–	4.5	5.4	26.5	2.3	5.2	–	Xin et al., 2016
Chemical digestion	–	5.0	7.6	–	25	4.4	–	Xin et al., 2016
Chemical digestion	–	2.76	–	–	–	–	–	Badawy et al., 2013
Chemical digestion	31.18	7.04	0.22	5.02	0.93	0.61	9.07	Ghassa et al., 2021
Chemical digestion	46	2.0	–	0.85	–	1.5	2.7	Alavi et al., 2021
Chemical digestion	20.46	3.74	–	23.65	–	6.14	3.45	Nazerian et al., 2023
XRF	17.11	–	6.6	22	0.19	9.45	2.82	Horeh et al., 2016
XRF	48	–	–	0.87	–	1.52	2.8	Alavi et al., 2021
XRF	53.82	–	0.20	1.67	–	0.12	2.99	Hariyadi et al., 2022b
EDX	48.5	3.37	–	23.9	0.14	–	24.1	Li et al., 2013
EDX	48.5	3.37	–	23.9	0.14	–	–	Zeng et al., 2012
EDX	38.54	–	–	1.03	–	2.08	–	Hariyadi et al., 2022a

In chemical digestion method, metal analysis was done mainly using the inductively coupled plasma optical emission spectroscopy (ICP-OES) instrument. XRF, X-ray fluorescence spectroscopy; EDX, energy-dispersive X-ray spectroscopy analysis.

performance of bacterial and fungal-based bioleaching for recovery of major elements such as Co and Li from spent LIBs. Discussion on the quality and quantity of metabolites (bio-acids) produced due to interactions of LIB components (e.g., metals) with bacteria or fungi which drive the bioleaching process is scant. Application of possible biological and/or chemical methods for the recovery of Co and Li from the aqueous bioleaching media (e.g., transformation of dissolved metals into solid form through precipitation) was not sufficiently addressed in the past reviews. Understanding of the bioleaching kinetics is important to optimize the process performance which was found to be missing in the earlier reviews. From the circular economy perspective, critical discussion on the sustainability of the bleaching method for the recovery of valuable metals from spent LIB is necessary, but this was not considered previously.

The main objective of this review is to comprehensively analyze the recent developments in the literature on the application of microbial agents namely bacteria and fungi for the recovery of valuable metals (mainly Co and Li) from spent LIBs. The influence of various factors including bioleaching conditions (e.g., leaching medium pH, pulp density, aeration and substrate/energy source concentrations) and spent LIBs characteristics (e.g., powder particle size) on the recovery of valuable metals was assessed. Insights into microbe- metal interactions and the associated bioleaching mechanisms are presented. The sustainability of the bioleaching method is critically discussed. The key knowledge gaps that currently exist in literature and future research directions for further development of the bioleaching method with improved efficiency and sustainability are highlighted.

2. Overview of the development and chemistry of Li-ion batteries (LIBs)

The initial discovery of LIBs was done in 1970s. However, the first commercial LIB was produced by Sony in 1991 (Baum et al., 2022; Yang et al., 2022). In 2019, three scientists namely John B Goodenough, M Stanley Whittingham, and Akira Yoshino won the highly prestigious Nobel Prize in Chemistry for their pioneering works on the development of LIBs (Kamat, 2019; Service, 2019). In the battery technology, the key motivation is to use Li metal in the cathodic materials since Li is the most electropositive (−3.04 V) and lightest metal (molecular weight: 6.94 g/mol and specific gravity: 40.53 g/cm^3), therefore enabling the design of storage systems with high energy density (Tarascon and Armand, 2001). The key chemical reactions involving in the primary non-rechargeable LIBs (e.g., the common Zn/MnO_2 "Alkaline" cell) (Eqs. 1, 2) (Huggins, 2016; Roy et al., 2022) and secondary rechargeable LIBs

TABLE 2 Comparison of potential advantages and disadvantages of commonly used LIB recycling methods (Roy et al., 2021a, 2022; Golmohammadzadeh et al., 2022; Mao et al., 2022).

Recycling method	Advantages	Disadvantages
Direct recycling	Practically feasible to recover different components of spent LIBs	Recovered materials may not perform like virgin material
	Active materials can be recovered with original chemical structures	Mixing of cathode material could decrease the quality of the recycled material
	Energy efficient	Regeneration process is not developed yet
	Economically feasible	It is remains at laboratory-scale, not applied industrial-scale
Pyrometallurgy	All types of spent LIBs with different chemistries can be recycled without sorting or treatment	Loss of lithium in the recycling process (formation of slag)
	Recovery of metals as alloys due to direct melting	Not suitable to recover Fe, Al and Mn
	Fast and high efficiency (high recovery of various metals including Co, Co and Ni)	High energy demand (operation and maintenance)
	Direct feeding into furnace allows practical large-scale operation	Emission of dust and toxic gases (e.g., CO_2)
	No wastewater generation	Purity of final product is expected to be low
	Lower possessing steps compared to the hydrometallurgical method	Not a flexible process
Hydrometallurgy	Applicable to any LIBs chemistries	Recycling involves complex and multi-steps operation
	Process is flexible to recover a specific target metal	Need pre-treatment of spent LIBs (e.g., discharging, shredding, sieving and separation)
	High process efficiency with high purity of the extracted metals	Changes of cathode material structure due to acid treatment
	High environmental sustainability due to less emission of hazardous gases	Formation of large volume of corrosive (acidic) wastewater
	Cost-effective and less energy demand	Need additional capital investment for treatment of wastewater
Biohydrometallurgy (Bioleaching)	Environmentally friendly	Slow process kinetics
	Low operation cost and energy requirement	Long processing time
	Minimal use of chemical reagents	Not feasible in high toxic environment
	Achieve high efficiency at low metal concentration	Low efficiency at higher pulp density
	Less issue of toxic gas generation	Hard process control measures

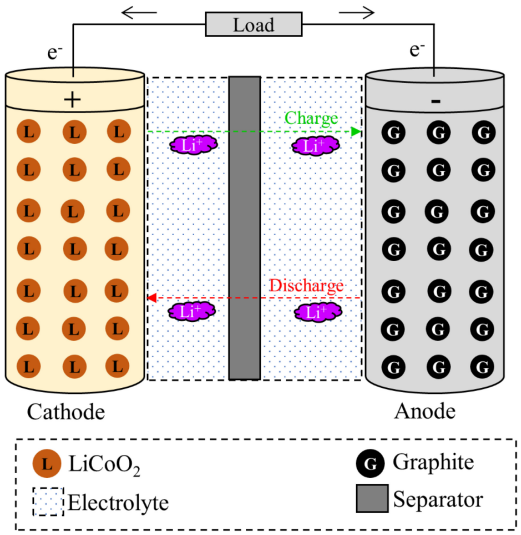

FIGURE 1
Schematic diagram for the different components of a typical LIB cell.

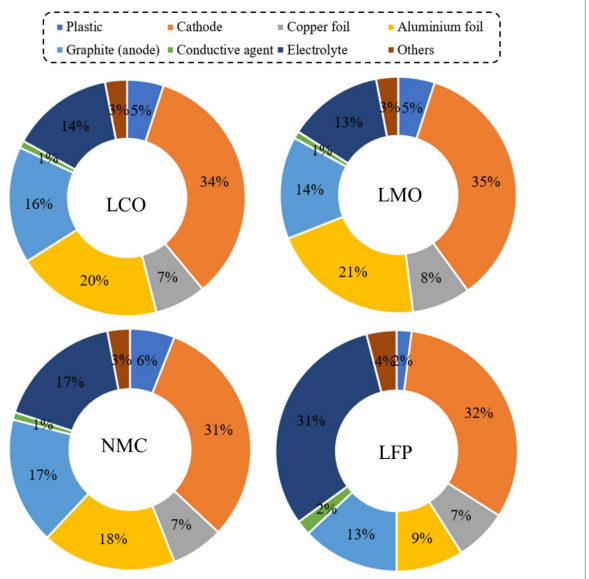

FIGURE 2
Weight fraction (wt %) of different components of LIBs with various cathode materials [adapted and modified from a previous study (Duan et al., 2022)]. LCO, $LiCoO_2$; LMO, $LiMn_2O_4$; NMC, $LiNi_xCo_yMn_zO_2$; and LFP, $LiFePO_4$.

(Eqs. 3, 4) are presented below (Moosakazemi et al., 2022; Roy et al., 2022). Additionally, the chemical reactions are involved in charge and discharge processes in LIBs having $LiCoO_2$ as the cathode and graphite as the anode are presented in Eq. (5) (Zeng et al., 2014).

2.1. Primary non-rechargeable LIBs

$$Li \rightarrow Li^+ + e^- \ (Anode) \quad (1)$$

$$Li^+ + e^- + MnO_2 \rightarrow LiMnO_2 \ (Cathode) \quad (2)$$

2.2. Secondary rechargeable LIBs

$$LiC_6(Lithiated\ graphite) \leftrightarrow C_6 + Li^+ + e^- \quad (3)$$

$$LiCoO_2 \leftrightarrow Li_{1-x}CoO_2 + xLi^+ + xe^- \quad (4)$$

$$LiCoO_2 + C_6 \underset{Discharge}{\overset{Charge}{\leftrightarrow}} Li_{(1-x)}CoO_2 + Li_xC_6 \quad (5)$$

The key components of a typical LIB include anode (negative electrode–natural or synthetic graphite), cathode (positive electrode–different formulations of Li-based metal oxide), separator (electrolyte resistant polymers, e.g., polypropylene or polyethylene), electrolyte (lithium salts dissolved in an organic solvent e.g., $LiPF_6$, $LiBF_4$, etc.) and battery casing materials, and aluminum and copper foil (Golmohammadzadeh et al., 2022; Roy et al., 2022; Alipanah et al., 2023). The schematic diagram of a typical LIB cell with different components is presented in **Figure 1**. The weight fraction of various components of a LIB cell is given in **Supplementary Table 1**. A typical $LiCoO_2$-based LIB contains 5% plastic, 34% $LiCoO_2$ (cathode), 16% graphite (anode), 7% copper foil, 20% aluminum foil, 1% conductive agent, 14% electrolyte and 3% others (**Figure 2**) (Duan et al., 2022). The variation of the percentage of different components in LIBs could be due to LIBs production from different manufacturers (Zeng et al., 2014). Based on the shape, LIBs are categorized into four types including (1) cylindrical, (2) coin, (3) prismatic, and (4) thin and flat LIBs (Tarascon and Armand, 2001). Graphite is commonly used as the anode in LIB with the theoretical specific capacity of 372 mAh/g (Griffiths, 2016). On the basis of battery chemistry, different cathode materials are used in LIB namely LCO: lithium cobalt oxide ($LiCoO_2$), NMC: lithium nickel manganese cobalt ($LiCo_xMn_yNi_{1-x-y}O_2$), LMO: lithium manganese oxide ($LiMn_2O_4$), LFP: lithium iron phosphate ($LiFePO_4$), and NCA: lithium nickel cobalt aluminum oxide ($LiNi_xCo_yAl_zO_2$) (Alipanah et al., 2021; Baum et al., 2022). The characteristics of these cathodic materials are presented in **Table 3**. According to the life cycle assessment (LCA) of the LIB, production of 1 Wh storage capacity of LIB is linked to a cumulative energy demand of 328 Wh and emission of 110 gCO_2eq of greenhouse gas (GHG) (Peters et al., 2017). The total cost for the production of one ton of LIB is US$ 77,708, and among the various components, the cost of the cathode material (e.g., $LiCoO_2$, US$ 2,946) is higher than other parts (Gratz et al., 2014) (**Supplementary Figure 3**). Due to considerable progress on LIB research and developments, the price of LIB is gradually decreasing, e.g., from 3.17 $/Wh in 1991 to 0.28 $/Wh in 2005 (Vanitha and Balasubramanian, 2013). Among these cathodes, $LiCoO_2$ is widely used in commercial applications (specifically in portable electronics) than others because $LiCoO_2$ is relatively thermally more stable and has high energy density than other types of batteries (Tarascon and Armand, 2001; Baum et al., 2022). For

the synthesis of LIBs, Li and Co are in greater demand compared to other metals due to their low relative abundance (Fan et al., 2020).

3. Pre-processing/pre-treatment of spent LIBs

Lithium-ion batteries (LIBs) have complex chemistry and structural configurations. Hence, pretreatment is applied for disintegrating this complex structure so that the downstream resource recovery processes would be easier (Premathilake et al., 2023). The pre-treatment has several benefits including enhancement of metal recovery rate, decrease of energy consumption, reduction of environmental risks and avoidance of safety risks (Hua et al., 2020). The pre-treatment process consists of the following five stages namely (1) sorting, (2) stabilization/discharge, (3) dismantling/disassembly (4) grinding/crushing and (5) separation (Hua et al., 2020; Ali et al., 2022). The sorting of spent LIBs is carried out based on the physical appearance (shape, size, density and magnetic properties) and chemistry (type of cathode materials) (Ali et al., 2022). Batteries can be sorted based on electrical parameters (static and dynamic) namely internal resistance, voltage, self-discharge rate and discharge capacity (Ali et al., 2022). Automatic sorting methods such as X-ray sensors and optical sensors are also developed (Yu et al., 2021). Spent LIBs for recycling may contain a small amount of residual charges which may cause spark and explosion during the dismantling of batteries due to the reaction of Li with atmospheric oxygen (Premathilake et al., 2023). Discharge is a process to stabilize the spent LIBs by removing the residual energy to eliminate short circuit/explosion in the downstream processes of recycling (Hua et al., 2020; Du et al., 2022). The spent batteries are discharged using various methods to drain out the residual charge to less than 0.5 V to avoid the occurrence of any fire and explosion (Roy et al., 2022). The brine/electrolyte method (using NaCl or Na_2SO_4 salt solution) is commonly applied for stabilization of spent LIBs. Other methods used in discharging/stabilization include electrical/ohmic discharge (using an external circuit), and cryogenic discharge (e.g., using liquid nitrogen) and thermal deactivation (heating at 100–150°C) (Yu et al., 2021; Ali et al., 2022). Disassembling of spent LIBs is commonly done in two ways namely manual disassembly (mainly employed in laboratories) and automatic disassembly (e.g., large-scale industrial recycling) (Du et al., 2022). Manual dismantling (physical teardown) is done using mechanical tools such as screwdrivers, pliers, bolt cutters, knives and saws. However, it may cause several safety problems and environmental effects (Premathilake et al., 2023). In the disassembling process, different components of a spent LIB cell including outer metal casing, plastic materials, separator, cathode, anode and other materials (glue, binder, electrolytes, wire, etc.) are separated, and taken for further treatment wherever necessary (Du et al., 2022). Crushing is a size reduction process in which shredding, hammer milling and granulating can be applied based on the size and shape requirement of the next step of the separation process (Ali et al., 2022). Crushing can be done in two ways such as dry crushing (without addition of water) or wet crushing (presence of water or other solution which inactivate lithium) (Yu et al., 2021). Mechanical crushing

TABLE 3 Characteristics of cathode materials used in LIBs and their typical applications (Vanitha and Balasubramanian, 2013; Griffiths, 2016; Harper et al., 2019; Alipanah et al., 2021; Roy et al., 2022).

Cathode type	Chemical formula	Structure type	Energy density (Wh/kg)	Voltage (V)	Capacity (mAh/g)	Power density (W/kg)	Safety/ stability	Calendar lifespan	Cycle lifespan	Year introduced	Key application
Lithium cobalt oxide (LCO)	$LiCoO_2$	Layered	203	4.40	274	20.3	Low	Poor	500–1,000	1991	Portable electronics (e.g., mobile phone and laptop)
Lithium iron phosphate (LFP)	$LiFePO_4$	Olivine	157.5	3.5	170	15.75	High	Good	2,000	1996	Electric vehicles, power tools, etc.
Lithium manganese oxide (LMO)	$LiMn_2O_4$	Spinel	144	4.1	148	14.4	Medium–high	Poor	300–700	1996	Electric vehicles, medical devices, e-bikes/scooters, power tools, etc.
Lithium nickel cobalt aluminum oxide (NCA)	$LiNi_xCo_yAl_zO_2$	Layered	200–260	3.60	200	–	Medium	Poor-good	500	1999	Electric vehicles, medical devices, laptops, etc.
Lithium nickel manganese cobalt (NMC)	$LiCo_xMn_yNi_{1-x-y}O_2$	Layered	155	4.6	200	25.5	Low–medium	Good	1,000–2,000	2008	Electric vehicles, power tools, e-bikes, etc.

is commonly used, and high efficiency can be achieved by using appropriate tools. The mechanical crushing enhances the contact surface of active cathode materials, and hence optimization of the recycling process is needed (Guimarães et al., 2022). A study evaluated the performance of three different types of grinding methods such as hammer, ceramic balls and knife mills for removal of electrode materials from spent LIBs (Takahashi et al., 2020). Notably, knife mill was effective for maximum recovery of cathode materials (i.e., achieved 11.2 wt % Co recovery) from the battery.

In the separation process, different parts of the crushed spent LIBs are separated based on their physicochemical properties such as size, density, hydrophobicity and ferromagnetism (Hua et al., 2020). The main aim of separation followed by purification is to separate active cathode materials (black mass) from other parts of spent batteries to achieve high recovery of valuable metals. The following separation processes are applied: (1) particle size fraction/sieving separation, (2) density/gravity separation (3) froth flotation separation, (4) magnetic separation and (5) electrostatic and eddy current separation (Ali et al., 2022). Other methods include mechanical separation (grinding and ultrasonic cleaning for separation of cathodes from foils), chemical dissolution (e.g., dissolution of organic binder by organic solvent and alkaline leaching) and thermal separation (high-temperature for separation of binder attached to the foils) (Yu et al., 2021). Based on the particle size distribution, the crushed material can be broadly divided into two fractions: fine fraction which mainly contains the active cathode materials, while the coarse fraction mostly consists of plastics, casing materials and separators (Premathilake et al., 2023). The mechanical separation is cost-effective and simple in operation, but results in low separation efficiency (Yu et al., 2021). However, organic solvent dissolution results in good separation and high recovery efficiency. The pre-processed/pre-treated spent LIB materials (in powder form) are taken for recycling of valuable metallic resources using various methods.

4. Overview of various methods for recycling of spent LIBs

The pre-treated spent LIB materials (mainly cathodic material) are taken to the next step of recycling process for the extraction of valuable metals. The following four methods such as direct recycling or three metallurgical-based methods (pyrometallurgy, hydrometallurgy and biohydrometallurgy) are commonly applied for the recovery of valuable metals from spent LIBs. In the direct recycling process, battery materials (e.g., cathode) are recovered with no or minimal change of their original chemical structure, and it is mainly carried out by physical and magnetic separation (Hua et al., 2020; Ali et al., 2022). Additionally, the surface and bulk properties of active battery materials can be restored using the chemical processes namely re-lithiation or hydrothermal methods (Ali et al., 2022). Pyrometallurgy (thermal processing) is a high temperature (500–1,000°C) thermal treatment which converts metal containing battery components into metallic alloy (Hua et al., 2020; Ali et al., 2022). Metals are converted into metal oxides. The pyrometallurgical process involves three main steps including pre-heating, plastic burnings and metal reducing. The thermal pre-treatments employed for the recovery of cathode materials include incineration, calcination and pyrolysis, and the enriched metals are processed using the roasting or smelting processes (Makuza et al., 2021). The efficiency of the pyrometallurgical method depends on various factors namely processing temperature, residence time, flux addition and types of purge gas (Makuza et al., 2021). Although pyrometallurgical process is industrially viable for large-scale recycling of spent LIBs, it shows poor performance toward Li recovery (Georgi-Maschler et al., 2012).

In hydrometallurgical method (aqueous processing), the valuable metals present in the cathodic materials are dissolved into a liquid at low temperature, followed by separation and purification to recover valuable metals (Ali et al., 2022; Du et al., 2022). In the metal leaching, various types of inorganic acids (HCl, HNO_3, H_2SO_4, and H_3PO_4) (Botelho Junior et al., 2021) or alkaline (e.g., NaOH) solutions are employed (Mao et al., 2022). Takahashi et al. (2020) investigated the leaching of Co from spent LIBs obtained from a cell phone company using various inorganic acid leaching agents [H_2SO_4, HNO_3, and HCl with or without reducing agent (H_2O_2)]. They found that the acid leaching using a combination of H_2SO_4 and H_2O_2 at the solution pH of 3.0 and temperature of 50°C resulted in the best Co recovery (98%). Another recent study from the same research group on metal recovery from the spent NMC type battery using 1 mol/L H_2SO_4 at the temperature of 90°C and solid-to-liquid ratio of 1:10, but without addition of a reducing agent achieved 100% extraction of Co, Li and Ni and 93% extraction of Mn (Guimarães et al., 2022). The three key steps of the hydrometallurgical method include leaching, precipitation and solvent extraction (Hua et al., 2020). Among the pyrometallurgical and hydrometallurgical processes, hydrometallurgical process is more advantageous because of less greenhouse gases (GHGs) (e.g., CO_2) emissions and low energy consumption (Vasconcelos et al., 2023). Additionally, hydrometallurgical processing results in the recovery of highly pure-grade Li. However, the above recycling methods (pyrometallurgy and hydrometallurgy) are not sustainable since the pyrometallurgical method is energy intensive and produces GHGs (Ali et al., 2022). Although the GHGs emission rate is lower in hydrometallurgical than pyrometallurgical method, it produces a high amount of corrosive wastewater which could damage the receiving water bodies if discharged without proper treatment (Ali et al., 2022).

In the hydrometallurgical process, H_2O_2 is usually used as a reducing agent for metal extraction from spent batteries using an inorganic-based leaching system (Takahashi et al., 2020). However, H_2O_2 is a chemical reagent that is explosive in nature and can easily disintegrate in the acidic (e.g., H_2SO_4) condition (Wu et al., 2020; Ma et al., 2021). Thus, for the development of environmentally friendly hydrometallurgical processes, considerable interest has emerged in the use of green reductants [e.g., antibiotic bacteria residues (ABR) and fruit peel] while using hydrometallurgical-based leaching process (Wu et al., 2020; Ma et al., 2021). In H_2SO_4 leaching system at the liquid-to-solid ratio of 30:1 ml/g, temperature of 90°C and reaction time of 2.5 h, the application of ABR (ABR to spent cathode powder: 0.8:1) resulted in the optimum recovery of various metals namely Co (98.50%), Li (99.90%), Ni (99.57%) and Mn (98.99%) (Ma et al., 2021). A subsequent study was conducted by the same research group in which the authors initially conducted thermal (350–750°C) reductive transformation of spent cathode powder in the presence of ABR (Ma et al., 2022). The highest recovery of various metals (Co: 99.5%, Li: 99.9%, Ni:

99.4%, and Mn: 99.9%) was obtained under low concentration acid leaching conditions (1 mol/L H_2SO_4) with a liquid-to-solid ratio of 20:1, reaction temperature of 60°C and reaction time of 1 h. Wu et al. (2020) used waste orange peel as the green reductant for metal extraction from spent LIBs. Citric acid-based leaching (1.5 M) with the orange peel dose of 5 mg/ml at the reaction temperature of 100°C, reaction duration of 4 h, and slurry density of 25 g/mL was effective for removal of various metals (Co, Li, Ni, and Mn), i.e., the leaching efficiency of metals varied between 80 and 99%.

The direct recycling is reported to be economically feasible with no considerable negative effects on the environment and energy efficient (Ali et al., 2022; Roy et al., 2022). Practically it is feasible to recover all battery materials including anodes, foils and electrolytes, and the process is most suitable for LFP type batteries (Roy et al., 2022). However, the key disadvantages are: (1) the maturity level of process is low (mainly at the laboratory scale, i.e., will take time to mature and commercialize), (2) the regeneration process is yet to be developed and (3) the mixing of cathode materials decreases the performance and value of the recycled products (Ali et al., 2022; Roy et al., 2022).

In recent years, increasing interests are given on the application of bio-hydrometallurgical (bioleaching) methods which use acid

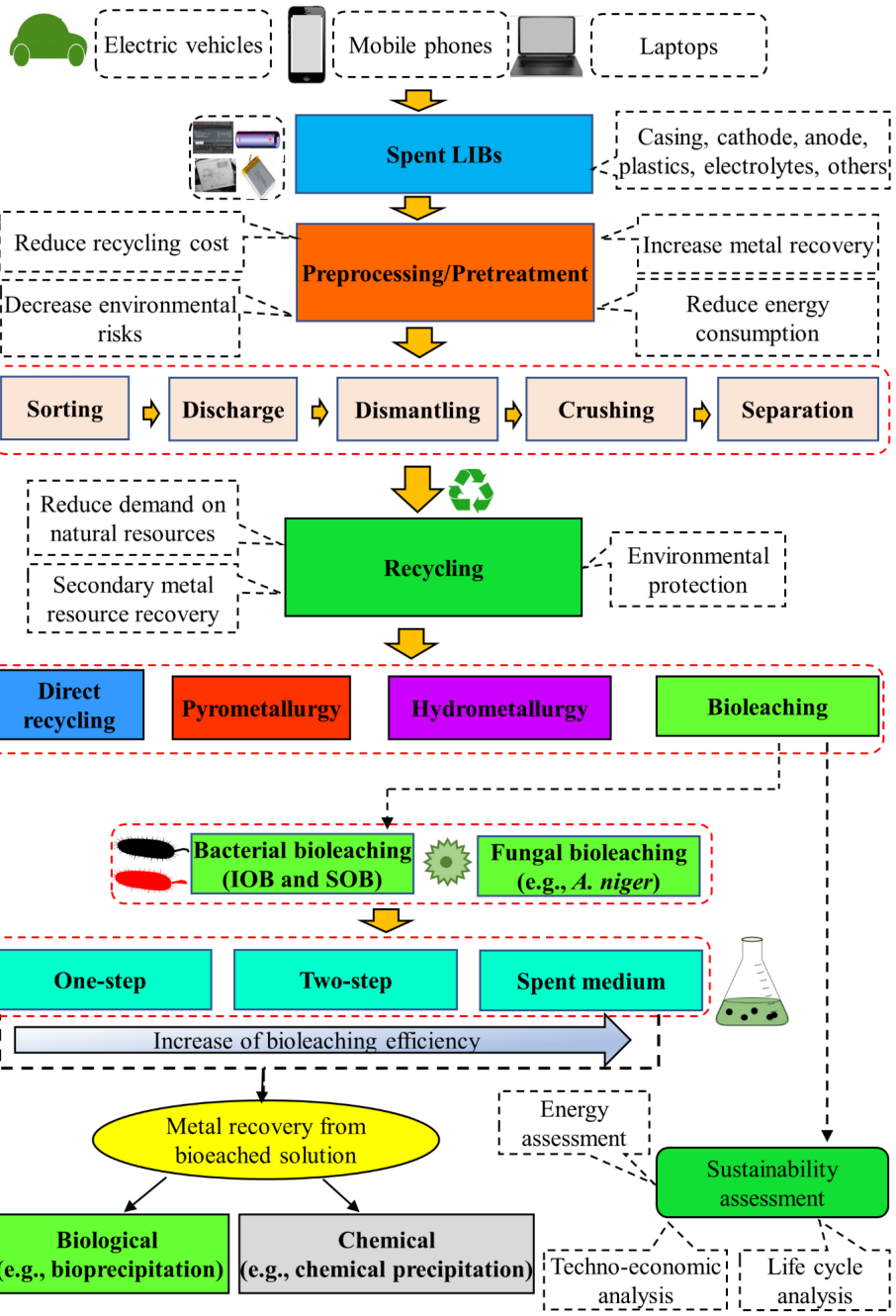

FIGURE 3
Flow-chart for recycling of spent LIBs.

producing microorganisms (bacteria or fungi) for the recovery of valuable metals from spent LIB since the bleaching process is cost-effective, environmentally friendly, less energy intensive, and has low emissions of GHGs as well as high efficiency (Hua et al., 2020; Roy et al., 2021a; Du et al., 2022). Other potential advantages include the requirement of minimal chemicals and water for bioleaching process, operational simplicity, no need of high skilled workers, selectivity toward metals, growth of most of the microbes under ambient conditions, and continued reuse of microbes (Roy et al., 2021a; Golmohammadzadeh et al., 2022; Ratnam et al., 2022). Microbial adaptation to toxic environments, genetic engineering of microbes using synthetic biology techniques, bioprospecting of novel biomining bacteria and storing of microbial agents have enhanced the accessibility of appropriate biocatalysts for applications in bioleaching (Kaksonen et al., 2018, 2020). Furthermore, the development of advanced microbial characterization tools has improved the understanding of metabolisms and metabolic activities of microbial communities and their abilities in the bioprocesses. Bioleaching has already been commercially applied for the removal of metals from low-grade sulfidic ores and for the pretreatment of refractory sulfidic gold-containing minerals (Kaksonen et al., 2020). At present, the application of bioleaching techniques for the recycling of toxic and complex waste materials such as spent LIBs have received considerable attention. However, the bioleaching process is slower than the hydrometallurgical process (Botelho Junior et al., 2021). The detailed information about the recovery of valuable metals from spent LIBs using bioleaching is presented in the next section. Additionally, a flow diagram containing the detailed procedures involved on the recycling of spent LIBs using bioleaching method is presented in **Figure 3**.

5. Microbial-based (bioleaching) recovery of valuable metals from spent LIBs

Bioleaching is a microbial-based natural chemical process in which insoluble solids are converted to soluble and extracted forms (Villares et al., 2016; Heydarian et al., 2018). Moreover, bioleaching is a promising emerging biotechnological process for recovery of secondary metal resources from spent LIBs, and could also contribute to achievement of the environmentally friendly circular economy (Orell et al., 2010; Villares et al., 2016). The bioleaching experiments are mainly conducted in three different ways namely (1) one-step bioleaching, (2) two-step bioleaching and (3) spent-medium bioleaching based on the types of interactions (direct/indirect) between microorganisms and the pre-processed spent LIBs (crushed and sieved powder form of spent LIBs) (Horeh et al., 2016; Biswal et al., 2018, 2022). The one-step method is a conventional approach in which pre-growth microorganisms are added as an inoculum to the leaching medium containing the spent LIBs powder. The leaching of metals from the complex spent LIBs powder matrix is driven by the continuous production of bioacids with the concurrent microbial growth (Biswal et al., 2022). The one-step method is suitable for spent LIBs containing a low amount of toxic components, e.g., pre-processed LIBs (e.g., water washing and drying) since the growth rate of microorganisms would be reduced due to toxicity effects. In the two-step method, the leaching organism is primarily grown (e.g., up to logarithmic phase) in the leaching medium for a specific time period for the production of bioacids. The LIB powered is then added to initiate the metal extraction process (Biswal et al., 2018, 2022). This method is suitable for spent LIBs containing toxic materials (without having any pre-treatments like washing and drying) which could hinder the growth of microorganisms with direct application. In both one-step and two-step methods, direct physical contact/interaction between microorganisms and spent LIB components occurs. In the spent medium method, the leaching is carried out by adding battery powder to the cell free medium (called spent medium), i.e., the microorganism is firstly fully grown in the medium for the production of bioacids, then the spent medium is obtained by removing the cells using various techniques such as centrifugation, filtration, or both (Biswal et al., 2018, 2022). The spent medium-based bioleaching can be applied to the spent LIBs containing diverse toxic components namely metals, electrolytes and organic solvents. Among the three types of bioleaching approaches, the spent medium bioleaching is most preferable since the leaching efficiency is usually higher in spent medium-based bioleaching tests compared to others (one-step or two-step method) (Horeh et al., 2016; Alavi et al., 2021; Lobos et al., 2021). Since there is no physical contact between microbial agents and spent LIBs particles in spent medium leaching, the individual process (biological and chemical) can be optimized (Bahaloo-Horeh et al., 2019). For example, the quality and quantity of biogenic acids can be enhanced during the initial growth experiments, while in the chemical leaching, the use of biogenic acid and higher pulp density can be explored since there is no issue of toxicity effects on hazardous components of LIBs due to absence of microbial cells. The bacterial-based leaching is conducted using basal salt/9K/modified 9k medium [$(NH_4)_2SO_4$, KCl, $K_2HPO_4.3H_2O$, $MgSO_4.7(H_2O)$, $Ca(NO_3)_2$, and $FeSO_4.7(H_2O)$] (Roy et al., 2021b) while fungal leaching is carried out using the sucrose medium [($NaNO_3$, KH_2PO_4, KCl, $MgSO_4.7H_2O$), yeast extract and sucrose] (Bahaloo-Horeh and Mousavi, 2017). The bioleaching experiments are conducted using single/pure culture microbial systems (Biswal et al., 2018) or consortia/mixed culture microbial systems (Heydarian et al., 2018; Alavi et al., 2021). The initial inoculum size for bacterial and fungal leaching is nearly 10^7 cells/spores per mL (Mishra et al., 2008; Bahaloo-Horeh and Mousavi, 2017).

5.1. Bacterial-based bioleaching for recovery of valuable metals from spent LIBs

The acidophilic sulfur-oxidizing bacteria (SOB) and iron-oxidizing bacteria (IOB) are widely used for the bioleaching of valuable metals from spent LIBs (Ghassa et al., 2020; Noruzi et al., 2022). The major SOB employed in the bioleaching of valuable metals from spent LIBs include *Acidithiobacillus thiooxidans*, *Sulfobacillus thermosulfidooxidans*, and *Alicyclobacillus* spp. while the dominant IOB applied for spent LIB bioleaching are *Acidithiobacillus ferrooxidans*, *Leptospirillum ferriphilum*, and *Sulfobacillus* spp. (Ghassa et al., 2020; Liu et al., 2020; Golmohammadzadeh et al., 2022). These SOB and IOB are called

chemolithoautotrophs which can utilize carbon dioxide (CO_2) as the carbon source (i.e., they obtain carbon by reductive fixation of atmospheric CO_2), while they utilize inorganic compounds such as ferrous ion (Fe^{2+}, IOB) and reduced S [elements sulfur (S^0), SOB] as an energy source (Hong and Valix, 2014). In the bacterial leaching, ferrous sulfate ($FeSO_4$), iron powder and pyrite (FeS_2) are also used as the source of iron and sulfur (Golmohammadzadeh et al., 2022). The IOB oxidizes Fe^{2+} to Fe^{3+}, while SOB oxidizes S^0 to SO_4^{2-} (Heydarian et al., 2018). Other chemolithoautotrophic bacteria namely *Acidithiobacillus caldus*, and *Ferroplasma* spp. are also applied for the bioleaching of metals from spent LIBs (Ghassa et al., 2020). A majority of the chemolithotrophic bacteria show high level of tolerance to metals toxicity (Işıldar et al., 2019).

Single or consortia acidophilic bacteria are used for the recovery of valuable metals (mainly Co and Li) from spent LIBs (**Table 4**). Biswal et al. (2018) used *A. thiooxidans* 80191 as the microbial agent and observed higher Li (66%) removal than Co (23%) under two-step bioleaching tests. Another study also used *A. thiooxidans* (PTCC 1717) (inoculum concentration: 10^7 cells/mL) for the metal extraction from spent LIBs (spent coin cells) in two-step bioleaching tests, and found higher recovery of Co (60%) and Li (99%) than Mn (20%) (Naseri et al., 2019b). Using an IOB, *A. ferrooxidans*, Roy et al. (2021b) obtained higher Co (94%) recovery compared to Li (60%) from spent LIBs at a high pulp density (100 g/L) in 3 days with continued refilling of the bacterial culture to the leaching medium for three cycles. Additional study from the same research group on the spent nickel-, manganese-, cobalt (NMC)-based LIBs using *A. ferrooxidans* at a higher pulp density (100 g/L) reported a higher extraction efficiency of various metals namely Co (82%), Li (89%), Mn (92%) and Ni (90%) (Jegan-Roy et al., 2021). Li et al. (2013) reported 47.6% dissolution of Co from spent LIB employing *A. ferrooxidans* as the leaching organism. Using the mixed culture consortia of *A. ferrooxidans* and *A. thiooxidans*, 67% Co and 80% Li were extracted from spent LIBs in the nutrient rich medium (Marcinčáková et al., 2016). However, the metal efficiency was considerably reduced (10.5% Co and 35% Li) when tested with the low nutrient medium which contains only elemental sulfur (4 g/L) and sulphuric acid. Another study also used the same mixed culture (*A. ferrooxidans* and *A. thiooxidans*), and found 50.4 % Co, 99.9% Li and 89.4% Ni recovery from spent LIBs used in laptops (Heydarian et al., 2018). However, using a mixed culture containing four different thermophilic bacteria (*A. caldus*, *L. ferriphilum*, *Sulfobacillus* spp. and *Ferroplasma* spp.), the bioleaching tests resulted in the dissolution of 99.9% Co, 84% Li and 99.7% Ni from spent LIB used in laptops. Do et al. (2022) performed spent NMC bioleaching using *A. ferrooxidans*, and reported 90.4% Co, 89.9% Li, 85.5% Ni, 91.8% Mn recovery in 6 h at a higher pulp density (100 g/L). Additionally, the authors attempted to regenerate cathode material (NMC_{111} and NMC_{622}) using the oxalate-based precipitated metals from the bioleached solution and found that the electrochemical stability of the regenerated cathode material was similar to that of commercial NMC (i.e., nearly 85% of capacity retention after 50 cycles at 100 mA/g). Liu et al. (2020) reported that bio-oxidative activity of microbial agents reduced due to metallic stress, as a result, the bioleaching efficiency is declined. However, addition of exogenous glutathione (GSH) which is a ubiquitous intracellular peptide with diverse functions (0.3 g/L), the bacterial intracellular reactive oxygen species (ROS) level decreased by 40% which resulted in 96.3% Co and 98.1% Li recovery at pulp density of 5% using microbial consortium of *L. ferriphilum* and *S. thermosulfidooxidans*.

A few studies have isolated acidophilic bacteria from the acid mine drainage, then applied them for metal extraction from spent LIBs (Hariyadi et al., 2022b; Putra et al., 2022). Hariyadi et al. (2022b) conducted bioleaching of spent LIBs using *A. ferrooxidans* cells isolated from water samples of a coal mine pond, and found recovery of 57.81% Co at medium pH of 2.5 in 14 days of incubation period. Another study from the same research group reported 73.95% dissolution of Co from spent LIBs at an optimum experimental condition of 10 g/L of pulp density, temperature of 30°C, pH of 2–4 and incubation period of 14 days with *A. ferrooxidans* inoculum size of 20% (v/v) (Putra et al., 2022). Overall, findings of these reports suggest that the metal removal efficiency varied among various studies which may be due to the difference in the leaching microorganisms (e.g., single vs. mixed culture), mode of leaching (one-step, two-step or spent medium), battery chemistry (e.g., characteristics of cathode materials) and leaching conditions (pH and pulp density). Additionally, in most of the studies, it was observed that the Li bioleaching efficiency was greater than that of Co.

5.2. Fungal-based bioleaching for recovery of valuable metals from spent LIBs

Fungi are the heterotrophic microorganisms which use organic carbon-based materials as the carbon source for their growth and metabolism (Bahaloo-Horeh et al., 2019). Several fungal species namely *Aspergillus niger*, *Aspergillus tubingensis*, *Penicillium simplicissimum*, and *Penicillium chrysogenum* are employed for the extraction of metals from electronic wastes (Bahaloo-Horeh et al., 2019; Işıldar et al., 2019; Lobos et al., 2021). However, in spent LIBs bioleaching, *A. niger* is highly favored due to less complexity in the growth and harvesting process and higher yields (Roy et al., 2021a). In contrast to bacteria, fungi have the greater capacity for tolerance to diverse toxic metals, having a shorter lag phase and faster leaching rate as well as fungi can grow in both acid- and alkaline-consuming wastes (Horeh et al., 2016). A study compared the metal tolerance capacity of three fungi species namely *A. niger* (ATCC 6275), *P. chrysogenum* (ATCC 10108) and *P. simplicissimum* (ATCC 48705) by exposing them 250 mg/L of $CoCl_2$ or LiCl solution over a period of 20 days (Lobos et al., 2021). Among the three fungal species, only *A. niger* developed tolerance to both metals since an increase of biomass production was observed.

Biswal et al. (2018) conducted fungal bioleaching of spent LIBs (pulp density: 0.25% w/v) using two isolated strains, *A. niger* MM1 and *A. niger* SG1 under cell-free spent medium. Both fungal strains were effective for the extraction of valuable metals from spent LIBs, i.e., 80–82% Co and 100% Li recovery were achieved. Horeh et al. (2016) used a pure culture of *A. niger* (PTCC 5210) for the recovery of various metals from spent mobile phone LIBs using three different approaches (one-step, two-step and cell-free spent medium). Among the three types of experimental conditions, the spent-free medium test exhibited highest performance for the extraction of numerous valuable metals including Co (45%),

TABLE 4 Bacterial-based bioleaching for recovery of valuable metals from spent Li-ion batteries (LIBs).

Bacteria	Key leaching condition	Bioleaching efficiency			Additional information	References
		Co	Li	Other metals		
A. thiooxidans (80191)	Pulp density: 0.25% (w/v), pH: 2.4	23%	60%	NA	Co and Li dissolution were higher in two-step bioleaching	Biswal et al., 2018
A. ferrooxidans (ATCC 19859)	Solid-to-liquid ratio: 5 g/L, pH: 2.5	65%	9.5%	NA	Higher solid/liquid ratios reduced leaching efficiency	Mishra et al., 2008
A. ferrooxidans (DSMZ, 1927)	Pulp density: 100 g/L	94%	60.30%	NA	For optimum metal extraction, replenishment of microbial culture was done every 24 h for 3 cycles	Roy et al., 2021b
A. ferrooxidans (DSMZ 1927)	Pulp density: 100 g/L	82%	89%	Mn: 92%, Ni: 90%	Leaching efficiency was increased with increase of sulphuric and ferric ion in the leaching medium as well as by replenishing the culture for three cycles	Jegan-Roy et al., 2021
A. ferrooxidans (DSMZ 1927)	Pulp density: 100 g/L	90.4%	89.9%	Mn: 91.8%, Ni: 85.5%	NMC (NMC_{111} and NMC_{622}) were regenerated from the oxalate-based coprecipitated product. The electrochemical stability of the regenerated NMC was similar to the commercial NMC.	Do et al., 2022
A. ferrooxidans (isolated)	Pulp density: 1% (s/v), bacteria inoculation: 5% (v/v), pH: 1.5	47.60%	NA	NA	Enhancement of cobalt dissolution was observed at higher redox potential	Li et al., 2013
A. thiooxidans (PTCC 1717)	Pulp density: 30 g/L, pH: 2.0	60%	99%	Mn: 20%	Bioleached spent LIB residue was safe to disposal as meets the TCLP limit	Naseri et al., 2019b
A. thiooxidans (PTCC 1647)	Pulp density: 40 g/L, pH: 2.0	88%	100%	Mn: 20%	The shrinking core model predicted that the diffusion of ferric ions plays a key role in metal leaching.	Naseri et al., 2019a
A. ferrooxidans (isolated)	Pulp density 1% (s/v)	99.90%	NA	NA	Enhancement of cobalt dissolution was noticed with addition of copper ions (0.75 g/L).	Zeng et al., 2012
A. ferrooxidans (isolated)	Pulp density 1% (s/v)	98.40%	NA	NA	Enhancement of cobalt dissolution was noticed with addition of silver ions (0.02 g/L).	Zeng et al., 2013
A. ferrooxidans (PTCC 1647)	Pulp density: 10 g/L	19.0%	67%	Mn: 50%, Ni: 34%	Ultrasonic treatment (203.5 W for 30 min) enhanced metal leaching efficiency.	Nazerian et al., 2023
A. ferrooxidans (isolated)	pH: 2.5, inoculum concentration: 20% (v/v)	57.8%	NA	NA	Highest Co recovery was found at an inoculum concentration of 20% (v/v) in 14 days of incubation time.	Hariyadi et al., 2022b
A. ferrooxidans (isolated)	Pulp density: 10 g/L, pH: 2- 4, inoculum concentration: 20% (v/v)	73.95%	NA	NA	Bacterial strain isolated from the acid mine drainage has the potential as oxidizing agent for recovery of metals (Co and Li) from spent LIBs.	Putra et al., 2022
L. ferriphilum (isolated)	Pulp density: 1% (w/v), pH: 1.0	NA	49%	NA	Leaching tests were done using pyrite (FeS_2, 16 g/L) as the energy source and LFP as the cathode material.	Xin et al., 2016
A. thiooxidans (isolated)	Pulp density: 1% (w/v), pH: 1.0	NA	98%	NA	Leaching tests were done using S^0 (16 g/L) as the energy source and LFP as the cathode material.	Xin et al., 2016
A. thiooxidans (isolated)	Pulp density: 1% (w/v), pH: 1.0,	NA	97%	Mn: 35%	Leaching tests were done using S^0 (16 g/L) as the energy source and LMO as the cathode material.	Xin et al., 2016
Mixed bacterial culture (isolated)	Pulp density: 2 g/L, pH: 7.0	NA	63.8%	NA	Adaptation of bacteria with LiCl solution (576 μM) enhanced leaching efficiency of bacteria to Li.	Hartono et al., 2017
Mixed culture of IOB and SOB (isolated)	Pulp density 10 g/L, pH: 1.5 (2.0 g/L sulfur + 2.0 g/L FeS_2)	90.00%	80.0%	NA	Acidolysis was the main mechanism for Li dissolution, whereas both acidolysis and redoxolysis contributed for Co dissolution.	Xin et al., 2009
Mixed culture 1	Iron sulfate: 36.7 g/L; sulfur: 5.0 g/L, pH: 1.5	50.40%	99.20%	Ni: 89.4%	Metal contents in spent LIB residue reduced to below the regulatory standard (USEPA), thus the bioleached LIBs can be reused or disposed safely	Heydarian et al., 2018
Mixed culture 1	Pulp density: 1% (w/v), pH: 2.0	99.95%	NA	Ni: 99.95%	High metal extraction yield observed in short time (3 days) in two-step leaching with addition of silver ions (0.02 g/L)	Noruzi et al., 2022
Mixed culture 1	Pulp density: 10% (w/v), pH: 1.8	53.20%	60.00%	Ni: 48.7%, Mn: 81.8%, Cu: 74.4%	Biogenic ferric ion-based critical metal leaching yield was further improved with addition 100 mM H_2SO_4.	Boxall et al., 2018

(Continued)

TABLE 4 (Continued)

Bacteria	Key leaching condition	Bioleaching efficiency			Additional information	References
		Co	Li	Other metals		
Mixed culture 2	Pulp density: 10 g/L, pH: 1.8	99.90%	84%	NA	Similar leaching results obtained by using iron scrap waste instead of chemical reagent ($FeSO_4.7H_2O$)	Ghassa et al., 2020
Mixed culture 1	Pulp density: 10 g/L, pH: 1.5	67%	80%	NA	Leaching efficiency was reduced to 35% Li and 10.5% Co in low nutrient medium	Marcinčáková et al., 2016
Mixed culture 3	Pulp density: 5% (w/v), pH: 1.25	96.3%	98.1%	NA	Reactive oxygen species (ROS) regulation by the exogenous addition of glutathione resulted higher metal leaching yield.	Liu et al., 2020
Mixed culture 4	Pulp density: 1% (w/v), pH: 1.0	96.0%	92.0%	Mn: 92%, Ni: 97%	The experiments were conducted using mixed culture and mixed energy source (S^0 + FeS_2) and NMC as cathode material	Xin et al., 2016
Mixed culture 4	Pulp density: 1% (w/v), pH: 1.0	NA	> 95%	Mn: > 95%	The experiments were conducted using mixed culture and mixed energy source (S^0 + FeS_2) and LMO as cathode material	Xin et al., 2016
Mixed culture 5	Pulp density: 2% (w/v), pH: 1.0	72.0%	89.0%	NA	Thermodynamics analysis shows bioleaching has much greater potential to happen compared to chemical leaching.	Niu et al., 2014
Mixed culture 6	Pulp density: 15 g/L, pH: 1.20	99.3%	100%	NA	Extracellular polymeric substances (EPS) secreted by bacteria enhanced metal removal.	Wu W. et al., 2019

Mixed culture 1: *A. ferrooxidans* and *A. thiooxidans*. Mixed culture 2: *A. caldus*, *L. ferriphilum*, *Sulfobacillus* spp. and *Ferroplasma* spp. Mixed culture 3: *L. ferriphilum* and *Sulfobacillus thermosulfidooxidans*. Mixed culture 4: *A. thiooxidans* and *L. ferriphilum*. Mixed culture 5: *Alicyclobacillus* spp. and *Sulfobacillus* spp. Mixed culture 6: *L. ferriphilum* spp. and *S. thermosulfidooxidans* spp. *A. thiooxidans*, *Acidithiobacillus thiooxidans*; *L. ferriphilum*, *Leptospirillum ferriphilum*; NA, absence of data.

Li (95%) and other metals (e.g., Cu: 100%, Mn: 70%, and Al: 65%). Subsequent experiments from the same research group using *A. niger* (PTCC 5210) reported the highest Co (64%) and Ni (54%) recovery at lower (1%, w/v) pulp density, but the recovery of other four metals (Cu: 100%, Li: 100%, Mn: 77% and Al: 75%) was optimum at higher (2%, w/v) pulp density (Bahaloo-Horeh and Mousavi, 2017).

A recent study isolated *A. niger* from waste spices (Candlenut), and 57% Co and 72% Li recovery was obtained in 21 days of incubation time (Hariyadi et al., 2022a). Using a mixed fungal culture (*A. niger* and *A. tubingensis*), Alavi et al. (2021) investigated the bioleaching of valuable metals from spent cellphone LIBs using three different types of carbon sources (pure sucrose, impure sucrose and vinasse from an ethanol industry) under three types of leaching methods. The bioleaching was optimum with the spent medium test having vinasse as the carbon source, i.e., the recovery of Co and Li was nearly 60 and 95%, respectively, whereas the recovery of another three metals (Mn, Ni, and Al) was varied between ~80 and 98%. To enhance the metals toxicity tolerance level of *A. niger* (PTCC 5010), Bahaloo-Horeh et al. (2018) gradually increased the pulp density in the leaching medium from 0.3 to 1.0% (w/v) to adopt the *A. niger* to the toxic metal environment. Bioleaching tests showed that the adapted *A. niger* exhibited higher leaching efficacy for diverse metal elements from mobile phone-based spent LIBs including Co (38%), Li (100%), Cu (94%), Mn (72%), Al (62%), and Ni (45%). A study compared the metal dissolution performance of two different types of fungal species [*A. niger* (PTCC 5010) and *P. chrysogenum* (PTCC 5037)] (Kazemian et al., 2020), and the authors noticed that the *A. niger* (76.31%) demonstrated higher Li leaching capability than *P. chrysogenum* (54.6%). In total, most of the studies used *A. niger* as the microbial agent for the fungal bioleaching of spent LIBs (**Table 5**). Among various fungal species, *A. niger* is capable of tolerating metals toxicity from spent LIBs, and hence exhibited higher metal bioleaching efficiency. Like bacterial-based bioleaching, Li recovery was higher than Co in fungal-based bioleaching.

5.3. Quality and quantity of bioacids production in bacterial and fungal bioleaching

Bioacids or biogenic acids are the metabolites produced by the microbial agents during their growth in the leaching medium with or without supplementation of spent LIBs, and they primarily contribute to the extraction of metals from the spent LIB solid matrices (Biswal et al., 2018, 2022). In bacterial-based leaching [specifically SOB (e.g., *A. thiooxidans*)] with the use of elemental sulfur as the energy source and electron donor, biogenic sulfuric acid (H_2SO_4) is produced by oxidation of S^0 (Biswal et al., 2018). With the use of *A. thiooxidans* (80191), the pure culture growth medium resulted in the production of 10.2 mM biogenic H_2SO_4, while the H_2SO_4 production significantly decreased by nearly fivefold (1.7 mM) with the addition of 1% (w/v) S^o as the energy source and 0.25% (w/v) spent LIB powder (one-step leaching) (Biswal et al., 2018). Using the *A. ferrooxidans* strain (DSMZ, 1927), Roy et al. (2021b) reported 0.17 M production of H_2SO_4 under the leaching condition of 100 mg/L spent LIB pulp density and 45 g/L $FeSO_4$. However, the H_2SO_4 concentration increased by nearly 3 times (0.52 M) with the increase of $FeSO_4$ dose to 150 g/L.

In fungal bioleaching, mostly sucrose and glucose are used as a carbon and energy source, and the microbial metabolism (through the Krebs cycle) results in the production of diverse

organic acids (carboxylic acids) namely citric, gluconic, oxalic, malic, fumaric, lactic, pyruvic and succinic acids, etc (Bahaloo-Horeh and Mousavi, 2017; Bahaloo-Horeh et al., 2019). Using two isolated *A. niger* strains (MM1 and SG1), Biswal et al. (2018) reported only the production of citric acid with 76.9–102.4 mM in the pure culture medium (without spent LIBs), but the citric acid concentration was reduced to nearly half (40.7–43.1 mM) with the one-step bioleaching. Similar observations were also reported by two earlier bioleaching works since the citric acid was the dominant metabolite produced by the metabolism of sucrose, and the concentration of citric acid is usually lower in one-step/two-step bioleaching (133 mg/L) compared to cell free spent medium leaching (8,078 mg/L) (Horeh et al., 2016; Bahaloo-Horeh and Mousavi, 2017). Kim et al. (2016) found that *A. niger* isolate (KUC5254) produced a significant amount of citric acid (118.8 mM) than oxalic acid (0.8 mM) in the sucrose (100 g/L) growth medium.

A study compared the changes of quality of organic acid production by the unadapted and adapted *A. niger* (adapted by adding various doses of spent LIBs pulp densities), and only oxalic acid (up to 13,000 mg/L) was produced by the unadapted *A. niger*, whereas four different organic acids (oxalic, malic, citric and gluconic acid) were produced by the adapted *A. niger* with gluconic acid was the dominant metabolite (nearly 4,000–13,000 mg/L) with incubation time varied between 6 and 30 days (Bahaloo-Horeh et al., 2018). Overall, the quantity and quantity of bioacids production depends on the various factors namely the type of microbial agents (bacteria vs. fungi), leaching medium chemistry (e.g., composition and pH), type of energy/carbon sources, spent LIBs characteristics (e.g., quantity and quality of metals), pulp density, etc (**Supplementary Table 2**) (Biswal et al., 2018, 2022; Bahaloo-Horeh et al., 2019). The concentration of bioacids is usually higher in the pure culture growth medium (i.e., absence of spent LIBs) than that of the microbial growth in the presence of waste materials (one-step or two-step leaching) (Biswal et al., 2018). The decrease in the generation of bioacids by the addition of spent LIBs could be due to deactivation/suppression of enzyme activities responsible for the bioacid production by the toxic/inhibitory effects of metals or other components of spent LIBs (Naseri et al., 2022; Pourhossein and Mousavi, 2023).

5.4. Comparison of valuable metal recovery efficiency between bacterial, fungal and chemical leaching

A few studies compared the performance of valuable metals recovery of two types of biological leaching processes (bacteria vs. fungi) as well as the leaching efficiency between bioleaching and chemical leaching (i.e., using commercially synthesized chemical acids with concentrations similar to the concentration of bioacids produced in bioleaching) (Bahaloo-Horeh et al., 2018; Biswal et al., 2018; Noruzi et al., 2022). According to Biswal et al. (2018) between bacterial and fungal bioleaching, the metal extraction efficiency from spent LIBs was higher in fungal leaching (Co: 82% and Li: 100%) compared to bacterial leaching (Co: 23% and Li: 66%). Additional experiments using commercially

TABLE 5 Fungal-based bioleaching for recovery of valuable metals from spent Li-ion batteries (LIBs).

		Metal bioleaching efficiency				
Fungal	Key leaching condition	Co	Li	Other metals	Additional information	References
Aspergillus niger (PTCC 5210)	Pulp density: 1% (w/v); pH: 6.0	45%	95%	Cu: 100%, Mn: 70%, Al: 65%, Ni: 38%	Spent medium exhibited highest metal extraction yield. Also, bioacids yielded higher metal extraction than synthetic chemical acids.	Horeh et al., 2016
A. niger MM1/SG1 (isolated)	Pulp density: 0.25% (w/v); carbon source: sucrose; pH: 3.5	80–82%	100%	NA	Leaching efficiency was higher in cell-free spent medium. Also, bioacids yielded higher metal extraction than the synthetic chemical acid (citric acid).	Biswal et al., 2018
A. niger (PTCC 5210)	Pulp density: 1–2% (w/v), carbon source: sucrose	64%	100%	Cu: 100%, Mn: 77%, Al: 75%, Ni: 54%	Co and Ni recovery were higher at 1% pulp density, while Li, Cu, Al and Mn recovery was higher at 2% pulp density.	Bahaloo-Horeh and Mousavi, 2017
A. niger (PTCC 5210)	Pulp density: 1 % (w/v), carbon source: sucrose	38%	100%	Cu: 94%, Mn: 72%, Al: 62%, Ni: 45%	Adapted fungi showed higher metal leaching performance compared to unadopted fungi.	Bahaloo-Horeh et al., 2018
A. niger (PTCC 5010)	Pulp density: 10% (w/v), carbon source: glucose; pH: 4.5,	NA	73.3%	NA	*A. niger* showed higher metal leaching performance than *Penicillium chrysogenum*.	Kazemian et al., 2020
P. chrysogenum (PTCC 5037)	Pulp density: 10% (w/v), carbon source: glucose; pH: 4.5,	NA	54.6%	NA	*A. niger* showed higher metal leaching performance than *P. chrysogenum*.	Kazemian et al., 2020
A. niger (isolated)	Carbon sources: glucose, incubation time: 21 days	57%	72%	NA	Highest valuable metal recovery obtained in the one step process	Hariyadi et al., 2022a
Mixed culture 1	Pulp density: 1% (w/v), carbon source: sucrose, impure sucrose or vinasse	~60%	~95%	Mn: ~98%, Ni: ~80%, Al: ~82%	Spent medium leaching showed higher metal recovery efficiency with vanasse as the carbon source	Alavi et al., 2021

Mixed culture 1: *A. niger* and *Aspergillus tubingensis*. NA, absence of data.

synthesized of H_2SO_4 and citric acid with concentrations similar to those of bioacids showed that the percentage of valuable metal dissolution was higher (4–15%) in bioleaching compared to chemical reagent-assisted leaching method. Similar results were also obtained by another study in which authors compared critical metals removal efficacy between fungal leaching and chemical leaching (employing a mixture of commercial four types of carboxylic acids namely citric, gluconic, malic and oxalic acids) (Bahaloo-Horeh et al., 2018). The metal removal efficiency was higher in fungal-based leaching (38% Co and 100% Li) compared to commercial organic acid-based leaching (13% Co and 68% Li). According to a recent study, the recovery of Co and Ni from spent LIBs was higher in bacterial-based leaching (99.95% for both Co and Ni using *A. ferrooxidans* and *A. thiooxidans*) than chemical leaching [only 7.09% Co and 26.90% Ni using $Fe_2(SO_4)_3$ with the sulfate concentration similar to that in the bioleaching solution] (Noruzi et al., 2022). Xin et al. (2009) reported that the chemical simulation of acid solubilization (Fe^{2+}: 4 g/L and H_2SO_4 at pH of 1.0) resulted 621 mg/L Co and 303 mg/L Li recovery from spent LIBs powder. However, the bioacid leaching system achieved much higher metal dissolution (i.e., Co: 920 mg/L and Li: 470 mg/L) which is potentially due to continuous production of H_2SO_4 from biooxidation of S^0 by SOB. Additional work from the same research group on three types electric vehicle spent cathode materials (LMO, LFP, and NMC) also found that the metal dissolution was higher in bioleaching system containing mixed bacterial culture (*A. thiooxidans* and *L. ferriphilum*) and mixed energy source (S^0 and FeS_2), i.e., leaching of various metals in the bioacid system was 92% Li, 43.5% Co, 92% Mn, and 38.3% Ni, whereas the leaching of these metals in chemical simulation system was much lower, i.e., 65, 20, 52, and 18%, respectively.

Thermodynamics analysis shows that bioleaching is more thermodynamically feasible than chemical leaching (Niu et al., 2014). Niu et al. (2014) performed the thermodynamic analysis of the bacterial leaching (mixed culture of *Alicyclobacillus* spp. and *Sulfobacillus* spp.) and chemical leaching (H_2SO_4 + $FeSO_4$), and found that the change of free energy (ΔG) for the bacterial leaching (−3629.93 KJ/mol) was nearly 14 times higher than that of the chemical leaching (ΔG: −265.44 KJ/mol). The large difference in the free energy value between the two types of leaching suggests that the bioleaching has much higher potential to be a favorable compared to chemical leaching. In fungal bioleaching, multiple metabolites (organic acids) are produced, while in bacterial-based bioleaching only one metabolite (H_2SO_4) is produced. Thus, it is expected that higher metal recovery is possible by the chemical action of multiple metabolites in fungal leaching than bacterial leaching with single metabolite. The bioacids (carboxylic acids) produced in fungal leaching are mild, less toxic and biodegradable, while bacterial leaching produces inorganic acids such as H_2SO_4 which are corrosive and not easy to handle (Bahaloo-Horeh and Mousavi, 2017). Based on the pKa values of carboxylic acids, the pH of dilute solutions of carboxylic acids (equivalent to the fungal produced bioacids) is in the moderate acidic pH range between 3 and 5 (Moosakazemi et al., 2022). Sedlakova-Kadukova et al. (2020) compared the performance of three different bioleaching systems (bacterial consortia: *A. ferrooxidans* and *A. thiooxidans*, fungi: *A. niger* and yeast: *Rhodotorula mucilaginosa*) for the extraction of Li from lepidolite (Li-containing mineral). They found that the heterotrophic fungal and yeast bioleaching was faster (40 days) than autotrophic bacterial consortium bioleaching (336 days). Altogether, the fungal bioleaching has the following advantages including fungal isolates having higher capacity to tolerate toxic components of spent LIBs, and the ability to grow in a broad range of pH (pH: 2–8, i.e., both acid and alkaline environment) with shorter lag phase (Bahaloo-Horeh et al., 2019).

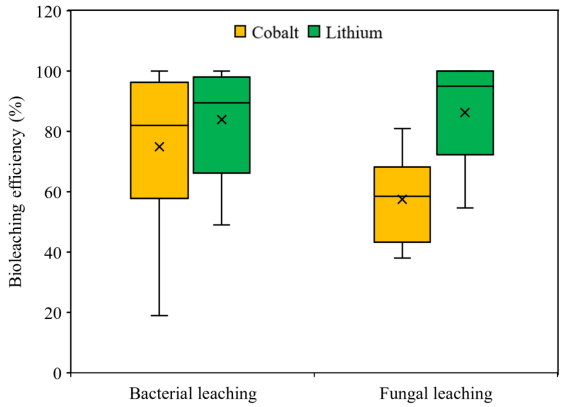

FIGURE 4
The Box and Whisker plot showing the comparative Co and Li leaching efficiency reported in literature using bacteria or fungi as the bioleaching agent.

For the comparative evaluation of variations in the dissolution of Co and Li in bacterial and fungal bioleaching, statistical analysis (Box and Whisker plot) was done using the literature data presented in **Table 4** (bacterial leaching) and **Table 5** (fungal leaching). The Box and Whisker plot (**Figure 4**) shows that in both types of bioleaching systems, Li dissolution was relatively higher than that of Co. Further analysis using the two-tailed Student *t*-test at 95% confidence interval ($P \leq 0.05$) reveals that the difference between Co and Li dissolution efficiency was statistically significant ($P < 0.05$) for the fungal leaching, but not for the bacterial leaching. Between the two types of bioleaching systems, Co dissolution seems to be higher in the bacterial-based leaching system, whereas fungal leaching appears to promote more Li solubilization than the bacterial system (**Supplementary Figure 4**). However, more studies (specifically fungal leaching) are needed for better comparison of the metal leaching performance of the two types of biological methods.

5.5. Recovery of valuable metals from the bioleached medium

Multiple microbial-driven reactions in the bioleaching process facilitate the extraction of metals from the complex solid matrix of spent LIBs as well as convert the hazardous fractions of spent LIBs into non-hazardous form (Naseri et al., 2019b). Thus, the bioleached medium is usually highly rich in diverse valuable metals including Co and Li, but they are mainly in the dissolved form. From the circularity and economic perspectives, the dissolved secondary metals can be recycled/recovered by transferring the dissolved form of the metals into the solid form through microbial-driven ad/or chemical-driven precipitation

reactions (Biswal et al., 2018). Biotechnological techniques such as bioprecipitation (e.g., employing metal reducing bacteria), biosorption (e.g., using living or dead biosorbents) and bio-electrochemical systems (e.g., microbial fuel cell and microbial electrolysis cell) can be applied for metal recovery (Sethurajan and Gaydardzhiev, 2021). The common precipitating agents used for the precipitation of metals include sulfides, carbonates and hydroxides. The pH of the medium plays a critical role for selective precipitation of the target metals. However, limited information is available on the recovery of valuable metals from the pregnant bioleached medium using biological methods. Biswal et al. (2018) used the fungal leaching solution for the recovery of Co and Li using the chemical precipitation method. Co recovery was attempted by adding three types of chemical reagents namely cobalt sulfide, cobalt hydroxide and cobalt oxalate which resulted in the Co recovery efficiency of 88–100%. Li was precipitated as lithium carbonate by adding sodium carbonate, and the Li recovery was 73.6%. Biogenic sulfide precipitation which is mediated by sulfate reducing bacteria (SRB) is used for metal recovery from secondary sources and natural ores (Sethurajan and Gaydardzhiev, 2021). The bioprecipitation reactions occur in the anoxic environment as shown in the following equations (Eqs. 6–8). Several studies have reported that SRB namely *Desulfovibrio vulgaris* are effective for bio-precipitation of Co as cobalt sulfide ($CoS \cdot xH_2O$) from the aqueous medium in sulfidic environment (Blessing et al., 2001; Mansor et al., 2020). In SRB-based bio-precipitation reactions (**Supplementary Figure 5**), organic carbon acts as an electron donor, while sulfate is acts as an electron acceptor (Sethurajan and Gaydardzhiev, 2021). Using acetic acid (CH_3COOH) as the model organic carbon source, the bio-precipitation reactions are presented in Eqs. 9, 10 (Kumar et al., 2015).

$$OM\ \left(Organic\ matter\right) + SO_4^{2-} \xrightarrow{SRB} H_2S + HCO_3^- \quad (6)$$

$$H_2S \rightarrow HS^- + H^+ \quad (7)$$

$$M^{2+} + HS^- \rightarrow MS_{(s)} + H^+ \left(Where\ M^{2+}\ Metal\ cation\right) \quad (8)$$

$$CH_3COOH + 2H_2O \rightarrow 2CO_2 + 8H^+ + 8e^- \quad (9)$$

$$SO_4^{2-} + 8H^+ + 8e^- \rightarrow S^{2-} + 4H_2O \rightarrow H_2S + M^{2+} \rightarrow MS + 2H^+ \quad (10)$$

5.6. Bioleaching kinetics

Bioleaching kinetic studies help to understand the nature and mechanism of the leaching process (Baniasadi et al., 2019). However, limited information is currently available on the kinetics of spent LIBs bioleaching. Although kinetics of bioleaching process is usually slower than other recycling processes namely conventional hydrometallurgy and pyrometallurgy, a few studies have reported that while using metallic ions (e.g., Cu^{2+} and Ag^+) as catalysts, the dissolution rate of metals was considerably enhanced (Zeng et al., 2013; Niu et al., 2015). Addition of catalytic ions accelerates electron transfer in the leaching solution (Zeng et al., 2013). With the application of 0.8 g/L Cu^{2+} into the bioleaching medium containing microbial consortia of *L. ferriphilum* (IOB) and *A. thiooxidans* (SOB), the solubilization rate of Zn and Mn from Zn–Mn batteries increased from 47.7 to 62.5% and from 30.9 to 62.4%, respectively (Niu et al., 2015). Additionally, the kinetic data were fitted with four different types of models (chemical reaction controlled model, shrinking sphere model, diffusion controlled model and product layer diffusion model), and the chemical reaction controlled model was most suitable to describe the kinetics data with the R^2 value of 0.9783. However, another study from the same research group on spent LIBs bioleaching using microbial consortia of *Sulfobacillus* spp. (IOB) and *Alicyclobacillus* spp. (SOB) achieved 72% Co and 89% Li at pulp density of 2% (w/v) (Niu et al., 2014). However, the researchers reported that the product layer diffusion model was best fitted to describe the kinetic data (R^2: 9,731). According to Baniasadi et al. (2019) the rate of bioleaching is controlled by the diffusion controlled model which is described as the shrinking core model. Sedlakova-Kadukova et al. (2020) also used the shrinking core model to describe the Li dissolution kinetics from lepidolite under three different microbial agent (bacteria, fungi and yeast) bioleaching systems. Other bioleaching studies on metal recovery from e-waste (e.g., printed circuit boards) also found that the shrinking core model was the most suitable for description of metal dissolution kinetics (Faraji et al., 2018; Arslan, 2021; Ilyas et al., 2022). In addition to metal ion catalysts, the application of ultrasonication (Nazerian et al., 2023) and reducing agents (Ghassa et al., 2020) is explored to enhance metal dissolution kinetics, but in-depth studies are needed to understand the associated kinetics mechanisms.

6. Factors impacting the performance of bioleaching process

The metal dissolution rate from spent LIBs in the bioleaching process depends on both biotic and abiotic factors (Moazzam et al., 2021; Sethurajan and Gaydardzhiev, 2021). The biotic factors include the type of microbial agents (bacteria vs. fungi). However, the abiotic factors include the leaching solution chemistry (e.g., concentration of nutrients and energy/carbon source and pH), environmental parameters (e.g., temperature), and other factors namely pulp density, spent LIBs particle size, aeration, and catalyst (**Supplementary Table 3**). The influence of the key parameters on the bioleaching performance is discussed below.

6.1. Composition of leaching medium

The quality and quantity of leaching medium components including nutrients and energy and carbon source considerably impact on the microbial growth and production of metabolites, and finally the bioleaching performance (Roy et al., 2021a). In bacterial leaching involving autotrophic microorganisms, various inorganic reagents such as S^0, Fe^{2+} (e.g., $FeSO_4.7H_2O$) and pyrite (FeS_2) are used as an energy source (Bahaloo-Horeh et al., 2019). To reduce the overall recycling cost, iron-containing waste materials like iron

scrap are applied instead of commercial reagents ($FeSO_4.7H_2O$) for the bacterial leaching of spent LIBs and a similar level of metal recovery (Co and Ni) was achieved in both cases (Ghassa et al., 2020). In fungal leaching, which is mediated by the heterotrophic microbial agents, organic carbon (sucrose or glucose) is used as the carbon source (Roy et al., 2021a). Organic carbon containing industrial wastes namely vanasse can be utilized as carbon source in fungal leaching (Alavi et al., 2021).

In a recent study, with the increase of Fe_2SO_4 concentration from 45 to 150 g/L, the dissolution of Co was enhanced from 44.51 to 94.02%, while Li was increased from 42.92 to 60.30% (Roy et al., 2021b). Li et al. (2013) conducted the bioleaching study of spent LIBs using *A. ferrooxidans* at the Fe^{2+} concentration in the range between 25 and 65 mg/L, and an optimum Co recovery (48.2%) was achieved at the Fe^{2+} dose of 45 mg/L. The increase of Co recovery was related to the increase of the redox potential with the change of the Fe^{2+} dose in the leaching system. A study investigated the bioacids production by *A. niger* using sucrose as the carbon source with concentration ranging from 50 to 150 g/L (Bahaloo-Horeh and Mousavi, 2017). Higher production of various bioacids (citric acid: 26,478 mg/L, malic acid: 1,832.53 mg/L, gluconic acid: 8,433.76 mg/L) was obtained under the optimal sucrose dose of 116.90 g/L, fungal inoculum concentration of 3.45% (v/v) and leaching medium pH of 5.44.

In addition to carbon [e.g., organic carbon for heterotrophic and inorganic carbon (CO_2) for autotrophic]/energy source, microorganisms require nutrients like N and P for their growth (cell synthesis) and activity (Mills et al., 2008; Biswal and Chang, 2022). Thus, inorganic reagents such as ammonium sulfate [$(NH_4)_2SO_4$] (e.g., as a source of N) and potassium dihydrogen phosphate (KH_2PO_4)/dipotassium hydrogen phosphate (K_2HPO_4) (e.g., as a source of P) are added to the medium as nutrients to support the microbial growth (Marcinčáková et al., 2016). A study compared the ($LiCoO_2$ content: 27.2%) bioleaching performance of a microbial consortia (*A. ferrooxidans* and *A. thiooxidans*) for spent LIBs in two different media: (1) synthetic nutrient medium (called 9K medium) containing all the nutrients and energy source, and (2) low nutrient medium containing only H_2SO_4 and S_0 as the energy source (Marcinčáková et al., 2016). Nutrient-rich medium exhibited higher metal removal (Co: 67% and Li: 80%) than nutrients limiting medium (Co: 1.5% and Li: 35%). Overall, the bioleaching kinetics could be impacted by changes of the substrate concentration which serves as an electron donor and/or source of energy. Thus, bioleaching medium should be provided with an optimum concentration of substrates to achieve the highest microbial growth and metabolism as well as the highest recovery of metals from spent LIBs. The increase of substrate dose beyond the optimum concentration could show inhibitory effects to microbial activity and the optimum substrate doses could vary for different microbes.

6.2. Leaching medium pH

The acidity (pH) of the leaching medium generally controls the growth of leaching bacteria and bacterial-based catalytic reactions which is optimum up to nearly pH 3.5 (Mishra et al., 2008). Most of the acidophilic bacteria (e.g., IOB and SOB) show optimum growth at the pH range of 2.0–2.5 (Bosecker, 1997). Li et al. (2013) performed the bioleaching of spent LIB using *A. ferrooxidans* at the pH range of 1.0–4.0 and the highest Co recovery was obtained (47.6%) at the pH of 1.5. The fungal-based bioleaching can be performed in a wider pH range between 3.0–7.0 (Moazzam et al., 2021). Ijadi Bajestani et al. (2014) reported that *A. ferrooxidans*-based bioleaching at an initial pH of 1.0 with LIBs particle size of 1.62 μm and the initial Fe^{3+} concentration of 9.7 g/L demonstrated optimum removal of various metals (93.7% Co, 87% Ni and 67% Cd) from spent batteries (Ni-Cd and Ni-MH). The optimum pH for the *A. niger*-based bioleaching is nearly 5.0. In a fungal bioleaching test, it was observed that an initial pH of 5.44 with sucrose concentration of 116.90 g/L and inoculum size of 3.45% (v/v) results in a maximum production of various metabolites (citric acid, malic acid and gluconic acid) (Bahaloo-Horeh and Mousavi, 2017). In the bioleaching tests, the pH of the leaching medium usually increases (consumption of bioacids) initially after the addition of spent LIBs powder due to its alkaline nature of Li-based compounds in LIB (Heydarian et al., 2018). Li is an alkaline metal which highly reacts with water and produces lithium hydroxide in aqueous medium (Heydarian et al., 2018). Furthermore, in bacterial leaching, the oxidation of Fe^{2+} to Fe^{3+} by IOB resulted in a decrease of pH due to proton consumption as shown in the following equation (Eq. 11) (Ijadi Bajestani et al., 2014). Together, the leaching kinetics could be influenced by the changes of solution pH since it impacts the microbial growth and its activity. The optimum pH for a bioleaching process depends on the selected microbial agents and the operating systems.

$$Fe^{2+} + \frac{1}{4}O_2 + H^+ \xrightarrow{IOB} Fe^{3+} + \frac{1}{2}H_2O \quad (11)$$

6.3. Pulp density

The toxicity level of the leaching environment could change with the change of pulp density dose since metals and other hazardous components of spent LIB could exert toxicity effects to the microbial agents (Biswal et al., 2022). At higher pulp density, the metal ions (e.g., Co^{2+} and Li^+) in the spent LIBs induce oxidative stress on the leaching microorganisms (Liu et al., 2020). In a simulated bioleaching experiments using acidophilic microbial consortium (*L. ferriphilum* and *S. thermosulfidooxidans*), at a pulp density of 4% (w/v) $LiCoO_2$ powder, the intracellular ROS level in the mixed culture was enhanced from 0.82 to 6.02 in 24 h, which was nearly three times greater than the control test at 0% pulp density (2.04) (Liu et al., 2020). Niu et al. (2014) compared the valuable metals leaching efficiency at pulp densities of 1–4%, and observed that with the increase of pulp density from 1 to 4%, the amount of Co (declined from 52 to 10%) and Li (declined from 80 to 37%) dissolution was considerably reduced. The pulp density dose of 2% shows an optimum performance with 72% Co and 89% Li extraction being achieved. Naseri et al. (2019b) explored a two-step bioleaching of various metals from the spent lithium-ion coin cell at various pulp densities (10–50 g/) using the *A. thiooxidans*, and observed that the metal extraction decreased at higher pulp densities. The pulp density of 30 g/L resulted in optimum metal dissolution with 60% Co, 99% Li and 20% Mn removal. The decrease of metal removal efficiency at the higher pulp density is due to the reduction of microbial growth by environmental toxicity,

the increase of viscosity of leaching solution and the reduction of oxygen transfer (Naseri et al., 2019b). In total, an appropriate pulp density should be provided to the bioleaching system to achieve maximum microbial growth and metal extraction. With the increase of pulp density, the oxygen mass transfer may decrease due to the increase of viscosity of the leaching medium which ultimately could reduce the metal extraction kinetics (Roy et al., 2021a). For the commercialization, bioleaching at higher pulp density is required.

6.4. Temperature

Temperature strongly influences the microbial growth, and hence impacts the bioleaching efficiency (Niu et al., 2014). A majority of SOB and IOB as well as fungal species can grow well between 28 and 30°C (Bosecker, 1997). Using a mixed culture of *Alicyclobacillus* spp. (SOB) and *Sulfobacillus* spp. (IOB), Niu et al. (2014) investigated the effects of various temperatures (30–40°C) on metal bioleaching from spent LIBs with a mixed bacterial culture, and found that with the increase of temperature from 30 to 35°C, the leaching of Co and Li increased from 52 and 78% to 72 and 89%, respectively. Further increase of temperature to 40°C resulted in the decrease of leaching efficiency which is possible due to inhibition of microbial growth (Niu et al., 2014). The bioleaching experiments are usually conducted in the temperature range between 22–35°C (Moazzam et al., 2021). Together, temperature is considered as one of the critical factors which impacts the leaching kinetics. The leaching kinetic increases up to the optimum temperature, and then decreases due to reduction of microbial growth and its activity. Additionally, the changes of temperature impact the thermodynamics (e.g., Gibb's free energy) of various biochemical reactions according to the Arrhenius law of thermodynamics (Niu et al., 2014).

6.5. Aerobic environment (dissolved oxygen level)

Most of the acidophilic microorganisms, both bacteria (e.g., *A. ferrooxidans*) and fungi (e.g., *A. niger*) grow well under aerobic environments (Bosecker, 1997; Putra et al., 2022; Nazerian et al., 2023). Hence, sufficient oxygen/air should be supplied to the leaching medium (e.g., through aeration, stirring or shaking) to obtain optimum microbial activities and metal leaching efficiency. *A. ferrooxidans* gets energy for the growth through the oxidation of substrate, ferrous ions (electron donor) (i.e., oxidation of Fe^{2+} to Fe^{3+}) in which the dissolved oxygen (O_2) acts as a terminal electron acceptor (Liang et al., 2016; Liu et al., 2020). A recent bioleaching study using *A. ferrooxidans* isolated from the acid mine drainage reported that Co extraction from spent LIBs was nearly 74% with aeration (stirring) of the leaching medium, while Co leaching was reduced to nearly 52% without aeration (Putra et al., 2022). Overall, in aerobic bioleaching system, O_2 acts as an electron acceptor. Thus, sufficient dissolved oxygen should be available in the leaching medium to achieve faster leaching kinetics.

6.6. Addition of catalysts

Bioleaching is usually considered as the slow kinetics process due to inhibition of growth and metabolism of leaching microorganism by toxic effects of high concentration metals (Zhang et al., 2023). Hence, to accelerate the metal dissolution kinetics, several metallic ions (e.g., Ag^{+}, Cu^{2+}, Bi^{3+}, Hg^{2+}, and Co^{2+}) are added which accelerate the electron transfer and improve the metal removal performance (Niu et al., 2015). With the addition of 0.75 g/L of copper ions (Cu^{2+}), the bioleaching of Co from spent LIBs remarkably increased from 43.1 to 99.1% in 10 days leaching period (Zeng et al., 2012). Additional bioleaching experiments from the same research group reported that with the supplementation of leaching medium with 0.02 g/L of silver ions (Ag^{+}), the Co leaching rate was almost doubled within 7 days, i.e., the amount of Co dissolution increased from 43.1 to 98.4% (Zeng et al., 2013). Noruzi et al. (2022) also found similar results of the enhancement of metals extraction efficiency from spent LIBs with the addition of silver ions (0.02 g/L), i.e., up to 99.95% Co and Ni leaching was observed by the supplementation of leaching (two-step approach) medium with silver ions. The copper ion (Cu^{2+})-based (Eqs. 12, 13) and silver ion (Ag^{+})-based (Eqs. 14–16) catalytic reactions for the removal of Co and Li from spent LIBs are presented in Roy et al. (2021a) and Golmohammadzadeh et al. (2022).

$$Cu^{2+} + 2LiCoO_2 \leftrightarrow CuCo_2O_4 + 2Li^{+} \quad (12)$$

$$CuCo_2O_4 + 6Fe^{3+} \leftrightarrow 6Fe^{2+} + Cu^{2+} + Co^{2+} + 2O_2 \quad (13)$$

$$Ag^{+} + LiCoO_2 \leftrightarrow AgCoO_2 + Li^{+} \quad (14)$$

$$AgCoO_2 + 3Fe^{3+} \leftrightarrow 3Fe^{2+} + Ag^{+} + Co^{2+} + O_2 \quad (15)$$

$$4Fe^{2+} + O_2 + 4H^{+} \xrightarrow{Bacteria} 4Fe^{3+} + 2H_2O \quad (16)$$

In addition to metallic catalyst-based bioleaching, a few studies have applied ultrasonication (called sonobioleaching) to accelerate the leaching efficiency (Nazerian et al., 2023). Without ultrasonication, the leaching of Co, Li, Mn and Ni was 13, 57, 42 and 25%, respectively, with *A. ferrooxidans* at the pulp density of 10 g/L (Nazerian et al., 2023). However, with the application of ultrasonication (203.5 W for 0.5 h), the metal leaching efficiency was increased (Co: 19%, Li: 57%, Mn: 50% and Ni: 34%) and the leaching time was reduced to nearly half (shortened from 24 h to 12 h). The increase of bioleaching efficiency by the application of ultrasound is due to the following four mechanisms such as (1) increase of convective penetration in the leaching medium by disintegration of particles, (2) increase of temperature and pressure of the leaching medium by cavitation, (3) enhancement of the homogeneous and heterogeneous reactions (having metals as the catalysts/reactants) by ultrasound application, and (4) generation of various reactive radical species according to the following reactions (Eqs. 17–20), followed by the enhancement of the concentration of ferric ion (Eqs. 21–23) in the leaching medium that accelerates/stimulates the reaction rate (Nazerian et al., 2023). Overall, in the catalysts-based bioleaching system, an appropriate

dose of catalysts should be applied to the leaching medium to obtain maximum microbial growth and leaching efficiency. The addition of catalysts lowers the activation energy, and thus accelerates the reaction rate (Bahaloo-Horeh et al., 2019).

$$H_2O \rightarrow H^{\cdot} + HO^{\cdot} \quad (17)$$

$$H^{\cdot} + O_2 \rightarrow HOO^{\cdot} \quad (18)$$

$$2HO^{\cdot} \rightarrow H_2O_2 \quad (19)$$

$$2HOO^{\cdot} \rightarrow H_2O_2 + O_2 \quad (20)$$

$$Fe^{2+} + OH^{\cdot} \rightarrow Fe^{3+} + OH^{-} \quad (21)$$

$$Fe^{2+} + HO_2^{\cdot} \rightarrow Fe^{3+} + HO_2^{-} \quad (22)$$

$$Fe^{2+} + H_2O_2 \rightarrow Fe^{3+} + OH^{-} + OH^{\cdot} \quad (23)$$

6.7. Spent LIBs particle size

Mass transfer is one of the key factors which influences the bioleaching performance (Bahaloo-Horeh et al., 2019). The availability of contact surface of the particles of spent LIBs used for leaching impacts the mass transfer rate. Generally, with the decrease of particle size (i.e., higher surface are), the contact surface increases, and as a result the mass transfer also increases (Bahaloo-Horeh et al., 2019). The upsurge of mass transfer contributes to the higher removal of metals from spent LIBs. Appropriate mesh size is usually used to sieve and collect the desired smaller size particles spent LIBs powder after crushing and milling (Mishra et al., 2008). In a majority of the studies, the size of spent LIBs powder used in bioleaching tests largely varied between less than 75 and 300 μm (Mishra et al., 2008; Bahaloo-Horeh et al., 2018; Biswal et al., 2018). Nonetheless, a few studies used commercial $LiCoO_2$ powder for the bioleaching tests and the particle size varied between 105 and 130 μm (Liu et al., 2020). Together, to achieve higher metal extraction in bioleaching, an appropriate LIB particle size should be used since the mass transfer is limited at bigger particle size. Additionally, the biofilm development and microbe-metal interactions may be higher in smaller LIB particles due to high surface area, and stronger microbe-metal interactions could result in faster leaching kinetics.

7. Insights into bioleaching mechanisms: metal dissolution by microbe-material interactions

Several biochemical mechanisms are proposed to explain the bioleaching reactions (Işıldar et al., 2019). The bioleaching reactions are broadly categorized into three groups namely (1) acidolysis, (2) redoxolysis and (3) complexolysis (**Figure 5**) based on the types of energy and carbon sources used as well as the type of biological production of metabolites (e.g., bioacids) (Botelho Junior et al., 2021; Sethurajan and Gaydardzhiev, 2021). In acidolysis, metal transformation from insoluble to soluble form occurs by the produced bioacids and/or protons. In redoxolysis, the microbes are attached to the surface of waste materials to be leached through the biofilm formation and the extracellular polymers (EPS), triggering the metal solubilization due to electron transfer between the solid mineral in waste materials and the microbes. In the case of complexolysis, the metabolites (bioacids) produced by the microbes form the soluble metal-organic complex through chelation and complexation reactions (Sethurajan and Gaydardzhiev, 2021). For the bacterial–based leaching, two types of leaching mechanisms are proposed: (1) direct (contact) leaching, and (2) indirect (non-contact leaching) (Bahaloo-Horeh et al., 2019; Roy et al., 2021a). The direct mechanism mainly occurs in one-step and two-step bioleaching tests where there is a physical contact between the microorganisms and the spent LIBs particles (Bahaloo-Horeh et al., 2019). However, the indirect mechanisms are mainly applicable to the cells free spent medium bioleaching test (Bahaloo-Horeh et al., 2019). The bioleaching mechanism for the removal of Li is different from that of other metals (Co, Mn, and Ni), For example, Li leaching is mainly driven by the non-contact mechanism (acidolysis), while the contact mechanism [acid solubilization plus reduction of insoluble form of metals (Co^{3+}, Mn^{4+}, and Ni^{3+}) by Fe^{2+}] contributes to the removal of Co, Mn and Ni from spent LIBs (Xin et al., 2016). The extracellular polymeric substances (EPS) secreted by the bacteria play an important role in metal dissolution since strong attachment occurs between bacterial cell and spent LIBs particle through EPS by hydrophobic and electrostatic forces (Wang et al., 2018). Moreover, EPS concentrate Fe^{2+}/Fe^{3+} cycle inside the battery particle which accelerate the metal removal by reductive mechanism. EPS increases the electronic potential which accelerates electron transfer and metal solubilization. A few studies have reported that biosorption and bioaccumulation contribute to metal removal from spent batteries specifically in fungal leaching (Bahaloo-Horeh et al., 2019; Dusengemungu et al., 2021). Biosorption is a process of accumulation of metals onto the biomass through numerous physicochemical processes (e.g., adsorption). Bioaccumulation is a process of the transport of soluble metal ions into the living biomass through cell membrane which is facilitated by the different functional groups (amine, carboxyl, hydroxyl, phosphate and sulfate) present in the fungal mycelium (Dusengemungu et al., 2021).

7.1. Bacterial bioleaching mechanisms

7.1.1. Direct leaching

Under the direct leaching, the microbes attachment to the surface of the spent LIBs particle facilitates the electron transfer reactions (or electrochemical interactions) between the metal substrate in spent LIBs and the reduced metal ions (usually added externally) (Roy et al., 2021a). Since spent LIBs hardly contain any iron-sulfur containing minerals, S^0 and Fe^{2+} (e.g., in the form of $FeSO_4$) are usually added externally as a source of energy and electron donor to promote bacterial leaching. The direct microbial interactions between bacteria (e.g., SOB) and spent LIBs

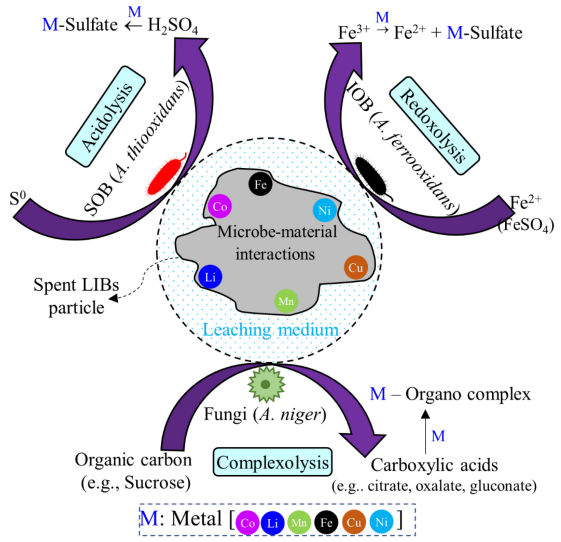

FIGURE 5
Key biochemical mechanisms for removal of metals from spent LIBs [adapted and modified from a previous study (Sethurajan and Gaydardzhiev, 2021)].

results in the formation of biogenic inorganic acid, H_2SO_4 due to the oxidation of S^0 and the concurrent oxidation of Fe^{2+} to Fe^{3+} also occurs (Eqs. 24–27) (Bahaloo-Horeh et al., 2019; Roy et al., 2021a). Both H_2SO_4 and Fe^{2+} act as oxidizing agents and facilitate the mobilization of metals from the spent LIB solid matrices. Xin et al. (2009) reported that acid-based solubilization (acidolysis) was the sole mechanism for valuable metal recovery from spent batteries in the sulfur (S^0)-based bioleaching system, whereas a combined effects of acid solubilization (acidolysis) and Fe^{2+} facilitated reduction (redoxolysis) contributed for the metal removal in the FeS_2 or S + FeS_2 bioleaching system.

$$S^0 + H_2O + \frac{3}{2}O_2 \xrightarrow{SOB\ (e.g.,\ A.\ thiooxidans)} H_2SO_4 \quad (24)$$

$$H_2SO_4 + M\,(s) \rightarrow MSO_4(aq) + 2H^+ \left(M = Metals\ in\ spent\ LIBs\right) \quad (25)$$

$$4LiCoO_2 + 3H_2SO_4 \rightarrow Co_3O_4\,(s) + 2Li_2SO_4\,(aq) + CoSO_4\,(aq) + 3H_2O + \frac{1}{2}O_2 \quad (26)$$

$$2Fe^{2+} + \frac{1}{2}O_2 + 2H^+ \xrightarrow{Bacteria} 2Fe^{3+} + H_2O \quad (27)$$

7.1.2. Indirect leaching

The indirect leaching is carried out by the lixiviants produced by the bacteria which chemically oxidize the reduced metal substrates in the spent LIBs (Bosecker, 1997). The IOB oxidizes Fe^{2+} to Fe^{3+}, then reduction reactions of Fe^{3+} lead to the production of protons (H^+ ions) which enhances the metals recovery efficiency (Eqs. 28–31). The aerobic metabolism of *A. ferrooxidans* is presented in **Figure 6**.

$$4Fe^{2+} + O_2 + 4H^+ \xrightarrow{IOB\ (e.g.,\ A.\ ferrooxidans)} 4Fe^{3+} + 2H_2O \quad (28)$$

$$Fe^{3+} + H_2O \rightarrow Fe(OH)^+ + H^+ \quad (29)$$

$$Fe^{3+} + 2H_2O \rightarrow Fe(OH)_2^+ + 2H^+ \quad (30)$$

$$Fe^{3+} + 3H_2O \rightarrow Fe(OH)_3^+ + 3H^+ \quad (31)$$

7.2. Fungal bioleaching mechanism

The fungal bioleaching mechanism mainly involves organic carboxylic acids (e.g., citric acid, oxalic acid and gluconic acid) produced by the heterotrophic fungal species during aerobic metabolism using sucrose as the carbon source (Bahaloo-Horeh and Mousavi, 2017). The metal solubilization by organic acids is mainly driven by the acidolysis and complexolysis reactions (by protons released by bioacids). However, the bioacids also change the oxidation potential of the leaching media, i.e., redoxolysis reaction (by anions from bioacids, e.g., citrate, oxalate, gluconate, etc.) and also contribute to the metal solubilization (Eqs. 32–43) (Biswal et al., 2018; Işıldar et al., 2019).

$$C_{12}H_{22}O_{11}(Sucrose) + H_2O \rightarrow C_6H_{12}O_6\,(Glucose) + C_6H_{12}O_6(Fructose) \quad (32)$$

$$C_6H_{12}O_6(Glucose) + 1.5O_2 \rightarrow C_6H_8O_7(Citric\ acid) + 2H_2O \quad (33)$$

$$C_6H_8O_7 \leftrightarrow (C_6H_7O_7)^- + H^+ \quad (34)$$

$$(C_6H_7O_7)^- + M^+\,(Metal) \leftrightarrow M\,[C_6H_7O_7]\,(Citric\ metallic\ complex) \quad (35)$$

$$C_6H_{12}O_6(Glucose) + 4.5O_2 \rightarrow 3C_2H_2O_4(Oxalic\ acid) + 3H_2O \quad (36)$$

$$C_2H_2O_4 \leftrightarrow (C_2HO_4)^- + H^+ \quad (37)$$

$$(C_2HO_4)^- + M^+\,(Metal) \leftrightarrow M\,[C_2HO_4]\,(Oxalic\ metallic\ complex) \quad (38)$$

$$C_6H_{12}O_6(Glucose) + O_2 \rightarrow C_6H_{10}O_6\,(Gluconolactone) + H_2O_2 \quad (39)$$

$$C_6H_{10}O_6(Gluconolactone) + H_2O \rightarrow C_6H_{12}O_7\,(Gluconic\ acid) + H_2O_2 \quad (40)$$

$$H_2O_2 \rightarrow H_2O + \frac{1}{2}O_2 \quad (41)$$

$$C_6H_{12}O_7 \leftrightarrow (C_6H_{11}O_7)^- + H^+ \quad (42)$$

$$(C_6H_{11}O_7)^- + M^+ \,(Metal) \;\leftrightarrow\; M\,[C_6H_{11}O_7] \quad (Gluconic\ metallic\ complex) \qquad (43)$$

8. Sustainability of bioleaching method for recycling of spent LIBs

Our literature review shows that most of previous studies mainly focused on the recycling of spent LIBs using various technologies, but limited information is available about the sustainability assessment of recycling technologies, especially the bioleaching method. The comparison of bioleaching and other recycling methods (e.g., pyrometallurgical and hydrometallurgical) from the sustainability viewpoint is usually done by performing comprehensive LCA which considers most of the environmental impacts of a recycling technique (Villares et al., 2016). A detailed LCA is required for scaling of the bioleaching process for industrial applications (Roy et al., 2022). A few studies have also performed techno-economic analysis (TEA) and energy assessment of the bioleaching process. According to a very recent study, the LCA results show the reduction of global warning potential (GWP) by nearly 8 times with the recycling of spent LIBs by bioleaching methods using *Gluconobacter oxydans* bacteria (6–19 kg CO_2 equivalent GWP per kg of recovered Co) compared to other technologies (e.g., hydrometallurgy using HCl, 43–91 kg CO_2 equivalent GWP per kg of recovered Co) (Alipanah et al., 2023). The TEA analysis projected a possible average profit of 21% for the processing of 10,000 tons/year of black mass (mostly cathode materials from spent LIBs). The economic viability of the bioleaching method is highly dependent on the purchasing price of spent LIBs (costs of collection and transportation). Moreover, the cost of chemical reagents used as the energy sources reagent (e.g., iron sulfate) and their consumption rate also have effects on the economic feasibility of the bioprocess (Alipanah et al., 2023). Sun et al. (2016) performed the LCA of recycling of spent Zn-Mn batteries using bacterial consortia (*Alicyclobacillus* spp. and *Sulfobacillus* spp.) at the pilot-scale operation mode. Among the tested 18 environmental impact parameters, the two parameters namely human toxicity (62.7 kg 1, 4- dichlorobenzene equivalent per kg of battery treatment) and marine ecotoxicity (0.46 kg 1, 4- dichlorobenzene equivalent per kg of battery treatment) were the main components of the environmental impact that get much attention. Among the various recycling processes, the pre-treatment processes such as mechanical cutting and crushing of spent LIBs accounted for the highest environmental impact.

Although limited information is available on the TEA for spent LIBs recycling using the bioleaching method, Işıldar (2018) compared the TEA for the recycling of printed circuit boards (PCBs) using three different routes (chemical, biological and hybrid approaches consisting of chemical plus biological methods). Notably, the total costs (a combination of operational costs and capital investment costs) for PCBs recycling using the biological method (EUR 0.616/kg PCB) was lower than that of the chemical (EUR 0.67/kg PCB) and hybrid methods (EUR 1.008/kg PCB). Thus, the TEA results suggest that the biological process is the most economically feasible method for the recovery of metals from e-wastes. Nevertheless, other critical factors including the potential environmental impacts, recovery yield and possible revenue generation need to be considered for selection of a specific recycling technology (Moazzam et al., 2021). For the overall costs associated with the recycling of spent LIBs, the cost of purchasing of spent LIBs was the major contributor (62–89%) of the total recycling cost (Alipanah et al., 2023). Boxall et al. (2018) computed the economic value of various metals recovered from the spent LIB by employing a sequential batch leaching process with biogenic ferric iron (mixed culture of IOB and SOB) and 100 mM H_2SO_4, and they reported the requirements to achieve the potential economic value of US$10,769 (Co: $9,558, Cu: $602, Ni:$332, Li: $257 and Mn:$20) for processing of one ton of spent LIBs. The maturity level which is measured by the technology readiness levels (TRL) of the biological method for e-wastes recycling seems to be lower [TRL > 4 (exploratory stage), operation at the column and tank reactors] compared to pyrometallurgical and hydrometallurgical methods (TRL > 6) (Moazzam et al., 2021).

9. Future research directions

- In most of the existing bioleaching studies, specific groups of microbial agents (e.g., *A. thiooxidans* and *A. ferrooxidans* in bacterial leaching, and *A. niger* in fungal leaching) are studied for their bioleaching performance. However, efforts should be made in future for isolation of acidophilic microbes from the acidic and metal contaminated sites (e.g., acid-mine drainage), followed by assessment of their bioleaching capacity.
- Since spent LIBs contain diverse toxic elements including critical metals and organic electrolytes/solvents, synthetic biology-based techniques (e.g., genetic engineering) can be applied to modify the metal tolerance genes in the microbial genome to enhance its tolerance level to the toxic elements of spent LIBs. The overall recycling cost may decease using the genetically modified microbes (engineered microbes) since a few pre-treatment processes (e.g., washing and drying of battery powder) can be omitted.
- Although numerous research works are performed on critical metal dissolution using bacterial and fungal bioleaching, limited information is currently available about the recovery of highly concentrated dissolved metal ions from the pregnant bioleached solution using biological methods, e.g., bio-precipitation employing the metal reducing bacteria. Recovery of high-grade valuable metals from spent LIBs electrodes would contribute not only to the economy, but also to achieving the circularity and a closed-loop bioprocess.
- Future studies should provide a better understanding of the leaching kinetics and thermodynamics of the bioleaching process. This would in turn help to gain insights into the potential mechanisms involved in the microbial-mediated metal solubilization.
- The existing literature has largely focused on the optimization of operating parameters to enhance the critical metal dissolution efficiency from spent LIBs powder, but

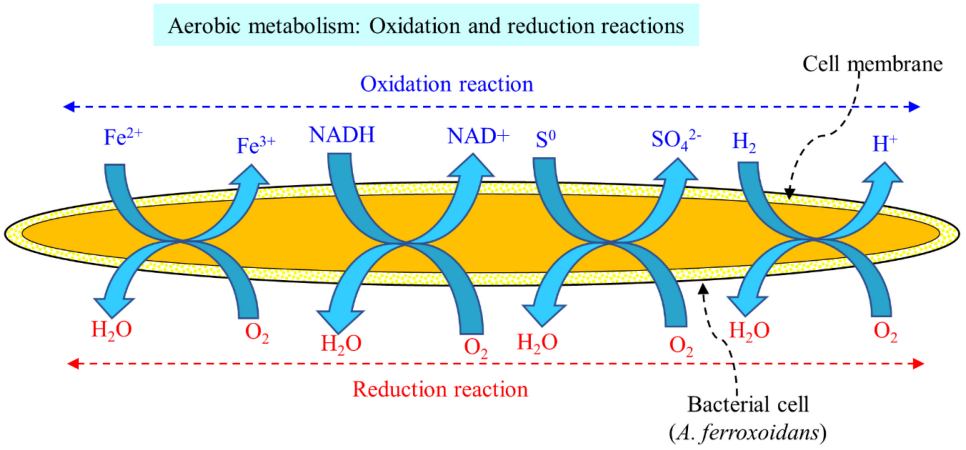

FIGURE 6
Oxidation and reduction reactions involving by aerobic metabolism of *Acidithiobacillus ferrooxidans* which contribute to the metal leaching [adapted and modified from a previous study (Valdés et al., 2008)].

more attention should be given to assess the economic, energy and environmental sustainability assessment of the bioleaching method.

10. Discussion and conclusion

Recycling of spent LIBs is necessary from the perspectives of sustainability, circular economy and environmental protection (Zeng et al., 2014; Mao et al., 2022). This review presents a comprehensive analysis of the current developments on the recovery of valuable metals (mainly Co and Li) from spent LIBs using microbial agents namely bacterial and fungal species. The efficiency of bioleaching processes reported in literature has large variations which could be due to differences in experimental, operational and/or environmental conditions adopted in different works including the type of microbial agents employed, changes of leaching medium chemistry, changes of spent LIBs chemistry (cathode materials), and environmental conditions (temperature) (Moazzam et al., 2021; Sethurajan and Gaydardzhiev, 2021). Between the two types of microbial agents, fungal leaching seems to result in higher overall valuable metal solubilization yield than bacterial leaching because heterophilic fungi exhibit high level of tolerance to the toxic leaching environment. Additionally, it produces multiple metabolites (organic carboxylic acids) than bacteria (Biswal et al., 2018, 2022). Fungi adopt different pathways to maintain their activity in toxic environments, for example, transformation of the solubilized form of metals into their insoluble forms by reaction of the produced bioacids (e.g., precipitation of metal oxalate).

Additionally, biosorption and intracellular bioaccumulation hinder the transport of metal ions into cells. The metal solubilization capacity of microbial agents can be improved by the adaptation method (i.e., enhancement of microbial resistance to toxic metals) by exposing the microbes to the toxic environment initially by gradually increasing spent LIBs pulp density (Bahaloo-Horeh et al., 2018), adding synthetic lithium and cobalt salt solutions (Lobos et al., 2021) or by adding metallic catalysts (Ag^{+} or Cu^{2+} ions) (Zeng et al., 2012, 2013). A few studies have applied microbial consortia (e.g., mixed culture of IOB and SOB) in the bioleaching process (Heydarian et al., 2018; Ghassa et al., 2020), and obtained a high metal leaching yield. The synergetic interactions of microbial consortia with battery powder could facilitate the production of bioacids/oxidizing agents that in turn accelerate metal dissolution. Among the two types of valuable metals, the solubilization rate of Li seems to be higher than Co in both bacterial and fungal leaching systems which could be related to its unique physicochemical properties including high instability, high chemical activity as well strong hydration power (i.e., formation LiOH) in aqueous medium (Wang et al., 2012; Wei et al., 2021). Bioleaching is successfully applied for the extraction of valuable metallic resources from ores in mining industry (Zhang et al., 2023). However, bioleaching of metals from spent LIBs has largely been carried out in the laboratory-scale. At present, the TRL (technology readiness level) of bioleaching processes for the recycling of e-waste is nearly 4 (i.e., exploratory research) (Moazzam et al., 2021). Hence, more studies (mainly pilot-scale) are needed to better understand the changes of the bioleaching performance with the changes of various operating parameters as well as the associated mechanisms so that the scale-up of the bioleaching process can be carried out for industrial-scale applications.

The commercial application of the bioleaching method for critical metal recovery from spent LIBs is limited due to its slow kinetics (Mishra et al., 2008). However, several techniques including application of metal catalyst (Cu^{2+} and Ag^{+}) (Zeng et al., 2012, 2013), ultrasound treatment (called sonobioleaching) (Nazerian et al., 2023) are adopted to enhance the bioleaching kinetics and/or metal recovery. A few studies have reported that the chemical-biological hybrid systems were effective for optimum recovery of valuable metals from spent LIBs (Dolker and Pant, 2019) as the *Lysinibacillus*–citric acid hybrid system was very efficient specifically for Co recover (98%). The bioleaching method is sustainable than other recycling technologies (e.g., pyrometallurgical and hydrometallurgical) because LCA-based

studies have reported that GWP of bioleaching is considerably lower than hydrometallurgy (Alipanah et al., 2023). TEA also shows that bioleaching is economically feasible than other recycling methods (e.g., chemical and hybrid technologies) (Işıldar, 2018).

The synthesis of LIBs (specifically electrode materials) largely depends on the natural resources which are limited, for example, natural graphite for anode and critical metals like Co and Li for cathode synthesis (Olivetti et al., 2017). Biomass or bio-waste which are usually rich in organic carbon and considered as a source of renewable energy (Ahmed et al., 2022). Presently, great interest is given for the development of biowaste-based electrode materials to produce eco-friendly LIBs (Ahmed et al., 2022; Ho et al., 2022). The electrical stability of biowaste-based LIBs is comparable to LIBs synthesized using natural materials.

To achieve energy sustainability, at present significant interest is given worldwide on the development of renewable energy (green energy). The potential sources of renewable energy include biomass energy, solar energy, hydro energy, wind energy, tidal energy and geothermal energy (Kalyani et al., 2015). The key advantages of renewable energy include they are abundant, renewable and environmentally friendly due to low or zero greenhouse gas (e.g., CO_2) emission (Kalyani et al., 2015). For biomass-based energy, various types of biomass or biowastes are used as a feedstock material for conversion them into bioenergy using biotechnological-based methods (Anwar et al., 2014). For example. lignocellulosic waste (e.g., agricultural waste) are used for the production of bioethanol (Anwar et al., 2014), whereas microalgae biomass is used for production biodiesel (Ray et al., 2022). Anaerobic digestion is also a promising technology for conversion of biomass to bioenergy (e.g., biomethane) (Milledge et al., 2019). Genetic and metabolic engineering tools are applied to engineer the organisms to enhance the bioenergy production (Brar et al., 2021).

The major conclusions drawn from this review on the recovery of valuable metals from spent LIBs using microbial agents are presented here.

- Spent LIBs are usually rich in various valuable metals namely Co and Li, but their concentrations vary with the change of cathode material chemistry.
- Lithium and cobalt-based LIBs are widely used in electrical and electronic devices due to their high energy density.
- Bioleaching is an eco-friendly and green technology which looks promising for effective recovery of valuable metals from spent LIBs.
- Acidophilic microorganisms including chemolithotrophic bacteria (IOB and SOB) and heterotrophic filamentous fungi (e.g., *A. niger*) are widely used for the dissolution of valuable metals from spent LIBs.
- Bioacids produced by the microbial agents [H_2SO_4 by bacteria and diverse organic carboxylic acids (e.g., oxalic, citric and gluconic acids) by fungi] mainly contribute to the metal dissolution.
- The major mechanisms involved in the solubilization of metals include acidolysis, redoxolysis and complexolysis.
- Several biotic (type of microbial agents) and abiotic factors (leaching medium composition, pH, pulp density, aeration, particle size of LIBs powder, temperature, etc.) considerably impact the critical metal recovery efficiency in bioleaching processes.
- The bioleaching process is thermodynamically feasible, and the process is also sustainable due to its minimal negative environmental impacts and cost-effective than other recycling technologies.
- In view of the promising resource recovery applications of the bioleaching process, efforts are needed to improve the technical maturity of this process toward its large-scale practical applications based on pilot studies and techno-economic assessments through multi-disciplinary collaboration.

Author contributions

BB: conceptualization, investigation, methodology, writing—original draft, and review and editing. RB: conceptualization, supervision, funding, and writing—review and editing. Both authors contributed to the article and approved the submitted version.

Funding

The senior research fellow appointment of BB was supported by the National Research Foundation (NRF), Singapore, and Ministry of National Development (MND), Singapore under its Cities of Tomorrow R&D Programme (CoT Award COT-V4-2019-6).

Conflict of interest

The authors declare that the research was conducted in the absence of any commercial or financial relationships that could be construed as a potential conflict of interest.

Publisher's note

Supplementary material

The Supplementary Material for this article can be found online at: https://www.frontiersin.org/articles/10.3389/fmicb.2023.1197081/full#supplementary-material

References

Aboelazm, E. A. A., Mohamed, N., Ali, G. A. M., Makhlouf, A. S. H., and Chong, K. F. (2021). "Recycling of cobalt oxides electrodes from spent lithium-ion batteries by electrochemical method," in *Waste recycling technologies for nanomaterials manufacturing*, eds A. S. H. Makhlouf and G. A. M. Ali (Cham: Springer International Publishing), 91–123. doi: 10.1007/978-3-030-68031-2_4

Ahmed, A. T. A., Soni, R., Ansari, A. S., Lee, C. Y., Kim, H.-S., Im, H., et al. (2022). Biowaste-derived graphitic carbon interfaced TiO2 as anode for lithium-ion battery. *Surf. Interfaces* 35:102404. doi: 10.1016/j.surfin.2022.102404

Alavi, N., Partovi, K., Majlessi, M., Rashidi, M., and Alimohammadi, M. (2021). Bioleaching of metals from cellphones batteries by a co-fungus medium in presence of carbon materials. *Bioresour. Technol. Rep.* 15:100768. doi: 10.1016/j.biteb.2021.100768

Ali, H., Khan, H. A., and Pecht, M. (2022). Preprocessing of spent lithium-ion batteries for recycling: Need, methods, and trends. *Renew. Sustain. Energy Rev.* 168:112809. doi: 10.1016/j.rser.2022.112809

Alipanah, M., Reed, D., Thompson, V., Fujita, Y., and Jin, H. (2023). Sustainable bioleaching of lithium-ion batteries for critical materials recovery. *J. Clean. Prod.* 382:135274. doi: 10.1016/j.jclepro.2022.135274

Alipanah, M., Saha, A. K., Vahidi, E., and Jin, H. (2021). Value recovery from spent lithium-ion batteries: A review on technologies, environmental impacts, economics, and supply chain. *Clean Technol. Recycl.* 1, 152–184. doi: 10.3934/ctr.2021008

Anwar, Z., Gulfraz, M., and Irshad, M. (2014). Agro-industrial lignocellulosic biomass a key to unlock the future bio-energy: A brief review. *J. Radiat. Res. Appl. Sci.* 7, 163–173. doi: 10.1016/j.jrras.2014.02.003

Arslan, V. (2021). Bacterial leaching of copper, zinc, nickel and aluminum from discarded printed circuit boards using acidophilic bacteria. *J. Mater. Cycles Waste Manag.* 23, 2005–2015. doi: 10.1007/s10163-021-01274-9

Badawy, S., Nayl, A., Elkhashab, R. A., and El-Khateeb, M. (2013). Cobalt separation from waste mobile phone batteries using selective precipitation and chelating resin. *J. Mater. Cycles Waste Manag* 16, 739–746. doi: 10.1007/s10163-013-0213-y

Bahaloo-Horeh, N., and Mousavi, S. M. (2017). Enhanced recovery of valuable metals from spent lithium-ion batteries through optimization of organic acids produced by *Aspergillus niger*. *Waste Manag.* 60, 666–679. doi: 10.1016/j.wasman.2016.10.034

Bahaloo-Horeh, N., Mousavi, S. M., and Baniasadi, M. (2018). Use of adapted metal tolerant *Aspergillus niger* to enhance bioleaching efficiency of valuable metals from spent lithium-ion mobile phone batteries. *J. Clean. Prod.* 197, 1546–1557. doi: 10.1016/j.jclepro.2018.06.299

Bahaloo-Horeh, N., Vakilchap, F., and Mousavi, S. M. (2019). "Bio-hydrometallurgical methods for recycling spent lithium-ion batteries," in *Recycling of spent lithium-ion batteries: Processing methods and environmental impacts*, ed. L. An (Cham: Springer International Publishing), 161–197. doi: 10.1007/978-3-030-31834-5_7

Baniasadi, M., Vakilchap, F., Bahaloo-Horeh, N., Mousavi, S. M., and Farnaud, S. (2019). Advances in bioleaching as a sustainable method for metal recovery from e-waste: A review. *J. Ind. Eng. Chem.* 76, 75–90. doi: 10.1016/j.jiec.2019.03.047

Baum, Z. J., Bird, R. E., Yu, X., and Ma, J. (2022). Lithium-ion battery recycling-overview of techniques and trends. *ACS Energy Lett.* 7, 712–719. doi: 10.1021/acsenergylett.1c02602

Biswal, B., Jadhav, U., Patil, D., and Yang, E.-H. (2022). "Physicochemical and biological methods for treatment of municipal solid waste incineration ash to reduce its potential adverse impacts on groundwater," in *Contaminants of emerging concerns and reigning removal technologies*, eds M. Kumar, S. Mohapatra, and K. Acharya (Boca Raton, FL: CRC Press), 221–255. doi: 10.1201/9781003247869-12

Biswal, B. K., and Chang, J. (2022). "Impact of *Arabidopsis thaliana* root exudates on dissimilatory nitrate reduction to ammonium (DNRA) activities in *Shewanella loihica* PV-4 and agricultural soil enrichments," in *Impact of COVID-19 on emerging contaminants: One health framework for risk assessment and remediation*, eds M. Kumar and S. Mohapatra (Singapore: Springer Nature Singapore), 211–229. doi: 10.1007/978-981-19-1847-6_9

Biswal, B. K., Jadhav, U. U., Madhaiyan, M., Ji, L., Yang, E.-H., and Cao, B. (2018). Biological leaching and chemical precipitation methods for recovery of Co and Li from spent lithium-ion batteries. *ACS Sustain. Chem. Eng.* 6, 12343–12352. doi: 10.1021/acssuschemeng.8b02810

Blessing, T. C., Wielinga, B. W., Morra, M. J., and Fendorf, S. (2001). CoIIIEDTA-reduction by *Desulfovibrio vulgaris* and propagation of reactions involving dissolved sulfide and polysulfides. *Environ. Sci. Technol.* 35, 1599–1603. doi: 10.1021/es001576r

Bosecker, K. (1997). Bioleaching: Metal solubilization by microorganisms. *FEMS Microbiol. Rev.* 20, 591–604. doi: 10.1111/j.1574-6976.1997.tb00340.x

Botelho Junior, A. B., Stopic, S., Friedrich, B., Tenório, J. A. S., and Espinosa, D. C. R. (2021). Cobalt recovery from li-ion battery recycling: A critical review. *Metals* 11:1999. doi: 10.3390/met11121999

Boxall, N. J., Cheng, K. Y., Bruckard, W., and Kaksonen, A. H. (2018). Application of indirect non-contact bioleaching for extracting metals from waste lithium-ion batteries. *J. Hazard. Mater.* 360, 504–511. doi: 10.1016/j.jhazmat.2018.08.024

Brar, A., Kumar, M., Soni, T., Vivekanand, V., and Pareek, N. (2021). Insights into the genetic and metabolic engineering approaches to enhance the competence of microalgae as biofuel resource: A review. *Bioresour. Technol.* 339:125597. doi: 10.1016/j.biortech.2021.125597

Dehaine, Q., Tijsseling, L. T., Glass, H. J., Törmänen, T., and Butcher, A. R. (2021). Geometallurgy of cobalt ores: A review. *Miner. Eng.* 160:106656. doi: 10.1016/j.mineng.2020.106656

Dewulf, J., Van der Vorst, G., Denturck, K., Van Langenhove, H., Ghyoot, W., Tytgat, J., et al. (2010). Recycling rechargeable lithium ion batteries: Critical analysis of natural resource savings. *Resour. Conserv. Recycl.* 54, 229–234. doi: 10.1016/j.resconrec.2009.08.004

Do, M. P., Jegan Roy, J., Cao, B., and Srinivasan, M. (2022). Green closed-loop cathode regeneration from spent NMC-based lithium-ion batteries through bioleaching. *ACS Sustain. Chem. Eng.* 10, 2634–2644. doi: 10.1021/acssuschemeng.1c06885

Dolker, T., and Pant, D. (2019). Chemical-biological hybrid systems for the metal recovery from waste lithium ion battery. *J. Environ. Manage.* 248:109270. doi: 10.1016/j.jenvman.2019.109270

Du, K., Ang, E. H., Wu, X., and Liu, Y. (2022). Progresses in sustainable recycling technology of spent lithium-ion batteries. *Energy Environ. Mater.* 5, 1012–1036. doi: 10.1002/eem2.12271

Duan, X., Zhu, W., Ruan, Z., Xie, M., Chen, J., and Ren, X. (2022). Recycling of lithium batteries—A review. *Energies* 15:1611. doi: 10.3390/en15051611

Dusengemungu, L., Kasali, G., Gwanama, C., and Mubemba, B. (2021). Overview of fungal bioleaching of metals. *Environ. Adv.* 5:100083. doi: 10.1016/j.envadv.2021.100083

Dyatkin, B., and Meng, Y. S. (2020). COVID-19 disrupts battery materials and manufacture supply chains, but outlook remains strong. *MRS Bull.* 45, 700–702. doi: 10.1557/mrs.2020.239

Fan, E., Li, L., Wang, Z., Lin, J., Huang, Y., Yao, Y., et al. (2020). Sustainable recycling technology for li-ion batteries and beyond: Challenges and future prospects. *Chem. Rev.* 120, 7020–7063. doi: 10.1021/acs.chemrev.9b00535

Faraji, F., Golmohammadzadeh, R., Rashchi, F., and Alimardani, N. (2018). Fungal bioleaching of WPCBs using *Aspergillus niger*: Observation, optimization and kinetics. *J. Environ. Manage.* 217, 775–787. doi: 10.1016/j.jenvman.2018.04.043

Georgi-Maschler, T., Friedrich, B., Weyhe, R., Heegn, H., and Rutz, M. (2012). Development of a recycling process for Li-ion batteries. *J. Power Sources* 207, 173–182. doi: 10.1016/j.jpowsour.2012.01.152

Ghassa, S., Farzanegan, A., Gharabaghi, M., and Abdollahi, H. (2020). Novel bioleaching of waste lithium ion batteries by mixed moderate thermophilic microorganisms, using iron scrap as energy source and reducing agent. *Hydrometallurgy* 197:105465. doi: 10.1016/j.hydromet.2020.105465

Ghassa, S., Farzanegan, A., Gharabaghi, M., and Abdollahi, H. (2021). Iron scrap, a sustainable reducing agent for waste lithium ions batteries leaching: An environmentally friendly method to treating waste with waste. *Resour. Conserv. Recycl.* 166:105348. doi: 10.1016/j.resconrec.2020.105348

Golmohammadzadeh, R., Faraji, F., Jong, B., Pozo-Gonzalo, C., and Banerjee, P. C. (2022). Current challenges and future opportunities toward recycling of spent lithium-ion batteries. *Renew. Sustain. Energy Rev.* 159:112202. doi: 10.1016/j.rser.2022.112202

Gratz, E., Sa, Q., Apelian, D., and Wang, Y. (2014). A closed loop process for recycling spent lithium ion batteries. *J. Power Sources* 262, 255–262. doi: 10.1016/j.jpowsour.2014.03.126

Griffiths, G. (2016). Review of developments in lithium secondary battery technology. *Underw. Technol.* 33, 153–163. doi: 10.3723/ut.33.153

Guimarães, L. F., Botelho Junior, A. B., and Espinosa, D. C. R. (2022). Sulfuric acid leaching of metals from waste Li-ion batteries without using reducing agent. *Miner. Eng.* 183:107597. doi: 10.1016/j.mineng.2022.107597

Hariyadi, A., Masago, A. R., Febrianur, R., and Rahmawati, D. (2022a). Optimization fungal leaching of cobalt and lithium from spent li-ion batteries using waste spices candlenut. *Key Eng. Mater.* 938, 177–182. doi: 10.4028/p-lkr100

Hariyadi, A., Sholikah, U., Gotama, B., and Ghony, M. A. (2022b). Biohydrometallurgy for cobalt recovery from spent li-ion batteries using acidophilic bacteria isolated from acid mine drainage. *Chem. J. Tek. Kim* 9, 88–96.

Harper, G., Sommerville, R., Kendrick, E., Driscoll, L., Slater, P., Stolkin, R., et al. (2019). Recycling lithium-ion batteries from electric vehicles. *Nature* 575, 75–86. doi: 10.1038/s41586-019-1682-5

Hartono, M., Astrayudha, M., Petrus, H., Wiratni, W., and Sulistyo, H. (2017). Lithium recovery of spent lithium-ion battery using bioleaching from local sources microorganism. *Rasayan J. Chem.* 10, 897–903. doi: 10.7324/RJC.2017.1031767

Heydarian, A., Mousavi, S. M., Vakilchap, F., and Baniasadi, M. (2018). Application of a mixed culture of adapted acidophilic bacteria in two-step bioleaching of spent lithium-ion laptop batteries. *J. Power Sources* 378, 19–30. doi: 10.1016/j.jpowsour.2017.12.009

Ho, C. W., Shaji, N., Kim, H. K., Park, J. W., Nanthagopal, M., and Lee, C. W. (2022). Thermally assisted conversion of biowaste into environment-friendly energy storage materials for lithium-ion batteries. *Chemosphere* 286:131654. doi: 10.1016/j.chemosphere.2021.131654

Hong, Y., and Valix, M. (2014). Bioleaching of electronic waste using acidophilic sulfur oxidising bacteria. *J. Clean. Prod.* 65, 465–472. doi: 10.1016/j.jclepro.2013.08.043

Horeh, N. B., Mousavi, S. M., and Shojaosadati, S. A. (2016). Bioleaching of valuable metals from spent lithium-ion mobile phone batteries using *Aspergillus niger*. *J. Power Sources* 320, 257–266. doi: 10.1016/j.jpowsour.2016.04.104

Hua, Y., Zhou, S., Huang, Y., Liu, X., Ling, H., Zhou, X., et al. (2020). Sustainable value chain of retired lithium-ion batteries for electric vehicles. *J. Power Sources* 478:228753. doi: 10.1016/j.jpowsour.2020.228753

Huang, T., Liu, L., and Zhang, S. (2019). Recovery of cobalt, lithium, and manganese from the cathode active materials of spent lithium-ion batteries in a bio-electro-hydrometallurgical process. *Hydrometallurgy* 188, 101–111. doi: 10.1016/j.hydromet.2019.06.011

Huggins, R. A. (ed.). (2016). "Primary, non-rechargeable batteries," in *Energy storage: Fundamentals, materials and applications*, (Cham: Springer International Publishing), 291–307. doi: 10.1007/978-3-319-21239-5_16

Ijadi Bajestani, M., Mousavi, S. M., and Shojaosadati, S. A. (2014). Bioleaching of heavy metals from spent household batteries using *Acidithiobacillus ferrooxidans*: Statistical evaluation and optimization. *Sep. Purif. Technol.* 132, 309–316. doi: 10.1016/j.seppur.2014.05.023

Ilyas, S., Srivastava, R. R., Kim, H., and Ilyas, N. (2022). Biotechnological recycling of hazardous waste PCBs using *Sulfobacillus thermosulfidooxidans* through pretreatment of toxicant metals: Process optimization and kinetic studies. *Chemosphere* 286:131978. doi: 10.1016/j.chemosphere.2021.131978

Işıldar, A. (2018). *Metal recovery from electronic waste: Biological versus chemical leaching for recovery of copper and gold*. Boca Raton, FL: CRC Press.

Işıldar, A., van Hullebusch, E. D., Lenz, M., Du Laing, G., Marra, A., Cesaro, A., et al. (2019). Biotechnological strategies for the recovery of valuable and critical raw materials from waste electrical and electronic equipment (WEEE) – A review. *J. Hazard. Mater.* 362, 467–481. doi: 10.1016/j.jhazmat.2018.08.050

Jegan-Roy, J., Srinivasan, M., and Cao, B. (2021). Bioleaching as an eco-friendly approach for metal recovery from spent NMC-based lithium-ion batteries at a high pulp density. *ACS Sustain. Chem. Eng.* 9, 3060–3069. doi: 10.1021/acssuschemeng.0c06573

Kaksonen, A. H., Boxall, N. J., Gumulya, Y., Khaleque, H. N., Morris, C., Bohu, T., et al. (2018). Recent progress in biohydrometallurgy and microbial characterisation. *Hydrometallurgy* 180, 7–25. doi: 10.1016/j.hydromet.2018.06.018

Kaksonen, A. H., Deng, X., Bohu, T., Zea, L., Khaleque, H. N., Gumulya, Y., et al. (2020). Prospective directions for biohydrometallurgy. *Hydrometallurgy* 195:105376. doi: 10.1016/j.hydromet.2020.105376

Kalyani, V., Dudy, M., and Pareek, S. (2015). Green energy: The need of the world. *J. Manag. Eng. Inf. Technol.* 2, 2394–8124.

Kamat, P. V. (2019). Lithium-ion batteries and beyond: Celebrating the 2019 Nobel prize in chemistry – A virtual issue. *ACS Energy Lett.* 4, 2757–2759. doi: 10.1021/acsenergylett.9b02280

Kazemian, Z., Larypoor, M., and Marandi, R. (2020). Evaluation of myco-leaching potential of valuable metals from spent lithium battery by *Penicillium chrysogenum* and *Aspergillus niger*. *Int. J. Environ. Anal. Chem.* 103, 514–527. doi: 10.1080/03067319.2020.1861605

Kim, M.-J., Seo, J.-Y., Choi, Y.-S., and Kim, G.-H. (2016). Bioleaching of spent Zn–Mn or Ni–Cd batteries by *Aspergillus* species. *Waste Manag.* 51, 168–173. doi: 10.1016/j.wasman.2015.11.001

Kumar, N., Chaurand, P., Rose, J., Diels, L., and Bastiaens, L. (2015). Synergistic effects of sulfate reducing bacteria and zero valent iron on zinc removal and stability in aquifer sediment. *Chem. Eng. J.* 260, 83–89. doi: 10.1016/j.cej.2014.08.091

Li, L., Zeng, G., Luo, S., Deng, X., and Xie, Q. (2013). Influences of solution pH and redox potential on the bioleaching of $LiCoO_2$ from spent lithium-ion batteries. *J. Korean Soc. Appl. Biol. Chem.* 56, 187–192. doi: 10.1007/s13765-013-3016-x

Liang, G., Li, P., Liu, W., and Wang, B. (2016). Enhanced bioleaching efficiency of copper from waste printed circuit boards (PCBs) by dissolved oxygen-shifted strategy in *Acidithiobacillus ferrooxidans*. *J. Mater. Cycles Waste Manag.* 18, 742–751. doi: 10.1007/s10163-015-0375-x

Lin, L., Lu, Z., and Zhang, W. (2021). Recovery of lithium and cobalt from spent Lithium- Ion batteries using organic aqua regia (OAR): Assessment of leaching kinetics and global warming potentials. *Resour. Conserv. Recycl.* 167:105416. doi: 10.1016/j.resconrec.2021.105416

Liu, X., Liu, H., Wu, W., Zhang, X., Gu, T., Zhu, M., et al. (2020). Oxidative stress induced by metal ions in bioleaching of $LiCoO_2$ by an acidophilic microbial consortium. *Front. Microbiol.* 10:3058. doi: 10.3389/fmicb.2019.03058

Lobos, A., Harwood, V. J., Scott, K. M., and Cunningham, J. A. (2021). Tolerance of three fungal species to lithium and cobalt: Implications for bioleaching of spent rechargeable Li-ion batteries. *J. Appl. Microbiol.* 131, 743–755. doi: 10.1111/jam.14947

Ma, Y., Liu, X., Zhou, X., Tang, J., Gan, H., and Yang, J. (2022). Reductive transformation and synergistic action mechanism in the process of treating spent lithium-ion batteries with antibiotic bacteria residues. *J. Clean. Prod.* 331:129902. doi: 10.1016/j.jclepro.2021.129902

Ma, Y., Zhou, X., Tang, J., Liu, X., Gan, H., and Yang, J. (2021). Reaction mechanism of antibiotic bacteria residues as a green reductant for highly efficient recycling of spent lithium-ion batteries. *J. Hazard. Mater.* 417:126032. doi: 10.1016/j.jhazmat.2021.126032

Makuza, B., Tian, Q., Guo, X., Chattopadhyay, K., and Yu, D. (2021). Pyrometallurgical options for recycling spent lithium-ion batteries: A comprehensive review. *J. Power Sources* 491:229622. doi: 10.1016/j.jpowsour.2021.229622

Mansor, M., Cantando, E., Wang, Y., Hernandez-Viezcas, J. A., Gardea-Torresdey, J. L., Hochella, M. F. J., et al. (2020). Insights into the biogeochemical cycling of cobalt: Precipitation and transformation of cobalt sulfide nanoparticles under low-temperature aqueous conditions. *Environ. Sci. Technol.* 54, 5598–5607. doi: 10.1021/acs.est.0c01363

Mao, J., Ye, C., Zhang, S., Xie, F., Zeng, R., Davey, K., et al. (2022). Toward practical lithium-ion battery recycling: Adding value, tackling circularity and recycling-oriented design. *Energy Environ. Sci.* 15, 2732–2752. doi: 10.1039/D2EE00162D

Marcinčáková, R., Kadukova, J., Mrazikova, A., Velgosova, O., Luptakova, A., and Ubaldini, S. (2016). Metal bioleaching from spent lithium-ion batteries using acidophilic bacterial strains. *Inżynieria Miner. R* 17, 117–120.

Martins, L. S., Guimarães, L. F., Botelho Junior, A. B., Tenório, J. A. S., and Espinosa, D. C. R. (2021). Electric car battery: An overview on global demand, recycling and future approaches towards sustainability. *J. Environ. Manage.* 295:113091. doi: 10.1016/j.jenvman.2021.113091

Miao, Y., Liu, L., Zhang, Y., Tan, Q., and Li, J. (2022). An overview of global power lithium-ion batteries and associated critical metal recycling. *J. Hazard. Mater.* 425:127900. doi: 10.1016/j.jhazmat.2021.127900

Milledge, J. J., Nielsen, B. V., Maneein, S., and Harvey, P. J. (2019). A brief review of anaerobic digestion of algae for bioenergy. *Energies* 12:1166. doi: 10.3390/en12061166

Mills, M. M., Moore, C. M., Langlois, R., Milne, A., Achterberg, E., Nachtigall, K., et al. (2008). Nitrogen and phosphorus co-limitation of bacterial productivity and growth in the oligotrophic subtropical North Atlantic. *Limnol. Oceanogr.* 53, 824–834. doi: 10.4319/lo.2008.53.2.0824

Mishra, D., Kim, D.-J., Ralph, D. E., Ahn, J.-G., and Rhee, Y.-H. (2008). Bioleaching of metals from spent lithium ion secondary batteries using *Acidithiobacillus ferrooxidans*. *Waste Manag.* 28, 333–338. doi: 10.1016/j.wasman.2007.01.010

Moazzam, P., Boroumand, Y., Rabiei, P., Baghbaderani, S. S., Mokarian, P., Mohagheghian, F., et al. (2021). Lithium bioleaching: An emerging approach for the recovery of Li from spent lithium ion batteries. *Chemosphere* 277:130196. doi: 10.1016/j.chemosphere.2021.130196

Mokarian, P., Bakhshayeshi, I., Taghikhah, F., Boroumand, Y., Erfani, E., and Razmjou, A. (2022). The advanced design of bioleaching process for metal recovery: A machine learning approach. *Sep. Purif. Technol.* 291:120919. doi: 10.1016/j.seppur.2022.120919

Moosakazemi, F., Ghassa, S., Jafari, M., and Chelgani, S. C. (2022). Bioleaching for recovery of metals from spent batteries – A review. *Miner. Process. Extr. Metall. Rev.* doi: 10.1080/08827508.2022.2095376

Naseri, T., Bahaloo-Horeh, N., and Mousavi, S. M. (2019a). Bacterial leaching as a green approach for typical metals recovery from end-of-life coin cells batteries. *J. Clean. Prod.* 220, 483–492. doi: 10.1016/j.jclepro.2019.02.177

Naseri, T., Bahaloo-Horeh, N., and Mousavi, S. M. (2019b). Environmentally friendly recovery of valuable metals from spent coin cells through two-step bioleaching using *Acidithiobacillus thiooxidans*. *J. Environ. Manage.* 235, 357–367. doi: 10.1016/j.jenvman.2019.01.086

Naseri, T., Pourhossein, F., Mousavi, S. M., Kaksonen, A. H., and Kuchta, K. (2022). Manganese bioleaching: An emerging approach for manganese recovery from spent batteries. *Rev. Environ. Sci. Biotechnol.* 21, 447–468. doi: 10.1007/s11157-022-09620-5

Nayak, M., Suh, W. I., Cho, J. M., Kim, H. S., Lee, B., and Chang, Y. K. (2020). Strategic implementation of phosphorus repletion strategy in continuous two-stage cultivation of *Chlorella* sp. HS2: Evaluation for biofuel applications. *J. Environ. Manage.* 271:111041. doi: 10.1016/j.jenvman.2020.111041

Nayak, M., Suh, W. I., Lee, B., and Chang, Y. K. (2018). Enhanced carbon utilization efficiency and FAME production of *Chlorella* sp. HS2 through combined supplementation of bicarbonate and carbon dioxide. *Energy Convers. Manag.* 156, 45–52. doi: 10.1016/j.enconman.2017.11.002

Nazerian, M., Bahaloo-Horeh, N., and Mousavi, S. M. (2023). Enhanced bioleaching of valuable metals from spent lithium-ion batteries using ultrasonic treatment. *Korean J. Chem. Eng.* 40, 584–593. doi: 10.1007/s11814-022-1257-2

Niu, Z., Huang, Q., Wang, J., Yang, Y., Xin, B., and Chen, S. (2015). Metallic ions catalysis for improving bioleaching yield of Zn and Mn from spent Zn-Mn batteries at high pulp density of 10%. *J. Hazard. Mater.* 298, 170–177. doi: 10.1016/j.jhazmat.2015.05.038

Niu, Z., Zou, Y., Xin, B., Chen, S., Liu, C., and Li, Y. (2014). Process controls for improving bioleaching performance of both Li and Co from spent lithium ion batteries at high pulp density and its thermodynamics and kinetics exploration. *Chemosphere* 109, 92–98. doi: 10.1016/j.chemosphere.2014.02.059

Noruzi, F., Nasirpour, N., Vakilchap, F., and Mousavi, S. M. (2022). Complete bioleaching of Co and Ni from spent batteries by a novel silver ion catalyzed process. *Appl. Microbiol. Biotechnol.* 106, 5301–5316. doi: 10.1007/s00253-022-12056-0

Olivetti, E. A., Ceder, G., Gaustad, G. G., and Fu, X. (2017). Lithium-ion battery supply chain considerations: Analysis of potential bottlenecks in critical metals. *Joule* 1, 229–243. doi: 10.1016/j.joule.2017.08.019

Orell, A., Navarro, C. A., Arancibia, R., Mobarec, J. C., and Jerez, C. A. (2010). Life in blue: Copper resistance mechanisms of bacteria and Archaea used in industrial biomining of minerals. *Biotechnol. Adv.* 28, 839–848. doi: 10.1016/j.biotechadv.2010.07.003

Peters, J. F., Baumann, M., Zimmermann, B., Braun, J., and Weil, M. (2017). The environmental impact of Li-Ion batteries and the role of key parameters – A review. *Renew. Sustain. Energy Rev.* 67, 491–506. doi: 10.1016/j.rser.2016.08.039

Pourhossein, F., and Mousavi, S. M. (2023). Improvement of gold bioleaching extraction from waste telecommunication printed circuit boards using biogenic thiosulfate by *Acidithiobacillus thiooxidans*. *J. Hazard. Mater.* 450:131073. doi: 10.1016/j.jhazmat.2023.131073

Premathilake, D. S., Botelho Junior, A. B., Tenório, J. A. S., Espinosa, D. C. R., and Vaccari, M. (2023). Designing of a decentralized pretreatment line for EOL-LIBs based on recent literature of lib recycling for black mass. *Metals* 13:374. doi: 10.3390/met13020374

Putra, R. A., Al Fajri, I., and Hariyadi, A. (2022). Metal bioleaching of used lithium-ion battery using acidophilic ferrooxidans isolated from acid mine drainage. *Key Eng. Mater.* 937, 193–200. doi: 10.4028/p-sd859o

Qazi, A., Hussain, F., Rahim, N. A. B. D., Hardaker, G., Alghazzawi, D., Shaban, K., et al. (2019). Towards sustainable energy: A systematic review of renewable energy sources, technologies, and public opinions. *IEEE Access* 7, 63837–63851. doi: 10.1109/ACCESS.2019.2906402

Raj, A., Panchireddy, S., Grignard, B., Detrembleur, C., and Gohy, J.-F. (2022). Bio-based solid electrolytes bearing cyclic carbonates for solid-state lithium metal batteries. *ChemSusChem* 15:e202200913. doi: 10.1002/cssc.202200913

Ratnam, M. V., Senthil, K. K., Samraj, S., Abdulkadir, M., and Rao Nagamalleswara, K. (2022). Effective leaching strategies for a closed-loop spent lithium-ion battery recycling process. *J. Hazard. Toxic Radioact. Waste* 26:4021055. doi: 10.1061/(ASCE)HZ.2153-5515.0000671

Ray, A., Nayak, M., and Ghosh, A. (2022). A review on co-culturing of microalgae: A greener strategy towards sustainable biofuels production. *Sci. Total Environ.* 802:149765. doi: 10.1016/j.scitotenv.2021.149765

Roy, J. J., Cao, B., and Madhavi, S. (2021a). A review on the recycling of spent lithium-ion batteries (LIBs) by the bioleaching approach. *Chemosphere* 282:130944. doi: 10.1016/j.chemosphere.2021.130944

Roy, J. J., Madhavi, S., and Cao, B. (2021b). Metal extraction from spent lithium-ion batteries (LIBs) at high pulp density by environmentally friendly bioleaching process. *J. Clean. Prod.* 280:124242. doi: 10.1016/j.jclepro.2020.124242

Roy, J. J., Rarotra, S., Krikstolaityte, V., Zhuoran, K. W., Cindy, Y. D.-I., Tan, X. Y., et al. (2022). Green recycling methods to treat lithium-ion batteries E-waste: A circular approach to sustainability. *Adv. Mater.* 34:2103346. doi: 10.1002/adma.202103346

Sagues, W. J., Yang, J., Monroe, N., Han, S.-D., Vinzant, T., Yung, M., et al. (2020). A simple method for producing bio-based anode materials for lithium-ion batteries. *Green Chem.* 22, 7093–7108. doi: 10.1039/D0GC02286A

Sedlakova-Kadukova, J., Marcincakova, R., Luptakova, A., Vojtko, M., Fujda, M., and Pristas, P. (2020). Comparison of three different bioleaching systems for Li recovery from lepidolite. *Sci. Rep.* 10:14594. doi: 10.1038/s41598-020-71596-5

Service, R. F. (2019). Lithium-ion battery development takes Nobel. *Science* 366:292. doi: 10.1126/science.366.6463.292

Sethurajan, M., and Gaydardzhiev, S. (2021). Bioprocessing of spent lithium ion batteries for critical metals recovery – A review. *Resour. Conserv. Recycl.* 165:105225. doi: 10.1016/j.resconrec.2020.105225

Sun, M., Wang, Y., Hong, J., Dai, J., Wang, R., Niu, Z., et al. (2016). Life cycle assessment of a bio-hydrometallurgical treatment of spent Zn–Mn batteries. *J. Clean. Prod.* 129, 350–358. doi: 10.1016/j.jclepro.2016.04.058

Swain, B. (2017). Recovery and recycling of lithium: A review. *Sep. Purif. Technol.* 172, 388–403. doi: 10.1016/j.seppur.2016.08.031

Takahashi, V. C. I., Botelho Junior, A. B., Espinosa, D. C. R., and Tenório, J. A. S. (2020). Enhancing cobalt recovery from Li-ion batteries using grinding treatment prior to the leaching and solvent extraction process. *J. Environ. Chem. Eng.* 8:103801. doi: 10.1016/j.jece.2020.103801

Tarascon, J.-M., and Armand, M. (2001). Issues and challenges facing rechargeable lithium batteries. *Nature* 414, 359–367. doi: 10.1038/35104644

Valdés, J., Pedroso, I., Quatrini, R., Dodson, R. J., Tettelin, H., Blake, R., et al. (2008). *Acidithiobacillus ferrooxidans* metabolism: From genome sequence to industrial applications. *BMC Genomics* 9:597. doi: 10.1186/1471-2164-9-597

Vanitha, M., and Balasubramanian, N. (2013). Waste minimization and recovery of valuable metals from spent lithium-ion batteries – a review. *Environ. Technol. Rev.* 2, 101–115. doi: 10.1080/21622515.2013.853105

Vasconcelos, D., da, S., Tenório, J. A. S., Botelho Junior, A. B., and Espinosa, D. C. R. (2023). Circular recycling strategies for LFP batteries: A review focusing on hydrometallurgy sustainable processing. *Metals* 13:543. doi: 10.3390/met13030543

Villares, M., Işıldar, A., Mendoza Beltran, A., and Guinee, J. (2016). Applying an ex-ante life cycle perspective to metal recovery from e-waste using bioleaching. *J. Clean. Prod.* 129, 315–328. doi: 10.1016/j.jclepro.2016.04.066

Wang, J., Tian, B., Bao, Y., Qian, C., Yang, Y., Niu, T., et al. (2018). Functional exploration of extracellular polymeric substances (EPS) in the bioleaching of obsolete electric vehicle LiNixCoyMn1-x-yO2 Li-ion batteries. *J. Hazard. Mater.* 354, 250–257. doi: 10.1016/j.jhazmat.2018.05.009

Wang, Y., Yi, J., and Xia, Y. (2012). Recent progress in aqueous lithium-ion batteries. *Adv. Energy Mater.* 2, 830–840. doi: 10.1002/aenm.201200065

Wei, C., Zhang, Y., Tian, Y., Tan, L., An, Y., Qian, Y., et al. (2021). Design of safe, long-cycling and high-energy lithium metal anodes in all working conditions: Progress, challenges and perspectives. *Energy Storage Mater.* 38, 157–189. doi: 10.1016/j.ensm.2021.03.006

Wu, W., Liu, X., Zhang, X., Li, X., Qiu, Y., Zhu, M., et al. (2019). Mechanism underlying the bioleaching process of $LiCoO_2$ by sulfur-oxidizing and iron-oxidizing bacteria. *J. Biosci. Bioeng.* 128, 344–354. doi: 10.1016/j.jbiosc.2019.03.007

Wu, Y., Wang, W., Ming, J., Li, M., Xie, L., He, X., et al. (2019). An exploration of new energy storage system: High energy density, high safety, and fast charging lithium ion battery. *Adv. Funct. Mater.* 29:1805978. doi: 10.1002/adfm.201805978

Wu, Z., Soh, T., Chan, J. J., Meng, S., Meyer, D., Srinivasan, M., et al. (2020). Repurposing of fruit peel waste as a green reductant for recycling of spent lithium-ion batteries. *Environ. Sci. Technol.* 54, 9681–9692. doi: 10.1021/acs.est.0c02873

Xi, G., Xu, H., and Yao, L. (2015). Study on preparation of NiCo ferrite using spent lithium-ion and nickel–metal hydride batteries. *Sep. Purif. Technol.* 145, 50–55. doi: 10.1016/j.seppur.2015.03.002

Xin, B., Zhang, D., Zhang, X., Xia, Y., Wu, F., Chen, S., et al. (2009). Bioleaching mechanism of Co and Li from spent lithium-ion battery by the mixed culture of acidophilic sulfur-oxidizing and iron-oxidizing bacteria. *Bioresour. Technol.* 100, 6163–6169. doi: 10.1016/j.biortech.2009.06.086

Xin, Y., Guo, X., Chen, S., Wang, J., Wu, F., and Xin, B. (2016). Bioleaching of valuable metals Li, Co, Ni and Mn from spent electric vehicle Li-ion batteries for the purpose of recovery. *J. Clean. Prod.* 116, 249–258. doi: 10.1016/j.jclepro.2016.01.001

Yang, J.-L., Zhao, X.-X., Ma, M.-Y., Liu, Y., Zhang, J.-P., and Wu, X.-L. (2022). Progress and prospect on the recycling of spent lithium-ion batteries: Ending is beginning. *Carbon Neutralization* 1, 247–266. doi: 10.1002/cnl2.31

Yu, D., Huang, Z., Makuza, B., Guo, X., and Tian, Q. (2021). Pretreatment options for the recycling of spent lithium-ion batteries: A comprehensive review. *Miner. Eng.* 173:107218. doi: 10.1016/j.mineng.2021.107218

Yu, X., Yu, S., Yang, Z., Gao, H., Xu, P., Cai, G., et al. (2022). Achieving low-temperature hydrothermal relithiation by redox mediation for direct recycling of spent lithium-ion battery cathodes. *Energy Storage Mater.* 51, 54–62. doi: 10.1016/j.ensm.2022.06.017

Zeng, G., Deng, X., Luo, S., Luo, X., and Zou, J. (2012). A copper-catalyzed bioleaching process for enhancement of cobalt dissolution from spent lithium-ion batteries. *J. Hazard. Mater.* 199–200, 164–169. doi: 10.1016/j.jhazmat.2011.10.063

Zeng, G., Luo, S., Deng, X., Li, L., and Au, C. (2013). Influence of silver ions on bioleaching of cobalt from spent lithium batteries. *Miner. Eng.* 49, 40–44. doi: 10.1016/j.mineng.2013.04.021

Zeng, X., Li, J., and Singh, N. (2014). Recycling of spent lithium-ion battery: A critical review. *Crit. Rev. Environ. Sci. Technol.* 44, 1129–1165. doi: 10.1080/10643389.2013.763578

Zhang, S.-D., Qi, M.-Y., Guo, S.-J., Sun, Y.-G., Tan, X.-X., Ma, P.-Z., et al. (2022). Advancing to 4.6 V review and prospect in developing high-energy-density LiCoO2 cathode for lithium-ion batteries. *Small Methods* 6:2200148. doi: 10.1002/smtd.202200148

Zhang, X., Shi, H., Tan, N., Zhu, M., Tan, W., Daramola, D., et al. (2023). Advances in bioleaching of waste lithium batteries under metal ion stress. *Bioresour. Bioprocess.* 10:19. doi: 10.1186/s40643-023-00636-5

frontiers | Frontiers in Microbiology

TYPE Original Research
PUBLISHED 09 June 2023
DOI 10.3389/fmicb.2023.1194871

OPEN ACCESS

EDITED BY
Muhammad Zahid,
The University of Lahore, Pakistan

REVIEWED BY
Brahim Bouizgarne,
Université Ibn Zohr, Morocco
Carolina Paz Quezada,
Universidad Catolica de la Santísima Concepción, Chile

*CORRESPONDENCE
Lifei Yu
✉ lfyu@gzu.edu.cn

RECEIVED 27 March 2023
ACCEPTED 29 May 2023
PUBLISHED 09 June 2023

CITATION
Chen J, Zhao Q, Li F, Zhao X, Wang Y, Zhang L, Liu J, Yan L and Yu L (2023) Nutrient availability and acid erosion determine the early colonization of limestone by lithobiontic microorganisms.
Front. Microbiol. 14:1194871.
doi: 10.3389/fmicb.2023.1194871

Nutrient availability and acid erosion determine the early colonization of limestone by lithobiontic microorganisms

Jin Chen[1], Qing Zhao[2], Fangbing Li[1], Xiangwei Zhao[1], Yang Wang[1], Limin Zhang[3], Jinan Liu[4], Lingbin Yan[1] and Lifei Yu[1]*

[1]Key Laboratory of Plant Resources Conservation and Germplasm Innovation in Mountainous Region (Ministry of Education), College of Life Sciences and Institute of Agro-Bioengineering, Guizhou University, Guiyang, Guizhou, China, [2]School of Mathematical Sciences, Guizhou Normal University, Guiyang, Guizhou, China, [3]Institute of Guizhou Mountain Resources, Guizhou Academy of Sciences, Guiyang, Guizhou, China, [4]Garden Greening Center of Logistics Management Office, Guizhou University, Guiyang, Guizhou, China

Introduction: Microorganisms, including the pioneer microorganisms that play a role in the early colonization of rock, are extremely important biological factors in rock deterioration. The interaction of microorganisms with limestone leads to biodeterioration, accelerates soil formation, and plays an important role in the restoration of degraded ecosystems that cannot be ignored. However, the process of microbial colonization of sterile limestone in the early stages of ecological succession is unclear, as are the factors that affect the colonization. Acid erosion (both organic and inorganic), nutrient availability, and water availability are thought to be key factors affecting the colonization of lithobiontic microorganisms.

Methods: In this study, organic acid (Oa), inorganic acid (Ia), inorganic acid+nutrient solution (Ia+Nut), nutrient solution (Nut), and rain shade (RS) treatments were applied to sterilized limestone, and the interaction between microorganisms and limestone was investigated using high-throughput sequencing techniques to assess the microorganisms on the limestone after 60days of natural placement.

Results: The results were as follows: (1) The abundance of fungi was higher than that of bacteria in the early colonization of limestone, and the dominant bacterial phyla were Proteobacteria, Bacteroidota, and Actinobacteriota, while the dominant fungal phyla were Ascomycota, Basidiomycota, and Chytridiomycota. (2) Acid erosion and nutrient availability shaped different microbial communities in different ways, with bacteria being more sensitive to the environmental stresses than fungi, and the higher the acidity (Ia and Oa)/nutrient concentration, the greater the differences in microbial communities compared to the control (based on principal coordinate analysis). (3) Fungal communities were highly resistant to environmental stress and competitive, while bacterial communities were highly resilient to environmental stress and stable.

Discussion: In conclusion, our results indicate that limestone exhibits high bioreceptivity and can be rapidly colonized by microorganisms within 60days in its natural environment, and both nutrient availability and acid erosion of limestone are important determinants of early microbial colonization.

KEYWORDS

biodeterioration, bioreceptivity, lithobiontic microorganism, corrosion, limestone

1. Introduction

Microbial colonization interferes with the integrity and esthetics of rock minerals (Trovão et al., 2019). Worldwide, most lithic artifacts have suffered irreversible biodegradation (Abdel Ghany et al., 2019; Trovão et al., 2019; Gambino et al., 2021; Zhang et al., 2021), for example, the Angkor sandstone monuments (Liu et al., 2018), the limestone walls of the old cathedral of Coimbra (Trovão et al., 2019), the Chaalis abbey (Mihajlovski et al., 2017), and the Feilaifeng limestone statue (Li et al., 2018). Southwest China is a typical carbonate area (Chen et al., 2022), where politics, economics, and culture are all linked to carbonate rocks. For example, policies in Southwest China are linked to the ecological restoration of areas exhibiting karstic desertification, and most building materials are limestone. The study of the biodeterioration of limestone is therefore of great value. Acids (both organic and inorganic) produced by colonizing biota are known key factors that lead to rock biodegradation (Zhang et al., 2019). Stone relic conservation science aims to slow or even eradicate the biodegradation of lithic relics caused by microorganisms and preserve their integrity. In contrast, according to ecological succession theory, acceleration of the biodeterioration of stones leads to the formation of relatively stable biological communities, promotes biomineralization, and accelerates soil formation. The clarification of the ecological succession process of colonizers and their interactions with the stone matrix is exceptionally important both for the conservation of lithic artifacts and for the promotion of soil formation. Microbial biodeterioration involves a series of processes, including biofilm formation, discoloration, salinization, mechanical damage, permeation, and organic matter production (Scheerer et al., 2009). The essence of microbial biodeterioration is the action of hydrogen ions from acidic corrosives produced by lithobiontic microorganisms on the rock matrix, resulting in dissolution, complexation, and chelation (Moroni and Pitzurra, 2008; Gadd, 2017a,b; Li et al., 2018). The acids produced are mainly organic acids such as oxalic and citric acid (Gadd, 1999; de Oliveira Mendes et al., 2020) and inorganic acids, such as HNO_2, HNO_3, H_2SO_3, and H_2SO_4 (Warscheid et al., 1991; Warscheid and Braams, 2000; Moroni and Pitzurra, 2008). The organisms involved in rock biodeterioration mainly include bacteria, Cyanobacteria, fungi, algae, lichens, and mosses (Scheerer et al., 2009; Pinheiro et al., 2019; Zhang et al., 2019). In recent years, the study of lithobiontic microorganisms has made great progress, from determining the role of single microbial species (Gerrits et al., 2021) to determining the role of multiple microbial species (Crispim and Gaylarde, 2005; Trovão et al., 2020) on rocks, and the study of rock biodeterioration is flourishing. Various organisms on rocks, such as fungi, algae, and lichens, have been extensively reported on, but bacteria and archaea have been relatively less reported on (Pinheiro et al., 2019). Regarding fungi, most studies have focused on the biodegradation of limestone caused by fungal strains that can be isolated and cultured (Trovão et al., 2020, 2021), while relatively little attention has been paid to other fungal taxa that colonize limestone under natural conditions.

Because of the poor availability of water and organic matter on rocks, pioneer microorganisms colonizing rocks generally have the ability to utilize small amounts of water, inorganic matter, and airborne organic matter (Villa et al., 2016). In addition, rocks provide little shelter for microorganisms other than the pores and cracks on the rocks, so lithobiontic microorganisms are often exposed to conditions of drastic temperature changes and strong UV light (Walker and Pace, 2007). In response to these conditions, lithobiontic microbes often form specific biofilms based on their nutrient and growth requirements to increase their adaptation to extreme environments (Gorbushina, 2007). Compared to microorganisms in other environments, lithobiontic microorganisms are characterized by (1) low taxonomic diversity but high synergistic and metabolic activity (Villa et al., 2015); (2) phylogenetic similarity and high specificity worldwide (Gorbushina and Broughton, 2009); and (3) pigments, exopolymeric substances, and efficient DNA repair systems that allow survival on the rock (Gómez-Silva, 2018). Rock surface pH, porosity, permeability, mineral composition, texture, geometry, shading, and timing of colonization affect the composition and structure of lithobiontic microbial communities (Miller et al., 2012; Brewer and Fierer, 2018; Liu et al., 2018, 2020; Abdel Ghany et al., 2019; Chen et al., 2022). A decrease in rock surface pH is generally regarded as more serious biodeterioration (Pinheiro et al., 2019). In addition, air is an important factor influencing the structure and composition of lithobiontic microbial communities, especially as air near cities contains organic pollutants that can be a source of energy for microorganisms (Mitchell and Gu, 2000; Villa et al., 2016).

Limestone is one of the rock types that are more susceptible to biodeterioration. Softness, brightness, and easy sculptability increase the bioreceptivity of limestone (Miller et al., 2012; Pinheiro et al., 2019; Chen et al., 2022). The inorganic compounds in limestone are good substrates for the growth of various microorganisms, with microorganisms obtaining the required elements by secreting organic acids (Warscheid et al., 1991). For example, *Nitrosomonas* spp. can secrete nitric acid and *Thiobacillus* spp. can secrete sulfuric acid, thereby obtaining the necessary chemoenergetic nutrients (Warscheid and Braams, 2000). Our previous study reported on the microbial taxa (and their functional genetic variations) on carbonate rock under natural conditions with various weathering times (Chen et al., 2022). However, it is not clear which microorganisms take the lead in colonizing limestone under natural conditions, or whether acid erosion or nutrient availability promote microbial colonization. Therefore, to understand the effects of acid erosion (organic and inorganic acids), nutrient availability, and rainfall on microbial colonization, we set up a total of five treatments: organic acid (Oa), inorganic acid (Ia), inorganic acid + nutrient solution (Ia + Nut), nutrient solution (Nut), and rain shade (RS). We focused on the following questions: what are the early colonizing microbial species on limestone surfaces in the subtropical climate zone? What are the ecological strategies of bacterial and fungal communities during colonization of limestone surfaces? What factors influence the colonization of limestone surfaces by microorganisms? To clarify these questions, we selected sterilized limestone sand-sized grains as the study material and applied different treatments to investigate the colonization patterns of various microbes. Our study provides new insights into the potential conservation of limestone artifacts and the soil-forming role of limestone in karst areas.

2. Materials and methods

2.1. Experimental design and sample processing

We chose limestone, which is commonly found in southwest China, as the study material. The limestone was purchased from a

specialized stone factory and was uniformly processed to a particle size that could pass through a 3-mm but not 1.5-mm sieve. The limestone samples were sterilized in a sterilizer at 180°C for 2 h and cooled. Next, 300 g were placed in a 100 mm × 95 mm × 55 mm plastic grid (Supplementary Figure S1H). Before adding the samples, a sterilized piece of gauze with an approximate pore size of 1 mm was placed in each compartment of the grid to prevent leakage of the added samples. In addition, an *in situ* weather station (Supplementary Figure S1B) was installed to observe the meteorological elements such as temperature, humidity, atmospheric pressure, and rainfall at the experimental site (26°25′42.65″, 106°39′59.65″), and readings were taken every 10 min. The experiment ran from January 15 to March 15, 2022.

To explore the relationship between limestone dissolution and microbial colonization, we set up six groups, i.e., addition of nutrient solution (Nut; Supplementary Figure S1G), addition of organic acid (Oa; Supplementary Figure S1D), addition of inorganic acid (Ia; Supplementary Figure S1E), addition of inorganic acid and nutrient solution (Ia + Nut; Supplementary Figure S1F), control (CK; Supplementary Figure S1C), and rain shade (RS; Supplementary Figure S1C) groups. Hoagland's solution is a complex nutrient solution containing large amounts of macronutrients and micronutrients required by a variety of organisms. Therefore, for the Nut group, a concentration gradient was set up involving five nutrient concentrations (40 mL each; Supplementary Table S1), i.e., 5, 10, 15, 20, and 25 mL Hoagland's solution mixed with water (for example, 5 mL Hoagland's solution in 35 mL water, and so on). The Nut concentrations and ratios were based on previous descriptions (Rajan et al., 2019). We selected oxalic acid, which is commonly found in rocks undergoing biodeterioration, as the corrosive organic acid for this experiment. For the Oa group, we set up a concentration gradient involving five oxalic acid concentrations (40 mL each), i.e., 0.1, 0.2, 0.4, 0.8, and 1.6 mmol/L. The Oa concentrations were based on the concentrations of 0.3–0.7 mmol/L in rocks undergoing biodeterioration reported by Sheng et al. (1997). We selected hydrochloric acid, which is often used as the dissolution acid for carbonate-related experiments (Sun et al., 2010), as the strong dissolution acid for this experiment. For the Ia group, we set up a concentration gradient involving five hydrochloric acid concentrations (40 mL each), i.e., 0.1, 0.2, 0.4, 0.8, and 1.6 mol/L. For the Ia + Nut group, we set up the same concentration gradient of hydrochloric acid as in the Ia group, and after the reaction was completed (after 24 h), we added 15 mL Hoagland's solution diluted to 40 mL with water. For the Nut, Oa, and Ia groups, after 24 h, 40 mL sterile water was added to give a final volume of 80 mL. For the CK and RS groups, 80 mL sterile water was used. After each rainfall event, we added an equal amount of sterile water to the RS group based on the amount of rainfall recorded by the weather station. We conducted three replicates of each treatment to give a total of 66 samples.

2.2. Sampling and assessment of limestone samples

It has been found that fungi grow on modern limestone surfaces after 60 days of infection (Abdel Ghany et al., 2019). Therefore, after the limestone samples had been left outdoors for 60 days, we scooped them out with a sterile steel spoon and placed them in labeled plastic bags. For high-throughput sequencing, to obtain microorganisms samples for DNA extraction, we added 50 g of the limestone samples to about 125 mL sterile water, washed them with an ultrasonic cleaner for 15 s to ensure that the microorganisms on the limestone were washed into the sterile water, and then passed the solution through a 0.02-μm filter membrane. Next, 50 g of the limestone samples was used for pH determination and 50 g was converted into powder with a ball mill and passed through a 0.053-mm sieve for X-ray diffraction (XRD) analysis (to investigate the structure of the limestone samples) and Fourier transform infrared spectroscopy (FTIR) analysis (to characterize the atomic groups in the limestone samples). The remainder of the limestone samples were passed through a 0.053-mm sieve to obtain the powder remaining on the rock surface, which was placed in plastic bags for physicochemical experiments. We assessed the organic nitrogen (ON) and total carbon (TC) content of the powder samples using an organic elemental analyzer (all the C obtained by the analyzer should represent the TC because most of the samples are carbonate rocks). In addition, we assessed the organic carbon (OC) content of the powder samples using the H_2SO_4-$K_2Cr_2O_7$ heating method (Bao, 2000).

2.3. DNA extraction and PCR amplification

Total microbial genomic DNA was extracted from the membrane (0.02-μm) samples using an E.Z.N.A.® soil DNA Kit (Omega Bio-tek, Norcross, GA, United States) according to the manufacturer's instructions. The quality and concentration of DNA were determined using 1.0% agarose gel electrophoresis and a NanoDrop® ND-2000 spectrophotometer (Thermo Scientific Inc., United States). The DNA was then kept at −80°C prior to further use.

For bacteria, the V3–V4 hypervariable regions (468 bp) of the 16S rRNA gene were targeted using primer pairs 338F (5′-ACTCCTACGGGAGGCAGCAG-3′) and 806R (5′-GGACTACH VGGGTWTCTAAT-3′; Liu et al., 2016). For fungi, the internal transcribed spacer region (about 300 bp) was targeted using primer pairs ITS1F (5′-CTTGGTCATTTAGAGGAAGTAA-3′) and ITS2R (5′-GCTGCGTTCTTCATCGATGC-3′; Adams et al., 2013). The 16S PCR reaction mixture included 4 μL 5 × Fast Pfu buffer, 2 μL 2.5 mM dNTPs, 0.8 μL each primer (5 μM), 0.4 μL Fast Pfu polymerase, 10 ng template DNA, and ddH_2O to give a final volume of 20 μL. The ITS PCR reaction mixture included 2 μL 10 × buffer, 2 μL 2.5 mM dNTPs, 0.8 μL each primer (5 μM), 0.2 μL rTaq polymerase, 0.2 μL bovine serum albumin, 10 ng template DNA, and ddH_2O to give a final volume of 20 μL.

The PCR amplification cycling conditions were as follows: initial denaturation at 95°C for 3 min, denaturing at 95°C for 30 s (27 cycles for 16S and 35 cycles for ITS), annealing at 55°C for 30 s, and extension at 72°C for 45 s, and single extension at 72°C for 10 min, ending at 4°C. All samples were amplified in triplicate. The PCR products were extracted after 2% agarose gel electrophoresis and purified using an AxyPrep DNA Gel Extraction Kit (Axygen Biosciences, Union City, CA, United States) according to the manufacturer's instructions. They were then quantified using a Quantus™ Fluorometer (Promega, United States). Purified amplicons were pooled in equimolar amounts and paired-end sequenced on an Illumina MiSeq PE300 platform (Illumina, San Diego, United States) according to standard protocols by Majorbio Bio-Pharm Technology Co. Ltd. (Shanghai, China). The raw sequencing reads were deposited into the US National Center for

Biotechnology Information (NCBI) Sequence Read Archive (SRA) database (accession number: PRJNA944278).

2.4. Sequencing data processing and quality control

Raw FASTQ files were de-multiplexed using an in-house perl script, quality-filtered using fastp v0.19.6 (Chen et al., 2018), and merged using FLASH v1.2.7 (Magoč and Salzberg, 2011) based on the following criteria: (i) 300-bp reads were truncated at any site with a mean quality score of <20 over a 50 bp sliding window and truncated reads <50 bp were discarded, (ii) reads containing ambiguous characters were also discarded, and (iii) only overlapping sequences >10 bp were assembled according to their overlapping sequence. The maximum mismatch ratio of the overlapping region was set at 0.2. Reads that could not be assembled were discarded. The optimized sequences were then clustered into operational taxonomic units (OTUs) using UPARSE v7.1 (Edgar, 2013) with a 97% sequence similarity level. The most abundant sequence for each OTU was selected as a representative sequence. The taxonomy of each OTU representative sequence was analyzed using RDP Classifier v2.2 (Wang et al., 2007) and 16S and ITS rRNA gene databases (Silva v138 for bacteria and Unite v8.0 for fungi) using a confidence threshold of 0.7.

All sequences classified as chloroplast or mitochondria sequences were removed using the Majorbio Cloud platform (https://cloud.majorbio.com; Ren et al., 2022). Next, we selected the OTUs that were detected in ≥2 samples and that accounted for ≥5 occurrences across samples. Thereafter, samples were rarefied to the smallest observed number of reads to normalize for uneven sequencing effort.

2.5. Statistical analyses

All analyses were performed in the R Environment v4.2.2, and all plots were generated using the *ggplot2* package. The sequencing data were transformed to proportions using total-sum scaling (TSS) normalization (McKnight et al., 2019); the data were transformed using $\log10(x + x_0)$, where x is the original non-zero abundance count data and $x_0 = 0.1 \cdot \min(x)$ (Sunagawa et al., 2015). We used the pcoa() function in the *ape* package for unconstrained principal coordinate analysis (PCoA; Paradis et al., 2004). Permutational multivariate ANOVA (PerMANOVA) was performed with the adonis() function implemented in the *vegan* package (Dixon, 2003). We calculated the difference in richness between treatment groups using the aov() function in the *stats* package and the duncan.test() function in the *agricolae* package to perform a *post hoc* test (Steel and Torrie, 1980). We performed a two-sample permutation Student's *t*-test (one-tailed; Hervé, 2022) using the perm.t.test() function in the *RVAideMemoire* package.

To construct Oa, Ia, Ia + Nut, and Nut co-occurrence networks, we selected OTUs that were present in ≥8 of all 15 Ia, Oa, Nut, or Ia + Nut samples (each treatment group had five concentration subgroups and three replicates). We then calculated the correlation coefficient R and p *value* between pairs of OTUs using the corAndPvalue() function in the *WGCNA* package (Langfelder and Horvath, 2012), and we identified eligible pairs based on absolute $R > 0.75$ and *value of* $p < 0.01$. The *igraph* package (Csardi and Nepusz, 2006) was used for network construction. Regarding the network topology properties, we measured the relative importance of a network node in terms of the information centrality of the node, and used the ratio between the reduced value of the network efficiency after removing any node and the network efficiency of the network without removing any node as the information centrality of that arbitrary node, and we used the information centrality of the largest node in the network as the network vulnerability indicator (Shang et al., 2021). We used the glmer() function in the *lme4* package to fit a generalized linear mixed-effect model (GLMM; Bates et al., 2015), with different treatments as random effects. The glmm.hp.() function in the *glmm.hp* package was used to calculate the relative contribution of multiple environmental factors after performing GLMM based on hierarchical partitioning theory (Lai et al., 2022).

3. Results

3.1. Rock properties and climatic conditions

The XRD results after standard mapping comparison indicate that the main phase of our rock samples was carbonatite (Reig et al., 2002; Zhang et al., 2017; Supplementary Figure S2A). In addition, the strong absorption peak at point b in the FTIR map was at around 1,419 cm, which represents the stretching vibration within $[CO_3]^{2-}$, followed by point c at 875 cm and point d at 711 cm, which represent the bending vibration within $[CO_3]^{2-}$ (Reig et al., 2002; Shareef et al., 2008), while point a at 3,444 cm was produced by the water absorption of KBr during the production process (Yang et al., 2015; Supplementary Figure S2B). In summary, the XRD and FTIR results indicate that the main component of our sample was calcium carbonate.

Based on the meteorological data obtained from the *in situ* weather station we installed (Supplementary Figure S2C), the mean temperature at our test site during the 60-day period (from 2022-01-15 to 2022-03-15) was 4.56°C (−4.7 to 25.5°C), the mean relative humidity was 82.44% (18.30–99.90%), the accumulated rainfall was 85.6 mm, and the mean atmospheric pressure was 89 kPa (87.8–90 kPa).

3.2. Bacterial and fungal community diversity among treatments

Among the 66 samples (3 RS, 3 CK, 15 Ia, 15 Oa, 15 Nut, and 15 Ia + Nut samples), 7,417 distinct fungal OTUs were obtained from 4,020,249 high-quality sequences and 2,754 distinct bacterial OTUs were obtained from 2,665,071 high-quality sequences at a 97% similarity level. After retaining the eligible OTUs (detected in ≥2 samples and accounting for ≥5 occurrences across samples), there were 2,832 fungal OTUs and 529 bacterial OTUs. The sequence count data were normalized based on the minimum value. The diversity indices were then calculated based on these data. The Good's Coverage of the 66 samples varied from 99.43 to 99.80% for bacterial communities, with a mean of 99.65%, and from 98.78 to 99.97% for fungal communities, with a mean of 99.42% (Supplementary Table S2).

The dilution curves (Supplementary Figure S3), theoretical species richness [Chao1 and abundance-based coverage estimator (ACE)], and Good's Coverage showed that after 60 days, a certain number of microorganisms had colonized the surface of the limestone sand-sized grains, and the diversity of the fungal communities was higher than that of the bacterial communities.

Regarding the bacterial communities, all Nut concentrations and high Oa concentrations significantly reduced the richness (Figures 1A,B), while the Ia and Ia + Nut treatments did not significantly alter the richness (Figures 1C,D). In addition, RS treatment significantly reduced bacterial richness (Figures 1A–D). Regarding the fungal communities, RS treatment did not significantly change the richness (Figures 1E–H). In addition, compared to CK, all Ia + Nut treatments and low Ia concentrations significantly increased the fungal richness (Figures 1G,H), while the Nut and Oa treatments did not significantly increase the richness (Figures 1E,F).

Rain shade treatment did not significantly change the evenness of the bacterial or fungal communities (Supplementary Figures S4A–H). High Ia + Nut treatment significantly reduced the bacterial community evenness (Supplementary Figures S4C,D), while the other treatments did not significantly change it. In addition, the Nut treatments changed the fungal community evenness (Supplementary Figure S4E), while the other treatments did not.

3.3. Comparison of bacterial and fungal community composition among treatments

The dominant bacterial phyla based on mean relative abundance (>1% threshold) among all treatments were Proteobacteria (56.78%), Bacteroidota (32.85%), and Actinobacteriota (8.22%). In contrast, the mean relative abundances of Deinococcota (0.95%), Cyanobacteria (0.42%), Bdellovibrionota (0.40%), Firmicutes (0.15%), Chloroflexi (0.11%), and Patescibacteria (0.05) were < 1% (Figure 2A). The top 10 bacterial genera were *Flavobacterium* (22.34%), *Massilia* (19.19%), *Noviherbaspirillum* (6.95%), *Cytophaga* (7.41%), *Cellvibrio* (5.34%) *Caulobacter* (5.46%), *Arthrobacter* (5.27%), *Pseudomonas* (4.34%), and *Brevundimonas* (2.68%; Supplementary Figure S5A).

The dominant fungal phyla based on mean relative abundance (>1% threshold) among all treatments were Ascomycota (57.82%), Basidiomycota (35.58%), and Chytridiomycota (4.45%). In contrast, the mean relative abundance of Mortierellomycota (0.15%) was <1% (Figure 2B). The top six fungal genera were *Epicoccum* (12.67%), *Symmetrospora* (9.37%), *Cladosporium* (9.05%), *Vishniacozyma* (4.62%), *Itersonilia* (4.47%), and *Botrytis* (2.19%; Supplementary Figure S5B).

3.4. Differences in microbial communities among treatments

Our PCoA and Adonis tests showed that bacterial and fungal communities exhibited significant separation regarding different Nut, Oa, Ia, and Ia + Nut concentrations, and that bacterial communities ($0.71 > R^2 > 0.47$, $p = 0.001$) differed more than fungal communities ($0.44 > R^2 > 0.35$, $p = 0.001$) for the treatments (Figure 3). In addition, UpSet plots showed that most OTUs were shared between the different treatments (Supplementary Figure S6).

We calculated the Bray–Curtis dissimilarity distances for bacterial and fungal communities between the treatment groups and the CK group, and the treatment groups and the RS group. For bacteria, there was a significant Nut effect, with the distances significantly increasing with Nut concentration (Supplementary Table S3; Supplementary Figures S7A,B). However, there were no significant acidity (Oa, Ia, or Ia + Nut) effects (Supplementary Figure S7). For fungi, there were no significant differences in the Bray–Curtis

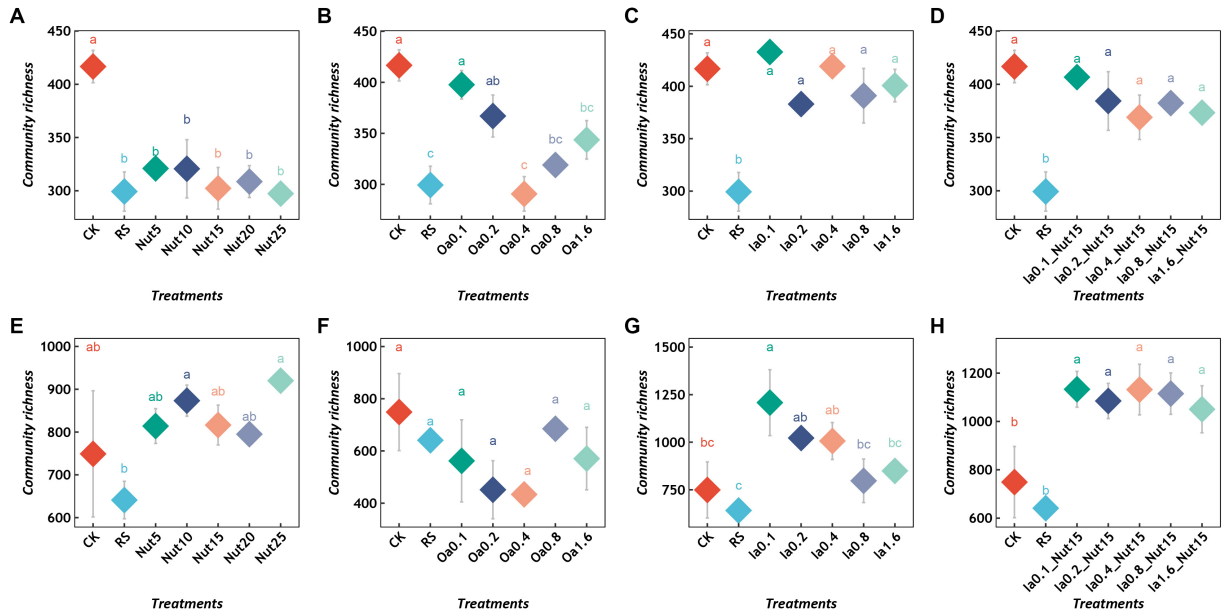

FIGURE 1
Richness of bacterial **(A–D)** and fungal **(E–H)** communities under different treatment conditions. Different lowercase letters indicate significant differences between groups (p <0.05), and the same lowercase letters indicate no significant differences between groups. RS, rain shade; Nut, nutrient; Oa, organic acid; Ia, inorganic acid; Ia+Nut, inorganic acid+Nutrient; and values after each treatment indicate concentration.

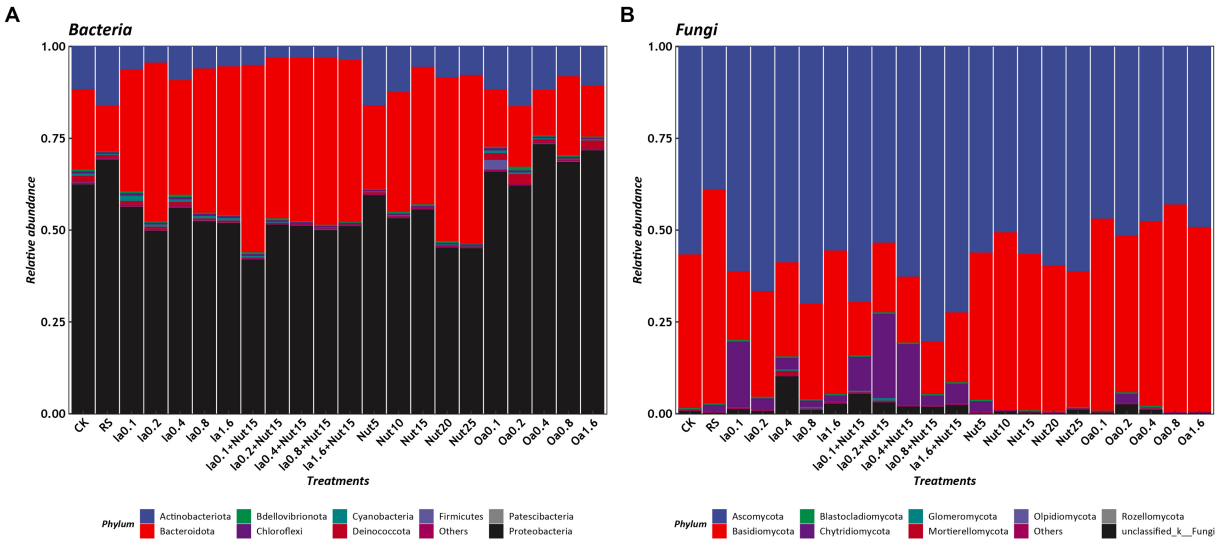

FIGURE 2
Relative abundances of phyla under different treatment conditions (**A**: bacteria, **B**: Fungi). RS, rain shade; Nut, nutrient; Oa, organic acid; Ia, inorganic acid; Ia+Nut, inorganic acid+nutrient; values after each treatment indicate concentration.

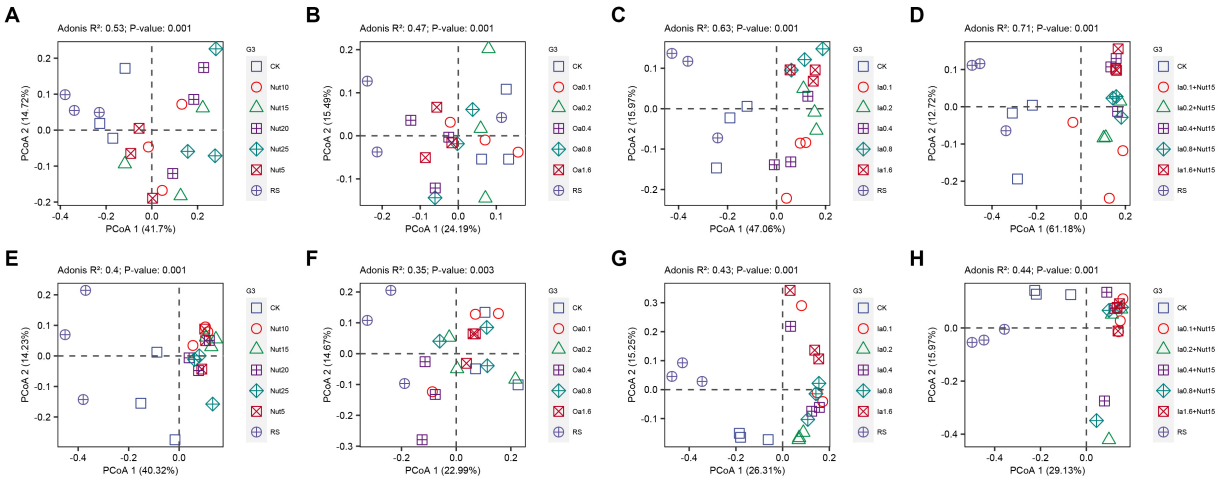

FIGURE 3
Principal coordinate analysis (PCoA) of bacterial **(A–D)** and fungal **(E–H)** communities under different treatment conditions. RS, rain shade; Nut, nutrient; Oa, organic acid; Ia, inorganic acid; Ia +Nut, inorganic acid+nutrient; and values after each treatment indicate concentration.

dissimilarity distance among the treatment groups and CK, or the treatment groups and RS (Supplementary Figure S8).

In summary, there were significant differences in bacterial and fungal community composition among the groups, but a large proportion was shared. In addition, the bacterial communities were more sensitive to the treatments than the fungal communities, especially regarding Nut concentrations.

3.5. Bacterial and fungal co-occurrence networks

For both fungal and bacterial communities, the proportion of positive correlations (among all correlations) was higher than the proportion of negative correlations in the Oa, Ia, Ia + Nut, and Nut networks, while the Nut network had a greater proportion of negative correlations. More negative correlations indicate increased competition between species, which occurred for both fungal and bacterial communities in the Nut treatment group (Supplementary Figure S9; Supplementary Table S4).

For the Nut network, strong correlations ($R > 0.25$) were more common among bacterial OTUs than fungal OTUs, while weak correlations ($-0.25 < R < 0.25$) were less common among bacterial OTUs than fungal OTUs. For the Oa and Ia + Nut networks, the negative correlations were stronger among bacterial OTUs than fungal OTUs, while the positive correlations were weaker among bacterial OTUs than fungal OTUs. For the Ia network, the negative correlations were weaker among bacterial OTUs than fungal OTUs, while the positive correlations were stronger among bacterial OTUs than fungal OTUs (Figure 4; Supplementary Figure S9).

When considering the significant correlations for a given threshold ($R > 0.75$, $p < 0.01$), the number of positive correlation edges was greater than the number of negative correlation edges for both fungal and bacterial communities (Supplementary Table S4). In addition, the permutation Student's *t*-test showed that the number of nodes was significantly lower in the bacterial networks than the fungal networks, but the edge density (i.e., the ratio of the number of edges to the number of all possible edges) was significantly higher (Supplementary Table S5). A higher edge density indicates more efficient network information transfer, higher resilience to environmental stress, and easier achievement of dynamic stability. The networks showed that the bacterial communities were more tightly connected, more complex, and more resilient to environmental stress, but less resistant to environmental stress than the fungal communities.

3.6. Relative contribution of environmental factors to microbial richness

Generalized linear mixed-effect models showed that bacterial and fungal richness increased with OC and ON and decreased with TC among the various treatments (Figure 5). In addition, fungal richness increased with pH, while bacterial richness decreased with pH. To investigate the relative contributions of the above four environmental factors to bacterial and fungal richness, we calculated their contributions after multivariate GLMM modeling based on hierarchical partitioning (Supplementary Figure S10). The results showed that OC had the highest relative contribution to bacterial richness, while TC had the highest relative contribution to fungal richness.

4. Discussion

4.1. Bacterial and fungal communities on limestone

The bacterial taxa found in this study are similar to those found in previous studies (Miller et al., 2008, 2009; Miller, 2010; Chimienti et al., 2016), but differ in terms of the dominant taxa. At the phylum level, the dominant bacteria found in this study were Proteobacteria (56.78%), Bacteroidota (32.85%), and Actinobacteriota (8.22%; Figure 2A). Proteobacteria is a key chemolithotroph involved in biotic degradation (Scheerer et al., 2009; Miller, 2010), most taxa of Bacteroidota are halophiles, and Actinobacteriota can lower the pH of rock surfaces and can be used as an indicator of biodeterioration (Scheerer et al., 2009). The microbial communities on the surfaces of Italian and French limestone tombstones and monasteries were reported to be dominated by Cyanobacteria and Alphaproteobacteria (Mihajlovski et al., 2017; Gambino et al., 2021). The microbial communities on the surfaces of 149 limestone and granite gravestone samples from three continents were reported to be dominated by Proteobacteria, Cyanobacteria, and Bacteroidetes (Brewer and Fierer, 2018).

At the phylum level, the dominant fungi found in this study were Ascomycota (57.82%) and Basidiomycota (35.58%; Figure 2B), similar to results from a previous study (Gómez-Cornelio et al., 2012). At the genus level, some of the rock-inhabiting fungal species (belonging to the genera *Cladosporium*, *Epicoccum*, and *Botrytis*) were the same as those found in previous studies (Gómez-Cornelio et al., 2012; Trovão et al., 2020), while some endemic taxa (such as *Vishniacozyma*, *Itersonilia*, and *Symmetrospora*) were also found (Supplementary Figure S5B). It is worth noting that some species of the genera *Cladosporium*, *Epicoccum*, and *Botrytis* have been found to have a potential for biodeterioration (Gómez-Cornelio et al., 2012; Li et al., 2018; Trovão et al., 2020).

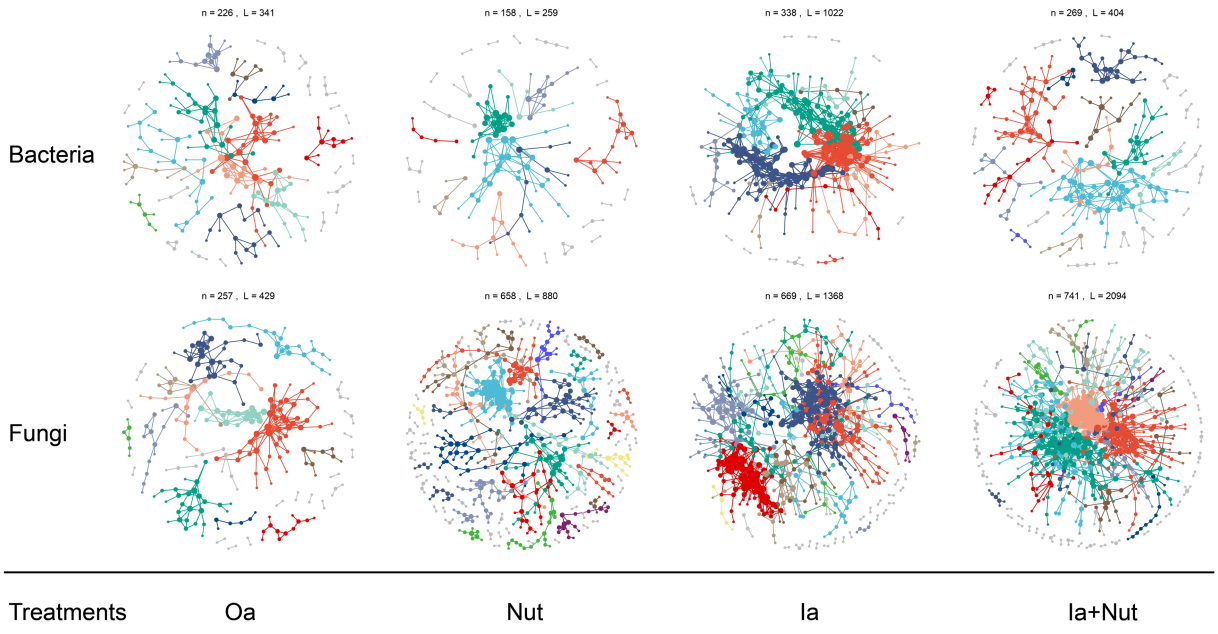

FIGURE 4
Bacterial and fungal co-occurrence networks on limestone under different treatment conditions. Large modules with ≥5 nodes are shown in different colors, and smaller modules are shown in gray. RS, rain shade; Nut, nutrient; Oa, organic acid; Ia, inorganic acid; Ia+Nut, inorganic acid+nutrient.

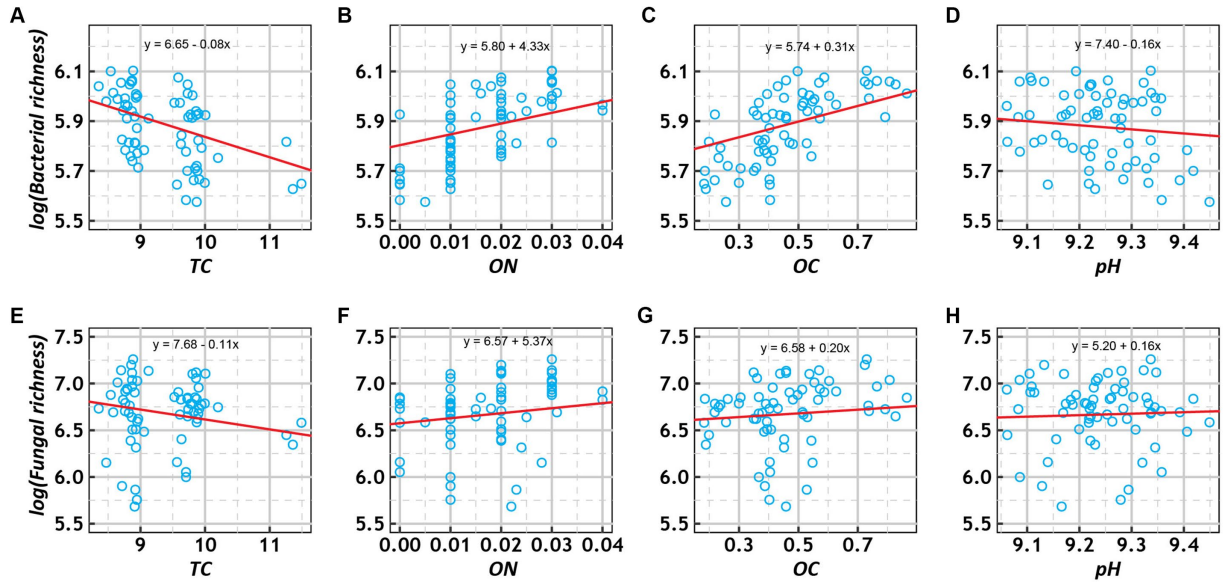

FIGURE 5
Scatter plots of the relationships of log-transformed richness (bacterial: **A–E**; fungal: **E–H**) with total carbon (TC, %), organic nitrogen (ON, %), organic carbon (OC, %), and pH under various treatment conditions. The trend lines represent the best-fit lines according to generalized linear mixed-effects models (GLMMs).

4.2. Response of bacterial and fungal communities to different treatments

Cyanobacteria are often the first colonizers and first microbes to perform ecosystem functions because their photoautotrophic metabolism is based on the ability to use light to produce energy and organic matter and to collect micronutrients, oxygen, carbon dioxide, and water from the surrounding air (Pinheiro et al., 2019). However, the relative abundance of Cyanobacteria in this study was low (Figure 2A). It is important to note that the above studies all assessed bacterial composition patterns under natural conditions, whereas in this study, Oa and Ia treatments were imposed (Supplementary Figure S1). This led to the interesting phenomenon of inorganic material produced by limestone dissolution allowing Proteobacteria, which depends on chemoenergetic inorganic nutrients, to colonize the limestone surfaces in large numbers (Figure 2A).

The dominant fungi differ between different climatic conditions, with filamentous fungi dominating in mild and humid environments, and the so-called microcolonial black fungi dominating in arid and semi-arid climates (Sterflinger and Piñar, 2013; Selbmann et al., 2015; Pinheiro et al., 2019). In our experimental site, which is located in a subtropical climate zone, filamentous fungi such as *Cladosporium* and *Epicoccum* were two of the dominant genera on the limestone surfaces (Supplementary Figure S5B), which is similar to what has been reported previously (Gómez-Cornelio et al., 2012; Pinheiro et al., 2019; Trovão et al., 2020).

Fungi can secrete more Oa than bacteria (Abdel Ghany et al., 2019) and grow mycelia that can damage rocks (Gaylarde et al., 2003; Dakal and Cameotra, 2012; Trovão et al., 2019). In this study, different concentrations of acids/nutrients shaped the bacterial and fungal communities; the bacterial communities were less resistant to the environmental stresses (different concentrations of acids/nutrients) than the fungal communities, so the abundance of fungi was higher than that of bacteria (Figure 3). Among the fungal genera found, *Cladosporium* and *Epicoccum* were both filamentous fungi; they may have been dominant because mycelia increase the efficiency of nutrient uptake (Fukasawa et al., 2020), which can increase the competitiveness of fungi compared to bacteria. Therefore, it is unsurprising that the abundance of fungi was higher than that of bacteria for the acid/nutrient treatments.

4.3. Adaptation of limestone lithogenic microorganisms

Typically, fungal communities are more able to persist in arid environments than bacterial communities and are more resistant to drought, while bacterial communities have good resilience under suitable conditions, i.e., they are able to recover rapidly (Barnard et al., 2013; de Vries et al., 2018). The limestone samples were in a chronic water deficit environment, which resulted in higher fungal abundance than bacterial abundance and a higher resistance to environment stress among the fungi compared to the bacteria, which were more resilient to the arid environment than the fungi (Figures 1, 3, 4; Supplementary Table S5). In addition, among the different treatments, Nut decreased bacterial richness (Figure 1A). Conversely, Ia + Nut increased fungal richness (Figure 1H). We hypothesized that fungi are better adapted to the limestone surface environment and are more competitive than bacteria during the early colonization process. The species richness and evenness of the fungal community were higher than those of the bacterial community after the sterile limestone sand-sized grains were subjected to natural conditions for 60 days (Figure 1; Supplementary Figure S4). Oa and Nut might hinder bacterial colonization, while Ia + Nut promoted fungal colonization, suggesting that the fungal community might be better adapted to limestone surfaces than bacteria (Figure 1). In addition, we speculate that rainfall may be the main source of bacterial

communities on limestone surfaces, while the environment may be the main source of fungal communities (Figure 1).

Based on our findings, we believe that limestone can be protected from biodeterioration in several ways. First, biodeterioration is the result of a combination of physical and biochemical mechanisms (Gadd, 2017b). Among the biochemical mechanisms, inorganic and organic acids are important influences. As carbonic acid is a very common inorganic acid that is mainly formed when excessively high concentrations of CO_2 in the air dissolve in water (Gadd, 2017b; Liu et al., 2020), CO_2 concentrations should be monitored to prevent carbonic acid in rainwater from dissolving limestone. Second, phototrophs such as Cyanobacteria are thought to be an important group of organisms in rock biodeterioration that are able to use photosynthesis to assimilate CO_2 into organic forms for subsequent colonizers (Sand and Bock, 1991; Crispim et al., 2006; Vázquez-Nion et al., 2018). Therefore, protecting limestone from direct sunlight as much as possible will slow the growth of lithobiontic Cyanobacteria and thus reduce the biodeterioration of the limestone. Third, rainfall, as an important environmental factor, is associated with a variety of biodeterioration processes, such as discoloration, distortions, blackening, and patina formation (Liu et al., 2020). Hence, limestone surfaces should be protected from rainfall to reduce colonization by microorganisms in the rainfall. Fourth, as it has been found that microorganisms cultured from the rinds of biodeteriorated rock surfaces can still cause damage to rocks (Gómez-Cornelio et al., 2012), microorganisms growing on limestone rocks undergoing biodeterioration need to be removed to avoid further erosion.

5. Conclusion

This study investigated microbial colonization of limestone surfaces after 60 days of treatment with various Nut, Oa, Ia, Ia + Nut, and Nut concentrations, providing a new perspective on microbial–rock interactions. We draw the following three main conclusions. First, fungi and bacteria exhibited different colonization patterns during the 60 days that the limestone was left in its natural environment. Fungi were more resistant to environmental stress and able to colonize the limestone surfaces rapidly and in large numbers, showing higher richness and competitiveness, while bacterial communities, although less diverse, were more complex and resilient to environmental stress, with an increased ability to recover rapidly. Second, the rock surface environment (acid erosion and nutrient availability) determined the early colonization by microorganisms, with different concentrations of Nut, Oa, and Ia all shaping the microbial communities in different ways. The higher the acidity (Ia and Oa), the greater the differences (compared to the CK) in microbial communities. The bacteria were less resistant to environmental stress than the fungi, and there was an obvious Nut concentration gradient effect for bacteria. Third, the richness of bacterial and fungal communities were influenced by OC, ON, TC, and pH, with OC being an important determinant of bacterial community richness and TC being an important determinant of fungal community richness. However, this study lacks a quantitative analysis of how limestone surface characteristics such as roughness and porosity affect microbial colonization. In addition, the limestone surface environment changed drastically over time, and this study did not assess the microbial colonization in different periods. Therefore, studies on the ecological succession of microorganisms on limestone surfaces in different periods should be conducted to provide a scientific basis for the conservation of limestone artifacts and early ecological succession in karst areas.

Data availability statement

The datasets presented in this study can be found in online repositories. The names of the repository/repositories and accession number(s) can be found at: https://www.ncbi.nlm.nih.gov/, PRJNA944278.

Author contributions

LYu conceived the project. JC, FL, XZ, QZ, LZ, JL, and LYa collected samples in the field. JC, FL, XZ, YW, and LYan performed data analysis. JC, FL, and XZ performed the experiment. JC and LYu wrote the manuscript. All authors contributed to the article and approved the submitted version.

Funding

This work was supported by the 13th Five-year National Key Research and Development Plan (grant number 2016YFC0502604); the Construction Program of Biology First-class Discipline in Guizhou (grant number GNYL[2017]009); and the Postgraduate Education Innovation Program in Guizhou Province (grant number YJSKYJJ[2021]079).

Acknowledgments

We would like to thank the editors and reviewers for their selfless help.

Conflict of interest

The authors declare that the research was conducted in the absence of any commercial or financial relationships that could be construed as a potential conflict of interest.

Publisher's note

Supplementary material

The Supplementary material for this article can be found online at: https://www.frontiersin.org/articles/10.3389/fmicb.2023.1194871/full#supplementary-material

References

Abdel Ghany, T. M., Omar, A. M., Elwkeel, F. M., Al Abboud, M. A., and Alawlaqi, M. M. (2019). Fungal deterioration of limestone false-door monument. *Heliyon* 5:e02673. doi: 10.1016/j.heliyon.2019.e02673

Adams, R. I., Miletto, M., Taylor, J. W., and Bruns, T. D. (2013). Dispersal in microbes: fungi in indoor air are dominated by outdoor air and show dispersal limitation at short distances. *ISME J.* 7, 1262–1273. doi: 10.1038/ismej.2013.28

Bao, S. (2000) *Soil and Agricultural Chemistry Analysis*. Beijing: China Agriculture Press Co., Ltd

Barnard, R. L., Osborne, C. A., and Firestone, M. K. (2013). Responses of soil bacterial and fungal communities to extreme desiccation and rewetting. *ISME J.* 7, 2229–2241. doi: 10.1038/ismej.2013.104

Bates, D., Mächler, M., Bolker, B., and Walker, S. (2015). Fitting linear mixed-effects models using lme4. *J. Stat. Softw.* 67, 1–48. doi: 10.18637/jss.v067.i01

Brewer, T. E., and Fierer, N. (2018). Tales from the tomb: the microbial ecology of exposed rock surfaces. *Environ. Microbiol.* 20, 958–970. doi: 10.1111/1462-2920.14024

Chen, J., Li, F., Zhao, X., Wang, Y., Zhang, L., Yan, L., et al. (2022). Change in composition and potential functional genes of microbial communities on carbonatite rinds with different weathering times. *Front. Microbiol.* 13:1024672. doi: 10.3389/fmicb.2022.1024672

Chen, S., Zhou, Y., Chen, Y., and Gu, J. (2018). Fastp: an ultra-fast all-in-one FASTQ preprocessor. *Bioinformatics* 34, i884–i890. doi: 10.1093/bioinformatics/bty560

Chimienti, G., Piredda, R., Pepe, G., van der Werf, I. D., Sabbatini, L., Crecchio, C., et al. (2016). Profile of microbial communities on carbonate stones of the medieval church of san Leonardo di Siponto (Italy) by Illumina-based deep sequencing. *Appl. Microbiol. Biotechnol.* 100, 8537–8548. doi: 10.1007/s00253-016-7656-8

Crispim, C. A., and Gaylarde, C. C. (2005). Cyanobacteria and biodeterioration of cultural heritage: a review. *Microb. Ecol.* 49, 1–9. doi: 10.1007/s00248-003-1052-5

Crispim, C. A., Gaylarde, P. M., Gaylarde, C. C., and Neilan, B. A. (2006). Deteriogenic cyanobacteria on historic buildings in Brazil detected by culture and molecular techniques. *Int. Biodeterior. Biodegrad.* 57, 239–243. doi: 10.1016/j.ibiod.2006.03.001

Csardi, G., and Nepusz, T. (2006). The igraph software package for complex network research. *Int. J. Complex Syst.* 5:1965.

Dakal, T. C., and Cameotra, S. S. (2012). Microbially induced deterioration of architectural heritages: routes and mechanisms involved. *Environ. Sci. Eur.* 24:36. doi: 10.1186/2190-4715-24-36

de Oliveira Mendes, G., Murta, H. M., Valadares, R. V., da Silveira, W. B., da Silva, I. R., and Costa, M. D. (2020). Oxalic acid is more efficient than sulfuric acid for rock phosphate solubilization. *Miner. Eng.* 155:106458. doi: 10.1016/j.mineng.2020.106458

de Vries, F. T., Griffiths, R. I., Bailey, M., Craig, H., Girlanda, M., Gweon, H. S., et al. (2018). Soil bacterial networks are less stable under drought than fungal networks. *Nat. Commun.* 9:3033. doi: 10.1038/s41467-018-05516-7

Dixon, P. (2003). VEGAN, a package of R functions for community ecology. *J. Veg. Sci.* 14, 927–930. doi: 10.1111/j.1654-1103.2003.tb02228.x

Edgar, R. C. (2013). UPARSE: highly accurate OTU sequences from microbial amplicon reads. *Nat. Methods* 10, 996–998. doi: 10.1038/nmeth.2604

Fukasawa, Y., Savoury, M., and Boddy, L. (2020). Ecological memory and relocation decisions in fungal mycelial networks: responses to quantity and location of new resources. *ISME J.* 14, 380–388. doi: 10.1038/s41396-019-0536-3

Gadd, G. M. (1999). Fungal production of citric and oxalic acid: importance in metal speciation, physiology and biogeochemical processes. *Adv. Microb. Physiol.* 41, 47–92. doi: 10.1016/s0065-2911(08)60165-4

Gadd, G. M. (2017a). Fungi, Rocks, and Minerals. *Elements* 13, 171–176. doi: 10.2113/gselements.13.3.171

Gadd, G. M. (2017b). Geomicrobiology of the built environment. *Nat. Microbiol.* 2:16275. doi: 10.1038/nmicrobiol.2016.275

Gambino, M., Lepri, G., Štovícek, A., Ghazayarn, L., Villa, F., Gillor, O., et al. (2021). The tombstones at the monumental cemetery of Milano select for a specialized microbial community. *Int. Biodeterior. Biodegrad.* 164:105298. doi: 10.1016/j.ibiod.2021.105298

Gaylarde, C., Ribas Silva, M., and Warscheid, T. (2003). Microbial impact on building materials: an overview. *Mater. Struct.* 36, 342–352. doi: 10.1007/BF02480875

Gerrits, R., Wirth, R., Schreiber, A., Feldmann, I., Knabe, N., Schott, J., et al. (2021). High-resolution imaging of fungal biofilm-induced olivine weathering. *ChGeo* 559:119902. doi: 10.1016/j.chemgeo.2020.119902

Gómez-Cornelio, S., Mendoza-Vega, J., Gaylarde, C. C., Reyes-Estebanez, M., Morón-Ríos, A., De la Rosa-García, S. D. C., et al. (2012). Succession of fungi colonizing porous and compact limestone exposed to subtropical environments. *Fungal Biol.* 116, 1064–1072. doi: 10.1016/j.funbio.2012.07.010

Gómez-Silva, B. (2018). Lithobiontic life: "Atacama rocks are well and alive". *Antonie Van Leeuwenhoek* 111, 1333–1343. doi: 10.1007/s10482-018-1033-9

Gorbushina, A. A. (2007). Life on the rocks. *Environ. Microbiol.* 9, 1613–1631. doi: 10.1111/j.1462-2920.2007.01301.x

Gorbushina, A. A., and Broughton, W. J. (2009). Microbiology of the atmosphere-rock interface: how biological interactions and physical stresses modulate a sophisticated microbial ecosystem. *Annu. Rev. Microbiol.* 63, 431–450. doi: 10.1146/annurev.micro.091208.073349

Hervé, M. (2022) RVAideMemoire: Testing and plotting procedures for biostatistics. Available at: https://CRAN.R-project.org/package=RVAideMemoire

Lai, J., Zou, Y., Zhang, S., Zhang, X., and Mao, L. (2022). Glmm.Hp: an R package for computing individual effect of predictors in generalized linear mixed models. *J. Plant Ecol.* 15, 1302–1307. doi: 10.1093/jpe/rtac096

Langfelder, P., and Horvath, S. (2012). Fast R functions for robust correlations and hierarchical clustering. *J. Stat. Softw.* 46, 1–17. doi: 10.18637/jss.v046.i11

Li, T., Hu, Y., Zhang, B., and Yang, X. (2018). Role of Fungi in the formation of patinas on Feilaifeng limestone, China. *Microb. Ecol.* 76, 352–361. doi: 10.1007/s00248-017-1132-6

Liu, X., Koestler, R. J., Warscheid, T., Katayama, Y., and Gu, J.-D. (2020). Microbial deterioration and sustainable conservation of stone monuments and buildings. *Nat. Sustain* 3, 991–1004. doi: 10.1038/s41893-020-00602-5

Liu, X., Meng, H., Wang, Y., Katayama, Y., and Gu, J.-D. (2018). Water is a critical factor in evaluating and assessing microbial colonization and destruction of Angkor sandstone monuments. *Int. Biodeterior. Biodegrad.* 133, 9–16. doi: 10.1016/j.ibiod.2018.05.011

Liu, C., Zhao, D., Ma, W., Guo, Y., Wang, A., Wang, Q., et al. (2016). Denitrifying sulfide removal process on high-salinity wastewaters in the presence of Halomonas sp. *Appl. Microbiol. Biotechnol.* 100, 1421–1426. doi: 10.1007/s00253-015-7039-6

Magoč, T., and Salzberg, S. L. (2011). FLASH: fast length adjustment of short reads to improve genome assemblies. *Bioinformatics* 27, 2957–2963. doi: 10.1093/bioinformatics/btr507

McKnight, D. T., Huerlimann, R., Bower, D. S., Schwarzkopf, L., Alford, R. A., and Zenger, K. R. (2019). Methods for normalizing microbiome data: an ecological perspective. *Methods Ecol. Evol.* 10, 389–400. doi: 10.1111/2041-210X.13115

Mihajlovski, A., Gabarre, A., Seyer, D., Bousta, F., and Di Martino, P. (2017). Bacterial diversity on rock surface of the ruined part of a French historic monument: the Chaalis abbey. *Int. Biodeterior. Biodegrad.* 120, 161–169. doi: 10.1016/j.ibiod.2017.02.019

Miller, A. Z. (2010) Primary bioreceptivity of limestones from the mediterranean basin to phototrophic microorganisms.

Miller, A. Z., Laiz, L., Dionísio, A., Macedo, M. F., and Saiz-Jimenez, C. (2009). Growth of phototrophic biofilms from limestone monuments under laboratory conditions. *Int. Biodeterior. Biodegrad.* 63, 860–867. doi: 10.1016/j.ibiod.2009.04.004

Miller, A. Z., Laiz, L., Gonzalez, J. M., Dionísio, A., Macedo, M. F., and Saiz-Jimenez, C. (2008). Reproducing stone monument photosynthetic-based colonization under laboratory conditions. *Sci. Total Environ.* 405, 278–285. doi: 10.1016/j.scitotenv.2008.06.066

Miller, A. Z., Sanmartín, P., Pereira-Pardo, L., Dionísio, A., Saiz-Jimenez, C., Macedo, M. F., et al. (2012). Bioreceptivity of building stones: a review. *Sci. Total Environ.* 426, 1–12. doi: 10.1016/j.scitotenv.2012.03.026

Mitchell, R., and Gu, J.-D. (2000). Changes in the biofilm microflora of limestone caused by atmospheric pollutants. *Int. Biodeterior. Biodegrad.* 46, 299–303. doi: 10.1016/S0964-8305(00)00105-0

Moroni, B., and Pitzurra, L. (2008). Biodegradation of atmospheric pollutants by fungi: a crucial point in the corrosion of carbonate building stone. *Int. Biodeterior. Biodegrad.* 62, 391–396. doi: 10.1016/j.ibiod.2008.03.011

Paradis, E., Claude, J., and Strimmer, K. (2004). APE: analyses of Phylogenetics and evolution in R language. *Bioinformatics* 20, 289–290. doi: 10.1093/bioinformatics/btg412

Pinheiro, A. C., Mesquita, N., Trovão, J., Soares, F., Tiago, I., Coelho, C., et al. (2019). Limestone biodeterioration: a review on the Portuguese cultural heritage scenario. *J. Cult. Herit.* 36, 275–285. doi: 10.1016/j.culher.2018.07.008

Rajan, P., Lada, R. R., and MacDonald, M. T. (2019). Advancement in indoor vertical farming for microgreen production. *Am. J. Plant Sci.* 10, 1397–1408. doi: 10.4236/ajps.2019.108100

Reig, F. B., Adelantado, J. V., and Moya Moreno, M. C. (2002). FTIR quantitative analysis of calcium carbonate (calcite) and silica (quartz) mixtures using the constant ratio method. *Talanta* 58, 811–821. doi: 10.1016/s0039-9140(02)00372-7

Ren, Y., Yu, G., Shi, C., Liu, L., Guo, Q., Han, C., et al. (2022). Majorbio cloud: a one-stop, comprehensive bioinformatic platform for multiomics analyses. *iMeta* 1:e12. doi: 10.1002/imt2.12

Sand, W., and Bock, E. (1991). Biodeterioration of mineral materials by microorganisms—biogenic sulfuric and nitric acid corrosion of concrete and natural stone. *Geomicrobiol J.* 9, 129–138. doi: 10.1080/01490459109385994

Scheerer, S., Ortega-Morales, O., and Gaylarde, C. (2009). Microbial deterioration of stone monuments--an updated overview. *Adv. Appl. Microbiol.* 66, 97–139. doi: 10.1016/s0065-2164(08)00805-8

Selbmann, L., Zucconi, L., Isola, D., and Onofri, S. (2015). Rock black fungi: excellence in the extremes, from the Antarctic to space. *Curr. Genet.* 61, 335–345. doi: 10.1007/s00294-014-0457-7

Shang, Q., Zhang, B., Li, H., and Deng, Y. (2021). Identifying influential nodes: a new method based on network efficiency of edge weight updating. *Chaos* 31:033120. doi: 10.1063/5.0033197

Shareef, K. M., Omer, L. A., and Garota, S. A. (2008). Predicting the chemical composition of gallstones by FTIR spectroscopy. *Biomed. & Pharmacol. J.* 1, 25–30.

Sheng, A., Li, X., and Wu, S. (1997). The composition characteristics of low-molecular-weight organic acids in soil and their roles on soil material cycling. *Plant Nutr. Fertil Sci* 3, 363–371.

Steel, R. G. D., and Torrie, J. H. (1980). *Principles and Procedures of Statistics, A Biometrical Approach*. New York: McGraw-Hill Kogakusha, Ltd.

Sterflinger, K., and Piñar, G. (2013). Microbial deterioration of cultural heritage and works of art — tilting at windmills? *Appl. Microbiol. Biotechnol.* 97, 9637–9646. doi: 10.1007/s00253-013-5283-1

Sun, B., Zhou, Q., Chen, X., Xu, T., and Hui, S. (2010). Effect of particle size in a limestone–hydrochloric acid reaction system. *J. Hazard. Mater.* 179, 400–408. doi: 10.1016/j.jhazmat.2010.03.018

Sunagawa, S., Coelho, L. P., Chaffron, S., Kultima, J. R., Labadie, K., Salazar, G., et al. (2015). Structure and function of the global ocean microbiome. *Science* 348:1261359. doi: 10.1126/science.126135

Trovão, J., Portugal, A., Soares, F., Paiva, D. S., Mesquita, N., Coelho, C., et al. (2019). Fungal diversity and distribution across distinct biodeterioration phenomena in limestone walls of the old cathedral of Coimbra, UNESCO world heritage site. *Int. Biodeterior. Biodegrad.* 142, 91–102. doi: 10.1016/j.ibiod.2019.05.008

Trovão, J., Soares, F., Tiago, I., Catarino, L., Portugal, A., and Gil, F. (2021). A contribution to understand the Portuguese emblematic Ançã limestone bioreceptivity to fungal colonization and biodeterioration. *J. Cult. Herit.* 49, 305–312. doi: 10.1016/j.culher.2021.04.003

Trovão, J., Tiago, I., Catarino, L., Gil, F., and Portugal, A. (2020). In vitro analyses of fungi and dolomitic limestone interactions: bioreceptivity and biodeterioration assessment. *Int. Biodeterior. Biodegrad.* 155:105107. doi: 10.1016/j.ibiod.2020.105107

Vázquez-Nion, D., Silva, B., and Prieto, B. (2018). Influence of the properties of granitic rocks on their bioreceptivity to subaerial phototrophic biofilms. *Sci. Total Environ.* 610-611, 44–54. doi: 10.1016/j.scitotenv.2017.08.015

Villa, F., Stewart, P. S., Klapper, I., Jacob, J. M., and Cappitelli, F. J. B. (2016). Subaerial biofilms on outdoor stone monuments: changing the perspective toward an ecological framework. *Bioscience* 66, 285–294. doi: 10.1093/biosci/biw006

Villa, F., Vasanthakumar, A., Mitchell, R., and Cappitelli, F. (2015). RNA-based molecular survey of biodiversity of limestone tombstone microbiota in response to atmospheric Sulphur pollution. *Lett. Appl. Microbiol.* 60, 92–102. doi: 10.1111/lam.12345

Walker, J. J., and Pace, N. R. (2007). Endolithic microbial ecosystems. *Annu. Rev. Microbiol.* 61, 331–347. doi: 10.1146/ANNUREV.MICRO.61.080706.093302

Wang, Q., Garrity, G. M., Tiedje, J. M., and Cole, J. R. (2007). Naive Bayesian classifier for rapid assignment of rRNA sequences into the new bacterial taxonomy. *Appl. Environ. Microbiol.* 73, 5261–5267. doi: 10.1128/aem.00062-07

Warscheid, T., and Braams, J. (2000). Biodeterioration of stone: a review. *Int. Biodeterior. Biodegrad.* 46, 343–368. doi: 10.1016/S0964-8305(00)00109-8

Warscheid, T., Oelting, M., and Krumbein, W. (1991). Physico-chemical aspects of biodeterioration processes on rocks with special regard to organic pollutants. *Int. Biodeterior.* 28, 37–48. doi: 10.1016/0265-3036(91)90032-M

Yang, N., Kuang, S., and Yue, Y. (2015). Infrared spectra analysis of several common anhydrous carbonate minerals. *MinPe* 35, 37–42. doi: 10.19719/j.cnki.1001-6872.2015.04.007

Zhang, G., Gong, C., Gu, J., Katayama, Y., Someya, T., and Gu, J.-D. (2019). Biochemical reactions and mechanisms involved in the biodeterioration of stone world cultural heritage under the tropical climate conditions. *Int. Biodeterior. Biodegrad.* 143:104723. doi: 10.1016/j.ibiod.2019.104723

Zhang, Y., Sun, Q., and Geng, J. (2017). Microstructural characterization of limestone exposed to heat with XRD, SEM and TG-DSC. *Mater. Charact.* 134, 285–295. doi: 10.1016/j.matchar.2017.11.007

Zhang, Y., Wu, F., Su, M., He, D., Gu, J.-D., Guo, Q., et al. (2021). Spatial and temporal distributions of microbial diversity under natural conditions on the sandstone stelae of the Beishiku Temple in China. *Int. Biodeterior. Biodegrad.* 163:105279. doi: 10.1016/j.ibiod.2021.105279

frontiers | Frontiers in Microbiology

TYPE Original Research
PUBLISHED 28 September 2023
DOI 10.3389/fmicb.2023.1229873

OPEN ACCESS

EDITED BY
Maqshoof Ahmad,
The Islamia University of Bahawalpur, Pakistan

REVIEWED BY
Decai Jin,
Chinese Academy of Sciences (CAS), China
Rajiv Das Kangabam,
Assam Agricultural University, India
Sara Fareed Mohamed Wahdan,
Suez Canal University, Egypt

*CORRESPONDENCE
Rasheed A. Adeleke
✉ rasheed.adeleke@nwu.ac.za

RECEIVED 27 May 2023
ACCEPTED 01 September 2023
PUBLISHED 28 September 2023

CITATION
Raimi AR, Ezeokoli OT and Adeleke RA (2023) Soil nutrient management influences diversity, community association and functional structure of rhizosphere bacteriome under vegetable crop production.
Front. Microbiol. 14:1229873.
doi: 10.3389/fmicb.2023.1229873

Soil nutrient management influences diversity, community association and functional structure of rhizosphere bacteriome under vegetable crop production

Adekunle R. Raimi, Obinna T. Ezeokoli and Rasheed A. Adeleke*

Unit for Environmental Sciences and Management, North-West University, Potchefstroom, South Africa

Introduction: Rhizosphere bacterial communities play a crucial role in promoting plant and soil ecosystem health and productivity. They also have great potential as key indicators of soil health in agroecosystems. Various environmental factors affect soil parameters, which have been demonstrated to influence soil microbial growth and activities. Thus, this study investigated how rhizosphere bacterial community structure and functions are affected by agronomic practices such as organic and conventional fertiliser application and plant species types.

Methods: Rhizosphere soil of vegetable crops cultivated under organic and conventional fertilisers in different farms was analysed using high-throughput sequencing of the 16S rRNA gene and co-occurrence network pattern among bacterial species. The functional structure was analysed with PICRUSt2 pipeline.

Results: Overall, rhizosphere bacterial communities varied in response to fertiliser type, with soil physicochemical parameters, including NH_4, PO_4, pH and moisture content largely driving the variations across the farms. Organic farms had a higher diversity richness and more unique amplicon sequence variants than conventional farms. Bacterial community structure in multivariate space was highly differentiated across the farms and between organic and conventional farms. Co-occurrence network patterns showed community segmentation for both farms, with keystone taxa more prevalent in organic than conventional farms.

Discussion: Module hub composition and identity varied, signifying differences in keystone taxa across the farms and positive correlations between changes in microbial composition and ecosystem functions. The organic farms comprised functionally versatile communities characterised by plant growth-promoting keystone genera, such as *Agromyces*, *Bacillus* and *Nocardioides*. The results revealed that organic fertilisers support high functional diversity and stronger interactions within the rhizosphere bacterial community. This study provided useful information about the overall changes in soil microbial dynamics and how the changes influence ecosystem functioning under different soil nutrient management and agronomic practices.

KEYWORDS

fertilizers, microbial networks, agroecosystem, soil-plant-microbe interactions, 16S rRNA gene sequencing, plant-soil ecology

Introduction

Soil microbes participate in nutrient cycling, organic matter decomposition and energy flow, which are key in sustaining soil ecosystem functions (Ling et al., 2022). However, soil nutrient management, soil properties and climatic conditions, which vary across geographic locations alter how soil ecosystem function through a possible shift in microbial diversity and functions (Ge et al., 2008; Ahkami et al., 2017; Yang et al., 2021). Substantial responses to changes in land use and soil nutrient build-up have been reported for both plant and soil microbial communities, with potential consequences for ecosystem functioning (Nielsen et al., 2015). Soil microbial diversity is vast and its interactions with other ecosystem components (e.g., vegetation and soil parameters) are complex, which significantly impacts the correlation between soil microbial diversity and ecosystem functions in response to disturbances (Garnica et al., 2020). Thus, insights into soil bacteriome structure and how it is affected by agronomic practices are key to making informed decisions that will promote agroecosystem sustainability.

Currently, organic and conventional fertilizers are the main agro-inputs for improving soil nutrient content (Musyoka et al., 2017). Improved soil nutrient content enhances overall plant health by altering the soil parameters and predisposing the selection of certain rhizosphere bacterial communities with unique ecosystem functions. Consequently, the plant and microbes interactions in the soil, along with the above-ground productivity, are affected by the type of fertilizer applied (Ahkami et al., 2017). Using phospholipid fatty acids, a study has reported that organically managed soil enhanced bacterial and fungal biomass, with an increase in total microbial metabolic activity and soil organic matter. Thus, soil nutrient management types could drastically impact soil ecosystem functioning, through the imbalances caused by fertilizer application and nutrient deposition (Martínez-García et al., 2018).

Furthermore, plant species or genotypes influence the synthesis of unique exudates and extracellular enzymes, which impact microscale spatial patterns in soil bacterial communities and differentially stimulate the growth of specific microbial groups under different ecosystems across geographic locations (Hoch et al., 2019; Yan et al., 2021). Usually, plants exert a selective influence on their rhizo-microbiome to acquire key beneficial traits (Jaramillo et al., 2016), indicating rhizosphere microbial communities are a reflection of plant species and plant-beneficial genetic functions. For example, legumes harbor bacteria with nitrogenases that enhance their N-fixing ability (Lugtenberg, 2015). Similarly, plant-associated microbes, which perform functions such as nitrate reduction, denitrification, nutrient solubilization, and production of phytohormones such as indole acetic acid, ethylene and siderophore are a reflection of the host plant's needs (Raimi et al., 2017). These microbial functions influence plant productivity and health, which in turn drive soil bacterial diversity and ecosystem functions (Mendes et al., 2013).

Soil parameters vary by geographic location and primarily provide similar conditions that affect the activities of plants and their associated microbiome to soil microbes (Mendes et al., 2013). Studies have shown that factors such as soil pH, carbon, organic matter and nutrient content drive spatial patterns of soil microbial diversity within an ecosystem (Bardgett and Caruso, 2020; Nan et al., 2020). Spatial patterns of soil microbial community due to plant species and fertilizer types and how it relates to bacterial taxonomic and functional profiles remain largely underexplored. Increase in land-use intensification is reported to alter soil microbial composition (Felipe-Lucia et al., 2020) and keystone taxa, which are crucial for microbial community structure and ecosystem functioning (Banerjee et al., 2018). Due to the importance and unique role of keystone taxa, their interactions or loss can trigger a shift in microbiome structure (Yang et al., 2021). Interactions between microbial community members have been widely assessed using microbial co-occurrence network analysis (Li et al., 2018; Xu et al., 2022). Thus, co-occurrence patterns and microbial networks are key to understanding how bacterial community interactions and keystone taxa distribution and functions change under different agronomic practices (Huang et al., 2019; Hernandez D. J. et al., 2021).

Consequently, this study assessed the effects of fertilizer type (organic vs. conventional) and plant species type on the microbial dynamics (including keystone taxa) and ecosystem functions of vegetable rhizosphere soil across different farms. It is hypothesized that fertilizer type in each of the farming systems predisposes the selection of certain rhizobacterial communities, which possess diverse but unique functional gene repertoire of agronomic importance. Results from this study could provide baseline information useful in predictive modeling for manipulating soil bacterial communities to improve agroecosystems. Similarly, the approach used in this study could unravel keystone taxa with unique biomarker potential for monitoring soil health and productivity in a given nutrient management system.

Experimental procedures

Description of the study sites and rhizosphere soil sampling

Rhizosphere soils were collected from four vegetable farms located in the North West (farms B and S) and Gauteng (farms J and T) provinces of South Africa. Farm B (26°42′55.0″S 27°04′59.6″E) and farm S (26°47′43.5″S 27°02′18.3″E) are situated in JB marks municipality, while farm J (26°11′40.1″S 28°03′58.3″E) and farm T (26°03′16.0″S 27°40′13.3″E) are in Johannesburg and West Rand District municipalities, respectively. The North West province is characterized as a semi-arid climate while the Gauteng province is classified as a mild climate that is neither humid nor too hot (www.sa-venues.com/weather/). Average annual temperature and rainfall are 22.36°C and 36.6 mm for North West province and 20.64°C and 56.11 mm for Gauteng province. The average annual relative humidity for North West and Gauteng provinces are 37.8 and 50.22%, respectively (Weather and Climate, 2023). Vegetable farming is a major agricultural production in the two provinces, with higher production in the North West compared with the Gauteng province (Macaskill, 2016). The farms have been cultivating various vegetables, including cabbage, lettuce, onions, and spinach for over 2 years on the same plot. The Gauteng province farms (farm J and T) practice conventional farming, using chemical fertilizers, pesticides and fungicides, whereas the farms in the North West province (farm B and S) practice mainly organic farming, utilizing plant and animal waste. The organic farms use compost, green waste, and animal manure (poultry, sheep, goat, and cow), while the conventional farms use chemical fertilizers including NPK fertilizers, urea, ammonium nitrate, diammonium phosphate, and pesticides such as carbamates, organophosphates and pyrethroid (Personal communication).

Sampling was conducted in the summer (October–February) of 2021. Based on visual inspection, rhizosphere soils of healthy vegetables of the same age and size including, *Allium cepa* (onion), *Brassica oleracea* (cabbage), *Lactuca sativa* (lettuce), and *Spinacia oleracea* (spinach), were sampled from each farm as described by Barillot et al. (2013), with some modifications. Briefly, vegetables were uprooted and shaken vigorously to remove bulk soil from the roots. Thereafter, the rhizosphere soil was collected by hand-shaking several undamaged roots to release the adhering soil into a sterile beaker. Five replicate samples were collected for each plant per farm and an equal quantity (50 g each) of the soils from the same vegetable for each farm were pooled to obtain a composite sample. An additional sample of the rhizosphere soil was collected from each farm; a different vegetable type was sampled at each farm, bringing the total number of study samples to 20. Samples were immediately placed in sterile zip-lock bags, transported to the laboratory on ice and stored for further analysis.

Physicochemical parameters and enzyme analyzes of rhizosphere soil

The soil pH was measured from a 1:2.5 soil-water suspension using a pre-calibrated pH meter (HQ40d Hach, United States), while the electrical conductivity (EC) was determined with an EC meter. The amounts of macronutrients (N, P, K, and Ca), micronutrients (Mn, Fe, Zn, and Cu), heavy metals (Pb, Cd, Cr, Hg, and As) and exchangeable cations (Ca^{2+}, Mg^{2+}, K^{+}, and Na^{+}) in the soil were determined using the inductively coupled plasma mass spectrometry (ICP-MS), following standard procedure (Bulska and Wagner, 2016). Other physicochemical properties, such as soil texture (sand, silt, and clay proportion), cation exchange capacity (CEC), moisture and organic matter (OM) content, and the soil enzyme activities, including acid and alkaline phosphatases, β-glucosidase, urease and dehydrogenase activity were analyzed at the Eco-Analytical, North-West University, South Africa, following standardized methods described by the Soil Science Society of South Africa (SSSSA, 1990).

High-throughput sequencing of 16S rRNA gene

Soil community DNA was extracted using Power Soil DNA extraction kits (Qiagen, Hilden, Germany) following the manufacturer's instructions. The DNA concentration was measured with a Qubit fluorometer (Invitrogen, Carlsbad, CA, United States) and the integrity was checked using gel electrophoresis with a 1% agarose gel. Extracted DNA was normalized to equimolar concentrations (5 ng/μl) using 0.1 M Tris-HCl (pH 8.5) and the partial 16S rRNA gene (V3-V4 region), a universal barcode for the characterization of bacteria, was amplified in a polymerase chain reaction (PCR) using Illumina-barcoded 341F and 805R primers (Klindworth et al., 2013). The 16S rRNA gene library was prepared as described by van Wyk et al. (2017). Paired-end (2 × 300 bp) sequencing of the gene libraries was performed on the Illumina MiSeq sequencer using the Nextera v3 kit (Illumina Inc., San Diego, CA, United States). Sequencing was performed at the sequencing facility of the Unit for Environmental Sciences and Management, North-West University, Potchefstroom, South Africa.

Bioinformatics

The 16S rRNA gene sequence reads were demultiplexed and trimmed of barcodes using MiSeq Reporter software (Illumina Inc., San Diego, CA, United States) and then quality checked with FastQC (v. 0.11.5) (Babraham Bioinformatics, UK). Low-quality reads were trimmed with trimmomatic software (v. 0.38) (Bolger et al., 2014) and reads with mean nucleotide base quality score of less than 20 (Phred Q score) were removed. Reads were analyzed using the Quantitative Insight into Microbial Ecology v2 platform (QIIME 2, Release 2020.11; Bolyen et al., 2019). Quality-filtered reads were denoised and clustered into amplicon sequence variants (ASVs) using DADA2 denoiser (Callahan et al., 2016) with a pre-trained classifier of the SILVAngs rRNA gene reference (release 138) (Quast et al., 2013). After singleton removal, the ASV table was rarefied to an even depth before the taxonomic assignment and diversity analyzes in QIIME 2. Alpha diversity indices such as the Shannon-Wiener index, inverse Simpson index, Chao1 richness estimator and phylogenetic diversity were analyzed in R v 4.1.1 (R Development Core Team, 2018).

Predicted functional metagenomic profile of rhizosphere bacterial communities

The functional metagenomic profile of the absolute abundance of microbial genera was predicted using the Tax4Fun2 package (Wemheuer et al., 2020) in R (R Development Core Team, 2018). Firstly, the ASVs were searched against the 16S rRNA gene reference sequences using the basic local alignment search tool (BLAST) via the *runRefBlast* function. Thereafter, the functional prediction was evaluated using the *makeFunctionalPrediction*, where the ASVs were summarized based on the results of the next neighbor search (Wemheuer et al., 2018). Predicted profiles were annotated based on the Kyoto Encyclopaedia of Genes and Genomes (KEGG) orthology (KO) pathways (Kanehisa et al., 2012). KO terms and metabolic pathways were generated for the ASVs and the relative abundance of the functional genes was calculated. To gain insights into the influence of agronomic practices on bacterial community functional genes, only a few of the KO terms contributing to major ecosystem functions (e.g., organic matter decomposition and biogeocycling), plant growth and nutrient metabolism were investigated.

Co-occurrence network

Bacterial community co-occurrence patterns were analyzed by constructing ecological networks using the Random matrix theory (RMT)-based method in the molecular ecological network analysis (MENA) pipeline[1] (Faust and Raes, 2016). To assess the impact of fertilizer type on soil bacterial structure, organic and conventional farm networks were constructed. Network complexity was reduced by using only ASVs present in at least 40% of the samples across the organic and conventional farms and the Pearson correlation coefficient was employed for data transformation. Using a multilevel modularity optimization algorithm, bacterial community groups

1 http://ieg4.rccc.ou.edu/mena

were identified by clustering networks into modules (Blondel et al., 2008). Node connectivity was established based on among-module connectivity (Pi) and within-module connectivity (Zi); creating four sub-categories of nodes (a) peripheral ($Zi < 2.5$; $Pi < 0.62$), (b) connectors ($Zi < 2.5$; $Pi > 0.62$), (c) module hubs ($Zi > 2.5$; $Pi < 0.62$) and (d) network hubs ($Zi > 2.5$; $Pi > 0.62$) (Guimera and Amaral, 2005). The networks were visualized in Gephi v 0.9.2.

Statistical analyzes

All statistical analyzes were performed in R software (v.4.1.1) unless otherwise stated. The significance for all tests was set at $p < 0.05$ and the data was tested across fixed factors: farms, fertilizer types (organic vs. conventional farms) and vegetable species. Data normality was tested using the Shapiro–Wilk test and non-normal data was transformed with $\log_{10}$, square root or sine to fit a normal distribution. Normal or non-normal data were analyzed using parametric or non-parametric tests, respectively. Correlation between soil physicochemical and enzyme activity data was tested using Pearson or Spearman rank correlation for normalized or non-normal datasets. The community structure across the farms, and between organic and conventional farm soil was visualized with a nonmetric multidimensional scaling (NMDS) plot and a cluster dendrogram using vegan and dendextend (v. 1.12.0) (Galili, 2015) packages in R studio. Differences in multivariate space across the fixed factors were performed with Bray-Curtis dissimilarity using permutational multivariate analysis of variance (PERMANOVA) and Permutational test for homogeneity of multivariate dispersion (PERMDISP). Linear Discriminant Analysis (LDA) Effect size (LEfSe) (Segata et al., 2011) was performed to detect differentially abundant genera (Mann–Whitney U test or Kruskal-Wallis test, p-value < 0.05; LDA score > 2) between the farms, organic and conventional farms and plant species using microeco package in R software (Liu et al., 2021). Subsequently, the LEfSe results were visualized as bar plots. An indicator species functional analysis was performed for predicted KO terms to detect the most discriminatory KOs between the fixed factors. KO terms with false discovery rate (FDR)-adjusted $p < 0.05$ and an indicator value of > 0.1 were taken to be discriminant for the fixed factors. Redundancy analysis (RDA) was performed in R software to show the physicochemical parameters that best explain the variations in the microbial community composition.

Data availability statement

The 16S rRNA gene sequence data for this study are available in the sequence read archives (SRA) of the National Centre for Biotechnological Information under a BioProject with SRA accession no PRJNA904574 (https://www.ncbi.nlm.nih.gov/bioproject/904574).

Results

Rhizosphere soil physicochemical properties

The soil physicochemical parameters varied across the fixed factors with no particular trend. A near-neutral pH range was observed across the farms, with the conventional farms having a higher pH than the organic farms (Table 1). The moisture and OM content ranged from 1.06–1.42% and 4.98–5.89%, respectively. Organic farms largely had a higher CEC and OM content than conventional farms. Farms mostly had low quantities of microelements and heavy metals, except for Pb and As in farm J (Table 1). Soil texture was mainly classified as sandy-clay-loam for organic farms and sandy-loam for conventional farms. Some of the soil physicochemical properties significantly (Kruskal-Wallis test, $p < 0.05$) differed across the farms (Table 1), while only the differences in OM, clay proportion, CEC, NH_4, P, and Cu were statistically significant (Mann–Whitney or t-test, $p < 0.05$) across the fertilizer types.

Soil enzyme activities

The soil enzyme activities were significantly (Kruskal-Wallis H test, $p < 0.05$) different across the farms and fertilizer type, except for alkaline phosphatase, which was not influenced by the fertilizer type. Mostly, the enzyme activities were higher for organic farms compared to conventional farms (Table 2). The alkaline and acid phosphatases had a very low range of activities across the farms. Comparing among farms, farm B had the highest dehydrogenase and β-glucosidase activities, while farm S had the highest activity for urease. Farm J had the lowest urease activity, which is approximately five, 12 and 23 folds lower compared to farms B, T, and S, respectively (Table 2). The main effect of crop type and the interactions between the fixed factors on soil enzyme activities were not statistically significant (Kruskal-Wallis H test, $p > 0.05$).

Diversity and community structure of bacterial amplicon sequence variants

A total of 1,933,349 16S rRNA gene reads was obtained from all samples, with a mean read count of 96,667 per sample. Quality-filtered reads were clustered into 28,604 ASVs after pruning low count and low variance features. The ASVs were rarefied to an equal depth of 74,170 (rarefaction curve in Supplementary Figure S1) before examining the treatment effects. The distribution and richness of ASVs differed substantially across the farms, with farm S having the highest number of unique ASVs (Figure 1A). Observed ASVs were higher in organic compared to conventional farms and 276 ASVs were shared among all the farms (Figures 1A,B). Comparing the shared ASVs in the organic (Supplementary Figure S2A) with the conventional (Supplementary Figure S2B) farms, 1,222 and 313 ASVs were exclusive to the organic and conventional farms, respectively (Figure 1B). Similarly, ASV richness differed across the rhizosphere of each vegetable species. Unique ASVs were higher in cabbage, followed by lettuce and onion rhizosphere, while spinach and lettuce rhizosphere share more ASVs (Supplementary Figure S3).

The alpha diversity indices measured were not significantly influenced by the main effect of fertilizer type and plant species, except for the inverse Simpson index, which was significant (ANOVA, $F = 3.65$, $p = 0.035$) across the farms, with the pairwise comparison (Tukey HSD, P-adjusted = 0.0218) showing differences between farms T and S. In addition, the combined effects of the fixed factors (fertilizer type and plant species) and their interactions had no significant effect (general linear model, $p > 0.05$) on the alpha diversity indices measured.

10.3389/fmicb.2023.1229873

TABLE 1 Selected soil physicochemical properties across farms and fertilizer types.

Parameters	Organic		Conventional	
	Farm B	Farm S	Farm J	Farm T
pH (H_2O)	7.05 ± 0.15^{a}	7.52 ± 0.13^{a}	7.62 ± 0.6^{a}	7.68 ± 1.1^{a}
Moisture (%)	1.27 ± 0.2^{a}	1.06 ± 0.12^{a}	1.42 ± 0.4^{a}	1.39 ± 0.2^{a}
OM (%)	5.89 ± 0.12^{a}	5.37 ± 0.11^{b}	4.98 ± 0.19^{b}	5.13 ± 0.19^{b}
TOC	1.62 ± 0.21^{c}	2.44 ± 0.02^{b}	2.99 ± 0.48^{a}	1.68 ± 0.11^{c}
EC (mS cm^{-1})	0.44 ± 0.0^{b}	0.44 ± 0.0^{b}	0.22 ± 0.0^{c}	0.70 ± 0.0^{a}
CEC (cmol [+]) kg $^{-1}$	11.68 ± 0.21^{b}	29.29 ± 1.62^{a}	8.42 ± 1.12^{c}	10.24 ± 1.42^{bc}
NO_3 (mg l^{-1})	135.82 ± 1.72^{a}	65.34 ± 1.53^{c}	35.96 ± 3.52^{d}	125.96 ± 4.39^{b}
PO_4 (mg l^{-1})	10.52 ± 0.44^{b}	11.03 ± 1.25^{ab}	10.45 ± 1.28^{b}	14.19 ± 1.82^{a}
NH_4 (mg l^{-1})	1.04 ± 0.1^{b}	1.12 ± 0.09^{b}	1.53 ± 0.1^{b}	4.28 ± 0.44^{a}
SO_4 (mg l^{-1})	35.54 ± 1.32^{c}	70.13 ± 2.17^{a}	15.37 ± 2.17^{d}	53.79 ± 3.03^{b}
HCO_3 (mg l^{-1})	15.25 ± 0.48^{b}	42.71 ± 1.41^{a}	36.61 ± 3.13^{a}	36.61 ± 3.94 ^{a}
P (mg kg $^{-1}$)	42.5 ± 3.27^{b}	14.3 ± 1.73^{c}	72.2 ± 3.25^{a}	40.2 ± 2.34^{b}
K (mg l^{-1})	17.2 ± 0.97^{bc}	19.55 ± 0.94^{ab}	16.42 ± 1.81^{c}	53.56 ± 1.81^{a}
Na (mg l^{-1})	16.78 ± 0.68^{b}	16.78 ± 0.87^{b}	10.28 ± 1.56^{c}	30.81 ± 2.53^{a}
Ca (mg l^{-1})	32.86 ± 2.61^{b}	33.26 ± 1.89^{b}	13.63 ± 3.56^{c}	51.7 ± 3.61^{a}
Mg (mg l^{-1})	18.21 ± 1.02^{a}	17.26 ± 0.89^{a}	6.2 ± 1.24^{b}	17.5 ± 2.20^{a}
Cl (mg l^{-1})	42.19 ± 2.1^{b}	30.14 ± 3.09^{c}	12.76 ± 2.6^{d}	99.62 ± 3.76^{a}
Fe (mg l^{-1})	0.51 ± 0.02^{a}	0.0 ± 0.00^{c}	0.01 ± 0.0^{bc}	0.03 ± 0.0^{b}
Cu (mg l^{-1})	0.03 ± 0.00^{c}	0.05 ± 0.00^{b}	0.19 ± 0.00^{a}	0.05 ± 0.00^{b}
Zn (mg l^{-1})	0.0 ± 0.00^{c}	0.0 ± 0.00^{c}	0.14 ± 0.00^{a}	0.01 ± 0.00^{b}
Pb (mg/kg)	5.46 ± 0.18^{d}	53.29 ± 0.91^{b}	91.27 ± 0.24^{a}	8.25 ± 0.10^{c}
As (mg/kg)	2.68 ± 0.16^{c}	3.69 ± 0.0b	12.35 ± 0.61^{a}	3.47 ± 0.0^{b}
Hg (mg/kg)	0.04 ± 0.0^{b}	0.11 ± 0.0^{b}	2.91 ± 0.18^{a}	0.05 ± 0.0^{b}
Pd (mg/kg)	0.26 ± 0.02^{b}	0.37 ± 0.0^{a}	0.17 ± 0.0^{c}	0.18 ± 0.0^{c}
Cd (mg/kg)	0.03 ± 0.0^{c}	0.085 ± 0.0^{b}	0.16 ± 0.0^{a}	0.02 ± 0.0^{c}
Particle size (>2 mm)	3.8 ± 0.78^{c}	29.9 ± 2.43^{a}	5.2 ± 0.68^{b}	0.4 ± 0.00^{d}
Clay (%)	23.1 ± 0.75^{a}	27.4 ± 2.56^{a}	12.6 ± 0.86^{c}	17.9 ± 1.76^{b}
Sand (%)	65.4 ± 2.72^{b}	64.0 ± 3.91^{b}	76.3 ± 2.66^{a}	65.8 ± 4.3^{b}
Silt (%)	11.5 ± 0.86^{b}	8.6 ± 1.84^{a}	11.1 ± 1.72^{b}	16.3 ± 1.8^{c}

Values are mean ± SD ($n = 4$). EC, electrical conductivity; CEC, cation exchange capacity; OM, Organic matter; TOC, Total organic carbon. Values with different superscript letters for each farm (across rows) are significantly different based on the non-parametric Kruskal-Wallis H test or the parametric analysis of variance (ANOVA) test.

TABLE 2 Important rhizosphere soil enzyme activities across the farms.

Parameters	Organic		Conventional	
	Farm B	Farm S	Farm J	Farm T
Dehydrogenase	249.4 ± 7.09^{a}	156.28 ± 6.61^{c}	171.17 ± 2.1^{b}	89.39 ± 0.78^{d}
β-glucosidase	140.98 ± 2.41^{a}	124.53 ± 0.47^{b}	108.09 ± 1.19^{c}	83.28 ± 0.22^{d}
Alkaline phosphatase	0.26 ± 0.01^{b}	0.52 ± 0.04^{a}	0.52 ± 0.02^{a}	0.26 ± 0.02^{b}
Acid phosphatase	0.51 ± 0.02^{a}	0.52 ± 0.02^{a}	0.52 ± 0.00^{a}	0.26 ± 0.01^{b}
Urease	10.83 ± 0.48^{c}	49.81 ± 1.74^{a}	2.17 ± 0.06 ^{d}	25.99 ± 0.24^{b}

Values are mean ± SD ($n = 4$) followed by superscript letters across the rows. The superscripts are significant differences based on the non-parametric Kruskal-Wallis H test or parametric independent sample ANOVA test across the farms. The unit of measurement for the enzyme are INF μg g^{-1} 2 h^{-1} (dehydrogenase), P-nitrophenol μg g^{-1} h^{-1} (β-glucosidase, acid and alkaline phosphatase) and NH_4-N μg g^{-1} 2 h^{-1} (urease).

Bacterial community structure was highly differentiated across the farms and between the organic and conventional farms in multivariate space. Although the bacterial community structure in the organic farms (farms B and S) are somewhat differentiated, they are jointly less similar to conventional farms (farms J and T) (Figure 2A); the community structural pattern is also supported by the hierarchical

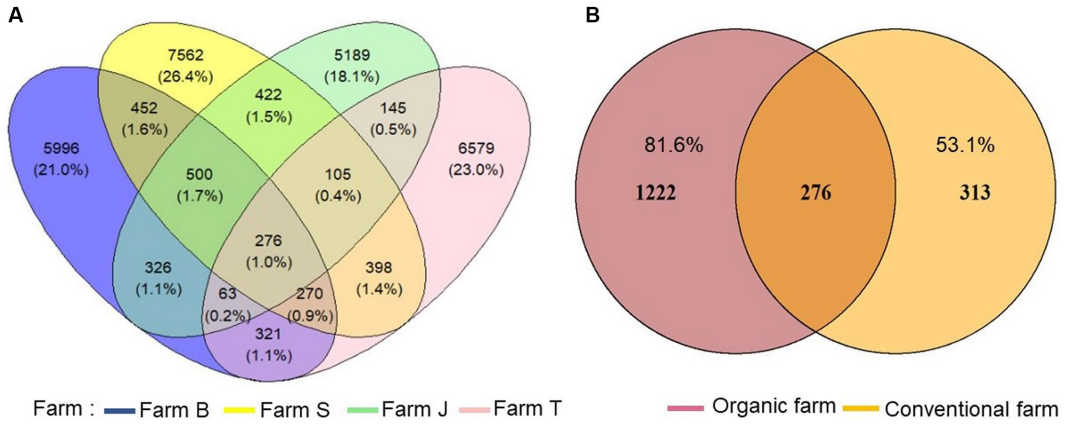

FIGURE 1
Comparison of unique and shared amplicon sequence variants (ASVs) richness. **(A)** ASV richness across the farms, **(B)** unique ASVs between organic and conventional farms.

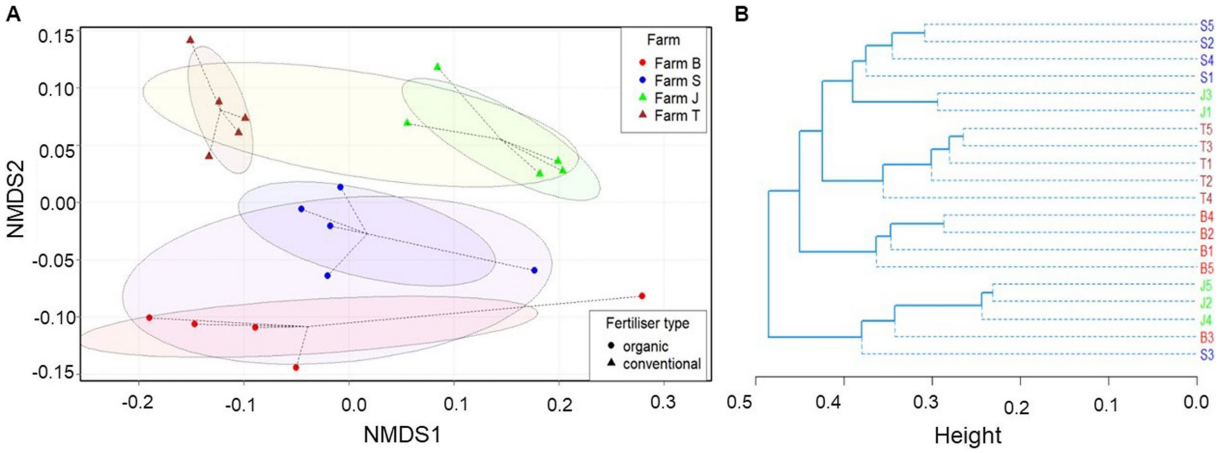

FIGURE 2
Bray-Curtis dissimilarity between bacterial communities. **(A)** Comparison of observed ASVs between organic and conventional fertilization and across farms based on non-metric multidimensional scaling (NMDS). **(B)** Unweighted paired group mean arithmetic (UPGMA) hierarchical cluster dendrogram. The eclipses in the NMDS plot show 95% confidence intervals (standard error) in multivariate space within the group centroids, while the dotted lines indicate the distance of each sample to its group centroid in multivariate space. The stress plot (Supplementary Figure S5B) for the NMDS showed that the original dissimilarities are well preserved (stress = 0.165047) in the reduced number of dimensions.

clustering (Figure 2B). Moreover, the bacterial community composition was significantly different between the farms (PERMANOVA, $p = 0.001$) and across organic and conventional farms (PERMANOVA, $p = 0.009$), contributing about 39.01 and 11.74% of the variations in the models and a PERMDISP of 0.073 and 0.269, respectively. Significant variation was observed between farms B and T, J and T, and S and T. However, the plant species had no significant (PERMAOVA, $p = 0.568$) effect on the bacterial community structure, which was not clearly differentiated (Supplementary Figure S4). The non-significant and low dispersion rate in the bacterial community across the farms (Supplementary Figure S5A) suggests the results depicted by the NMDS plot in Figure 2A are reliable. The stress plot run for the NMDS plot is below 0.2 (Supplementary Figure S5B). The effect of fertilizer type and plant species interaction on the bacterial community structure was not significant (Supplementary Table S1).

Dominant and differentially abundant rhizosphere bacterial communities

Across all datasets, the relatively more abundant classifiable ASVs belonged to nine phyla and 19 major genera. Across the farms, the most relatively abundant (>5%) phyla were Actinobacteria (32.3%), Proteobacteria (25.4%), Acidobacteria (8.4%), Firmicutes (7.6%), Chloroflexi (7.6%), and Planctomyces (5.7%) (Figure 3A). The relatively more abundant (> 5%) genera across the farms are *Bacillus*, *Rubrobacter*, *Gemmatimonas*, *Solirubrobacter*, RB41, *Nocardioides* and *Bryobacter* (Figure 3B). *Bacillus* and *Nocardioides* were relatively more abundant in conventional farms, with their highest abundance found in farm J, while *Rubrobacter* and *Solirubrobacter* were more abundant in organic farms, mainly in farms B and S, respectively. Across the plant species, the bacterial community composition at the phylum and genus taxa levels were not particularly different; however, at the

phylum level, Chloroflexi, Planctomycetes and Gemmatimonadetes were relatively most abundant in cabbage, whereas Actinobacteria, Proteobacteria and Firmicutes were the most abundant phyla in onion (Supplementary Figure S6A) compared to other vegetables. Cabbage had the highest relative abundance of *Bacillus* and *Rubrobacter*, whereas onion had the highest relative abundance of *Nocardioides*, *Streptomyces* and *Solirubrobacter* (Supplementary Figure S6B).

Linear discriminant analysis (LDA) effect size (LEFSe) showed that a total of 205 features were discriminant across the farms (Kruskal-Wallis H rank-sum test, $p < 0.05$; LDA score > 2.0; Supplementary Table S2) while only 18 features were discriminant for organic farms vs. conventional farms (LDA score > 2.4; Supplementary Table S3). No taxa was discriminant across the plant species after multiplicity adjustment (Kruskal-Wallis rank-sum test; $p > 0.05$). The genera *Rubrobacter* and *Microlunatus* were highly discriminant in organic farms (Figure 4A), while *Nocardioides*, *Ilumatobacter*, *Lysobacter*, and *Marmoricola*, were significantly discriminant in conventional farms (Figure 4A). Some of the bacterial communities that were significant and differentially abundant (FDR-adjusted $p < 0.05$, LDA score > 2.0) at the genus taxa across the farms are shown in Figure 4B. *Rubrobacter* and uncultured Conexibacteraceae were more discriminant in farm B, while Pira4lineage and uncultured bacterial Clone C112 were discriminant in farm T. In farm S, Uncultured Actinomycetales, Thermoactinomyces, and *Tumebacillus* were found to be discriminant. The discriminant features in conventional farms, *Marmoricola* and *Lysobacter,* were mainly from farm J. Before multiplicity adjustment of the LEFSe results for plant species type, *Pseudomonas*, *Paracoccus* and *Candidatus Udaeobacter* were discriminant ($p > 0.05$, LDA score > 2.0) and abundant in cabbage, onion, and spinach, respectively (Figure 4C), while lettuce rhizosphere soil showed no discriminant feature.

Bacterial functional profile and differentially abundant agroecological important enzymes

The KO terms and pathways predicted for all the ASVs were 6,429 and 279, respectively. After multiplicity adjustment, 17 of the predicted pathways were significant for fertilizer type factor (Kruskal-Wallis rank sum test, $p < 0.05$; LDA > 0.181; Supplementary Table S4), while no significant pathway was observed for the plant species factor. Across the farms, a total of 161 functions were significant (Kruskal-Wallis rank sum test, $p < 0.05$; LDA > 0.274) after multiplicity adjustment (Supplementary Table S5). Seventeen abundant KO terms, contributing to important agroecological processes such as the synthesis or metabolism of N, P, C, S, and Fe compounds were compared across the farms (Figure 5). Predicted KO terms, including nitrogenase, acid and alkaline phosphatase, ferric chelate reductase and aminocyclopropane-1-carboxylate (ACC) deaminase, had low relative abundance in organic compared to conventional farms. Based on the Bray-Curtis distance, the predicted pathways in organic farms and conventional farms clustered separately as shown by the hierarchical cluster dendrogram plot in Figure 5.

A higher relative abundance of K01505, K02217, K07405, K01187, and K03332 was predicted in the rhizosphere of cabbage relative to other plant species. Similarly, K00368, K02585, K01183, K07406, and K02013 were higher for ASVs from spinach than in other plant species, while onion had the least abundance of predicted KOs (Supplementary Table S6). The major functional profile group of the bacterial communities at taxa rank level 1 is metabolism, followed by environmental information, and genetic and cellular processes. Using LEfSe, it was revealed there are differences in the abundances of key enriched pathways across the fixed factors

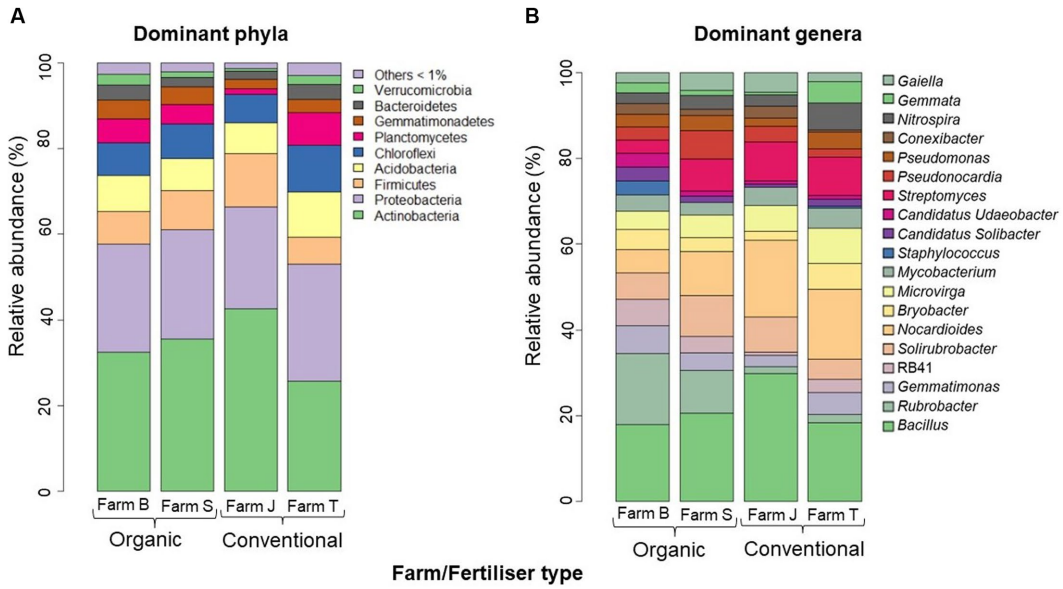

FIGURE 3
Average relative abundance (>5%) of dominant phylotypes across the farms. **(A)** Dominant Phyla **(B)** Dominant Genus taxa. The phylotypes with average relative abundance below 1% and the unculturable and unclassified at the genus taxa level were expunged from the plot. The bar plots were constructed based on the average relative abundance per farm site in R studio.

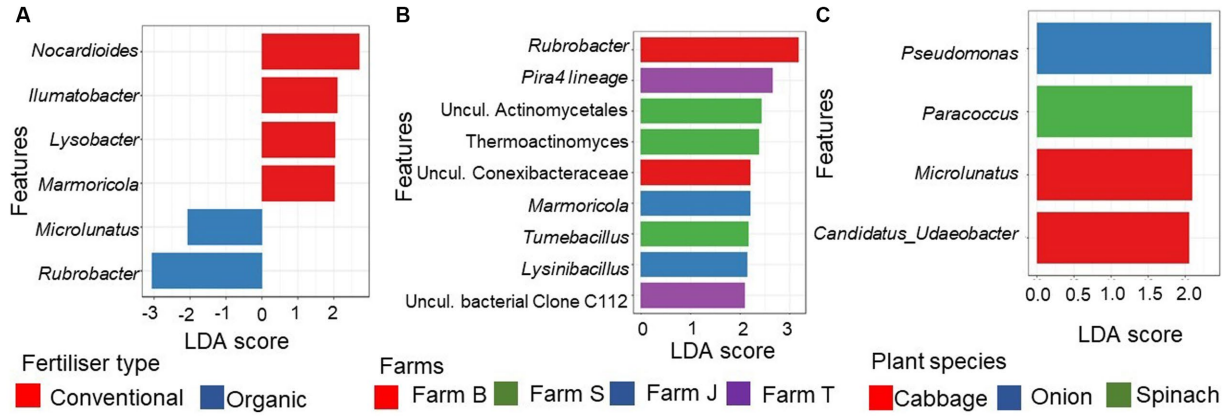

FIGURE 4
Differentially abundant genera of the rhizosphere bacterial communities. **(A)** Top 6 statistically significant discriminant (FDR-adjusted p-value < 0.1, LDA score > 2.4) genera between organic and conventional farms **(B)** Top 9 discriminant (FDR-adjusted p-value < 0.05, LDA score > 2.0) between the farms. **(C)** Differentially abundant genera (FDR-adjusted p-value < 0.1, LDA score > 2.0) between the plant species. The bar plot was generated using the Linear Discriminant Analysis (LDA) Effect size (LefSe) in the R using the microeco package. Uncul., uncultured.

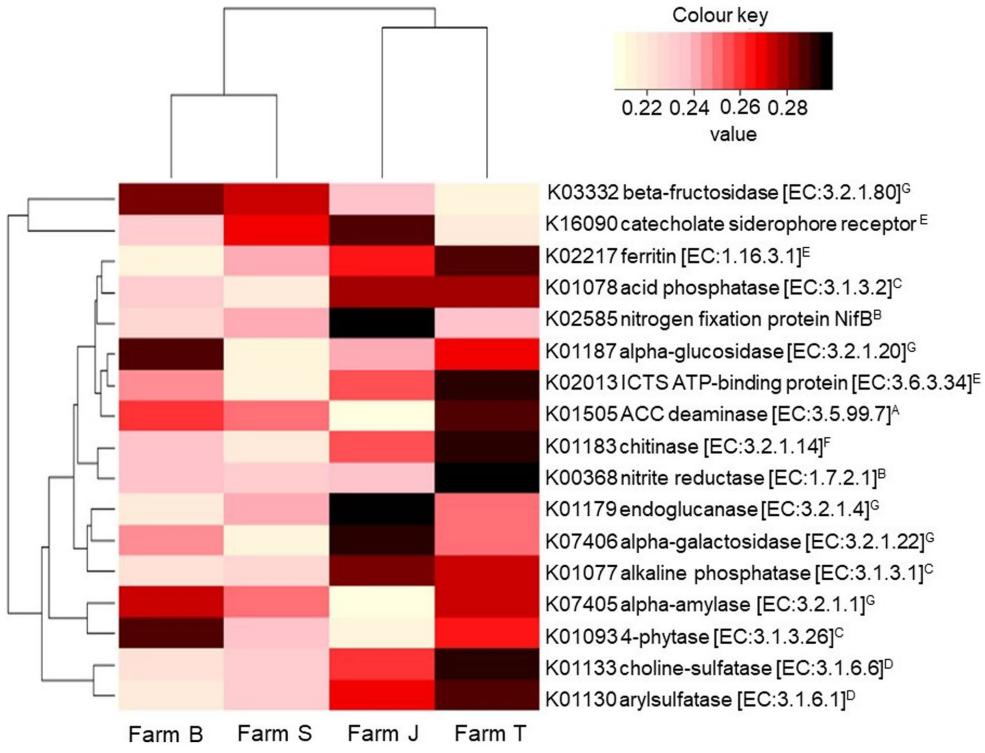

FIGURE 5
Relative abundance of KEGG Orthology terms contributing to important agroecosystem functions. The hierarchical clustering dendrograms are based on the mean Bray-Curtis distance between the farms. The color range for the relative abundance is scaled across the farms. The superscripts by the enzyme commission (EC) number indicate (A); ACC, (B); N-fixation, (C); phosphorous mineralization, (D); sulfur mineralization (E); soil iron balance, (F); biocontrol, and (G); soil C breakdown. ICT, iron complex transport system.

(Kruskal-Wallis rank-sum test, $p < 0.05$, LDA > 0.2). Organic farms had more differentially abundant pathways compared to conventional farms. Amino acid, arginine, proline metabolism, C-fixation and citrate cycle pathways were discriminant in the organic farm (Supplementary Table S4), while sulfur, phosphonate and phosphinate metabolism were more abundant in the conventional farms. Farm T, followed by farm J had the highest number of important enriched pathways (Supplementary Table S5). Xenobiotic degradation and terpenoid and polyketide metabolism were differentially abundant in farm J while bacterial secretion, translation and genetic information system were more abundant in farm T (Supplementary Table S5).

Relationship between biological and physicochemical properties

Although there were no significant correlations between some of the soil enzyme activities and physicochemical parameters (Supplementary Table S7), beta-glucosidase had a significantly positive correlation with pH ($r = 0.32$, $p = 0.001$) and PO_4 ($r = 0.12$, $p = 0.045$) but negative correlation with OM ($r = -0.69$, $p = 0.015$), NH_4^+ ($r = -0.72$, $p = 0.005$) and K ($r = -0.30$, $p = 0.019$). Both alkaline and acid phosphatase significantly ($p < 0.05$) correlated with TOC, positively and Cl, negatively. Moreover, alkaline phosphatase correlated positively with NO_3 while acid phosphatase correlated positively with pH and EC. In addition, dehydrogenase had significant correlations that were negative with pH, PO_4, NH_4 and K but positive with OM and TOC. Although there exists either a positive or negative correlation between the soil enzymes and moisture content, Ca and sand, the correlations were not significant. Similarly, though not significant, there were correlations between the species function percentage of bacterial community with the soil parameters (Supplementary Figure S7).

The RDA plot showed that the soil physicochemical properties contributed 34.5% (R-squared adjusted value) of the variation in the bacterial community structure. Farms and fertilizer type-specific clustering were observed, especially for the organic farms (Figure 6). Among the physicochemical parameters in the RDA model, TOC, OM, EC, and CEC were statistically significant (ANOVA, $p < 0.05$) (Supplementary Table S8). Similarly, there were significant correlations between the environmental variables and the distance matrix (Mantel, $p < 0.05$) (Supplementary Table S8). Overall, the plot showed that soil physicochemical properties largely influenced the variations observed in the bacterial community (Figure 6). PO_4, Na, and NH_4 had more impact on the bacterial community structure in farm T, while moisture, TOC, sand, and pH, had more influence on bacterial community structure in the organic farms (farms B and S).

Co-occurrence analysis

Some of the ASVs had significant ($r = 0.70$, $p < 0.05$) positive correlations with the environmental traits, which produced a significant (Mantel, $p = 0.001$) effect on the network connectivity. The significant ASVs and node connectivity were found to be significant for two major phyla: Actinobacteria (Mantel, $r = 0.120$, $p = 0.022$) and Acidobacteria (Mantel, $r = 0.344$, $p = 0.009$). From the topological metrics (Table 3), both organic and conventional farm networks were non-random as inferred from the significant power-law distribution for each network ($R^2_{organic} = 0.88$, $p < 0.05$; $R^2_{conventional} = 0.84$, $p < 0.05$) and the higher values of some of the structural features in the empirical compared to the random networks (Table 3). The empirical network consisted of 247 nodes and 704 edges (Figure 7A) for the organic farms and 284 nodes and 1,027 edges for the conventional farms (Figure 7B).

A higher level of positive (~72%) associations occurred among the bacterial communities in the organic farms compared to conventional farms, which had a higher negative (~33%) association. Though community segmentation was apparent in both networks, the organic farms had a more profound fragmentation. Moreover, a higher network complexity was observed for organic farms compared to conventional farms, which had more numbers of smaller modules and edges than organic farms. The module hubs were not of similar parameters, with organic farms (Figure 7A) having more bacterial communities compared to conventional farms (Figure 7B). Actinobacteria, Acidobacteria, Proteobacteria and Chloroflexi were dominant in the keystone nodes. No network hub was observed for both networks. While Actinobacteria occurred as a major node that highly connects modules in both networks (Figure 7), Bacteroides, Proteobacteria, Acidobateria and Chloroflexi are other connectors in the organic farm network. The keystone nodes comprised the genera *Bacillus*, *Nocardioides*, *Blastocatella*, and *Saccharomonsospora*. A major connector in conventional farms is *Agromyces* while organic farms are dominated by the family Micrococcaceae, Roseiflexaceae, Blastocatellaceae, Xanthobacteraceae, and Chitinophagaceae (Figure 7).

Discussion

Soil microbes significantly contribute to ecosystem functions through organic matter decomposition, nutrient cycling, and mineralization. These functions and plant ecosystems are influenced by agronomic practices such as soil nutrient management and cropping systems. Thus, this study provided insights into the rhizosphere soil bacterial community structure and functions of vegetable crops cultivated under organically and conventionally managed soil in different farms. Functional profiling and differentially abundant taxa of rhizosphere bacteria allowed for the identification of rare microbial communities with unique potentials in agroecosystems, emphasizing the benefits of understanding soil microbiome dynamics to reveal specific patterns, functions and strategies used by microbes under different agronomic conditions.

Soil physicochemical parameters influence nutrient richness

The fact that soil nutrients and structure drive plant growth and soil microbial diversity is well established (Bach et al., 2010; Xu et al., 2022). Some of the soil parameters, including pH, EC, moisture content, NH_4^+ and NO_3^- were not significant across the farms, However, except for pH and P, the measured values were relatively not within the optimal range required for the productivity of most crops, including vegetables (Rosen and Eliason, 2005; Warncke et al., 2009; Liu and Hanlon, 2018). Contrary to our results, low moisture content has been reported in chemically fertilized soils (Rachwał et al., 2021) and a higher pH in organically managed soil (Diacono and Montemurro, 2010; Aziz et al., 2017). Higher levels of organic matter increase soil water holding capacity through soil aggregation, signifying soil organic matter and moisture content are strongly correlated (Rajkai et al., 2015). Although organic farms typically have higher organic matter content and soil texture type that support high moisture content, our results showed that conventional farms had higher moisture content, possibly due to other factors such as time of sampling and irrigation system. Compared to conventional farms, soils in the organic farms largely had higher clay content, CEC and OM content; this is in agreement with the observations from other studies (Han et al., 2016; Rigane et al., 2020). Among the farms, farm S, which is organically managed, had the highest particle size (Table 1). Soil particle sizes impact soil aeration and structure, while high clay content and CEC strongly drive the fixation of key soil nutrients

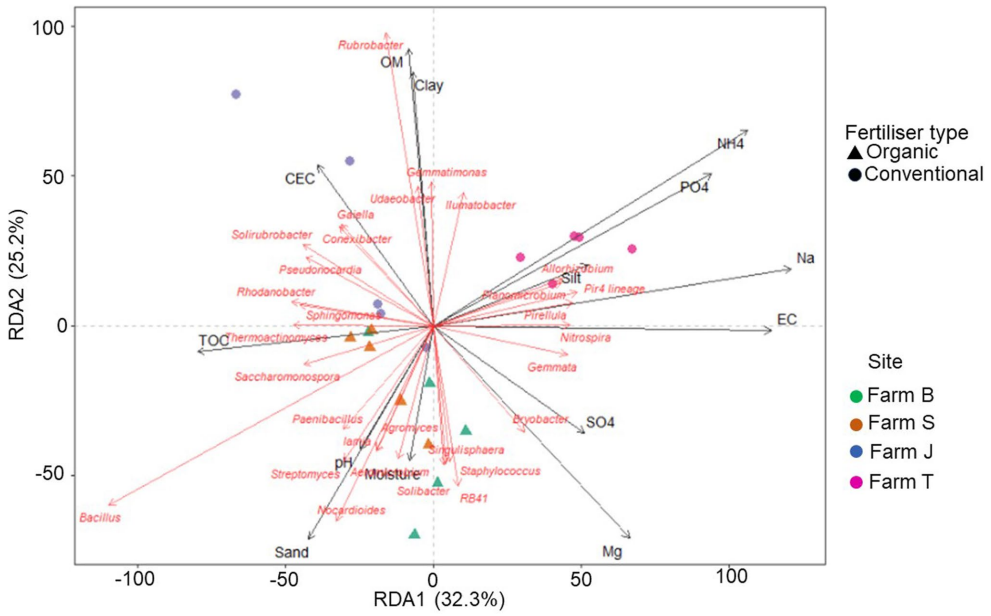

FIGURE 6
Redundancy analysis (RDA) triplot showing the correlation between bacterial community relative abundance (for 30 major genera) and explanatory variables (physicochemical factors). The first species axis (RDA) is significant ($p < 0.05$).

(Ramos et al., 2018; Kome et al., 2019). Being negatively charged, clay particles adsorb positive ions such as Ca^{2+}, Fe^{3+}, K^{+}, and NH_4^{+} which are key indicators of soil nutrient richness (Tomašić et al., 2021). In contrast, our results show that in the organic farms (Farm B and S), which had higher clay content, some of the positive ions, including NH_4^{+}, K^{+}, and Ca^{2+} were relatively lower suggesting other factors, including irrigation, could have influenced the soil nutrient levels.

Soil enzyme activities in organically and conventionally managed soil

High activity of soil enzymes, including dehydrogenase, β-glucosidase and urease activities have been reported in organic farms (Hernandez T. et al., 2021; Pittarello et al., 2021). Extracellular enzyme production has been positively correlated with high microbial biomass and diversity in the community. Such reports are consistent with our results that showed a high activity of β-glucosidase across organic farms, validating the comparatively higher C mineralization in organic farms compared to conventional farms; compost and manure applied in organic farms are rich in carbon substrate (Zang et al., 2018; Cordero et al., 2019). Acid and alkaline phosphatase activities are optimal at pH 3.0–5.5 and 8.5–11.5, suggesting the low activities across the farms may be linked to the soil neutral pH (Neina, 2019). Soil enzyme activities dynamically respond to soil nutrient management, which influences soil parameters, particularly pH, OM, moisture content and nutrient content (Pan et al., 2013; Koishi et al., 2020). A significant correlation between soil pH and dehydrogenase, β-glucosidase and acid phosphatase suggests pH is a key factor driving enzyme activities (Pan et al., 2013). The observed positive correlation of β-glucosidase with OM indicates the specificity of the enzyme to soil C, which is a fraction of the total soil OM (Meena and Rao, 2021). Corroborating with our result of reduced enzyme activities in the conventional farm, excessive use of chemical fertilizers has been reported to hinder soil enzyme activities (Pittarello et al., 2021; Rachwał et al., 2021). Thus, the types of fertilizers used in plant cultivation affect changes in soil conditions, such as enzyme activities which may cause variations in the dynamics of the associated soil microbial community (Liu and Hanlon, 2018; Ullah et al., 2019).

Rhizosphere bacterial community diversity and structure

Soil properties, especially organic matter drive bacterial growth and metabolism, suggesting the bacterial richness across the farms is related to soil conditions (Peltoniemi et al., 2021; Rachwał et al., 2021). This was evidenced in the RDA triplot (Figure 6), which revealed a significant correlation between the soil parameters and some bacterial communities. Soil physical and biological parameters, including OM, moisture and nutrient content, pH, dehydrogenase, β-glucosidase, and urease, support improved soil and plant health, which in turn influence the rhizosphere bacteria composition (Yan et al., 2021). Rhizosphere microbiome has some analogous traits with its associated plants, suggesting plant selective impact on rhizosphere microbes and consequently shaping rhizobacterial assemblage (Ling et al., 2022). Similar to other studies, though only the inverse Simpson diversity index was significant, the differences in alpha diversity across the farms suggest fertilizer types influence bacterial community richness (Hu et al., 2011; Acharya et al., 2021). According to Hermans et al. (2017) and Kamaa et al. (2011), bacterial communities respond to prevailing soil nutrient management types, which vary across landscapes; this is in agreement with our results which revealed differences in bacterial communities across the different farms, as depicted by the NMDS plot (Figure 2A). However, the bacterial community structure of soils from similar fertilizer types showed some differences, an indication that other site-specific factors, such as the source and type of seeds, fertilizers, and irrigation systems not considered in this study, may be responsible.

TABLE 3 Topological properties of empirical and random networks between bacterial communities of organic and conventional farm.

Network indices	Organic		Conventional	
	ENI	100 RNI	ENI	100 RNI
Average clustering coefficient	0.129	0.043 ± 0.006	0.216	0.309 ± 0.011
Average path distance	6.183	3.467 ± 0.038	2.791	2.545 ± 0.027
Geodesic efficiency	0.215	0.321 ± 0.003	0.456	0.435 ± 0.003
Harmonic geodesic distance	4.648	3.115 ± 0.025	2.191	2.300 ± 0.017
Centralization of degree	0.073	0.073 ± 0.000	0.326	0.326 ± 0.000
Centralization of betweenness	0.122	0.074 ± 0.008	0.067	0.090 ± 0.010
Centralization of stress centrality	17.228	0.299 ± 0.028	2.725	0.590 ± 0.055
Centralization of eigenvector centrality	0.210	0.184 ± 0.015	0.175	0.173 ± 0.003
Density	0.019	0.019 ± 0.000	0.050	0.050 ± 0.000
Reciprocity	1.000	1.000 ± 0.000	1.000	1.000 ± 0.000
Transitivity	0.192	0.061 ± 0.006	0.131	0.254 ± 0.005
Connectedness	0.801	0.958 ± 0.021	0.471	0.980 ± 0.017
Efficiency	0.981	0.984 ± 0.000	0.900	0.952 ± 0.001
Hierarchy	0.000	0.000 ± 0.000	0.000	0.000 ± 0.000
Lubeness	1.000	1.000 ± 0.000	1.000	1.000 ± 0.000
Modularity	0.676	0.406 ± 0.006	0.210	0.166 ± 0.004

ENI, Empirical Network Indices; RNI, Random Network indices.

Important bacterial phyla, including Actinobacteria, Proteobacteria, Acidobacteria, Firmicutes and Chloroflexi, which were relatively abundant across the farms have been reported in similar studies (Ezeokoli et al., 2020; Zhang et al., 2022). These phyla usually exist in C-rich niches, such as the rhizosphere, which supports high metabolic activities and fast microbial growth. The variation in taxa abundance across crop species may be due to differences in root architecture and exudates, which differentially stimulate the growth of rhizosphere microbial communities (Hoch et al., 2019; Yan et al., 2021). Similarly, this may have influenced the higher ASVs abundance observed in cabbage compared to other crop species, suggesting the need to further explore factors influencing rhizobacteria diversity variability in different crop species under similar conditions. Several studies have identified core bacterial microbiomes primarily using taxonomic assignment; however, for detailed knowledge of microbial dynamics, it has become imperative to further identify soil microbes using key functions that are commonly expressed (Ling et al., 2022). For instance, Gemmatimonadetes, a recently classified phylum found among the major phyla in the cabbage soil have species that contribute to C-fixation through chlorophototrophy (Thiel et al., 2018). In addition, predominant genera, such as *Bacillus*, *Nocardioides*, *Pseudomonas*, *Rubrobacter*, and *Lysobacter,* which are constantly enhanced in the rhizosphere, contribute to key microbial functions and processes, such as biogeochemical cycling, organic matter decomposition, mineralization and processes that are crucial to agroecosystem sustainability (Raimi et al., 2017; Adeleke et al., 2019).

Ecological functions of differentially abundant rhizosphere bacterial community

The differentially abundant *Rubrobacter* in organic farms is underexplored despite its ecological restoration and engineering potential, which is attributed to its ability to survive in low-nutrient soil and under intense desiccation (Baubin et al., 2021). Similarly, *Lysinibacillus* and *Pseudomonas* predominant in organic farm soils are well-known plant growth-promoting rhizobacteria involved in N-fixation, phytohormone production and P solubilization (Li et al., 2017; Vignesh et al., 2021; Shahwar et al., 2023). *Candidatus Udaeobacter*, a differentially abundant genus in the spinach rhizosphere, exhibits multidrug resistance and the ability to evade the harmful effects of antimicrobials (Willms et al., 2020). The unique properties of these genera suggest they are suitable indicator species for assessing the soil nutrient status. In contrast to the organic farms, conventional farms had differentially abundant *Norcardioides*, *Lysobacter*, *Ilumatobacter*, and *Marmoricola*. *Nocardioides* participate in bioremediation, especially organochlorine degradation such as lindane pesticide and chloroaromatics, making them a crucial candidate for soil remediation strategy (Ito et al., 2019; Singh and Singh, 2019). *Lysobacter* is a well-known biocontrol agent (Lin et al., 2021) while *Ilumatobacter* and *Marmoricola* participate in C and N cycling, respectively (Edgmont et al., 2012; Liu et al., 2023). Although soil microbes have been extensively classified, the high proportion of unclassified sequences in this study gave credence to the fact that the majority of soil microbiomes are yet to be fully identified and characterized (Delgado-Baquerizo, 2019; Furtak et al., 2020). However, metagenomics, a leading and relatively recent technique for effective analysis of diverse environments has advanced microbial diversity knowledge, offering valuable strategies for optimizing the cultivation of yet uncultured species (Kulski, 2016; Mendes et al., 2017).

Nitrogenase and NifT play key roles in the N-cycle, while cellulases break down cellulose and polysaccharide, and chitinase degrades chitins, contributing to C and N levels in the ecosystem (Glick, 2012). Corroborating the report by Ling et al. (2022), alpha-glucosidase and beta-fructokinase were highly predicted in organic farms, possibly due to the high level of C supplied by compost and animal manure, suggesting a more sustainable soil microbial community may

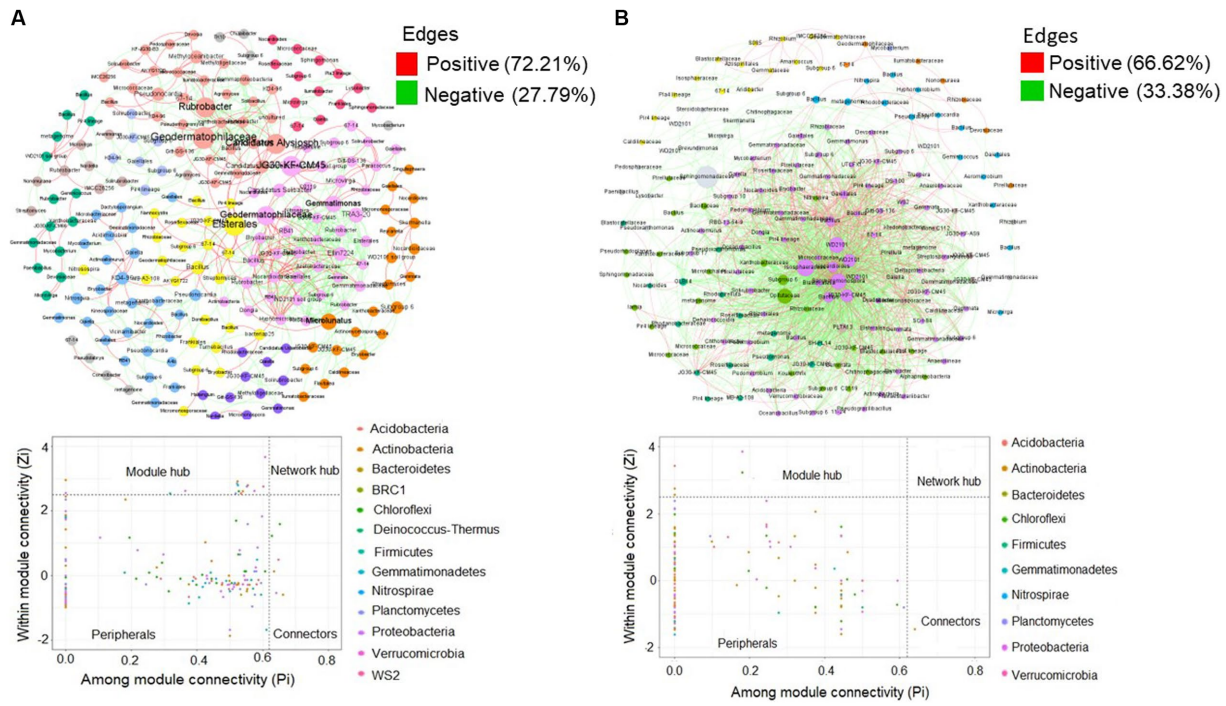

FIGURE 7
Co-occurrence networks of bacterial communities and classification of nodes for detection of keystone taxa within ecological networks in **(A)** organic and **(B)** conventional farm rhizosphere soil. The nodes represent bacterial species (round shape), colored according to the community modularity class. Node sizes are proportional to their degree of distribution, and nodes having less than two connections have been removed. Edges are network connections signifying significant (FDR-adjusted $p < 0.01$) associations between nodes. Positive associations are colored red, while negative associations are colored blue. Detected module hubs in the two farm networks are linked with Acidobacteria, Actinobacteria, Proteobacteria and Chloroflexi, while the connectors are affiliated with Actinobacteria for both organic and conventional farms. The co-occurrence network statistics are presented in Table 3.

be achieved through organic amendments that increased these key enzymes. Bacterial communities such as *Bacillus*, *Enterobacter*, *Citrobacter*, and *Pseudomonas* detected have been previously reported with N-fixing ability due to their nitrogenases (Gomez-Garzon et al., 2017; Li et al., 2017). On the contrary, nitrite reductase genes driving the denitrification pathway in the N-cycle were significantly abundant in Farm T, which is a conventional farm, establishing the fact that these genes play a crucial role in preventing groundwater pollution caused by nitrate compounds due to excessive chemical fertilizer application (Liu et al., 2020). Arylsulfatase and choline-sulfatase drive the sulfur content in the soil and are usually activated under sulfur-deficient conditions (Cregut et al., 2013; Sánchez-Romero and Olguin, 2015). Surprisingly, these genes were highly prevalent in conventional farms (Farm T and J) (Figure 5), suggesting other factors, including available sulfur, forms of sulfur compounds and other nutrient complexes in the soil may have influenced the prevalence of these enzymes (Siwik-Ziomek et al., 2016). In addition, the high abundance of enzyme coding genes predicted in the rhizosphere of cabbage compared to other vegetables could enhance soil nutrient richness and in turn drive increased soil microbial composition and diversity (de Bruijn, 2015; Xu et al., 2022). While variations across geographic locations drive changes in soil physicochemical parameters (Moore et al., 2022), the changes may in turn influence soil microbial and enzyme activities (Meena and Rao, 2021), suggesting the reason for some of the variations observed across the farms. Thus, it may be recommended toward best practices to always understand agronomic soil parameters for appropriate selection of efficient soil nutrient management.

Microbial co-occurrence network and keystone taxa

Microbial co-occurrence structure greatly impacts community assembly, abundance and diversity (Pan et al., 2021). Soil nutrient management (types of fertilizer applied) and plant species have been reported to influence the network structure of soil bacterial communities (Xue et al., 2018; Xu et al., 2022). The network analysis showed that conventionally managed soil had high numbers of bacterial communities with negative links, which may indicate weak connections among microbial associations. This observation was corroborated by Huang et al. (2019), who attributed the distinctly weakened ecological interactions between soil microbes to long-term chemical fertilization. In contrast, the higher level of positive interactions in the organic farms may signify greater ecological cooperation among the microbial communities for diverse ecosystem functions and consequently; a network structure with high stability and high-order level complexity (Xue et al., 2018; Gu et al., 2019). Profound community fragmentation was noticed for organic farm networks. According to Hernandez D. J. et al. (2021), ecological stress greatly influences the complexity and stability of microbial networks, indicating fragmentation may not necessarily be due to fertilizer types. Thus, other factors such as soil types, irrigation and land preparation that impact soil microbial diversity may be influential.

In microbial networks, modules comprise species, which are interconnected with more frequent and intensive interactions than other parts of the community (Ling et al., 2022). Compared to conventional

farms, the organic farms had high numbers of complex topological structures and modules, which suggests high niche differentiation in organic farms (Figure 7; Table 3). Unique microbes play key roles in the functioning of bacterial communities by contributing to the information current across the entire network (Banerjee et al., 2018). Similar to our observation, Gu et al. (2019) reported no network hubs in their study, suggesting unique phylotypes for specific functions are absent. However, some generalists, including *Bacillus*, *Nocardioides, Agromyces*, and *Blastocatella* were detected, signifying diverse keystone species that could drive the soil microbial communities in each of the farms (Gu et al., 2019). Module hub, network hub and connectors harbor keystone communities whose identification further improves the understanding of microbial community structure and interactions (Pan et al., 2021). In this study, *Bacillus* found in organic farms is a unique generalist, participating in nutrient solubilization and mineralization; therefore, can generate a niche for other plant growth-promoting rhizobacteria. On the other hand, the conventional farm network has *Agromyces* as a major connector, which is involved in xylan degradation; thus, may create a niche for microbial populations that cannot degrade polysaccharides (Rivas et al., 2004).

To further improve our agroecosystem management knowledge, we recommend that the impact of soil nutrient management on soil microbial diversity and functional structure be investigated across seasons. Data on crops cultivated in the previous seasons, irrigation systems and sources of fertilizers were not available, contributing to some of the limitations in this study.

Conclusion

This study revealed the soil bacterial community diversity and functions are influenced by farm sites and fertilizer types. Unique bacterial communities, which contribute to ecosystem functions were also differentiated across these fixed factors. To a large extent, the discovery of unique bacterial communities such as *Bacillus* and *Rubrobacter* with plant growth-promoting and niche-creation potentials across the farms could improve the understanding of soil microbial dynamics for enhancing soil and plant productivity. In addition, conventional farms had reduced keystone taxa compared to organic farms, signifying fertilizer types impact the abundance of keystone taxa, which is a key factor in ecosystem functioning. This study provided comprehensive details on rhizosphere soil bacterial diversity and functions, which could be useful in the identification of biomarker species for monitoring soil productivity in a particular nutrient management system. Keystone taxa, such as *Bacillus* and *Agromyces* could be a good source of microbial resources for bioformulation production. Overall, the findings provide a baseline for understanding how fertilizer types, organic and conventional fertilizers, impact soil bacteria community structure and related ecological functions. Such knowledge may be useful for monitoring invasive species or formulating a strategy for replenishing extinct beneficial species following land-use intensification or a particular agronomic practice.

Data availability statement

The datasets presented in this study can be found in online repositories. The names of the repository/repositories and accession number(s) can be found below: https://www.ncbi.nlm.nih.gov/, PRJNA904574.

Author contributions

RA: conceptualization, methodology, validation, formal analysis, investigation, resources, writing: review and editing, project administration. AR: validation, resources, writing—original draft, review and editing, methodology, validation, formal data analysis, and investigation. OE: validation, data analysis, writing—review and editing. All authors contributed to the article and approved the submitted version.

Funding

This research was funded by the National Research Foundation (NRF) South Africa, under grant number 116251 and the Technology Innovation Agency with grant number NWU SF2210012/TIA1396/01.

Acknowledgments

The authors appreciate Dr. Deidre Van Wyk, Ms. Mariska Kleyn, Ms. Sharon Mokubedi, Mr. Abram Mahlatsi, and Mrs. Lee Chanhaka for their various supports. The authors are also thanking the farm managers and supervisors, including Mr. Gilbert, Ms. Lerato, and Mr. Malungani, for their support and cooperation during sampling. The authors acknowledge the Centre for High-Performance Computing (CHPC), South Africa, for providing computational resources to this research study (grant number 116251). The views expressed in this study are those of the authors and not of the funding partners.

Conflict of interest

The authors declare that the research was conducted in the absence of any commercial or financial relationships that could be construed as a potential conflict of interest.

Publisher's note

Supplementary material

The Supplementary material for this article can be found online at: https://www.frontiersin.org/articles/10.3389/fmicb.2023.1229873/full#supplementary-material

References

Acharya, M., Ashworth, A. J., Yang, Y., Burke, J. M., Lee, A., and Acharya, R. S. (2021). Soil microbial diversity in organic and non-organic pasture systems. *PeerJ* 9:e11184. doi: 10.7717/peerj.11184

Adeleke, R. A., Nunthkumar, B., Roopnarain, A., and Obi, L. (2019). "Applications of plant-microbe interactions in agro-ecosystem" in *Microbiome in plant health and disease*. eds. V. Kumar, R. Prasad, M. Kumar and D. K. Choudhary (Singapore: Springer Nature), 1–34. doi: 10.1007/978-981-13-8495-0_1

Ahkami, A. H., Allen, R., Iii, W., Handakumbura, P. P., and Jansson, C. (2017). Rhizosphere rhizosphere engineering: enhancing sustainable plant ecosystem productivity. *Rhizosphere* 3, 233–243. doi: 10.1016/j.rhisph.2017.04.012

Aziz, M. A., Hazra, F., Salma, S., and Nursyamsi, D. N. (2017). Soil chemical characteristics of organic and conventional agriculture. *J. Trop. Soils* 21:19. doi: 10.5400/jts.2016.v21i1.19-25

Bach, E. M., Baer, S. G., Meyer, C. K., and Six, J. (2010). Soil Biology & Biochemistry Soil texture affects soil microbial and structural recovery during grassland restoration. *Soil Biol. Biochem.* 42, 2182–2191. doi: 10.1016/j.soilbio.2010.08.014

Banerjee, S., Schlaeppi, K., and van der Heijden, M. G. A. (2018). Keystone taxa as drivers of microbiome structure and functioning. *Nat. Rev. Microbiol.* 16, 567–576. doi: 10.1038/s41579-018-0024-1

Bardgett, R. D., and Caruso, T. (2020). Soil microbial community responses to climate extremes: resistance, resilience and transitions to alternative states. *Philos. Trans. R. Soc. B Biol. Sci.* 375:20190112. doi: 10.1098/rstb.2019.0112

Barillot, C. D. C., Sarde, C. O., Bert, V., Tarnaud, E., and Cochet, N. (2013). A standardized method for the sampling of rhizosphere and rhizoplane soil bacteria associated to a herbaceous root system. *Ann. Microbiol.* 63, 471–476. doi: 10.1007/s13213-012-0491-y

Baubin, C., Farrell, A. M., Šťovíček, A., Ghazaryan, L., Giladi, I., and Gillor, O. (2021). The role of ecosystem engineers in shaping the diversity and function of arid soil bacterial communities. *Soil* 7, 611–637. doi: 10.5194/soil-7-611-2021

Blondel, V. D., Guillaume, J. L., Lambiotte, R., and Lefebvre, E. (2008). Fast unfolding of communities in large networks. *J. Stat. Mech. Theory Exp.* 2008:P10008. doi: 10.1088/1742-5468/2008/10/P10008

Bolger, A. M., Lohse, M., and Usadel, B. (2014). Trimmomatic: a flexible trimmer for Illumina sequence data. *Bioinformatics* 30, 2114–2120. doi: 10.1093/bioinformatics/btu170

Bolyen, E., Rideout, J. R., Dillon, M. R., Bokulich, N. A., Abnet, C. C., Al-Ghalith, G. A., et al. (2019). Reproducible, interactive, scalable and extensible microbiome data science using QIIME 2. *Nat. Biotechnol.* 37, 852–857. doi: 10.1038/s41587-019-0209-9

Bulska, E., and Wagner, B. (2016). Quantitative aspects of inductively coupled plasma mass spectrometry. *Philos. Trans. R. Soc. A Math. Phys. Eng. Sci.* 374:20150369. doi: 10.1098/rsta.2015.0369

Callahan, B. J., McMurdie, P. J., Rosen, M. J., Han, A. W., Johnson, A. J. A., and Holmes, S. P. (2016). DADA2: high-resolution sample inference from Illumina amplicon data. *Nat. Methods* 13, 581–583. doi: 10.1038/nmeth.3869

Cordero, I., Snell, H., and Bardgett, R. D. (2019). High throughput method for measuring urease activity in soil. *Soil Biol. Biochem.* 134, 72–77. doi: 10.1016/j.soilbio.2019.03.014

Cregut, M., Piutti, S., Slezack-deschaumes, S., and Benizri, E. (2013). Compartmentalization and regulation of arylsulfatase activities in *Streptomyces* sp., *Microbacterium* sp. and *Rhodococcus* sp. soil isolates in response to inorganic sulfate limitation. *Microbiol. Res.* 168, 12–21. doi: 10.1016/j.micres.2012.08.001

de Bruijn, F. J. (2015). "Biological Nitrogen Fixation" in *Principles of Plant-Microbe Interactions: Microbes for Sustainable Agriculture*. ed. B. Lugtenberg (Cham: Springer), 215–224. doi: 10.1007/978-3-319-08575-3

Delgado-Baquerizo, M. (2019). Obscure soil microbes and where to find them. *ISME J.* 13, 2120–2124. doi: 10.1038/s41396-019-0405-0

Diacono, M., and Montemurro, F. (2010). Long-term effects of organic amendments on soil fertility. *A review. Agron. Sustain. Dev.* 30, 401–422. doi: 10.1051/agro/2009040. hal-00886539

Edgmont, C. A., Herfort, L., Tebo, B. M., Delorenzo, S., Bra, S. L., and Zuber, P. (2012). Ubiquitous dissolved inorganic carbon assimilation by marine Bacteria in the Pacific northwest Coastal Ocean as determined by stable isotope probing. *PLoS One* 7:e46695. doi: 10.1371/journal.pone.0046695

Ezeokoli, O. T., Bezuidenhout, C. C., Maboeta, M. S., Khasa, D. P., and Adeleke, R. A. (2020). Structural and functional differentiation of bacterial communities in post-coal mining reclamation soils of South Africa: bioindicators of soil ecosystem restoration. *Sci. Rep.* 10, 1759–1714. doi: 10.1038/s41598-020-58576-5

Faust, K., and Raes, J. (2016). CoNet app: inference of biological association networks using Cytoscape [version 1; referees: 2 approved with reservations]. *F1000Research* 5, 1–17. doi: 10.12688/F1000RESEARCH.9050.1

Felipe-Lucia, M. R., Soliveres, S., Penone, C., Fischer, M., Ammer, C., Boch, S., et al. (2020). Land-use intensity alters networks between biodiversity, ecosystem functions, and services. *Proc. Natl. Acad. Sci. U. S. A.* 117, 28140–28149. doi: 10.1073/pnas.2016210117

Furtak, K., Grządziel, J., Gałązka, A., and Niedźwiecki, J. (2020). Prevalence of unclassified bacteria in the soil bacterial community from floodplain meadows (fluvisols) under simulated flood conditions revealed by a metataxonomic approachss. *Catena* 188:104448. doi: 10.1016/j.catena.2019.104448

Galili, T. (2015). Dendextend: An R package for visualizing, adjusting and comparing trees of hierarchical clustering data and text mining dendextend: An R package for visualizing, adjusting, and comparing trees of hierarchical clustering. *Bioinformatics* 31, 3718–3720. doi: 10.1093/bioinformatics/btv428

Garnica, S., Rosenstein, R., and Schön, M. E. (2020). Belowground fungal community diversity, composition and ecological functionality associated with winter wheat in conventional and organic agricultural systems. *PeerJ* 8:e9732. doi: 10.7717/peerj.9732

Ge, Y., He, J. Z., Zhu, Y. G., Zhang, J. B., Xu, Z., Zhang, L. M., et al. (2008). Differences in soil bacterial diversity: driven by contemporary disturbances or historical contingencies? *ISME J.* 2, 254–264. doi: 10.1038/ismej.2008.2

Glick, B. R. (2012). Plant growth-promoting Bacteria: Mechanisms and applications. *Scientifica (Cairo)* 2012, 1–15. doi: 10.6064/2012/963401

Gomez-Garzon, C., Hernandez-Santana, A., and Dussan, J. (2017). A genome-scale metabolic reconstruction of *Lysinibacillus sphaericus* unveils unexploited biotechnological potentials. *PLoS One* 12, e0179666–e0179621. doi: 10.1371/journal.pone.0179666

Gu, S., Hu, Q., Cheng, Y., Bai, L., Liu, Z., Xiao, W., et al. (2019). Application of organic fertilizer improves microbial community diversity and alters microbial network structure in tea (*Camellia sinensis*) plantation soils. *Soil Tillage Res.* 195:104356. doi: 10.1016/j.still.2019.104356

Guimera, R., and Amaral, L. A. N. (2005). Functional cartography of complex metabolic networks. *Lett. Nat.* 433, 895–900. doi: 10.1038/nature03286.1

Han, S. H., An, J. Y., Hwang, J., Kim, S., Bin, , and Park, B. B. (2016). The effects of organic manure and chemical fertilizer on the growth and nutrient concentrations of yellow poplar (*Liriodendron tulipifera* Lin.) in a nursery system. *For. Sci. Technol.* 12, 137–143. doi: 10.1080/21580103.2015.1135827

Hermans, S. M., Buckley, H. L., Case, B. S., Curran-cournane, F., and Taylor, M. (2017). Bacteria as emerging indicators of soil condition. *Appl. Environ. Microbiol.* 83, 1–13. doi: 10.1128/AEM.02826-16

Hernandez, D. J., David, A. S., Menges, E. S., Searcy, C. A., and Afkhami, M. E. (2021). Environmental stress destabilizes microbial networks. *ISME J.* 15, 1722–1734. doi: 10.1038/s41396-020-00882-x

Hernandez, T., Berlanga, J. G., Tormos, I., and Garcia, C. (2021). Organic versus inorganic fertilizers: Response of soil properties and crop yield. *AIMS Geosci.* 7, 415–439. doi: 10.3934/geosci.2021024

Hoch, J. M. K., Rhodes, M. E., Shek, K. L., Dinwiddie, D., Hiebert, T. C., Gill, A. S., et al. (2019). Soil microbial assemblages are linked to plant community composition and contribute to ecosystem services on urban green roofs. *Front. Ecol. Evol.* 7:198. doi: 10.3389/fevo.2019.00198

Hu, J., Lin, X., Wang, J., Dai, J., Chen, R., Zhang, J., et al. (2011). Microbial functional diversity, metabolic quotient, and invertase activity of a sandy loam soil as affected by long-term application of organic amendment and mineral fertilizer. *J. Soils Sediments* 11, 271–280. doi: 10.1007/s11368-010-0308-1

Huang, R., McGrath, S. P., Hirsch, P. R., Clark, I. M., Storkey, J., Wu, L., et al. (2019). Plant–microbe networks in soil are weakened by century-long use of inorganic fertilizers. *Microb. Biotechnol.* 12, 1464–1475. doi: 10.1111/1751-7915.13487

Ito, K., Takagi, K., Kataoka, R., Kiyota, H., and Iwasaki, A. (2019). Dissipation, dehalogenation, and denitration of chloroaromatic compounds by *Nocardioides* sp. strain PD653: Characterization of the substrate specificity. *J. Pestic Sci.* 44, 171–176. doi: 10.1584/jpestics.D19-024

Jaramillo, J. E. P., Mendes, R., and Raaijmakers, J. M. (2016). Impact of plant domestication on rhizosphere microbiome assembly and functions. *Plant Mol. Biol.* 90, 635–644. doi: 10.1007/s11103-015-0337-7

Kamaa, M., Mburu, H., Blanchart, E., Chibole, L., Chotte, J. L., Kibunja, C., et al. (2011). Effects of organic and inorganic fertilization on soil bacterial and fungal microbial diversity in the Kabete long-term trial. *Kenya Biol. Fertil. Soils* 47, 315–321. doi: 10.1007/s00374-011-0539-3

Kanehisa, M., Goto, S., Sato, Y., Furumichi, M., and Tanabe, M. (2012). KEGG for integration and interpretation of large-scale molecular data sets. *Nucleic Acids Res.* 40, D109–D114. doi: 10.1093/nar/gkr988

Klindworth, A., Pruesse, E., Schweer, T., Peplies, J., Quast, C., Horn, M., et al. (2013). Evaluation of general 16S ribosomal RNA gene PCR primers for classical and next-generation sequencing-based diversity studies. *Nucleic Acids Res.* 41, e1–e11. doi: 10.1093/nar/gks808

Koishi, A., Bragazza, L., Maltas, A., Guillaume, T., and Sinaj, S. (2020). Long-term effects of organic amendments on soil organic matter quantity and quality in conventional cropping systems in Switzerland. *Agronomy* 10:1977. doi: 10.3390/agronomy10121977

Kome, G. K., Enang, R. K., and Tabi, F. O. (2019). Influence of clay minerals on some soil fertility attributes: A review. *Open J. Soil Sci.* 9, 155–188. doi: 10.4236/ojss.2019.99010

Kulski, J. K. (2016). "Next-generation sequencing — An overview of the history, tools, and 'Omic' applications" in *Next generation sequencing-advances, applications and challenges*. ed. J. Buxeraud (INTECH), 1–60.

Li, H. B., Singh, R. K., Singh, P., Song, Q. Q., Xing, Y. X., Yang, L. T., et al. (2017). Genetic diversity of nitrogen-fixing and plant growth promoting Pseudomonas species isolated from sugarcane rhizosphere. *Front. Microbiol.* 8, 1–20. doi: 10.3389/fmicb.2017.01268

Li, M., Zhang, J., Wu, B., Zhou, Z., and Xu, Y. (2018). Identifying keystone species in the microbial community based on cross-sectional data. *Curr. Gene Ther.* 18, 296–306. doi: 10.2174/1566523218666181008155734

Lin, L., Xu, K., Shen, D., Chou, S. H., Gomelsky, M., and Qian, G. (2021). Antifungal weapons of Lysobacter, a mighty biocontrol agent. *Environ. Microbiol.* 23, 5704–5715. doi: 10.1111/1462-2920.15674

Ling, N., Wang, T., and Kuzyakov, Y. (2022). Rhizosphere bacteriome structure and functions. *Nat. Commun.* 13, 836–813. doi: 10.1038/s41467-022-28448-9

Liu, C., Cui, Y., Li, X., and Yao, M. (2021). Microeco: an R package for data mining in microbial community ecology. *FEMS Microbiol. Ecol.* 97:fiaa255. doi: 10.1093/femsec/fiaa255

Liu, G., and Hanlon, E. (2018). *Soil pH range for optimum commercial vegetable production*. Florida: University of Florida, Institute of Food and Agricultural Sciences.

Liu, X., Pang, L., Yue, Y., Li, H., Chatzisymeon, E., Lu, Y., et al. (2023). Insights into the shift of microbial community related to nitrogen cycle, especially N2O in vanadium-polluted soil. *Environ. Pollut.* 322:121253. doi: 10.1016/j.envpol.2023.121253

Liu, X., Wang, Q., Li, L., Sun, X., Lv, A., and Chen, C. (2020). Characterization of aerobic denitrification genome sequencing of *Vibrio parahaemolyticus* strain HA2 from recirculating mariculture system in China. *Aquaculture* 526:735295. doi: 10.1016/j.aquaculture.2020.735295

Lugtenberg, B. (Ed.) (2015). *Principles of plant-microbe interactions: Microbes for sustainable agriculture*. Cham: Springer.

Martínez-García, L. B., Korthals, G., Brussaard, L., Jørgensen, H. B., and De Deyn, G. B. (2018). Organic management and cover crop species steer soil microbial community structure and functionality along with soil organic matter properties. *Agric. Ecosyst. Environ.* 263, 7–17. doi: 10.1016/j.agee.2018.04.018

Macaskill, C. (2016). Agriculture in the provinces. Agri Handb. South Africa, Johannesbg. *SimplyPhi Inf.* Available at: https://agribook.co.za/introduction/agriculture-in-the-provinces/. (Accessed December 30, 2022).

Meena, A., and Rao, K. S. (2021). Assessment of soil microbial and enzyme activity in the rhizosphere zone under different land use/cover of a semiarid region. *India. Ecol. Process.* 10, 1–12. doi: 10.1186/s13717-021-00288-3

Mendes, R., Garbeva, P., and Raaijmakers, J. M. (2013). The rhizosphere microbiome: significance of plant beneficial, plant pathogenic, and human pathogenic microorganisms. *FEMS Microbiol. Rev.* 37, 634–663. doi: 10.1111/1574-6976.12028

Mendes, L. W., Palma, L., Braga, P., Acacio, A., De Souza, D. G., Silva, G. G. Z., et al. (2017). Using metagenomics to connect microbial community biodiversity and functions. *Curr. Issues Mol. Biol.* 24, 103–118. doi: 10.21775/cimb.024.103

Moore, J. A., Kimsey, M. J., Garrison-johnston, M., Shaw, T. M., Mika, P., and Poolakkal, J. (2022). Geologic soil parent material influence on Forest surface soil chemical characteristics in the inland northwest, USA. *Forests* 13, 1–13. doi: 10.3390/f13091363

Musyoka, M. W., Adamtey, N., Muriuki, A. W., and Cadisch, G. (2017). Effect of organic and conventional farming systems on nitrogen use efficiency of potato, maize and vegetables in the central highlands of Kenya. *Eur. J. Agron.* 86, 24–36. doi: 10.1016/j.eja.2017.02.005

Nan, J., Chao, L., Ma, X., Xu, D., Mo, L., Zhang, X., et al. (2020). Microbial diversity in the rhizosphere soils of three Stipa species from the eastern inner Mongolian grasslands. *Glob. Ecol. Conserv.* 22:e00992. doi: 10.1016/j.gecco.2020.e00992

Neina, D. (2019). The role of soil pH in plant nutrition and soil remediation. *Appl. Environ. Soil Sci.* 2019, 1–9. doi: 10.1155/2019/5794869

Nielsen, U. N., Wall, D. H., and Six, J. (2015). Soil biodiversity and the environment. *Soil Biodiver. Environ.* 40, 1–28. doi: 10.1146/annurev-environ-102014-021257

Pan, Z., Chen, Y., Zhou, M., McAllister, T. A., and Guan, L. L. (2021). Microbial interaction-driven community differences as revealed by network analysis. *Comput. Struct. Biotechnol. J.* 19, 6000–6008. doi: 10.1016/j.csbj.2021.10.035

Pan, C., Liu, C., Zhao, H., and Wang, Y. (2013). European journal of soil biology changes of soil physico-chemical properties and enzyme activities in relation to grassland salinization. *Eur. J. Soil Biol.* 55, 13–19. doi: 10.1016/j.ejsobi.2012.09.009

Peltoniemi, K., Velmala, S., Fritze, H., Lemola, R., and Pennanen, T. (2021). Long-term impacts of organic and conventional farming on the soil microbiome in boreal arable soil. *Eur. J. Soil Biol.* 104:103314. doi: 10.1016/j.ejsobi.2021.103314

Pittarello, M., Ferro, N. D., Chiarini, F., and Morari, F. (2021). Influence of tillage and crop rotations in organic and conventional farming systems on soil organic matter, bulk density and enzymatic activities in a short-term field experiment. *Agronomy* 11:724. doi: 10.3390/agronomy11040724

Quast, C., Pruesse, E., Yilmaz, P., Gerken, J., Schweer, T., Yarza, P., et al. (2013). The SILVA ribosomal RNA gene database project: Improved data processing and web-based tools. *Nucleic Acids Res.* 41, 590–596. doi: 10.1093/nar/gks1219

R Development Core Team (2018). *A language and environment for statistical computing* R Foundation for Statistical Computing, 2.

Rachwał, K., Gustaw, K., Kazimierczak, W., and Waśko, A. (2021). Is soil management system really important? Comparison of microbial community diversity and structure in soils managed under organic and conventional regimes with some view on soil properties. *PLoS One* 16, 1–22. doi: 10.1371/journal.pone.0256969

Raimi, A., Adeleke, R., and Roopnarain, A. (2017). Soil fertility challenges and Biofertiliser as a viable alternative for increasing smallholder farmer crop productivity in sub-Saharan Africa. *Cogent Food Agric.* 3, 1–26. doi: 10.1080/23311932.2017.1400933

Ramos, F. T., Dores, E. F. C., Weber, O. L. S., Beber, D. C., Campelo, J. H., and Maia, J. C. D. S. (2018). Soil organic matter doubles the cation exchange capacity of tropical soil under no-till farming in Brazil. *J. Sci. Food Agric.* 98, 3595–3602. doi: 10.1002/jsfa.8881

Rigane, H., Medhioub, K., Rebai, A., and Ammar, E. (2020). Effects of compost and manure application rate on the soil Physico-chemical layers properties and plant productivity. *Waste Biomass Valorizat.* 11, 1883–1894. doi: 10.1007/s12649-018-0543-z

Rivas, R., Trujillo, M. E., Mateos, P. F., Martínez-Molina, E., and Velázquez, E. (2004). *Agromyces ulmi* sp. nov., xylanolytic bacterium isolated from Ulmus nigra in Spain. *Int. J. Syst. Evol. Microbiol.* 54, 1987–1990. doi: 10.1099/ijs.0.63058-0

Rajkai, K., Tóth, B., Barna, G., Hernádi, H., Kocsis, M., Makó, A., et al. (2015). Particle-size and organic matter effects on structure and water retention of soils. *Biol.* 70, 1456–1461. doi: 10.1515/biolog-2015-0176

Rosen, C. J., and Eliason, R. (2005). *Nutrient Management for Commercial Fruit & vegetable crops in Minnesota*. Minnesota: University of Minnesota Extension Service.

Sánchez-Romero, J. J., and Olguin, L. F. (2015). Choline sulfatase from *Ensifer* (*Sinorhizobium*) *meliloti*: characterization of the unmodified enzyme. *Biochem. Biophys. Rep.* 3, 161–168. doi: 10.1016/j.bbrep.2015.08.002

Segata, N., Izard, J., Waldron, L., Gevers, D., Miropolsky, L., Garrett, W. S., et al. (2011). Metagenomic biomarker discovery and explanation. *Genome Biol.* 12:R60. doi: 10.1186/gb-2011-12-6-r60

Singh, T., and Singh, D. K. (2019). Rhizospheric Microbacterium sp. P27 showing potential of Lindane degradation and plant growth promoting traits. *Curr. Microbiol.* 76, 888–895. doi: 10.1007/s00284-019-01703-x

Siwik-Ziomek, A., Lemanowicz, J., and Koper, J. (2016). Arylsulphatase activity and sulphate content in relation to crop rotation and fertilization of soil. *Int. Agrophysics* 30, 359–367. doi: 10.1515/intag-2015-0098

Shahwar, D., Mushtaq, Z., Mushtaq, H., Alqarawi, A. A., Park, Y., Alshahrani, T. S., et al. (2023). Role of microbial inoculants as bio fertilizers for improving crop productivity: A review. *Heliyon* 9, e16134. doi: 10.1016/j.heliyon.2023.e16134

SSSSA (1990). *Handbook of standard soil testing methods for advisory purposes*. Pretoria: Soil Science Society of South Africa.

Thiel, V., Tank, M., and Bryant, D. A. (2018). Diversity of Chlorophototrophic Bacteria revealed in the omics era. *Annu. Rev. Plant Biol.* 69, 21–49. doi: 10.1146/annurev-arplant-042817-040500

Tomašić, M., Žgorelec, Ţ., Jurišić, A., Kisić, I., Hernandez, T., Berlanga, J. G., et al. (2021). Cation exchange capacity of dominant soil types in the Republic of Croatia. *PLoS One* 16, 1–22. doi: 10.5513/JCEA01/14.3.1286

Ullah, S., Ai, C., Huang, S., Zhang, J., Jia, L., and Ma, J. (2019). The responses of extracellular enzyme activities and microbial community composition under nitrogen addition in an upland soil. *PLoS One* 14:e0223026. doi: 10.1371/journal.pone.0223026

van Wyk, D. A. B., Adeleke, R., Rhode, O. H. J., Bezuidenhout, C. C., and Mienie, C. (2017). Ecological guild and enzyme activities of rhizosphere soil microbial communities associated with Bt-maize cultivation under field conditions in north West Province of South Africa. *J. Basic Microbiol.* 57, 781–792. doi: 10.1002/jobm.201700043

Vignesh, M., Shankar, S. R. M., Mubarak Ali, D., and Hari, B. N. V. (2021). A novel Rhizospheric bacterium: *Bacillus velezensis* NKMV-3 as a biocontrol agent against Alternaria leaf blight in tomato. *Appl. Biochem. Biotechnol.* 194, 1–17. doi: 10.1007/s12010-021-03684-9

Warncke, D., Dahl, J., Jacobs, L., and Laboski, C. (2009). Nutrient Recommendations for 971 Field Crops in Michigan. *Michigan State University Extension Bulletin.* E2904, 1–32.

Weather and Climate (2023). *Climate zone and Historcal climate data*.

Wemheuer, F., Taylor, J. A., Daniel, R., Johnston, E., Meinicke, P., and Thomas, T. (2020). Tax4Fun2: Prediction of habitat-specific functional profiles and functional redundancy based on 16S rRNA gene sequences. *Environ. Microb.* 15, 1–12. doi: 10.1186/s40793-020-00358-7

Wemheuer, F., Taylor, J. A., Daniel, R., Johnston, E., Meinicke, P., Thomas, T., et al. (2018). Tax4Fun2: a R-based tool for the rapid prediction of habitat-specific functional profiles and functional redundancy based on 16S rRNA gene marker gene sequences. *bio Rxiv*. doi: 10.1101/490037

Willms, I. M., Rudolph, A. Y., Göschel, I., Bolz, S. H., Schneider, D., Penone, C., et al. (2020). Globally abundant "Candidatus Udaeobacter" benefits from release of antibiotics in soil and potentially performs trace gas scavenging. *mSphere* 5, 1–17. doi: 10.1128/msphere.00186-20

Xu, A., Li, L., Xie, J., Zhang, R., Luo, Z., Cai, L., et al. (2022). Bacterial diversity and potential functions in response to Long-term nitrogen fertilizer on the semiarid loess plateau. *Microorganisms* 10, 1–18. doi: 10.3390/microorganisms10081579

Xue, C., Ryan Penton, C., Zhu, C., Chen, H., Duan, Y., Peng, C., et al. (2018). Alterations in soil fungal community composition and network assemblage structure by different long-term fertilization regimes are correlated to the soil ionome. *Biol. Fertil. Soils* 54, 95–106. doi: 10.1007/s00374-017-1241-x

Yan, Y., Li, B., Huang, Z., Zhang, H., Wu, X., Farooq, T. H., et al. (2021). Characteristics and driving factors of rhizosphere bacterial communities of Chinese fir provenances. *Forests* 12:1362. doi: 10.3390/f12101362

Yang, F., Chen, Q., Zhang, Q., Long, C., Jia, W., and Cheng, X. (2021). Keystone species affect the relationship between soil microbial diversity and ecosystem function under land use change in subtropical China. *Funct. Ecol.* 35, 1159–1170. doi: 10.1111/1365-2435.13769

Zang, X., Liu, M., Fan, Y., Xu, J., Xu, X., and Li, H. (2018). The structural and functional contributions of β-glucosidase-producing microbial communities to cellulose degradation in composting. *Biotechnol. Biofuels* 11, 51–13. doi: 10.1186/s13068-018-1045-8

Zhang, Q., Zhao, W., Zhou, Z., Huang, G., Wang, X., Han, Q., et al. (2022). The application of mixed organic and inorganic fertilizers drives soil nutrient and bacterial community changes in teak plantations. *Microorganisms* 10:958. doi: 10.3390/microorganisms10050958

frontiers | Frontiers in Microbiology

TYPE Original Research
PUBLISHED 19 October 2023
DOI 10.3389/fmicb.2023.1285574

OPEN ACCESS

EDITED BY
Muhammad Zahid Mumtaz,
The University of Lahore, Pakistan

REVIEWED BY
M. Murali,
University of Mysore, India
Muhammad Atif Muneer,
Fujian Agriculture and Forestry University, China
Shaikhul Islam,
Bangladesh Agricultural Research Council, Bangladesh

*CORRESPONDENCE
Bong Soo Park
✉ bongsoo@tll.org.sg

RECEIVED 30 August 2023
ACCEPTED 28 September 2023
PUBLISHED 19 October 2023

CITATION
Suraby EJ, Agisha VN, Dhandapani S, Sng YH, Lim SH, Naqvi NI, Sarojam R, Yin Z and Park BS (2023) Plant growth promotion under phosphate deficiency and improved phosphate acquisition by new fungal strain, *Penicillium olsonii* TLL1.
Front. Microbiol. 14:1285574.
doi: 10.3389/fmicb.2023.1285574

Plant growth promotion under phosphate deficiency and improved phosphate acquisition by new fungal strain, *Penicillium olsonii* TLL1

Erinjery Jose Suraby[1], Valiya Nadakkakath Agisha[1], Savitha Dhandapani[1], Yee Hwui Sng[1], Shi Hui Lim[1], Naweed I. Naqvi[1,2], Rajani Sarojam[1], Zhongchao Yin[1,2] and Bong Soo Park[1]*

[1]Temasek Life Sciences Laboratory, National University of Singapore, Singapore, Singapore, [2]Department of Biological Sciences, National University of Singapore, Singapore, Singapore

Microbiomes in soil ecosystems play a significant role in solubilizing insoluble inorganic and organic phosphate sources with low availability and mobility in the soil. They transfer the phosphate ion to plants, thereby promoting plant growth. In this study, we isolated an unidentified fungal strain, POT1 (*Penicillium olsonii* TLL1) from indoor dust samples, and confirmed its ability to promote root growth, especially under phosphate deficiency, as well as solubilizing activity for insoluble phosphates such as $AlPO_4$, $FePO_4{\cdot}4H_2O$, $Ca_3(PO_4)_2$, and hydroxyapatite. Indeed, in vermiculite containing low and insoluble phosphate, the shoot fresh weight of Arabidopsis and leafy vegetables increased by 2-fold and 3-fold, respectively, with POT1 inoculation. We also conducted tests on crops in Singapore's local soil, which contains highly insoluble phosphate. We confirmed that with POT1, Bok Choy showed a 2-fold increase in shoot fresh weight, and Rice displayed a 2-fold increase in grain yield. Furthermore, we demonstrated that plant growth promotion and phosphate solubilizing activity of POT1 were more effective than those of four different *Penicillium* strains such as *Penicillium bilaiae*, *Penicillium chrysogenum*, *Penicillium janthinellum*, and *Penicillium simplicissimum* under phosphate-limiting conditions. Our findings uncover a new fungal strain, provide a better understanding of symbiotic plant-fungal interactions, and suggest the potential use of POT1 as a biofertilizer to improve phosphate uptake and use efficiency in phosphate-limiting conditions.

KEYWORDS

biofertilizer, *Penicillium olsonii* TLL1, phosphate deficiency stress, phosphate solubilizing fungus, plant growth promotion

1. Introduction

The availability of macro- and micronutrients plays a pivotal role in the growth and development of plants. Among the macronutrients, phosphorus is an essential element involved in metabolic processes and signal transduction pathways in plants (Nesme et al., 2018). Phosphate limitation is a major nutritional constraint as it affects plant growth development and

compromises optimal yields. Phosphate deficiency in agriculture has often been addressed by applying phosphate fertilizers, but the phosphate use efficiency in plants is only 5%–25% due to the rapid fixation into insoluble forms (Schnug and Haneklaus, 2016). Moreover, the over-application has led to loss of soil fertility and associated environmental hazards (Sharma et al., 2013).

Plants respond to phosphate limitation through various physiological, morphological, and biochemical strategies. One of the acclimatization responses is the root morphology change to acquire available phosphate. The plant root morphology is remodeled by inhibiting primary root elongation and enhancing the formation of lateral roots and root hairs, which increases the effective surface area (Peret et al., 2014).

In Arabidopsis, the transcription factor STOP1 (SENSITIVE TO PROTON RHIZOTOXICITY 1) regulates citrate and malate exudation by activating the expression of its downstream genes, *MATE and ALMT1* efflux transporters, respectively, which are important for Al tolerance (Sawaki et al., 2009). In addition, RAE1 functions as an E3 ligase ubiquitinating *STOP1* and controls the expression of STOP1-regulated *AtALMT1* in Al resistance and low Pi response (Zhang et al., 2019). The inhibition of primary root elongation under phosphate stress is often linked to iron accumulation in the root apical meristem (Ward et al., 2008) which is mediated by two genes in Arabidopsis, *LPR1* (Low Phosphate Root 1) encoding multicopper oxidase with ferroxidase activity and *PDR2* (Phosphate Deficiency Response 2) encoding single P-type ATPase (Ticconi et al., 2004; Svistoonoff et al., 2007). The interaction of LPR1-PDR2 results in the accumulation of iron in the root apical meristem (RAM) and elongation zone (EZ) leading to callose deposition at the cell walls of RAM and EZ. Callose deposition impairs the expression of the transcription factor, *SHR* (Short Root), which is required for root patterning (Petricka et al., 2012). This results in blocked cell-to-cell communication and reduced RAM activity (Muller et al., 2015). Phosphate-deficiency stress also promotes the accumulation of reactive oxygen species (ROS) and peroxidase in the cell walls of the root apical meristem (RAM) and elongation zone (EZ) in Arabidopsis plants. Peroxidase activity crosslinks cell wall components, which leads to cell wall stiffening, eventually reducing root cell expansion (Balzergue et al., 2017). Phosphate deprivation also leads to higher levels of nitric oxide (NO) in the roots (Wang et al., 2010; Royo et al., 2015). NO acts as a signal molecule that mediates multiple responses, including reduction of primary roots (Wu et al., 2014), development of lateral roots (Correa-Aragunde et al., 2004), growth of root hair (Lombardo et al., 2006), and reutilization of phosphate in the cell wall (Zhu et al., 2017) in phosphate deficiency in plants.

Phosphate-solubilizing microorganisms (PSM) help in phosphate assimilation from both organic and inorganic forms of phosphates in soil, making it available for plant uptake. Soluble phosphate acquisition by PSM is attributed to several mechanisms such as chelation and ion exchange processes, production of organic acids, secretion of microbial-derived enzymes such as acid phosphatases and phytases, and production of phytohormones (Bergkemper et al., 2016). Although PSM includes both fungi and bacteria, the phosphate-solubilizing activity of fungi is comparatively higher than that of bacteria (Khan et al., 2010). Mycorrhizal associations with the plant roots are the best-characterized beneficial interactions that help to mobilize soil nutrients and improve plant growth. However, endophytic fungi are the major contributors to phosphate solubilization in the Brassicaceae family as mycorrhizal associations are rare (Bonfante and Genre, 2010). Most of the phosphate-solubilizing fungi (PSF) have been reported in the genera *Penicillium* (Li et al., 2016), *Aspergillus* (Yin et al., 2015), and *Trichoderma* (Lei and Zhang, 2015) and have been utilized as microbial inoculants in a variety of crops for improved phosphate uptake, and thereby increased biomass and yield. For example, *Penicillium oxalicum* and *Aspergillus niger* increase the bioavailability of phosphate and promote maize growth in calcareous soil (Yin et al., 2015). *Penicillium guanacastense* was reported as a potent biological fertilizer as it enhances the growth of *Pinus massoniana* under phosphate-limiting conditions (Qiao et al., 2019). Though PSF from soil has been widely investigated, the phosphate solubilizing activity of airborne fungi is less explored. Recently, *Aspergillus hydei* sp. nov. was reported to be the first phosphate-solubilizing fungus reported in the air (Doilom et al., 2020). Efficient PSF is a promising eco-friendly strategy to improve phosphate uptake and promote plant growth in modern agriculture. Nevertheless, it remains unclear how symbiotic fungi control the growth condition and regulate gene expression of their host plants under phosphate limitation.

In this study, we identify a new airborne fungal strain *P. olsonii* TLL1 (POT1) and investigate gene regulation for root growth, especially under limited phosphate availability such as phosphate deficiency and insoluble phosphate conditions in the soil, testing its phosphate solubilizing capability by fungus-plant interaction. Furthermore, we show that POT1 as a biofertilizer functions in mono/dicot plants and propose that it can be applied effectively in phosphate-limiting soils in both upland and paddy environments.

2. Materials and methods

2.1. PSF strain and plant materials

PSF was isolated from indoor dust samples and monocultured on Pikovskaya agar containing 0.5% tricalcium phosphate (CaP), pH 6.8–7.2, by incubating at 25°C for 7 days.

For seedling growth, *Arabidopsis* WT (Col-0), Bok Choy (*Brassica rapa subsp. chinensis*), and Rice (Temasek Rice) seeds were germinated on media containing Murashige and Skoog salts, 0.25 mM MES, 10 g/L sucrose, and 0.8% agar.

2.2. Identification and genotyping of PSF strain

Total genomic DNA was extracted from the PSF strain using the CTAB method (Edel et al., 2001). One hundred nanograms of genomic DNA of the PSF strain were used to amplify five genetic loci such as internal transcribed spacer (*ITS*), translation elongation factor-1-α (*TEF1*α), small ribosomal subunit (*SSU*), large ribosomal subunit (*LSU*), and Mini-chromosome maintenance protein (*MCM7*) using Hi-fidelity Phusion DNA polymerase (White et al., 1990; Schmitt et al., 2009; Raja et al., 2011, 2017; Stielow et al., 2015). The genotyping was performed with primers in Supplementary Table S1. The PCR reaction profile consisted of initial denaturation at 98°C for 3 min, followed by 35 cycles of 98°C for 10 s, 55°C–68°C for 30 s, and 72°C for 1 min and a final extension of 72°C for 5 min. The sequences

of PCR amplicons were determined using Sanger's Sequencing, and the contigs were assembled using the Bioedit tool and were analyzed by BLAST searches at NCBI.

A phylogenetic tree was constructed using MEGA v. 7.0 separately for each genetic locus. The maximum-likelihood (ML) algorithm and Tamura Nei model were applied, with 1,000 bootstrap replications. Reference sequences of the genes from the genus *Penicillium* were also used for alignment. The final tree was presented with a bootstrap cutoff level above 65% (Visagie et al., 2014).

2.3. Colony morphology and microscopy analysis

The colony morphology of POT1 was studied by culturing it on PDA and MEA plates at 28 ± 2°C for 7 days. The colonization of POT1 was analyzed under full P conditions using co-staining with Wheat Germ Agglutinin-Alexa Fluor 488 conjugate (WGA-AF488) and propidium iodide (PI) as per the protocol mentioned in Redkar et al. (2018). Confocal analysis was performed using a TCS SP8 confocal laser scanning microscope (Leica, Germany). The excitation wavelength and detection wavelength for WGA-AF488 were 488 nm and 500–540 nm, respectively. For PI staining, the excitation wavelength and detection wavelength were 561 nm and 580–630 nm, respectively.

2.4. Bioassay for assessment of plant growth promoting potential

In vitro growth test of the Arabidopsis ecotype Col-0 was assessed in modified Hoagland's solution under full P, low P, and -P conditions with 0.50 mM, 0.01 mM, and 0 mM of KH_2PO_4 (pH 5.6), respectively (Millner and Kitt, 1992). Four-days-old Arabidopsis seedlings were transferred to the test media precultured with 100 µL of POT1 conidial spore suspension (10^8 spores/mL). The root length of the seedlings was estimated after 10 days using ImageJ software.[1] Other growth parameters such as shoot and root fresh weight were also determined.

The total phosphorus content in the shoot was measured by digesting 45 mg of the leaf or root tissue in 1 mL of 3:1 HNO_3/HCl in a microwave oven at 240°C for 15 min, and after digestion, it was diluted 10 times with water. The phosphorus content was determined using Agilent 720 Inductively Coupled Plasma-Optical Emission Spectrometry (ICP-OES; Agilent, United States).

2.5. Quantitative RT-PCR

The total RNA was isolated from shoots and roots of Arabidopsis plants grown in full P and low P conditions both with and without POT1 using FavorPrep™ plant total RNA mini kit (Favorgen, Taiwan). Subsequently, cDNAs were synthesized from 1 µg of total RNA samples using the iScript cDNA synthesis kit (Bio-Rad, United States). Quantitative real-time RT-PCR was then performed using the CFX96 Real-Time system (Bio-Rad, United States). Each reaction had a total volume of 20 µL, comprising 10 ng of template, 10 µL of SsoAdvanced Universal SYBR Green Supermix (Bio-Rad, United States), and 0.5 µM of each primer. The amplification conditions were set as follows: initial denaturation at 95°C for 30 s, followed by 40 cycles of denaturation at 95°C for 5 s, and annealing at 60°C for 30 s. The expression of *RAE1, STOP1, ALMT1*, and *MATE1* were analyzed with primers in Supplementary Table S2. Actin was used as the reference gene, and the gene expression level was analyzed by Genex Program (Bio-Rad, United States). The relative expression levels of each gene were normalized to their expression levels under full P conditions without POT1.

2.6. Determination of STOP1 protein levels in plants after POT1 inoculation

Full-length CDS of the *STOP1* gene was amplified from Arabidopsis cDNA using STOP1F: CACCATGGAAACTGAAGACGATTTGTGCAA and STOP1R: GAGACTAGTATCTGAAACAGACTCACCAAC and cloned in pENTR/D vector (Invitrogen, United States) and then transferred to pBCo-DC-3HA plant expression vector by Gateway cloning (Invitrogen, United States) using LR clonase enzyme II (Invitrogen, United States) to generate 35S: STOP1-3HA construct. The construct was then introduced into the Arabidopsis ecotype Columbia-0 (Col-0) through *Agrobacterium*-mediated floral dipping (Zhang et al., 2006). To detect STOP1 accumulation in plants, transgenic Arabidopsis seedlings harboring 35S: STOP1-3HA transgenes were grown in full P and -P conditions both with and without POT1 at pH 5.6 for 10 days. The plants (100 mg) were flash-frozen in liquid nitrogen and homogenized with 500 µL IP lysis buffer containing 1X complete protease inhibitor tablets (Roche, Germany). The total protein contents were separated on a 10% SDS-PAGE and STOP1-3HA proteins were analyzed by standard immunoblot using anti-HA antibody. Protein bands on the membrane were captured using the ChemiDoc Touch Imaging system (Bio-Rad, United States).

2.7. Determination of callose and NO

The roots excised from Arabidopsis plants grown under full P and low P conditions for 10 days were incubated for 2 h in 150 mM K_2HPO_4 and 0.01% aniline blue in the dark (Schenk and Schikora, 2015). Callose depositions were analyzed with an FV3000 confocal laser scanning microscope (Olympus, Japan) using a DAPI filter (excitation 370 nm and emission 509 nm).

For NO determination, the roots were treated with 10 µM DAF-FM DA (3-amino, 4-aminomethyl-2′, 7′-difluorescein diacetate) for 15 min, and samples were washed with HEPES buffer (pH 4.0) for 10 min (Lombardo and Lamattina, 2012). The fluorescence (excitation 495 nm and emission 515 nm) was observed using an FV3000 confocal laser scanning microscope (Olympus, Japan).

2.8. Analysis of insoluble phosphate-solubilizing activity of POT1

POT1 was cultured on Pikovskaya agar and NBRIP containing tricalcium phosphate (CaP), with a pH of 6.8–7.2. The colony diameter

1 https://imagej.nih.gov/ij/download/

(*D*) and the diameter of the circular zone of solubilized phosphorus (*d*) were determined, and the *d*/*D* ratio was calculated to find the phosphate-solubilizing rate.

For determination of soluble P concentration in broth, POT1 was cultured on Prune agar medium (40 mL/L prune juice, 1 g/L yeast extract, 2.5 g/L lactose, 2.5 g/L sucrose, 20 g/L agar, and pH 6.5) for 2 days in the dark and 3 days in the light for sporulation. The conidial spore suspension (10^8 spores/mL) was inoculated into 100 mL of modified Pikovskaya broth containing 1 g/L of sparingly soluble inorganic phosphates such as tricalcium phosphate (pH 7.0), iron phosphate (pH 2.5), aluminum phosphate (pH 4.0), and hydroxyapatite (pH 7.0) and incubated at 25°C and 120 rpm for 14 days. Uninoculated media with different P sources were also kept as controls. The cultures were centrifuged at 5000 rpm for 15 min, and the supernatant was filtered with a 0.22 µm syringe filter. The soluble phosphorus content was determined using phosphomolybdenum spectrophotometry.

2.9. Analysis of organic acids secreted by POT1

Cultures of POT1, grown under full P and low P were filtered using 0.22 µm filter, and 10 µL of the samples were analyzed on a Liquid Chromatography-Q Exactive Orbitrap Mass Spectrometer system (Thermo Fisher Scientific, United States). The multi-sampler was set to a 4°C temperature, and LC-separation was carried out using an Accucore C18 column (2.1 mm × 30 mm, 2.6 µm) at 22°C under a flow rate of 300 µL/min. The mobile phases for the reversed-phase (RP)-LC were solution A, 0.2% v/v formic acid in water; and solution B, 0.2% formic acid in 100% methanol. The MS was run in the negative mode for parallel reaction monitoring (PRM) using the ions listed in Supplementary Table S3. Calibration stock solutions were prepared and stored at −80°C, and in each batch, six-point calibration curves were generated with freshly prepared dilutions.

2.10. Analysis of plant growth by POT1 under insoluble phosphate conditions

For the soil test, vermiculite was used as nutrient-free soil for studying plant growth under insoluble phosphate conditions. It was washed three times with deionized water to remove any soluble P and air-dried at room temperature. To test plant growth by P solubilizing activity, POT1 mycelia (0.5 g) resuspended in 50 mL of sterile distilled water was inoculated into the vermiculite for 7 days prior to the transfer of the seedlings. To test plant growth by P solubilizing activity, POT1 mycelia (0.5 g) were drenched in vermiculite for 7 days prior to the transfer of the seedlings. Seven-days-old seedlings of Arabidopsis and Bok Choy were transferred to vermiculite and subjected to different phosphate sources.

The plants were irrigated twice a week with Hoagland's that contained full P (0.5 mM KH_2PO_4), low P (0.01 mM KH_2PO_4), -P (0 mM KH_2PO_4), tricalcium phosphate (0.5 mM CaP), aluminum phosphate (0.5 mM AlP), iron phosphate (0.5 mM FeP), and hydroxyapatite (0.5 mM HA) and were grown at 22°C (Arabidopsis) and 25°C (Bok Choy) under 75% relative humidity. Growth index parameters such as shoot fresh weight, leaf area index, number of leaves, and shoot P content were analyzed.

The anthocyanin content in leaves of Arabidopsis plants was determined following the protocol by Laby et al. (2000). Leaves of 14 days-old plants, both those co-cultivated with or without POT1, were divided into three distinct groups (leaves 1–4, 5–8, and 9–12). The leaves were extracted with 99:1 methanol: HCl (v/v) overnight at 4°C. The anthocyanin contents were determined by acquiring OD at 530 and 657 nm and were calculated using the formula: OD530-(0.25 × OD657) × extraction volume (mL) × 1/weight of the tissue.

2.11. Effect of POT1 under local soil conditions

The growth test of Bok Choy and Temasek Rice was conducted in soil collected from Lim Chu Kang, Singapore (N 1° 26′ 7.3284″, E 103° 42′ 48.456″). Before conducting the tests, a soil nutrient analysis was performed to determine the available nutrients in Lim Chu Kang soil and commercial soil used for the cultivation of Bok Choy and Rice. One kilogram of commercial and Lim Chu Kang soils was analyzed for nitrogen, phosphorus, potassium, calcium, magnesium, sodium, copper, manganese, zinc, and boron using Mehlich 3 extraction (Mehlich, 1984) followed by Agilent 720 Inductively Coupled Plasma-Optical Emission Spectrometry (ICP-OES; Agilent, United States) analysis. Ten grams of soil was mixed with 20 mL of sterile distilled water on a magnetic stirrer for 1 h, and the pH of the soil mixture was recorded using a pH meter.

For the growth test, POT1 mycelia (0.5 g per pot) and heat-killed POT1 were incorporated into Lim Chu Kang soil a week before transferring the Bok Choy and Rice seedlings. These plants were grown under greenhouse conditions, and the corresponding growth index parameters were subsequently examined.

2.12. Comparison of POT1 with other *Penicillium* species

The insoluble phosphate solubilizing activity of POT1 was analyzed with other *Penicillium* strains such as *P. bilaiae* (ATCC 20851), *P. chrysogenum* (NBRC 4626), *P. janthinellum* (NBRC 31133), and *P. simplicissimum* (NBRC 106922) in CaP-amended modified Pikovskaya broth. The phosphate solubilizing rate was determined using the following formula [(soluble phosphorus concentration of treatment-soluble phosphorus concentration of control)/inorganic phosphorus concentration of each experimental group × 100] described by Qiao et al. (2019). *An in vitro* growth test was carried out to compare the effect of POT1 with other *Penicillium* strains under -P conditions.

Additionally, vermiculite soil experiments were undertaken to further assess the ability of POT1 to solubilize CaP in comparison with other strains of *Penicillium*. Vermiculite was conditioned with 0.5 g of fungal mycelia for 7 days before transplanting Arabidopsis seedlings. The plants were then watered bi-weekly with a Hoagland's solution in which tricalcium phosphate served as the exclusive phosphorus source. Cultivated at a temperature of 22°C, growth metrics were analyzed to evaluate the effectiveness of the different strains in phosphate solubilization.

2.13. Statistical analysis

Statistical analysis was performed using GraphPad Prism software version 9.5 for Windows (GraphPad Software, United States). The data from replicate observations were analyzed using student's *t*-test, and significant differences among treatments were determined at $p < 0.05$ based on an unpaired two-tailed *t*-test.

3. Results

3.1. Identification and genotyping of POT1

The phylogenetic relationships between POT1 and the related fungal strains in maximum-likelihood trees were generated using five barcode markers such as *ITS*, *TEF1α*, *SSU*, *LSU*, and *MCM7*. The *ITS* sequence of POT1 clustered with two other strains of *P. olsonii* (bootstrap = 82) (Figure 1A; Supplementary Figure S1). The *TEF1α* sequences of POT1 clustered with five other strains of *P. olsonii* with a bootstrap value of 87 (Supplementary Figure S2). The *SSU* and *LSU* sequences of *P. olsonii* were also grouped with other strains of *P. olsonii* with bootstrap values of 97 and 99, respectively (Supplementary Figures S3, S4). The same or closely related *Penicillium* species were clustered as a clade on the resulting phylogenetic tree, while the out-group cluster of *Aspergillus* sp. formed non-similarity clusters. Except for *MCM7* (Supplementary Figure S5), all the sequences of the DNA barcode markers of the POT1 strain grouped with *P. olsonii* sequences, and the strain was ascertained as *P. olsonii*.

The colony morphology of POT1 was recorded after 7 days of growth on MEA and PDA (Figure 1B). When we stained the Arabidopsis roots co-cultivated with POT1 using WGA-AF488 and PI, the POT1 fungal hyphae appeared green and the plant root cell walls appeared red (Supplementary Figure S6). The co-staining revealed that POT1 colonized the surface of the roots without any penetration into the root cortical cells.

3.2. Plant root growth promotion by POT1 under P-sufficient and deficient conditions

We conducted experiments to assess the growth promotion of Arabidopsis mediated by *P. olsonii* TLL1 (POT1) under both P-sufficient and P-deficient media conditions (Supplementary Figure S7). Under P-sufficient conditions, Arabidopsis plants inoculated with POT1 exhibited 1.2-fold longer primary roots (Figures 1C,D), but there was no significant increase in shoot fresh weight, root fresh weight, or shoot P content compared to uninoculated plants (Figures 1E–G). Under P-deficient conditions, POT1-inoculated plants showed 2-fold longer primary root length (Figures 1H,I), and their shoot and root fresh weights significantly increased by 1.5- and 2-fold (Figures 1J,K), respectively, compared with uninoculated plants (Supplementary Table S4). Additionally, we tested the growth of Arabidopsis by POT1 inoculation under no P condition (Supplementary Figure S8A). Despite the absence of a phosphate source in the medium, the co-cultivated plants with POT1 showed 2-fold longer primary roots and 2-fold increased root fresh weight, whereas there was no difference in shoot fresh weight between inoculated and non-inoculated plants (Supplementary Figures S8B–D and Supplementary Table S5). The shoot phosphate content in plants inoculated with POT1 under no P conditions increased 1.5-fold compared to uninoculated plants (Supplementary Figure S8E).

3.3. Altered ALMT1 expression by POT1

To identify the role of *RAE1*, *STOP1*, *ALMT1*, and *MATE1* in promoting Arabidopsis growth by POT1, we quantified their relative expression in shoots and roots using qPCR (Figure 2 and Supplementary Table S6). Our results showed that the expression level of *RAE1*, *STOP1*, and *MATE1* showed no significant changes in response to phosphate sufficiency or deficiency in either shoots or roots (Figures 2A,B,D–F,H). However, the expression of *ALMT1* was increased under phosphate-deficient conditions in the root. Consistent with the root phenotype in Arabidopsis, *ALMT1* expression was decreased upon POT1 inoculation (Figure 2C). Under the phosphate-sufficient condition, *ALMT1* expression was significantly decreased in the shoots upon POT1 inoculation (Figure 2G).

3.4. STOP1 protein was unstable when co-cultivated with POT1

The interaction between POT1 and STOP1 protein under full P and low P conditions was demonstrated in the transgenic Arabidopsis plant. The STOP1 protein was found to be degraded by POT1 under both phosphate-sufficient and deficient conditions (Figure 3A). Under phosphate-deficient conditions, POT1 induced a greater decrease in STOP1 protein levels compared to phosphate-sufficient conditions.

3.5. Inhibition of callose deposition and NO accumulation by POT1

To confirm that POT1 inhibits the negative components of root growth, we investigated its effect on callose deposition and nitric oxide (NO) accumulation under phosphate-sufficient and deficient conditions. Under phosphate deficiency, POT1-inoculated plants showed decreased callose deposition in the root apical meristem compared to the massive callose formation observed in uninoculated plants (Figure 3B). However, under phosphate-sufficient conditions, no difference in callose deposition was observed in plants with or without POT1. The capability of POT1 to inhibit endogenous NO accumulation in roots was tested using the fluorescent probe DAF-FM DA. Green fluorescence was clearly observed under phosphate-deficient conditions, indicating phosphate-dependent NO production. In contrast, after inoculating POT1, the NO level in the root decreased, suggesting the involvement of POT1 in root development under phosphate deficiency (Figure 3C).

3.6. Quantitative assay for phosphate-solubilizing activity of POT1

When POT1 was grown on PVK and NBRIP media amended with $Ca_3(PO_4)_2$ for 7 days at 25°C, visible halo zones of dissolved phosphorus were observed, indicating recalcitrant phosphate

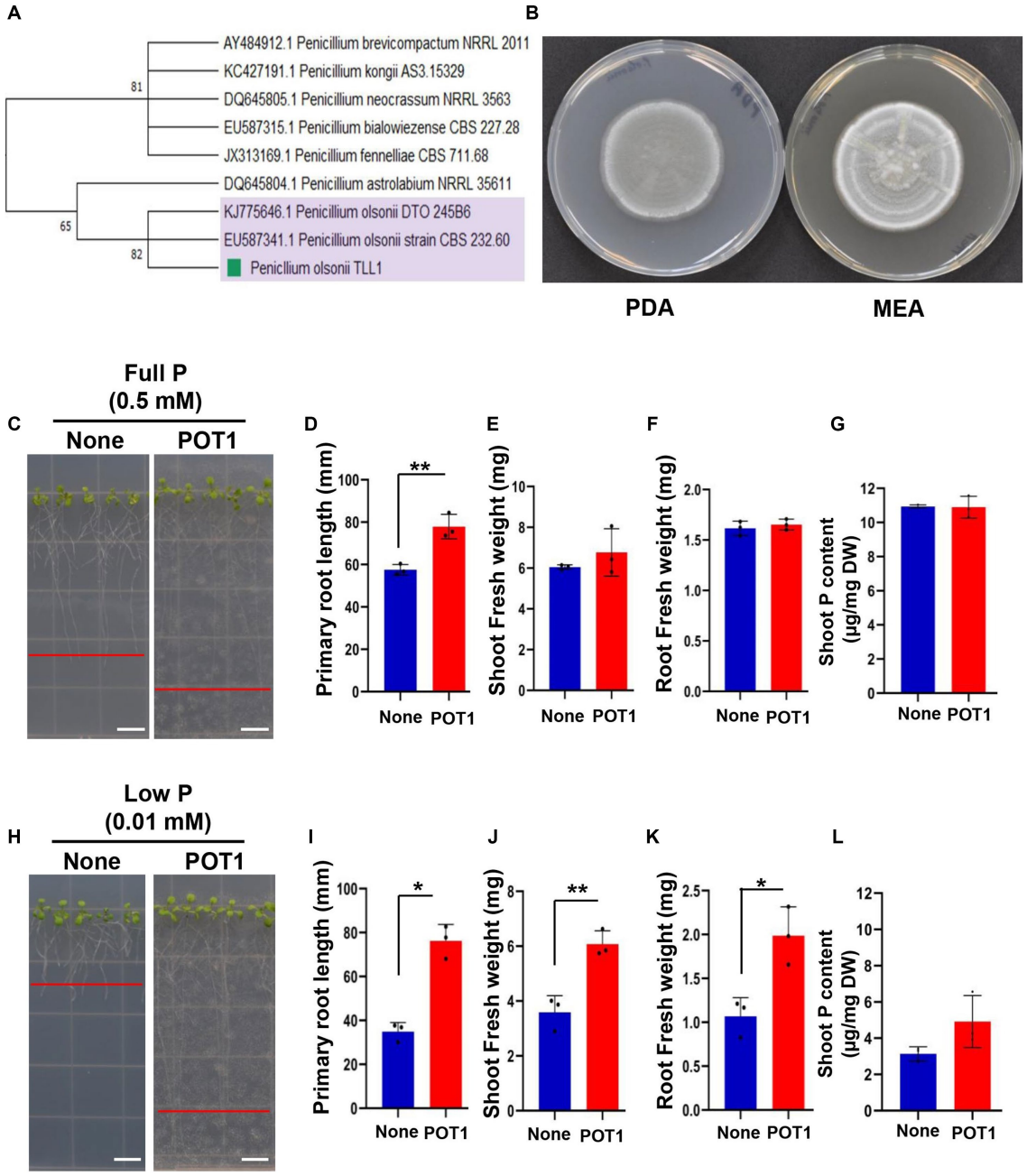

FIGURE 1
Identification of the phosphate-solubilizing fungus *Penicillium olsonii* TLL1 (POT1) and growth promotion of Arabidopsis by POT1 under P-sufficient and P-limiting conditions. **(A)** Phylogenetic tree generated from maximum likelihood (ML) analysis of POT1 based on *ITS* sequence data. Bootstrap values on 1,000 replications are shown at the nodes of the tree. **(B)** Colony morphology of POT1 cultured on (left) PDA and (right) MEA for 7 days. The scale bar represents 1 cm. **(C)** Arabidopsis plants grown in full P conditions both with and without POT1. Four-days-old plants were transferred to full P media pre-cultured with and without POT1 under *in vitro* conditions for 10 days. The scale bar represents 1 cm. The bar diagrams show **(D)** primary root length, **(E)** shoot fresh weight, and **(F)** root fresh weight of Arabidopsis Col-0 plants co-cultivated with POT1 in full P conditions for 10 days. The combined data from three independent experiments ($n = 3$; unpaired two-tailed *t*-test, $^{***}p < 0.001$; $^{**}p < 0.01$; $^{*}p < 0.05$) is shown. **(G)** The phosphate content in the shoot of Arabidopsis, following a 4 weeks co-cultivation with or without POT1. **(H)** Arabidopsis plants grown in low P conditions both with and without POT1. Four-days-old plants were transferred to low P media that had been either pre-cultured with POT1 or not and maintained *in vitro* for 10 days. The scale bar represents 1 cm. The bar diagrams show **(I)** primary root length, **(J)** shoot fresh weight, and **(K)** root fresh weight of Arabidopsis WT plants co-cultivated with POT1 in low P conditions for 10 days. The combined data from three independent experiments is represented ($n = 3$; unpaired two-tailed *t*-test, $^{***}p < 0.001$, $^{**}p < 0.01$, and $^{*}p < 0.05$). **(L)** The shoot phosphate content of Arabidopsis plants after a four-week co-cultivation with or without POT1 under low P conditions *in vitro* ($n = 3$; unpaired two-tailed *t*-test, $^{**}p < 0.01$).

solubilization (Figure 4A). When cultured on Pikovskaya and NBRIP media, POT1 showed a phosphate solubility index (*d*/*D* ratio) of 1.161 and 1.212, respectively (Figure 4B and Supplementary Table S7).

POT1 was found to solubilize tricalcium phosphate [$Ca_3(PO_4)_2$], hydroxyapatite [$Ca_{10}(PO_4)_6$ $(OH)_2$], aluminum phosphate ($AlPO_4$), and iron phosphate ($FePO_4{\cdot}4H_2O$) accompanied by a decline in the

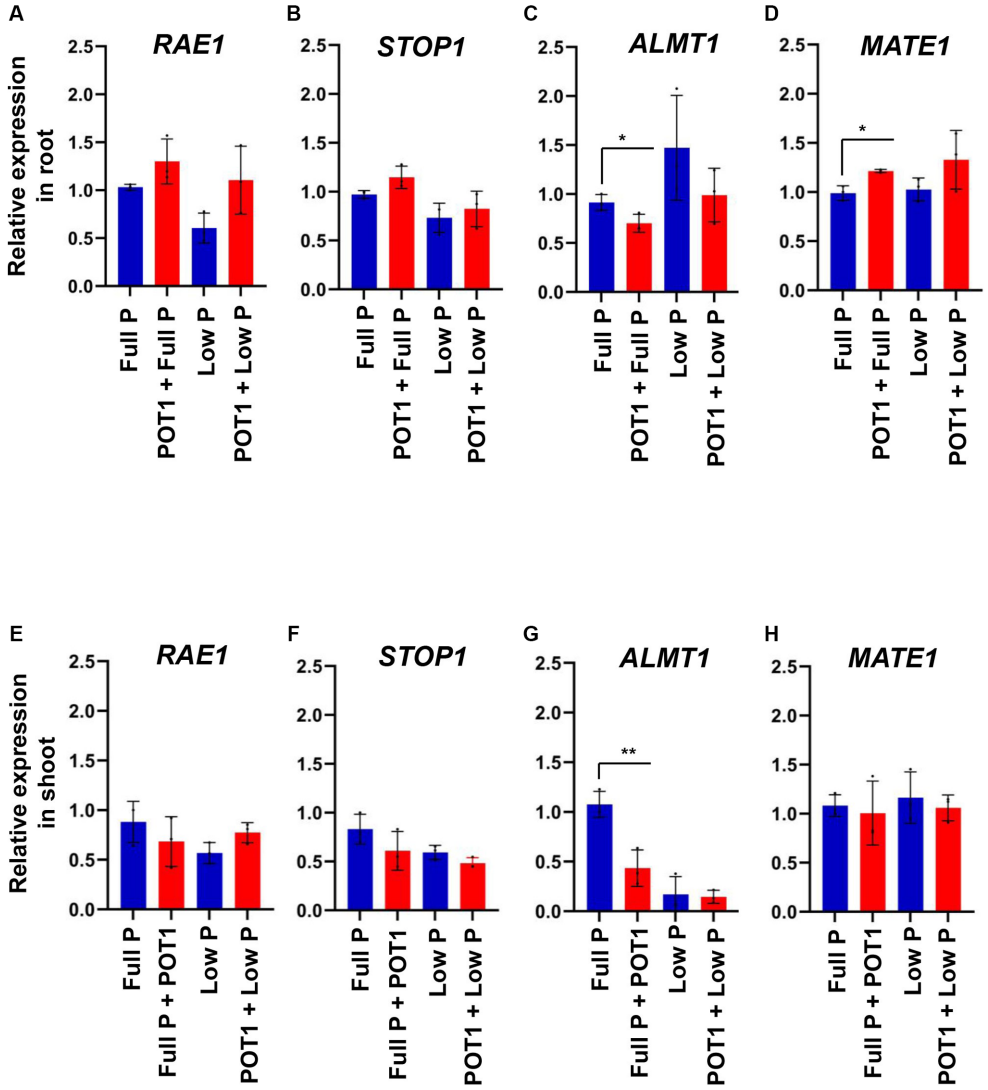

FIGURE 2
Gene expression analysis. Relative expression of **(A)** *RAE1*, **(B)** *STOP1*, **(C)** *ALMT1*, and **(D)** *MATE1* in roots of Arabidopsis when treated with and without *Penicillium olsonii* TLL1 (POT1) under full P and low P conditions. The relative expression of **(E)** *RAE1*, **(F)** *STOP1*, **(G)** *ALMT1*, and **(H)** *MATE1* in shoots of Arabidopsis when treated with POT1 under full P and low P conditions. Expression levels are shown relative to the mean expression of actin and normalized to those of full P conditions. The bar diagrams show combined data from three independent experiments ($n = 3$; unpaired two-tailed t-test, $^{**}p < 0.01$ and $^{*}p < 0.05$).

pH of the supernatants in modified PVK media (Supplementary Table S8). POT1 exhibited the highest phosphate-solubilizing activity in media containing $Ca_3(PO_4)_2$, followed by hydroxyapatite, aluminum phosphate, and iron phosphate (Figure 4C). In CaP and hydroxyapatite, the soluble phosphorus concentrations were 2.95 mg/mL and 1.574 mg/mL, respectively. POT1 could also solubilize $AlPO_4$ and $FePO_4$, releasing soluble P at concentrations of 0.924 mg/mL and 0.436 mg/mL, respectively, after 14 DPI (Figure 4D). The phosphate-solubilizing rate was 57% for CaP, 31% for hydroxyapatite, 20% for AlP, and 3% for FeP (Supplementary Table S8).

3.7. Secretion of organic acids by POT1

The organic acids released by POT1 were measured under both full P and low P conditions. The secretion of gluconic acid (238 mg/L) was higher under low P conditions, whereas the secretion of citric acid (212 mg/L) was higher under full P conditions (Supplementary Figure S9). The malic acid concentration in low P (3 mg/L) was reduced 45-fold when compared to full P conditions (136 mg/L). Similarly, the amount of succinic acid secreted by POT1 into low P culture filtrate was reduced 25-fold.

3.8. Growth promotion in Arabidopsis and leafy vegetables by POT1 under insoluble phosphate conditions

To investigate the growth promotion and phosphate-solubilizing capability of POT1 on Arabidopsis growth under P-sufficient and deficient conditions including insoluble P sources, we co-cultivated Arabidopsis plants in vermiculite,

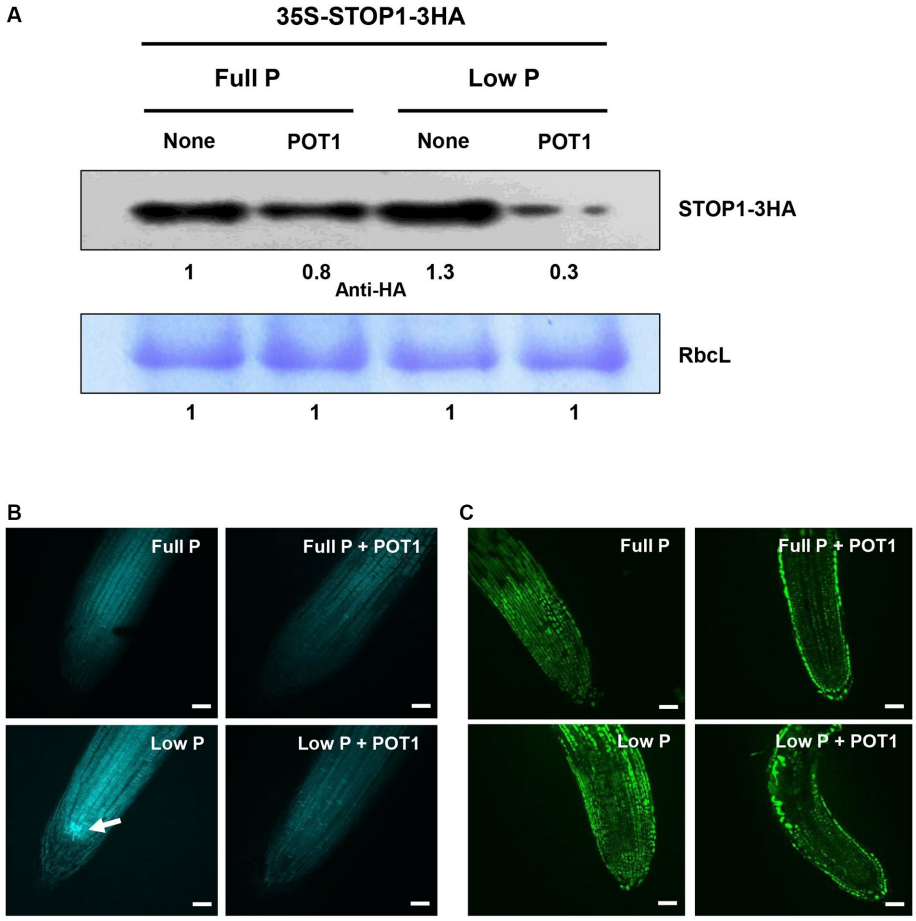

FIGURE 3
Effects of *Penicillium olsonii* TLL1 (POT1) inoculation on STOP1 accumulation, callose deposition, and NO accumulation in Arabidopsis. **(A)** Transgenic Arabidopsis plants expressing 35S: STOP1-3HA were grown under full P and low P with and without POT1 inoculation. STOP1 protein levels were analyzed by western blots using anti-HA antibodies. Stained gel bands of a large subunit of Rubisco (RbcL) were used as controls. **(B)** Callose deposition in Arabidopsis roots under full P and low P conditions, with both inoculated and uninoculated conditions of POT1. Four-days-old plants were transferred to full P media pre-cultured with and without POT1 under *in vitro* conditions for 10 days, and callose accumulation was analyzed in 1.5 cm root tips using aniline blue staining. The white arrowhead denotes callose deposition in the stem cell niche under phosphate-limiting conditions. Three independent experiments were carried out, and one representative experiment is shown. The scale bar represents 100 μm. **(C)** Nitric oxide (NO) accumulation in Arabidopsis roots under full P and low P conditions, with inoculated and uninoculated conditions of POT1. Four-days-old plants were transferred to full P media pre-cultured with and without POT1 under *in vitro* conditions for 10 days. NO accumulation was analyzed in 1.5 cm root tips using DAF-FM DA staining. The scale bar represents 100 μm.

which is a nutrient-free soil (Figure 5 and Supplementary Table S9). Arabidopsis plants grown in low P and insoluble P sources such as tricalcium phosphate (CaP), aluminum phosphate (AlP), iron phosphate (FeP), and hydroxyapatite (HA) conditions are stunted without POT1 inoculation (Figure 5A). Consistent with Arabidopsis growth condition, shoot fresh weight, leaf index, number of leaves, and shoot phosphate content were higher in POT1 inoculated plants compared to non-inoculated plants (Figures 5B–E; Supplementary Figure S10). The anthocyanin accumulation, a typical phenotype of plants grown under phosphate deficiency (Jiang et al., 2007), was lower in POT1-inoculated plants than in non-inoculated plants (Supplementary Figure S11 and Supplementary Table S10). Under no P condition in vermiculite soil, the shoot fresh weight, the number of leaves, leaf area index, and shoot P content of POT1-inoculated Arabidopsis plants were increased significantly, compared with non-inoculated plants (Supplementary Figure S12 and Supplementary Table S11). However, plants grown under no P condition still showed growth defects when compared with phosphate-sufficient plants.

We also examined whether POT1 colonization could promote the growth of leafy vegetable Bok Choy (*B. rapa* subsp. *chinensis*) under different phosphate sources by growing it in vermiculite (Figure 6A and Supplementary Table S12). After 4 weeks, Bok Choy plants grown in low P, tricalcium phosphate (CaP), aluminum phosphate (AlP), iron phosphate (FeP), and hydroxyapatite (HA) conditions without POT1 exhibited stunted growth. In contrast, the biomass of POT1-inoculated plants increased as indicated by fresh shoot weight, number of leaves, and leaf area index (Figures 6B–D; Supplementary Figure S13). Moreover, the total phosphate content was higher in all the inoculated plants under insoluble phosphate and low phosphate conditions, compared with non-inoculated Bok Choy (Figure 6E). When no P condition was simulated in vermiculite soil, the shoot fresh weight, number of leaves, and leaf area index of plants

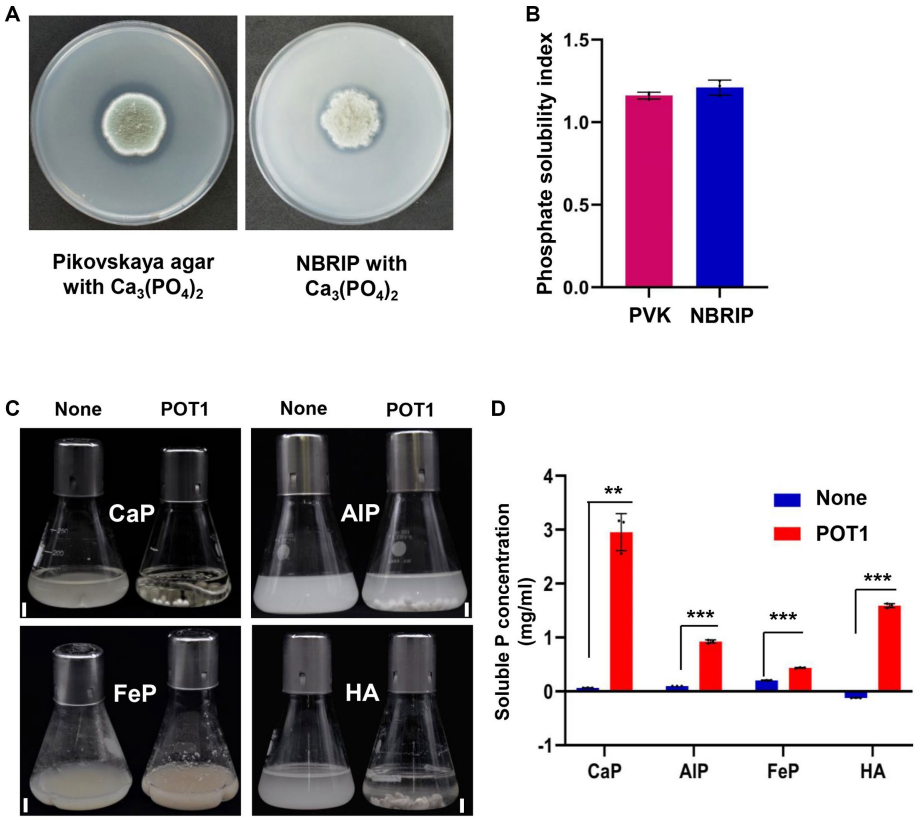

FIGURE 4
Insoluble phosphate solubilization activity of *Penicillium olsonii* TLL1 (POT1) under different recalcitrant P sources. **(A)** POT1 producing dissolved circular zones of phosphorus when cultured on Pikovskaya agar and NBRIP media amended with CaP for 7 days. **(B)** A bar diagram showing phosphate solubility indices of POT1 when cultured in Pikovskaya agar and NBRIP media amended with CaP for 7 days. **(C)** Phosphate-solubilizing potential of POT1 in various inorganic phosphorus compounds such as tricalcium phosphate (CaP), aluminum phosphate (AlP), iron phosphate (FeP), and hydroxyapatite (HA) after 14 days. Scale bar represents 1 cm. **(D)** Soluble P concentration produced by POT1 in different inorganic insoluble phosphates such as CaP, AlP, FeP, and HA. The POT1 spore suspension was inoculated in 100 mL-modified Pikovskaya media amended with CaP, AlP, FeP, and HA for 2 weeks and the soluble phosphate concentration was measured using phosphomolybdenum spectrophotometry. Three biological replicates of each treatment were analyzed ($n = 3$; unpaired two-tailed t-test, $^{***}p < 0.001$, $^{**}p < 0.01$, and $^{*}p < 0.05$). The error bars show the standard deviation.

increased in plants treated with POT1 compared to non-inoculated plants (Supplementary Figure S14). However, the biomass of the plants still decreased 7-fold compared to plants grown under full P conditions (Supplementary Table S13).

3.9. Growth promotion by POT1 under local soil conditions

We investigated whether POT1 functions in the local soil at Lim Chu Kang in Singapore on Bok Choy and Rice growth. Firstly, we analyzed the pH and macro/micro-nutrient content of the local soil. Our results showed that the pH of Lim Chu Kang soil was 6.5 higher than the pH of the commercial soil (5.7) (Supplementary Figure S15A), which was in the range of highest phosphate availability (Havlin, 2020) (Supplementary Figure S15B). Additionally, the phosphate content of the commercial soil was 4-fold higher than that of Lim Chu Kang soil (Supplementary Figure S15C). However, the phosphate content in Lim Chu Kang soil (50 mg/kg) indicated that they were still sufficient for plant growth (Philip et al., 2021). We also analyzed other macro/micro-nutrients such as nitrogen, potassium, calcium, magnesium, iron, sodium, copper, manganese, zinc, and boron in the commercial and Lim Chu Kang soils (Supplementary Figures S16A,B). Notably, the content of copper, manganese, and zinc in Lim Chu Kang soil was higher than that of the commercial soil (Supplementary Table S14).

For 4 weeks, we grew Bok Choy plants in Lim Chu Kang soil with/without POT1 (Supplementary Figure S17). We found that POT1 improved the growth conditions of the plants, as indicated by the increase in shoot fresh weight, number of leaves, and leaf index in POT1 inoculated plants (Figures 7A–D and Supplementary Table S15). Moreover, the total phosphorus content in the leaves of POT1-inoculated plants was higher than that of non-inoculated plants (Figure 7E and Supplementary Table S15). We also confirmed that POT1 promoted the growth of Rice, a monocot plant, in Lim Chu Kang soil (Figure 8; Supplementary Figure S18). The co-cultivation of Rice plants with POT1 resulted in increased plant height (Figures 8A,B), number of tillers (Figure 8C), and shoot phosphate content (Figure 8D) compared with plants grown without POT1 inoculation. Furthermore, the increased tiller number was accompanied by an increase in seed number (Figure 8E), and seed dry weight (Figure 8F) was also increased by POT1 inoculation (Supplementary Table S16).

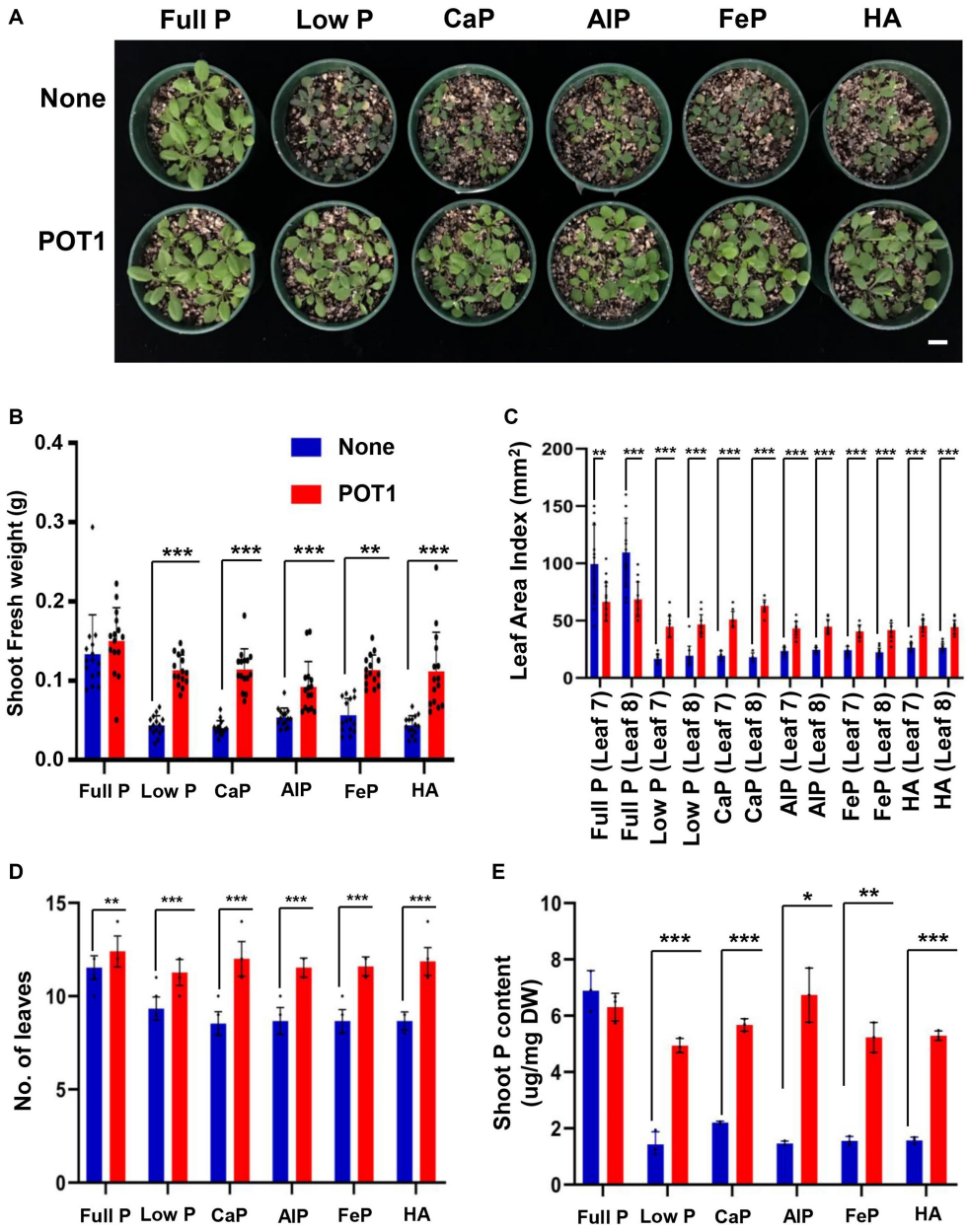

FIGURE 5
Penicillium olsonii TLL1 (POT1) promotes the growth of Arabidopsis under insoluble phosphate and phosphate-limiting conditions. **(A)** A representative image of *A. thaliana* WT plants grown in full P, low P, CaP, AlP, FeP, and HA as the sole source of P with and without POT1. Ten-days-old plants were transferred to vermiculite soil pre-inoculated with and without POT1 and were harvested after 2 weeks. The scale bar represents 1 cm. The bar diagrams represent **(B)** shoot fresh weight, **(C)** leaf area Index, and **(D)** number of leaves of *A. thaliana* WT plants grown in full P, low P, CaP, AlP, FeP, and HA with and without POT1 in vermiculite for 2 weeks. The combined data from 15 independent experiments were analyzed ($n = 15$; unpaired two-tailed *t*-test, ***$p < 0.001$, **$p < 0.01$, and *$p < 0.05$). **(E)** Shoot phosphate content of Arabidopsis plants grown in full P, low P, CaP, AlP, FeP, and HA with and without POT1 after 4 weeks ($n = 3$; unpaired two-tailed *t*-test, **$p < 0.01$).

In addition, we tested the effect of POT1 on plant growth under Lim Chu Kang soil conditions using heat-killed POT1 as a negative control. We found that shoot fresh weight, number of leaves, and leaf area index of Bok Choy were significantly higher in live POT1 inoculated plants compared to heat-killed POT1 and uninoculated plants (Supplementary Figure S19 and Supplementary Table S17). Similarly, in the Rice growth test, heat-killed POT1 was non-functional, as indicated by shorter plant height, lower tiller numbers, and reduced seed weight/number compared with live POT1 (Supplementary Figure S20 and Supplementary Table S18). These results suggest that the phosphate-solubilizing capability of POT1 helps plants absorb phosphate sources from soils containing insoluble phosphate, thereby increasing plant growth.

3.10. Comparison of five *Penicillium* strains on phosphate solubilizing activity and Arabidopsis growth

The capability of POT1 to solubilize tricalcium phosphate was evaluated against other *Penicillium* strains including *P. bilaiae*, *P. chrysogenum*, *P. janthinellum*, and *P. simplicissimum*

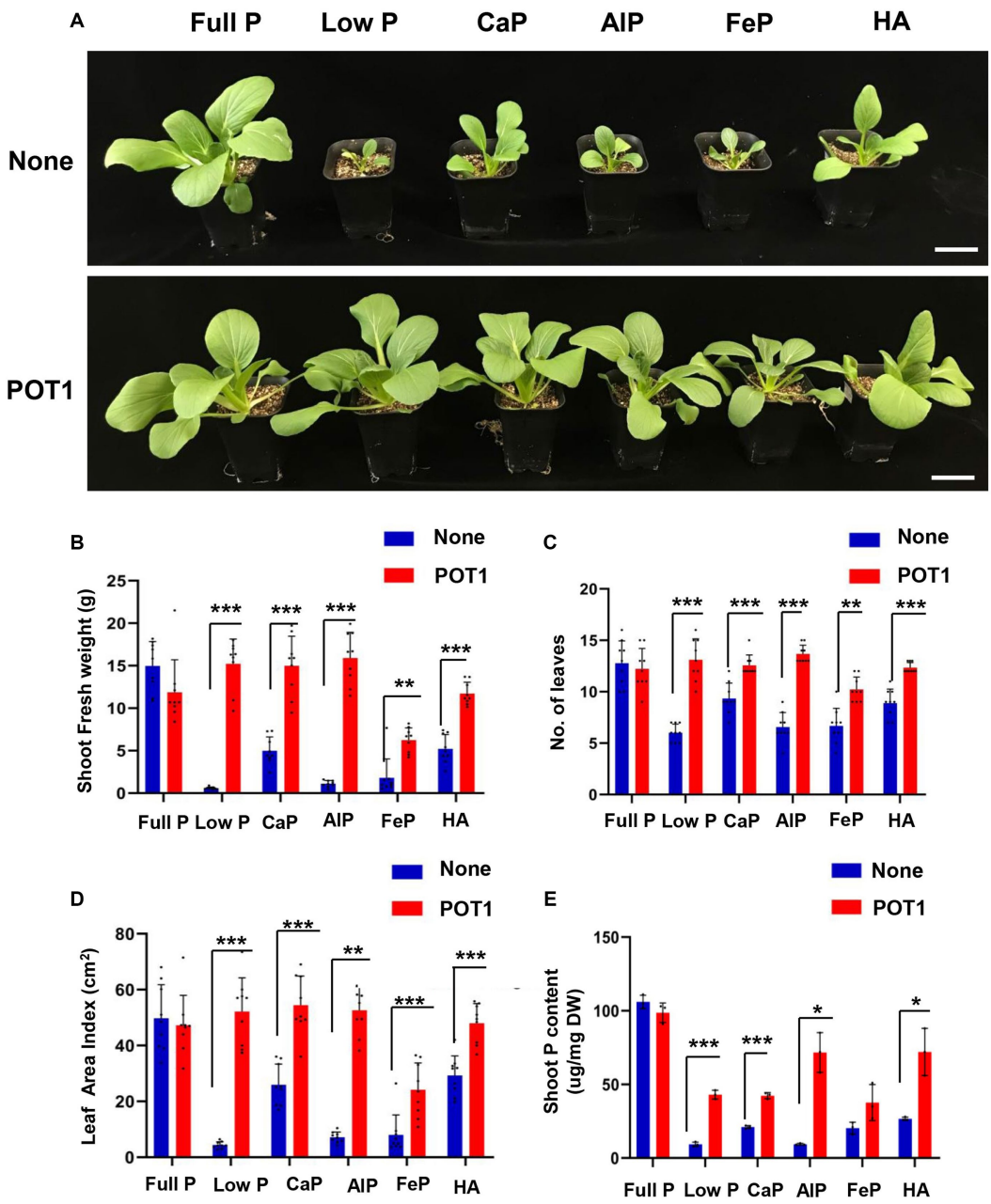

FIGURE 6
Penicillium olsonii TLL1 (POT1) promotes the growth of leafy vegetable Bok Choy under insoluble phosphate and phosphate-limiting conditions. **(A)** A representative image of Bok Choy plants grown in full P, low P, CaP, AlP, FeP, and HA as the sole source of P with and without POT1. Ten-days-old Bok Choy plants were transferred to nutrient-poor vermiculite soil pre-inoculated with and without POT1 and were harvested after 4 weeks. The scale bar represents 5 cm. The bar diagrams show **(B)** shoot fresh weight, **(C)** number of leaves, and **(D)** leaf area index of the 4th leaf of Bok Choy plants co-cultivated with POT1 in full P, low P, CaP, AlP, FeP, and HA conditions after 4 weeks. The combined data from nine independent experiments were analyzed ($n = 9$; unpaired two-tailed t-test, $^{***}p < 0.001$, $^{**}p < 0.01$, and $^{*}p < 0.05$). **(E)** Shoot phosphate content of Bok Choy plants co-cultivated with and without POT1 after 4 weeks ($n = 3$; unpaired two-tailed t-test, $^{**}p < 0.01$).

(Supplementary Figure S21). In mediums containing CaP, the soluble phosphate concentrations for *P. chrysogenum*, *P. janthinellum*, and *P. simplicissimum* were measured at 1.69 mg/mL, 1.84 mg/mL, and 1.97 mg/mL, respectively. The highest solubilizing activity was shown in *P. bilaiae* (3.44 mg/mL), followed by POT1 (3.06 mg/mL) (Supplementary Table S19). Based on these results, growth promotion activity was also compared between POT1 and the aforementioned *Penicillium* strains under phosphate-deficient conditions (Supplementary Figure S22A). All strains showed longer primary root lengths compared to the control, which was without any fungal inoculation. Among the five *Penicillium* strains, plants inoculated with POT1 had the longest primary root length (Supplementary Figure S22B). Similarly, shoot fresh weight in plants treated with POT1 (a 2-fold increase) was the highest among all the strains (Supplementary Figure S22C). Unexpectedly, no difference in shoot fresh weight was found between plants treated with

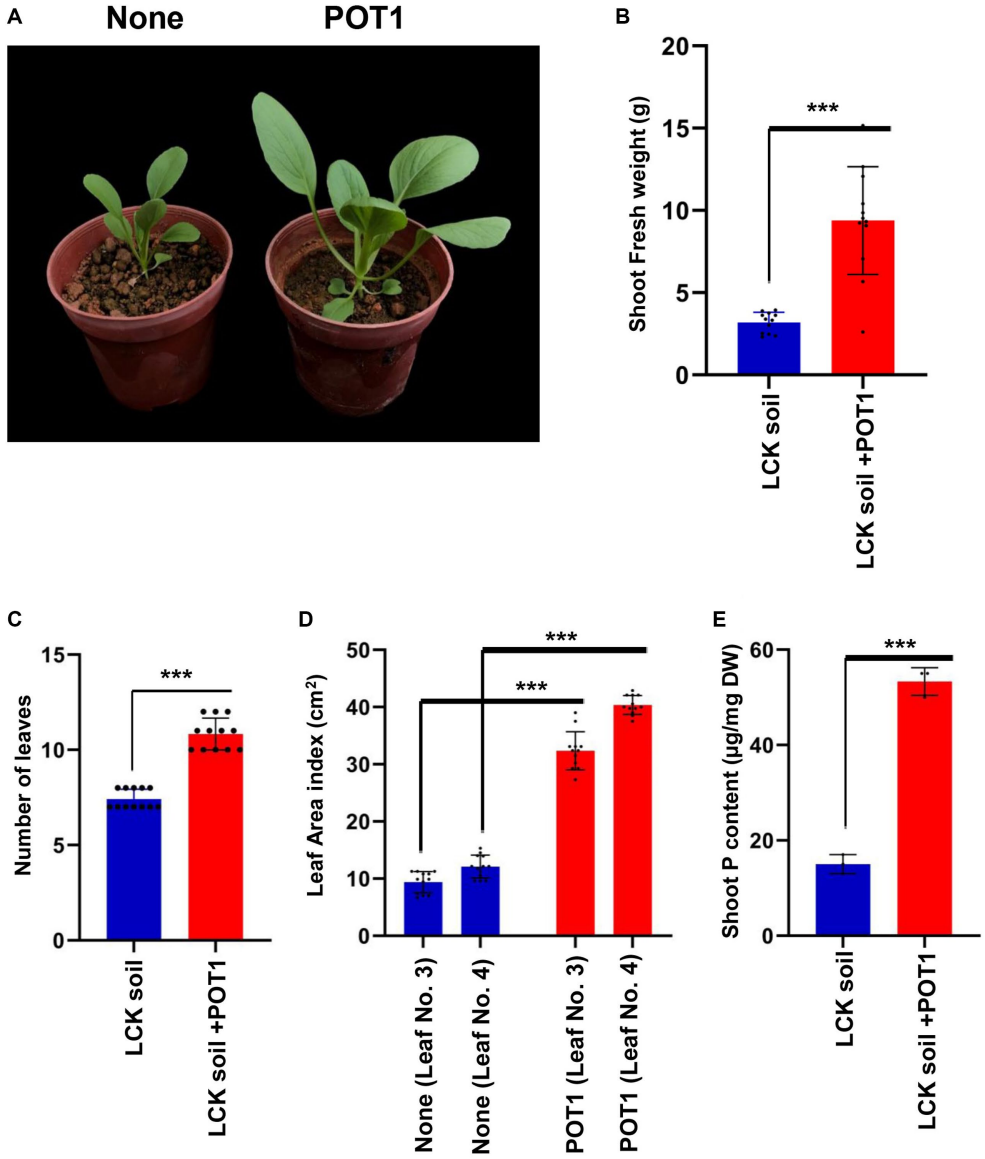

FIGURE 7
Penicillium olsonii TLL1 (POT1) promotes the plant growth index of leafy vegetables in Singapore's local soil. **(A)** A representative image of Bok Choy plants grown in Lim Chu Kang soil with and without POT1. Ten-days-old Bok Choy plants were transferred to Lim Chu Kang soil pre-inoculated with and without POT1 and harvested after 4 weeks. The scale bar represents 5 cm. The bar diagrams show **(B)** shoot fresh weight, **(C)** the number of leaves, and **(D)** the leaf area index of the 3rd and 4th leaves of Bok Choy plants co-cultivated with POT1 after 4 weeks. The combined data from 12 independent experiments are represented ($n = 12$; unpaired two-tailed t-test, $^{***}p < 0.001$, $^{**}p < 0.01$, and $^{*}p < 0.05$). **(E)** Shoot phosphate content of Bok choy plants co-cultivated with and without POT1 after 4 weeks ($n = 3$; unpaired two-tailed t-test, $^{**}p < 0.01$).

P. simplicissimum and control plants. Moreover, in the case of plants co-cultivated with *P. janthinellum*, a 2.56-fold decrease in shoot fresh weight was observed. Regarding root fresh weight, all inoculated plants exceeded the non-inoculated controls, with *P. chrysogenum* demonstrating the highest increase (Supplementary Figure S22D and Supplementary Table S20).

To investigate plant growth by the phosphate solubilizing activity of each fungus, we tested Arabidopsis growth in vermiculite using an insoluble phosphate source, which is calcium phosphate (CaP) (Supplementary Figure S23A). The shoot fresh weight of Arabidopsis inoculated with POT1 was higher than that of other strains under these conditions (Supplementary Figure S23B). Furthermore, we measured anthocyanin accumulation, which is a typical phosphate deficiency response in plants. The lowest anthocyanin content was observed in plants inoculated with POT1 and *P. simplicissimum* (Supplementary Figure S23C and Supplementary Table S21). Overall, these results indicate that POT1 demonstrated superior activity in comparison to the other *Penicillium* strains.

4. Discussion

In our study, we identified that the newly isolated fungal strain, *P. olsonii* TLL1 (POT1), has a high ability to solubilize phosphate and

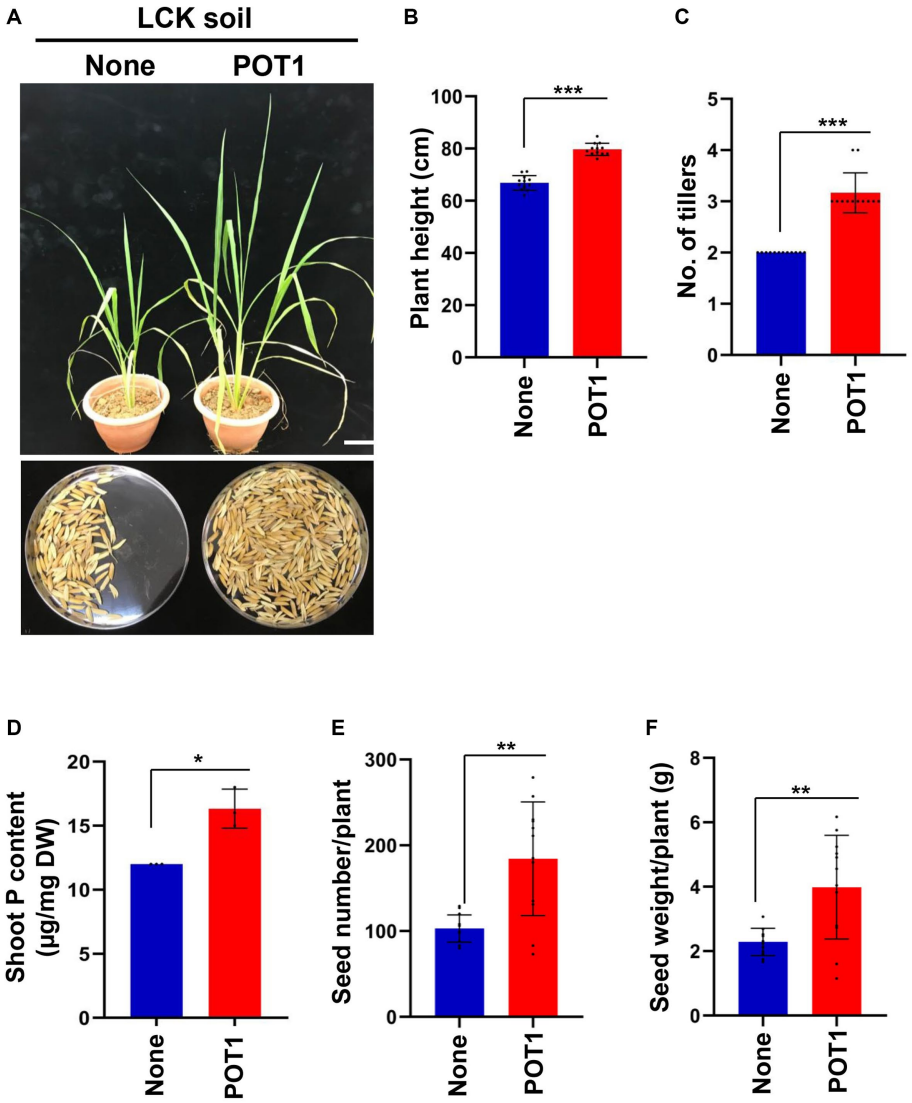

FIGURE 8
Penicillium olsonii TLL1 (POT1) promotes the plant growth index of rice in Singapore's local soil. **(A)** A representative image of rice grown in Lim Chu Kang soil with and without POT1 after 6 weeks. The scale bar represents 10 cm. Fourteen-days-old Rice seedlings were transferred to LCK soil pre-inoculated with and without POT1 and were grown for 3 months. The bar diagrams show **(B)** plant height, **(C)** number of tillers, **(D)** shoot phosphorus content after 6 weeks, **(E)** seed number per plant, and **(F)** seed weight per plant co-cultivated with and without POT1 in LCK soil. The combined data from 12 independent experiments were analyzed ($n = 12$; unpaired two-tailed t-test, ***$p < 0.001$, **$p < 0.01$, and *$p < 0.05$).

promote root elongation in Arabidopsis (Figure 1). Even if the phosphate source is completely omitted from the growth medium, the length of the primary root is longer with POT1 inoculation. Previously, several *Penicillium* spp. were isolated from the greenhouses of a botanical garden and *P. olsonii* was identified to be one of the predominant airborne fungal species (Rodolfi et al., 2003). Recently, the biocontrol activity and plant growth-promoting potential of *P. olsonii* strains isolated from different environments have also been revealed (Rojas et al., 2022; Tarroum et al., 2022). Here, we demonstrate the growth-promoting potential of POT1 especially under phosphate limiting conditions.

The STOP1 transcription factor is one of the crucial checkpoints in root development to phosphate deficiency stress in Arabidopsis. Our study shows that the STOP1 protein level is decreased by POT1 inoculation under full P and low P conditions, implying that the reduction of STOP1 protein leads to a low ALMT1 transcript level (Figures 2, 3A). STOP1 stability is reported to be post-translationally regulated by RAE1, an E3 ubiquitin ligase, thereby controlling primary root length and *STOP1* mutants, and RAE1 overexpressed plants have a long primary root under phosphate deficiency (Sawaki et al., 2009; Balzergue et al., 2017; Zhang et al., 2019). A recent report demonstrated that in Arabidopsis, the premature leaf senescence induced by the soil-borne fungus *Verticillium dahliae* is influenced by the protein elicitor PevD1, which is secreted by *V. dahliae*. When PevD1 is overexpressed or transferred by *V. dahliae*, it not only accelerates leaf senescence but also targets and stabilizes the senescence-related NAC transcription factor ORE1. This happens by interfering with ORE1's interaction with the RING-type ubiquitin E3 ligase NLA, leading to increased ethylene production and enhanced senescence (Zhang et al., 2021). Similarly, more research is needed to

identify specific elicitors that affect the degradation of STOP1 by RAE1.

Moreover, we confirmed that POT1 inhibited callose and NO accumulation in root cells under phosphate deficiency (Figures 3B,C). As negative factors of primary root elongation inhibiting cell-to-cell communication, callose deposition and NO are accumulated in the root apical meristem and entire root cells, respectively.

Despite being grown under low phosphate conditions, Arabidopsis' roots elongate normally due to the inhibition of callose and NO accumulation with root colonization of POT1. These metabolites can be degraded and scavenged by beta-1,3 glucanases and flavonoids, respectively (Wang et al., 2010; Burch-Smith and Zambryski, 2012; Duarte et al., 2014; Muller et al., 2015).

The secretion of β-1,3 glucanases by endophytic fungi is well documented as an antagonistic activity against invading fungal pathogens (Markovich and Kononova, 2003). Endophytic fungal communities with phosphate solubilizing activity associated with the rhizosphere of healthy maize and rice plants secrete β-1,3 glucanases, chitinases, and amylases (Potshangbam et al., 2017). Besides, *Aspergillus nidulans* and *Aspergillus oryzae* are reported to secrete flavonoids in cultures (Qiu et al., 2010). Taken together, we suggest that POT1 might control STOP1 protein stability and secrete beta-1,3 glucanases and flavonoids in low-phosphate environments. Thus, further studies are required to confirm the mechanism of post-translational regulation as well as the secretion of beta-1,3 glucanases and flavonoids by POT1 under phosphate-limiting conditions. Therefore, further study is required to determine whether POT1 can secrete and transfer a particular flavonoid and beta-1,3-glucanases to plant root cells using secondary metabolite and proteome analysis as well as investigate flavonoid content and beta-1,3-glucanase expression level induced by POT1 inoculation.

Organic acid secretion is the widely reported mechanism of phosphate solubilization, where PSFs break down insoluble phosphates by secreting organic acids onto soil surfaces (Rawat et al., 2021). Malic acid was most competent to solubilize CaP, followed by citric, formic, and succinic acids (Gaind, 2016). It has been reported that tartaric acid and citric acid were dominant in *Penicillium oxalicum* P4, while malic and citric acid dominated in *A. niger* P85 cultures when solubilizing tricalcium phosphate (Yin et al., 2015). The commercial strain, *P. bilaiae*, has been shown to produce oxalic and citric acids (Sanchez-Esteva et al., 2016). We have shown that in low P conditions, POT1 highly exudates gluconic acid while malic acid and citric acid are reduced.

The use of microbial inoculants has gained acceptance over chemical fertilizers as they are eco-friendly and help to improve soil health. The application of fungal species as biofertilizers to arable land to improve soil quality is emerging as an eco-friendly approach in modern agriculture (Kour et al., 2020). *P. bilaiae* was widely used as a biofertilizer, and several studies conducted in growth chambers and the field increased the biomass, phosphate uptake, and grain yield in wheat (*Triticum aestivum* L.) (Sanchez-Esteva et al., 2016), pea (Vessey and Heisinger, 2001), and lentil (Wakelin et al., 2007). Among the *Penicillium* genus, *P. bilaji*, *P. italicum*, *P. albidum*, *P. frequentans*, *P. simplicissimum*, *P. rubrum*, *P. expansum*, *P. oxalicum*, and *P. citrinum* have been commercially used as biofertilizers for the mobilization of P, Mn, Zn, Fe, Co, Cu, and Mo and biotic and abiotic stress tolerance (Odoh et al., 2020). *P. bilaiae* was reported to be effective in calcareous soil compared to moderately acidic soil (Sanchez-Esteva et al., 2016). In our study, we have confirmed that plant growth conditions in Arabidopsis, Bok Choy, and Rice in vermiculite and Singapore's local soil, which has low phosphate availability, are improved due to the P-solubilizing activity of POT1 (Figures 5–8).

Phosphate fixation in soil depends on edaphic factors such as pH, organic matter content, the presence of exchangeable cations such as Fe, Al, Ca, and Mg, and clay content, which contribute to phosphate insolubility. The phosphate added as agro fertilizer to the soil reacts with cation ions such as Al, Ca, and Fe and becomes fixed in the soil, which is inaccessible for uptake by the plant roots (Penn and Camberato, 2019). Hence, phosphate-solubilizing fungi (PSF) could be widely employed as a potential solution to improve phosphate uptake and use efficiency.

Phosphate-solubilizing fungi thrive in the rhizosphere and establish symbiotic associations with the root systems of plants. Endophytic fungi such as *Penicillium*, *Aspergillus*, *Trichoderma*, *Piriformospora*, and *Curvularia* are among the active PSF species involved in phosphate cycling (Mehta et al., 2019). The *P. guanacastense* JP-NJ2 strain has a high ability to solubilize aluminum phosphate (Qiao et al., 2019). The solubilization of recalcitrant phosphate sources by *Aspergillus* spp. and *Penicillium* spp. generally decreased the liquid medium pH for the solubilization of insoluble phosphate (Acevedo et al., 2014). Here, we confirmed the phosphate-solubilizing activity of POT1 in insoluble phosphate complexes such as tricalcium phosphate, aluminum phosphate, iron phosphate, and hydroxyapatite (Figure 4). Among these, the highest solubilizing capability is observed in culture media containing tricalcium phosphate (Figure 4D). In addition, we showed that POT1 was remarkably effective on root growth promotion and phosphate solubilizing activity in the phosphate-deficient medium and insoluble phosphate-contained soil when compared to other *Penicillium* strains such as *P. bilaiae*, *P. chrysogenum*, *P. janthinellum*, and *P. simplicissimum*. Thus, we suggest that POT1, which showed better activity than other *Penicillium* strains, can be used as a high-potential biofertilizer for both monocot and dicot crop growth as well as the different types of soil conditions, which are upland and paddy soil. Furthermore, combinations of various beneficial fungal strains are required for the evaluation of plant growth and viability tests among fungal strains. Overall, this study provides useful information for developing more efficient biofertilizers than the existing ones.

5. Conclusion

The optimal usage of chemical fertilizers is necessary to maintain ecosystem function and develop sustainable agriculture. Thus, application, research, and methodology developments of biofertilizers need to be emphasized on improving effective, stable, and non-toxic microbiome strains for promoting plant growth. Using POT1, a potential biofertilizer, our study provides information on the combined action of both phosphate-solubilizing function and inhibitor removal of primary root elongation, especially under phosphate-limiting conditions. Therefore, these findings will support the development of biofertilizers for improved phosphate use efficiency and apply to different types of plants, such as monocot and dicot plants, increasing the yield even under low or no phosphate conditions as well as different conditions of soil, such as upland and paddy soils. Further study is required to investigate the functions and changes of diversification in the soil ecosystem due to biotic interactions between soil microbiomes and POT1. Specifically, research should explore combinations of POT1

with other beneficial fungi and bacteria to identify microbiome combinations that maximize growth promotion and yield in crops. Moreover, in our study, there is limited data on the effects of POT1 on plant growth in acidic conditions and different soil textures. Further research is needed to explore the functions of POT1 under various field conditions. Taken together, our research would contribute toward a better solution for sustainable agriculture with reduced fertilizer cost, especially phosphate, increasing its use efficiency and increasing crop yield.

Data availability statement

The original contributions presented in the study are included in the article/Supplementary material, further inquiries can be directed to the corresponding author.

Author contributions

ES: Formal analysis, Investigation, Methodology, Project administration, Writing – original draft, Writing – review & editing. VA: Investigation, Writing – original draft, Writing – review & editing. SD: Formal analysis, Methodology, Writing – review & editing. YS: Formal analysis, Investigation, Visualization, Writing – review & editing. SL: Investigation, Writing – review & editing. NN: Supervision, Writing – review & editing. RS: Supervision, Writing – review & editing. ZY: Supervision, Writing – review & editing. BP: Conceptualization, Data curation, Formal analysis, Funding acquisition, Methodology, Project administration, Resources, Supervision, Validation, Visualization, Writing – original draft, Writing – review & editing.

Funding

The author(s) declare financial support was received for the research, authorship, and/or publication of this article. The work was supported by Temasek Life Sciences Laboratory core funding (3085).

Conflict of interest

This research finding has been filed with the Intellectual Property Office of Singapore (IPOS), Application No. 10202300767S. This patent was filed by ES, NN, RS, ZY, and BP.

The remaining authors declare that the research was conducted in the absence of any commercial or financial relationships that could be construed as a potential conflict of interest.

Publisher's note

All claims expressed in this article are solely those of the authors and do not necessarily represent those of their affiliated organizations, or those of the publisher, the editors and the reviewers. Any product that may be evaluated in this article, or claim that may be made by its manufacturer, is not guaranteed or endorsed by the publisher.

Supplementary material

The Supplementary material for this article can be found online at: https://www.frontiersin.org/articles/10.3389/fmicb.2023.1285574/full#supplementary-material

References

Acevedo, E., Galindo-Castaneda, T., Prada, F., Navia, M., and Romero, H. M. (2014). Phosphate-solubilizing microorganisms associated with the rhizosphere of oil palm (*Elaeis guineensis* Jacq.) in Colombia. *Appl. Soil Ecol.* 80, 26–33. doi: 10.1016/j.apsoil.2014.03.011

Balzergue, C., Dartevelle, T., Godon, C., Laugier, E., Meisrimler, C., Teulon, J. M., et al. (2017). Low phosphate activates STOP1-ALMT1 to rapidly inhibit root cell elongation. *Nat. Commun.* 8:15300. doi: 10.1038/ncomms15300

Bergkemper, F., Kublik, S., Lang, F., Kruger, J., Vestergaard, G., Schloter, M., et al. (2016). Novel oligonucleotide primers reveal a high diversity of microbes which drive phosphorous turnover in soil. *J. Microbiol. Methods* 125, 91–97. doi: 10.1016/j.mimet.2016.04.011

Bonfante, P., and Genre, A. (2010). Mechanisms underlying beneficial plant—fungus interactions in mycorrhizal symbiosis. *Nat. Commun.* 1:48. doi: 10.1038/ncomms1046

Burch-Smith, T. M., and Zambryski, P. C. (2012). Plasmodesmata paradigm shift: regulation from without versus within. *Annu. Rev. Plant Biol.* 63, 239–260. doi: 10.1146/annurev-arplant-042811-105453

Correa-Aragunde, N., Graziano, M., and Lamattina, L. (2004). Nitric oxide plays a central role in determining lateral root development in tomato. *Planta* 218, 900–905. doi: 10.1007/s00425-003-1172-7

Doilom, M., Guo, J. W., Phookamsak, R., Mortimer, P. E., Karunarathna, S. C., Dong, W., et al. (2020). Screening of phosphate-solubilizing fungi from air and soil in Yunnan, China: four novel species in *Aspergillus*, *Gongronella*, *Penicillium*, and *Talaromyces*. *Front. Microbiol.* 11:585215. doi: 10.3389/fmicb.2020.585215

Duarte, J., Francisco, V., and Perez-Vizcaino, F. (2014). Modulation of nitric oxide by flavonoids. *Food Funct.* 5, 1653–1668. doi: 10.1039/c4fo00144c

Edel, V., Steinberg, C., Gautheron, N., Recorbet, G., and Alabouvette, C. (2001). Genetic diversity of *Fusarium oxysporum* populations isolated from different soils in France. *FEMS Microbiol. Ecol.* 36, 61–71. doi: 10.1016/S0168-6496(01)00119-2

Gaind, S. (2016). Phosphate dissolving fungi: mechanism and application in alleviation of salt stress in wheat. *Microbiol. Res.* 193, 94–102. doi: 10.1016/j.micres.2016.09.005

Havlin, J. L. (2020). "Soil: fertility and nutrient management" in *Landscape and land capacity*. ed. Y. Wang (Boca Raton, FL: CRC Press), 251–265.

Jiang, C., Gao, X., Liao, L., Harberd, N. P., and Fu, X. (2007). Phosphate starvation root architecture and anthocyanin accumulation responses are modulated by the gibberellin-DELLA signaling pathway in Arabidopsis. *Plant Physiol.* 145, 1460–1470. doi: 10.1104/pp.107.103788

Khan, M. S., Zaidi, A., Ahemad, M., Oves, M., and Wani, P. A. (2010). Plant growth promotion by phosphate solubilizing fungi—current perspective. *Arch. Agron. Soil Sci.* 56, 73–98. doi: 10.1080/03650340902806469

Kour, D., Rana, K. L., Yadav, A. N., Yadav, N., Kumar, M., Kumar, V., et al. (2020). Microbial biofertilizers: bioresources and eco-friendly technologies for agricultural and environmental sustainability. *Biocatal. Agric. Biotechnol.* 23:101487. doi: 10.1016/j.bcab.2019.101487

Laby, R. J., Kincaid, M. S., Kim, D., and Gibson, S. I. (2000). The Arabidopsis sugar-insensitive mutants *sis*4 and *sis*5 are defective in abscisic acid synthesis and response. *Plant J.* 23, 587–596. doi: 10.1046/j.1365-313X.2000.00833.x

Lei, Z., and Zhang, Y. Q. (2015). Effects of phosphate solubilization and phytohormone production of *Trichoderma asperellum* Q1 on promoting cucumber growth under salt stress. *J. Integr. Agric.* 14, 1588–1597. doi: 10.1016/S2095-3119(14)60966-7

Li, Z., Bai, T., Dai, L., Wang, F., Tao, J., Meng, S., et al. (2016). A study of organic acid production in contrasts between two phosphate solubilizing fungi: *Penicillium oxalicum* and *Aspergillus Niger*. *Sci. Rep.* 6:25313. doi: 10.1038/srep25313

Lombardo, M. C., Graziano, M., Polacco, J. C., and Lamattina, L. (2006). Nitric oxide functions as a positive regulator of root hair development. *Plant Signal. Behav.* 1, 28–33. doi: 10.4161/psb.1.1.2398

Lombardo, M. C., and Lamattina, L. (2012). Nitric oxide is essential for vesicle formation and trafficking in Arabidopsis root hair growth. *J. Exp. Bot.* 63, 4875–4885. doi: 10.1093/jxb/ers166

Markovich, N. A., and Kononova, G. L. (2003). Lytic enzymes of *Trichoderma* and their role in plant defense from fungal diseases: a review. *Appl. Biochem. Microbiol.* 39, 341–351. doi: 10.1023/A:1024502431592

Mehlich, A. (1984). Mehlich 3 soil test extractant: a modification of Mehlich 2 extractant. *Commun. Soil Sci. Plant Anal.* 15, 1409–1416. doi: 10.1080/00103628409367568

Mehta, P., Sharma, R., Putatunda, C., and Walia, A. (2019). "Endophytic fungi: role in phosphate solubilization" in *Advances in endophytic fungal research*. ed. B. Singh (Cham: Springer), 183–209.

Millner, P. D., and Kitt, D. G. (1992). The Beltsville method for soilless production of vesicular-arbuscular mycorrhizal fungi. *Mycorrhiza* 2, 9–15. doi: 10.1007/BF00206278

Muller, J., Toev, T., Heisters, M., Teller, J., Moore, K. L., Hause, G., et al. (2015). Iron-dependent callose deposition adjusts root meristem maintenance to phosphate availability. *Dev. Cell* 33, 216–230. doi: 10.1016/j.devcel.2015.02.007

Nesme, T., Metson, G. S., and Bennett, E. M. (2018). Global phosphorus flows through agricultural trade. *Glob. Environ. Chang.* 50, 133–141. doi: 10.1016/j.gloenvcha.2018.04.004

Odoh, C. K., Eze, C. N., Obi, C. J., Anyah, F., Egbe, K., Unah, U. V., et al. (2020). "Fungal biofertilizers for sustainable agricultural productivity" in *Agriculturally important fungi for sustainable agriculture*. eds. A. N. Yadav, S. Mishra, D. Kour, N. Yadav and A. Kumar (Cham: Springer), 199–225.

Penn, C. J., and Camberato, J. J. (2019). A critical review on soil chemical processes that control how soil pH affects phosphorus availability to plants. *Agriculture* 9:120. doi: 10.3390/agriculture9060120

Peret, B., Desnos, T., Jost, R., Kanno, S., Berkowitz, O., and Nussaume, L. (2014). Root architecture responses: in search of phosphate. *Plant Physiol.* 166, 1713–1723. doi: 10.1104/pp.114.244541

Petricka, J. J., Winter, C. M., and Benfey, P. N. (2012). Control of Arabidopsis root development. *Annu. Rev. Plant Biol.* 63, 563–590. doi: 10.1146/annurev-arplant-042811-105501

Philip, V., George, E. R., Ghosh, S., and Yap, M. L. (2021). "Nutrient sufficiency range of soils and plants in Singapore" in *Soil science: fundamentals to recent advances*. eds. A. Rakshit, S. K. Singh, P. C. Abhilash and A. Biswas (Singapore: Springer), 669–681.

Potshangbam, M., Indira Devi, S., Sahoo, D., and Strobel, G. A. (2017). Functional characterization of endophytic fungal community associated with *Oryza sativa* L. and *Zea mays* L. *Front. Microbiol.* 8:325. doi: 10.3389/fmicb.2017.00325

Qiao, H., Sun, X. R., Wu, X. Q., Li, G. E., Wang, Z., and Li, D. W. (2019). The phosphate-solubilizing ability of *Penicillium guanacastense* and its effects on the growth of *Pinus massoniana* in phosphate-limiting conditions. *Biol. Open* 8:bio046797. doi: 10.1242/bio.046797

Qiu, M., Xie, R. S., Shi, Y., Zhang, H., and Chen, H. M. (2010). Isolation and identification of two flavonoid-producing endophytic fungi from *Ginkgo biloba* L. *Ann. Microbiol.* 60, 143–150. doi: 10.1007/s13213-010-0016-5

Raja, H. A., Miller, A. N., Pearce, C. J., and Oberlies, N. H. (2017). Fungal identification using molecular tools: a primer for the natural products research community. *J. Nat. Prod.* 80, 756–770. doi: 10.1021/acs.jnatprod.6b01085

Raja, H., Schoch, C. L., Hustad, V., Shearer, C., and Miller, A. (2011). Testing the phylogenetic utility of MCM7 in the Ascomycota. *MycoKeys* 1, 63–94. doi: 10.3897/mycokeys.1.1966

Rawat, P., Das, S., Shankhdhar, D., and Shankhdhar, S. C. (2021). Phosphate-solubilizing microorganisms: mechanism and their role in phosphate solubilization and uptake. *J. Soil Sci. Plant Nutr.* 21, 49–68. doi: 10.1007/s42729-020-00342-7

Redkar, A., Jaeger, E., and Doehlemann, G. (2018). Visualization of growth and morphology of fungal hyphae in planta using WGA-AF488 and propidium iodide co-staining. *Bio-protocol* 8:e2942. doi: 10.21769/bioprotoc.2942

Rodolfi, M., Lorenzi, E., and Picco, A. M. (2003). Study of the occurrence of greenhouse microfungi in a botanical garden. *J. Phytopathol.* 151, 591–599. doi: 10.1046/j.0931-1785.2003.00771.x

Rojas, E. C., Jensen, B., Jorgensen, H. J., Latz, M. A., Esteban, P., and Collinge, D. B. (2022). The fungal endophyte *Penicillium olsonii* ML37 reduces *fusarium* head blight by local induced resistance in wheat spikes. *J. Fungi* 8:345. doi: 10.3390/jof8040345

Royo, B., Moran, J. F., Ratcliffe, R. G., and Gupta, K. J. (2015). Nitric oxide induces the alternative oxidase pathway in Arabidopsis seedlings deprived of inorganic phosphate. *J. Exp. Bot.* 66, 6273–6280. doi: 10.1093/jxb/erv338

Sanchez-Esteva, S., Gomez-Munoz, B., Jensen, L. S., de Neergaard, A., and Magid, J. (2016). The effect of *Penicillium bilaii* on wheat growth and phosphorus uptake as affected by soil pH, soil P and application of sewage sludge. *Chem. Biol. Technol. Agric.* 3:21. doi: 10.1186/s40538-016-0075-3

Sawaki, Y., Iuchi, S., Kobayashi, Y., Kobayashi, Y., Ikka, T., Sakurai, N., et al. (2009). STOP1 regulates multiple genes that protect Arabidopsis from proton and aluminum toxicities. *Plant Physiol.* 150, 281–294. doi: 10.1104/pp.108.134700

Schenk, S., and Schikora, A. (2015). Staining of callose depositions in root and leaf tissues. *Bio-protocol* 5:e1429. doi: 10.21769/bioprotoc.1429

Schmitt, I., Crespo, A., Divakar, P. K., Fankhauser, J. D., Herman-Sackett, E., Kalb, K., et al. (2009). New primers for promising single-copy genes in fungal phylogenetics and systematics. *Persoonia* 23, 35–40. doi: 10.3767/003158509X470602

Schnug, E., and Haneklaus, S. H. (2016). "The enigma of fertilizer phosphorus utilization," in *Phosphorus in agriculture: 100% zero*, eds. E. Schnug and KokL. J. De (Dordrecht: Springer), 7–26

Sharma, S. B., Sayyed, R. Z., Trivedi, M. H., and Gobi, T. A. (2013). Phosphate solubilizing microbes: sustainable approach for managing phosphorus deficiency in agricultural soils. *Springerplus* 2:587. doi: 10.1186/2193-1801-2-587

Stielow, J. B., Levesque, C. A., Seifert, K. A., Meyer, W., Irinyi, L., Smits, D., et al. (2015). One fungus, which genes? Development and assessment of universal primers for potential secondary fungal DNA barcodes. *Persoonia* 35, 242–263. doi: 10.3767/003158515X689135

Svistoonoff, S., Creff, A., Reymond, M., Sigoillot-Claude, C., Ricaud, L., Blanchet, A., et al. (2007). Root tip contact with low-phosphate media reprograms plant root architecture. *Nat. Genet.* 39, 792–796. doi: 10.1038/ng2041

Tarroum, M., Romdhane, W. B., Al-Qurainy, F., Ali, A. A. M., Al-Doss, A., Fki, L., et al. (2022). A novel PGPF *Penicillium olsonii* isolated from the rhizosphere of *Aeluropus littoralis* promotes plant growth, enhances salt stress tolerance, and reduces chemical fertilizers inputs in hydroponic system. *Front. Microbiol.* 13:996054. doi: 10.3389/fmicb.2022.996054

Ticconi, C. A., Delatorre, C. A., Lahner, B., Salt, D. E., and Abel, S. (2004). Arabidopsis pdr2 reveals a phosphate-sensitive checkpoint in root development. *Plant J.* 37, 801–814. doi: 10.1111/j.1365-313X.2004.02005.x

Vessey, J. K., and Heisinger, K. G. (2001). Effect of *Penicillium bilaii* inoculation and phosphorus fertilisation on root and shoot parameters of field-grown pea. *Can. J. Plant Sci.* 81, 361–366. doi: 10.4141/P00-083

Visagie, C. M., Houbraken, J., Frisvad, J. C., Hong, S. B., Klaassen, C. H. W., Perrone, G., et al. (2014). Identification and nomenclature of the genus *Penicillium*. *Stud. Mycol.* 78, 343–371. doi: 10.1016/j.simyco.2014.09.001

Wakelin, S. A., Gupta, V. V. S. R., Harvey, P. R., and Ryder, M. H. (2007). The effect of *Penicillium* fungi on plant growth and phosphorus mobilization in neutral to alkaline soils from southern Australia. *Can. J. Microbiol.* 53, 106–115. doi: 10.1139/W06-109

Wang, B. L., Tang, X. Y., Cheng, L. Y., Zhang, A. Z., Zhang, W. H., Zhang, F. S., et al. (2010). Nitric oxide is involved in phosphorus deficiency-induced cluster-root development and citrate exudation in white lupin. *New Phytol.* 187, 1112–1123. doi: 10.1111/j.1469-8137.2010.03323.x

Ward, J. T., Lahner, B., Yakubova, E., Salt, D. E., and Raghothama, K. G. (2008). The effect of iron on the primary root elongation of Arabidopsis during phosphate deficiency. *Plant Physiol.* 147, 1181–1191. doi: 10.1104/pp.108.118562

White, T. J., Bruns, T., Lee, S., and Taylor, J. (1990). "Amplification and direct sequencing of fungal ribosomal RNA genes for phylogenetics" in *PCR protocols: a guide to methods and applications*. eds. M. A. Innis, D. H. Gelfand, J. J. Sninsky and T. J. White (London: Academic Press), 315–322.

Wu, A. P., Gong, L., Chen, X., and Wang, J. X. (2014). Interactions between nitric oxide, gibberellic acid, and phosphorus regulate primary root growth in Arabidopsis. *Biol. Plant.* 58, 335–340. doi: 10.1007/s10535-014-0408-7

Yin, Z., Shi, F., Jiang, H., Roberts, D. P., Chen, S., and Fan, B. (2015). Phosphate solubilization and promotion of maize growth by *Penicillium oxalicum* P4 and *Aspergillus Niger* P85 in a calcareous soil. *Can. J. Microbiol.* 61, 913–923. doi: 10.1139/cjm-2015-0358

Zhang, Y., Gao, Y., Wang, H. L., Kan, C., Li, Z., Yang, X., et al. (2021). *Verticillium dahliae* secretory effector PevD1 induces leaf senescence by promoting ORE1-mediated ethylene biosynthesis. *Mol. Plant* 14, 1901–1917. doi: 10.1016/j.molp.2021.07.014

Zhang, X., Henriques, R., Lin, S. S., Niu, Q. W., and Chua, N. H. (2006). *Agrobacterium*-mediated transformation of *Arabidopsis thaliana* using the floral dip method. *Nat. Protoc.* 1, 641–646. doi: 10.1038/nprot.2006.97

Zhang, Y., Zhang, J., Guo, J., Zhou, F., Singh, S., Xu, X., et al. (2019). F-box protein RAE1 regulates the stability of the aluminum-resistance transcription factor STOP1 in Arabidopsis. *Proc. Natl. Acad. Sci. U. S. A.* 116, 319–327. doi: 10.1073/pnas.1814426116

Zhu, X. F., Zhu, C. Q., Wang, C., Dong, X. Y., and Shen, R. F. (2017). Nitric oxide acts upstream of ethylene in cell wall phosphorus reutilization in phosphorus-deficient rice. *J. Exp. Bot.* 68, erw480–erw760. doi: 10.1093/jxb/erw480

Frontiers in Microbiology

Explores the habitable world and the potential of microbial life

The largest and most cited microbiology journal which advances our understanding of the role microbes play in addressing global challenges such as healthcare, food security, and climate change.

Discover the latest Research Topics

See more →

Frontiers

Avenue du Tribunal-Fédéral 34
1005 Lausanne, Switzerland
frontiersin.org

Contact us

+41 (0)21 510 17 00
frontiersin.org/about/contact